Distribution Agreement

In presenting this thesis or dissertation as a partial fulfillment of the requirements for an advanced degree from Emory University, I hereby grant to Emory University and its agents the non-exclusive license to archive, make accessible, and display my thesis or dissertation in whole or in part in all forms of media, now or hereafter known, including display on the world wide web. I understand that I may select some access restrictions as part of the online submission of this thesis or dissertation. I retain all ownership rights to the copyright of the thesis or dissertation. I also retain the right to use in future works (such as articles or books) all or part of this thesis or dissertation.

Signature:

_____ _____

Max R. Schroeder Date

Macrolide Resistance in *Streptococcus pneumoniae*

By

Max R. Schroeder
Doctor of Philosophy

Graduate Division of Biological and Biomedical Sciences
Microbiology and Molecular Genetics

David Stephens, M.D. Advisor	Timothy Read, Ph.D. Committee Member
Keith Klugman, M.D., Ph.D. Committee Member	William Shafer, Ph.D. Committee Member
Charles Moran, Ph.D. Committee Member	Jorge Vidal, Ph.D. Committee Member
Philip Rather, Ph.D. Committee Member	

Accepted:

Lisa A. Tedesco, Ph.D.
Dean of the James T. Laney School of Graduate Studies

Date

Macrolide Resistance in *Streptococcus pneumoniae*

By

Max R. Schroeder

B.A., Ohio Wesleyan University, 2009

Advisor: David S. Stephens, M.D.

An abstract of

A dissertation submitted to the Faculty of the
James T. Laney School of Graduate Studies of Emory University
in partial fulfillment of the requirements for the degree of
Doctor of Philosophy
in
Graduate Division of Biological and Biomedical Sciences
Microbiology and Molecular Genetics

2016

Abstract

Macrolide Resistance in *Streptococcus pneumoniae*

By Max R. Schroeder

Streptococcus pneumoniae, the pneumococcus, is an obligate commensal of the human nasopharynx, but an important opportunistic pathogen. The explosive, widespread use of macrolides in the last thirty years has been a strong selective pressure contributing to the expansion of macrolide-resistant *S. pneumoniae*. Macrolide resistance in pneumococci is primarily due to ribosomal methylation by a methyltransferase encoded by *erm*(B) and an efflux system encoded by *mef*(E)/*mel*, an operon of the macrolide efflux genetic assembly (Mega) element. These determinants are present on an expanding group of mobile composite genetic elements.

Through a prospective study of invasive pneumococcal disease (IPD) using established population-based surveillance, the incidence of IPD and macrolide-resistant IPD (MR-IPD) in Atlanta, Georgia from 2003-2013 was studied. The heptavalent pneumococcal conjugate vaccine (PCV-7) introduced in 2000 was previously found to decrease IPD and MR-IPD caused by PCV-7 vaccine serotypes through individual and herd protection. In this work, we demonstrated a continued decline of IPD and MR-IPD caused by PCV-7 serotypes and observed "serotype replacement" by serotypes 7F for IPD and 19A for MR-IPD. The increase in MR-IPD from 2003-2009 was largely due to the clonal expansion of the serotype 19A clonal complex 320 isolates that contained Tn*2010*, a new composite mobile element with both *erm*(B) and *mef*(E)/*mel*. We documented a rapid decline of these isolates following PCV-13 introduction.

By creating isogenic mutants, we assessed the contributions of dual macrolide resistance determinants in Tn*2010* for pneumococcal fitness and macrolide resistance. We found *erm*(B) confers high-level macrolide resistance in Tn*2010*-containing strains, but *mef*(E)/*mel* encoded efflux remains functional. We also identified and assessed high-level macrolide-resistant IPD isolates caused by insertions of Mega, Mega-2.IVa and Mega-2.IVc, associated with the pneumococcal pathogenicity island. Deletion of *mef*(E)/*mel* eliminated macrolide resistance in these isolates. Using *in vitro* competition experiments, we found that, in the presence of erythromycin, high-level macrolide-resistant *S. pneumoniae* (conferred by *erm*(B) or Mega-2.IVa) have a growth fitness advantage. These data indicate the ability of *S. pneumoniae* to generate high-level macrolide resistance by efflux or ribosomal methylation, that either high-level mechanism affords a selective advantage, and that the efflux pump may have additional biological functions.

Macrolide Resistance in *Streptococcus pneumoniae*

By

Max R. Schroeder

B.A., Ohio Wesleyan University, 2009

Advisor: David S. Stephens, M.D.

A dissertation submitted to the Faculty of the
James T. Laney School of Graduate Studies of Emory University
in partial fulfillment of the requirements for the degree of
Doctor of Philosophy
in
Graduate Division of Biological and Biomedical Sciences
Microbiology and Molecular Genetics

2016

ACKNOWLEDGMENTS

Thank you to all of those that have helped me become the scientist I am today. To my advisor Dr. David Stephens, I want to thank you for the years of support and encouragement. You have taught me to develop questions, address experimental setbacks, and look for the biological significance of the data. I am a better scientist today thanks to your example. Thank you also to my committee: Drs. Keith Klugman, Charles Moran, Philip Rather, Timothy Read, William Shafer, and Jorge Vidal. Your advice and direction over the years has helped me stay focused and ultimately complete this work. I would also like to thank Dr. David Weiss for your mentorship and ongoing investment into my graduate career; it is a pleasure to work with you. Thank you Dr. Scott Chancey and Dr. Dorothea Zähner for teaching me about *Streptococcus pneumoniae*. Also, thank you to Dr. Yih-Ling Tzeng for assistance in troubleshooting experiments, analyzing data, preparing presentations and papers, and ongoing support in the completion of this dissertation.

To Dr. Monica Farley and members of the Georgia Emerging Infections Program, past and present, thank you for maintaining the pneumococcal surveillance network and openly collaborating with me; without our collaboration much of my work would not exist. I truly appreciate all of the assistance you have provided. Emily Crispell thank you for helping me learn better ways to manipulate *S. pneumoniae* and for your constant positive outlook toward laboratory work. And Dr. Sarah Satola, you are a mentor in life and science, and I thank you for always listening and providing guidance.

My undergraduate professors and research advisors, Dr. Laura Tuhela-Reuning and Dr. Edward (Jed) Burtt were integral in my initial research training. Laura, your

excitement for microbiology is contagious and I caught it from you. Jed, you are a mentor and one of my best friends. Thank you for all the encouragement and advice over the years.

To my family, thank you for the support throughout my education. Mom and Dad, thank you for the love and encouragement throughout my many years of school. You have taken pride and shared news of all my accomplishments and you listened and provided words of wisdom during my difficulties. I am truly blessed to have parents like you. And Mom, thank you for always making time for my phone calls, even if I have nothing to talk about. Molly thank you for being an amazing sister and my oldest friend. Your enthusiasm for your career and love for others is inspiring. Jack, Kathleen, Jason, and Courtney thank you welcoming me into your family and for the love, support, and prayers throughout this journey. To my Atlanta family, Sandy, Luther, and Amelia I have loved the opportunity to spend so much time with you since moving to Atlanta in 2010. Graduate school certainly would have been unbearable without our many weekends together.

To my lovely wife to whom I dedicate this dissertation, Morgan, I thank you for you love and support. Throughout this journey of graduate school, you have been by my side. Thank you for accompanying me on late night trips to the lab to streak out a strain, providing advice on preparing better presentations, and proofreading almost everything I write. Your optimism is a joy. Thank you for the years of support. Now that this journey is coming to an end, I look forward to our next adventures.

TABLE OF CONTENTS

LIST OF TABLES AND FIGURES

Chapter 2

Chapter 3

Appendix B

Appendix C

Appendix D

Chapter 1: Introduction

I. The Pneumococcus

Streptococcus pneumoniae, the pneumococcus, is an obligate commensal of the human nasopharynx, an opportunistic pathogen and a leading cause of death for children worldwide (1). In 2007, the World Health Organization estimated that up to 1.6 million people died each year due to pneumococcal infections including almost one million children under the age of five (2). In addition to severe invasive disease including bacteremia and meningitis, the pneumococcus causes localized, non-invasive infections such as otitis media and pneumonia. *S. pneumoniae* is identified through growth on blood agar as alpha-hemolytic colonies that are sensitive to optochin, a quinine analogue that was used in the treatment of lobar pneumonia in the early twentieth century. Despite a lack of catalase production, *S. pneumoniae* is aerotolarant. Microscopically, pneumococci are classified as a Gram-positive diplococcic due to their characterized lancet-shaped cell morphology. There are over 90 serotypes of *S. pneumoniae* that are distinguished based on differences in the structure of capsular polysaccharide expressed (3).

A. Discovery

S. pneumoniae was independently co-discovered by George Miller Sternberg from the United States and Louis Pasteur from France (4, 5). In September of 1880, Sternberg identified *Micrococcus lanceolatus*, later named *S. pneumoniae*, by inoculating rabbits with his own saliva (6). In December of the same year, Pasteur also inoculated rabbits with saliva of a boy who died of rabies (7). After the rabbits died, both Sternberg and

Pasteur isolated and cultivated diplococcal bacteria from the blood of the rabbits and in their publications the two microbiologists described the same organism. Although Pasteur is often credited as the discoverer of the pneumococcus (5), Sternberg was the first to photograph the pneumococcus and isolate the organism from several carriers. Subsequent researchers found the pneumococcus to be a common colonizer in the human upper-respiratory tract and a frequent cause of pneumonia (4, 5).

B. Capsular Polysaccharide

When initially describing the microscopic appearance of the pneumococcus in 1881, Pasteur described an aureole that surrounded the diplococci (7) which was later identified as polysaccharide capsule. In 1916 Laura Stryker from the U.S. found pneumococcal virulence to be dependent on the presence of the capsule, as capsule loss was associated with a reduction of virulence (8). In 1900 the German physician Friedrich Neufeld described bile solubility of the pneumococcus as a key microbiological identifying feature (4, 9). A few years later in 1904 Neufeld first published the Quellung reaction (10) which has remained as a gold standard for serotyping of *S. pneumoniae*. In the Quellung reaction bacterial cells are treated with capsule specific antibodies that bind to capsular polysaccharide and cause capsule swelling that may be observed microscopically. Today PCR-based molecular methods are used to complement Quellung reactions (11). Over 90 pneumococcal capsular polysaccharide serotypes have been identified to date (3, 12).

C. Transforming Principle

Groundbreaking experiments that lead to the identification of DNA as the hereditary material in cells were first performed with *S. pneumoniae*. In 1928, Frederick

Griffith published the first observation of bacterial transformation (13). In his experiments, Griffith inoculated mice with bacterial cultures from smooth (encapsulated) or rough (unencapsulated) pneumococcal isolates and found that only mice inoculated with the smooth isolate died. Furthermore, smooth pneumococci were isolated from dead mice and rough pneumococci were isolated from surviving mice. When bacterial cultures were heat-killed prior to inoculation all inoculated mice survived. When Griffith used a combination of live rough bacteria with heat-killed smooth bacteria, the inoculated mice died and live smooth *S. pneumoniae* were isolated from the dead mice. Therefore, the presence of the heat-killed "smooth" pneumococci contributed an unknown factor to the "rough" pneumococci which transformed the organism to a smooth phenotype, and the phenomenon was termed the "transforming principle."

Continuing the work of Griffith, three medical doctors in the United States, Oswald Avery, Colin MacLeod, and Maclyn McCarty determined that the transforming principle was DNA (14, 15). In their experiments the heat-killed smooth bacterial lysate was separated into purified DNA, RNA, proteins, lipids, and carbohydrates, and each fraction was combined with the rough bacteria as an inoculum (15). Through meticulous purification methods they ascertained that purified DNA was capable of transforming rough bacteria *in vivo* into smooth bacteria that resulted in death of the mice. The conclusion was that DNA is the transforming principle from the Griffith experiment and thus DNA is the hereditary material of life.

II. Pathogenesis

A. Non-Invasive Diseases

The pneumococcus is an opportunistic pathogen with high rates of asymptomatic carriage based on age, race, and socioeconomic status. The highest rates of carriage are in young children. Studies have found that up to 75% of children under the age of 5 and 30% of adults living in households with young children are colonized by *S. pneumoniae.* Pneumococcal acquisition and colonization is considered a prerequisite for disease as it provides an opportunity for the bacteria to migrate from the nasopharynx to local or systemic sites of infection (16).

1. Acute Otitis Media

Otitis media is an infection of the middle ear that results in ear pain, fluid accumulation, sometimes drainage from the ear, loss of hearing, and low-grade fever. Interestingly, acute otitis media is the most common reason for pediatric office visits in the U.S. with more than 20 million visits annually coded as otitis media. Although the majority of cases of otitis media are caused by viruses, bacterial otitis media is common and *S. pneumoniae* is the most common cause of bacterial otitis media. Migration of colonizing *S. pneumoniae* from the nasopharynx to the middle ear using the Eustachian tube as the passageway may result in acute otitis media. Otitis media is often a self-limiting infection for which clearance can occur without the need of antibiotic intervention (17). In Europe, ibuprofen is typically prescribed for treatment of otitis media to reduce discomfort due to middle ear inflammation. In the U.S., otitis media is often treated with antibiotics such as amoxicillin, or for patients with a penicillin allergy, macrolides. Added benefits of antibiotic treatment include shortening the duration of

infection and reducing the risk of permanent hearing damage (17, 18). Interestingly, recent studies in mice have found increased pneumococcal colonization and translocation of pneumococci to the middle ear following vaccination with live attenuated influenza virus (19, 20). This suggests vaccination of children with FluMist®, the quadrivalent live attenuated influenza vaccine, might increase the risk of pneumococcal otitis media.

2. Pneumonia

Pneumococcal pneumonia is the most common type of community-acquired pneumonia worldwide (21). In 2015, pneumococcal pneumonia was the cause of an estimated 922,000 deaths of children under five years old representing 15% of deaths of children in this age group (22, 23). The highest rates of pneumococcal pneumonia occur in developing countries, specifically Sub-Saharan Africa. Pneumonia is medical syndrome wherein the alveoli, or microscopic air sacs, become inflamed. While a variety of microorganisms may cause pneumonia, bacteria and viruses are the most common etiologic agents. Pneumococci descend from the nasopharynx to the lower respiratory tract where they may infect the alveoli, often as a secondary infection following the common cold virus or influenza. Symptoms of pneumococcal pneumonia are acute and include cough with green or blood-tinged mucus, chest pain, malaise, nausea and vomiting, diarrhea, and fever. Influenza has a high association with pneumococcal disease, specifically pneumonia (24, 25). During the 1918 influenza pandemic, co-infection with influenza and *S. pneumoniae* may have caused extensive pulmonary thrombosis that contributed to the high mortality of this pandemic (26). Respiratory syncytial virus (RSV) also had a significant association with pneumococcal pneumonia (27).

B. Invasive Pneumococcal Diseases (IPD)

During acute local infection by *S. pneumoniae*, the pneumococcus may reach the bloodstream and disseminate to other sterile sites, such as joints or the meninges.

1. Bacteremia

When pneumococci replicate in the bloodstream, the infection is classified as pneumococcal bacteremia or septicemia. Bacteremia is often associated with fever that may be accompanied by shaking chills, hypotension, gastrointestinal distress, and altered sensory perception. Bloodstream infections are life-threatening and may result in the systemic inflammatory response syndrome. Historically, the pneumococcus was an important cause of endocarditis. Though the molecular mechanisms are still not fully understood (28), there is evidence that colonization of the nasopharynx, by pneumococci especially in young children, may lead directly to bloodstream entry from the nasopharynx to cause occult bacteremia, e.g. bacteremia without a local pneumococcal infection (29, 30). Improved patient outcomes are attributed to antibiotic therapy when treated with macrolides (31) or combination therapy (32).

2. Meningitis

Spread of pneumococci directly from a non-invasive infection (e.g. otitis media) or via bacteremia to the subarachnoid space containing the meninges is termed meningitis. Meningitis is a life-threatening disease of inflammation of the subarachnoid space and meninges, the protective outer membranes that line the brain and spinal cord. Meningeal infection and associated inflammation can lead to cerebral edema and infection of blood vessels that can result in collateral damage to the brain parenchyma, which may lead to coma and death (33). With a variety of agents causing meningitis,

identification of the pathogen is critical in implementing a successful treatment regimen. In pneumococcal meningitis, about half of all surviving patients experience neurological sequelae and approximately 25% of children experience moderate or severe symptoms (34). *S. pneumoniae* has remained the leading cause of bacterial meningitis in the United States, where it is responsible for three times as many cases of bacterial meningitis as the next leading agents (35). Though the mechanisms are still unknown, *S. pneumoniae* is thought to penetrate the blood-brain barrier through a receptor-mediate process (36). Pneumococci present in the blood adhere to the specific receptors that allow the organism to cross the blood brain barrier.

III. Treatment and Prevention

A. Antibiotic Therapy

During the mid-1990s, the emergence and high prevalence of penicillin resistance among *S. pneumoniae* resulted in a shift in the recommended treatment for non-meningitis pneumococcal infections from beta-lactams to macrolides. Macrolides are often used as the first line of treatment against upper respiratory tract infections and community acquired pneumonia. Macrolides are defined by a complex macrocyclic structure with a 14-, 15-, or 16-membered lactone ring substituted with neutral or amino sugar groups. Macrolides inhibit bacterial protein synthesis by binding to the large 50S ribosomal subunit and disrupting protein elongation by causing the dissociation of the peptidyl-tRNA. The introduction of new macrolides and their widespread use beginning in the 1990s resulted in increased macrolide resistant in *S. pneumoniae* (37, 38).

Erythromycin, discovered in 1952, is a 14-membered macrolide produced by *Streptomyces erythraeus* (39). After the discovery of erythromycin and other naturally-produced macrolides, research focused on the creation of synthetic and semisynthetic macrolides (40). Azithromycin and clarithromycin are semisynthetic macrolides approved for use in the United States. Others macrolides are approved in different countries worldwide or are used as a growth supplement in animals. Macrolides bind reversibly to the 23S rRNA at a site near the peptidyl transferase center of the 50S ribosomal subunit. This binding occurs in pre-structured ribosomal assemblies (41). The smaller macrolides (14- and 15-membered) partially block the nascent peptide channel to inhibit the elongating peptide chain while larger macrolides (16-membered) fully block the nascent peptide channel and cause ribosomal disassociation that reversibly inhibits protein synthesis (42). Though distinct in chemical structure, the antibiotics lincosamide and streptogramin have overlapping binding sites with macrolides and similar mechanisms of action.

B. Vaccines

During World War I, as many as one million people participated in various clinical trials of heat-killed whole pneumococcal cell-based vaccines, but the efficacy of these vaccines was not established (4, 43). During World War II the United States military had a successful clinical trial using a tetravalent capsule polysaccharide vaccine, but the success of penicillin for treatment of bacterial infection virtually eliminated commercial interest in pursuing vaccine development (44). It was not until 1977 that the first pneumococcal polysaccharide vaccine, PPSV-14, with capsular polysaccharide antigens from 14 serotypes of *S. pneumoniae* (serotype 1, 2, 3, 4, 6A, 7F, 8, 9N, 12F, 14,

18C, 19F, 23F, and 25), became licensed in the U.S. (45). In 1984, PPSV-14 was replaced by PPSV-23, which contained capsular polysaccharide antigens individually extracted from serotypes 1, 2, 3, 4, 5, 6B, 7F, 8, 9N, 9V, 10A, 11A, 12F, 14, 15B, 17F, 18C, 19A, 19F, 20, 22F, 23F, and 33F, combined to create the final formulation (46). The effectiveness of this vaccine has been challenged but it has continued to be recommended for adults at risk of pneumococcal disease including individuals aged 65 years and older (47, 48).

The pneumococcal conjugate vaccine (PCV-7), containing seven capsular polysaccharides of serotypes 4, 6B, 9V, 14, 18C, 19F, and 23F conjugated to the CRM_{197} diphtheria protein, was licensed in 2000 for use in children under five years old in the United States (49, 50). Following PCV-7 introduction, clonal expansion of non-vaccine strains was observed worldwide (51-53). The emergence of non-PCV-7 serotypes resulted in development of additional PCV formulations. In 2010, an additional six serotypes (1, 3, 5, 6A, 7F, and 19A conjugated to CRM_{197}) were added to the PCV-7 serotypes to create the 13-valent conjugate vaccine (PCV-13), which replaced PCV-7 in the U.S. (50, 54). In addition to direct protection, pneumococcal conjugate vaccines have yielded sustained reductions in pneumococcal carriage of vaccine serotypes (55) and also disease caused by vaccine serotypes in unvaccinated (herd protection) (56, 57). The continued expansion of pneumococcal conjugate vaccination into developing countries is greatly reducing the global burden of pneumococcal disease (50).

IV. Macrolide Resistance

As noted widespread macrolide use is associated with increased macrolide resistance in *S. pneumoniae* (37, 38). Clinical failures of macrolide treatment of pneumococcal infections have been reported for lower respiratory tract infections (58) and bacteremia (59, 60). The widespread use of macrolides provides a selective pressure that has contributed to the expansion of macrolide-resistant *S. pneumoniae* (37, 61). Globally, erythromycin resistance among *S. pneumoniae* is geographically variable but ranges from <10% to >50% of isolates (62).

A. Mechanisms of Macrolide Resistance

Macrolide resistance in *S. pneumoniae* is mediated through three distinct mechanisms: modification of the macrolide ribosomal target site, macrolide efflux, and chromosomal mutations to macrolide binding sites.

1. Ribosomal Modification

Erythromycin ribosomal methylase (*erm*) family genes encode an adenine-specific N-methyltransferases that methylates the 23 rRNA to prevent antibiotic binding (63). When present in *Escherichia coli* the 23S rRNA is methylated at A2058, which is considered to be the target for methylation and macrolide binding (64). The ribosomal methylase found in *S. pneumoniae* is encoded by the *erm*(B) gene whose gene product dimethylates this target site of the 23S rRNA (65). Ribosomal methylation by Erm(B) confers resistance to macrolides, lincosamide, and streptogramin B, which is characterized as the MLS_B phenotype (63). In addition to the expanded spectrum of resistance, *erm*(B) provides high-level resistance to macrolides (erythromycin MICs ≥256 μg/ml).

The induction of *erm*(B) allows high-level translation of Erm(B) in the presence of inducers such as erythromycin (66). In the pneumococcus, *erm*(B) expression may be inducible or constitutively expressed to high levels. As expression of *erm* genes is frequently repressed in the absence of inducing drugs through a mechanism of translational attenuation, *erm*(B) expression has been proposed to have a bacterial fitness cost (67-69). A recent study found that a *Staphylococcus aureus* strain expressing *erm*(C) was outcompeted by *S. aureus* expressing catalytically-inactive *erm*(C) (68), supporting the need for tight regulation of expression. Interestingly, deletion of the leader sequence of *erm*(B) in *S. pneumoniae* was found to confer resistance to telithromycin, the first-generation ketolide which is a semi-synthetic macrolide antibiotic, by allowing constitutive expression (70).

2. Macrolide Efflux

Macrolide efflux in *S. pneumoniae* is the most common cause of macrolide resistance in North America (62, 71). Pneumococcal macrolide efflux is encoded by the *mef*(E)/*mel* operon and occurs through an poorly understood mechanism of macrolide binding and membrane targeting for efflux (72). Macrolide resistance in *S. pneumoniae* requires both *mef*(E) and *mel* (73, 74). These genes are carried on the macrolide efflux genetic assembly (Mega) element and are expressed from a single promoter inducible by 14- and 15-membered macrolides (e.g. erythromycin and azithromycin) (74-76). Expression of *mef*(E) and *mel* is tightly controlled through transcriptional attenuation (75).

The first gene, *mef*(E) shares 90% sequence identity with *mef*(A) from *Streptococcus pyogenes* (77, 78). In *S. pneumoniae*, *mef*(E) encodes a 405 amino acid

protein that belongs to the major facilitator superfamily, which utilizes proton motive force-driven efflux to expel molecules from cells (77). The second gene, *mel* (also *msr*(D)) is a homolog of the *S. aureus* gene *mrsA* (78), which encodes an ATP-binding cassette (ABC) transporter protein but lacks typical hydrophobic, membrane-binding domains and is thought to interact with chromosomally encoded transmembrane complexes (74). Mef(E) and Mel have been shown to operate as a dual efflux pump in *S. pneumoniae* (74). A recent study in *Escherichia coli* suggests a physical interaction between Mef(E) and Mel and that Mel may bind macrolides and localize to the membrane (79).

S. pneumoniae with *mef*(E)/*mel* have been shown to have an M phenotype, which is resistance to 14- and 15-membered macrolides (e.g. erythromycin and azithromycin) while retaining susceptibility to lincosamides and streptogramin B (77). While most *mef*(E)/*mel*-containing strains are resistant to low levels (1-8 µg/ml) of erythromycin, strains with increased expression of *mef*(E)/*mel* have increased levels of macrolide resistance (80). Induction of *mef*(E)/*mel* by macrolides causes increased expression and thus increased levels of macrolide resistance (to ≥16 µg/ml) (66, 74). In addition to macrolides, the presence of *mef*(E)/*mel* has been shown to increase resistance to the human antimicrobial peptide LL-37, which was also found to induce expression of the efflux pump (81). This suggests the macrolide efflux pump may be expressed during nasopharyngeal colonization and prime *mef*(E)/*mel*-containing pneumococci for exposure to macrolide antibiotics.

3. Ribosomal Mutations

Point mutations in 23S rRNA at or near the macrolide binding residue A2058 (*E. coli* ribosome) have resulted in macrolide resistance (82, 83). Mutations of ribosomal proteins L4 and L22 confer macrolide resistance in pathogenic and nonpathogenic bacteria including pneumococci. L4 and L22 are ribosomal proteins with domains on the surface of the ribosome as well as tentacles that extend into the exit tunnel in proximity to the macrolide-binding site (84). In *E. coli*, a Lys-63-Glu change in the L4 protein (*rplD*) as well as a triple amino acid deletion of Met-82, Lys-83, and Glu-84 from L22 (*rplV*) confer resistance to macrolides (85, 86). A variety of additional L4 and L22 mutations have also been found to confer macrolide resistance (87, 88). While the overall incidence is rare, some L4 and L22 mutations have resulted in macrolide resistance in *S. pneumoniae* (82).

4. Dual Macrolide Resistance Genotype

S. pneumoniae containing both *erm*(B) and *mef*(E)/*mel* were first reported in the late-1990s (89, 90) and are now found worldwide (62). The dual macrolide resistance genotype occurred in 12% of global isolates collected from 2003-2004, which is twice the frequency reported from 1999-2000 (62). In 2004, 18.4% of *S. pneumoniae* isolates from the United States were found to have the dual *erm*(B) and *mef*(E)/*mel* genotype (71); and in a study published this year, up to 52% of macrolide-resistant isolates from Arizona were found to contain both macrolide resistance genes (91). Tn*2010* has been identified as the composite mobile element that contains *erm*(B) and *mef*(E)/*mel* (Mega) (92). Tn*2010* was first identified in *S. pneumoniae* serotype 19. Following introduction of the 7-valent pneumococcal conjugate vaccine (PCV-7) the “replacement” serotype 19A

(ST320) with Tn*2010* emerged (93). ST320 is a multidrug resistant strain that appears to represent a "capsule switch" from serotype 19F and is responsible for global pandemic in the wake of PCV-7 introduction (53, 94). This emergence of *S. pneumoniae* with dual macrolide resistance determinants is intriguing. The high-level and broader resistance conferred by *erm*(B) would predict that *mef*(E)/*mel* is functionally redundant in *erm*(B)-containing *S. pneumoniae*.

B. Dissemination of Resistance Determinants

1. Macrolide Resistance Chromosomal Locations

The *mef*(E)/*mel*-containing genetic element Mega is found in six distinct chromosomal sites within the pneumococcal genome (76, 95, 96). Mega insertion sites are distributed around the chromosome: (I) a phosphomethylpyrimidine kinase (TIGR4 SP_1598), (II) a DNA-3-methyladenine glycosylase (SP_0180), (III) a capsule biosynthesis gene (SP_0103), (IV) the RNA methyltransferase *rumA* (SP_1029) (76), (V) *orf6* of Tn*916*-like elements (95), and (VI) a novel insertion into a *S. suis* homolog element found in *S. pneumoniae* (96). Due to genetic variations at insertion site IV, this class is subdivided: (IVa) Mega and IS*Smi* element insertion along with deletion of the 30.7 kb pneumococcal pathogenicity island-1 (PPI-1), and (IVb) simple insertion of Mega into *rumA* with intact PPI-1, and (IVc) same as IVa with a *S. equi* subspecies *zooepidmicus*-related ICE (42 kb) inserted upstream of Mega (96). The Mega element is horizontally transferred through transformation and homologous recombination between pneumococci but the element per se lacks genes required for transposition (76). Analysis of the insertion sites revealed a putative target sequence of 5'-TTTCCNCAA-3' about six base pairs upstream of the insertion and Tn*916*-like coupling sequences (96). The genes

required for Mega transposition may be present on other conjugative elements of the pneumococcal genome and in non-*S. pneumoniae* commensal organisms (76, 96). However, Mega is infrequently transferred through transposition but once stabilized can be widely disseminated through horizontal DNA exchange and homologous recombination.

Tn*916* is the prototype conjugative transposon that contains the tetracycline resistance gene *tet*(M), and is found in many Gram-positive bacteria. Tn*916* may incorporate additional antibiotic resistance determinants which comprise larger Tn*916*-like composite elements (97). The history and molecular mechanisms of the Tn*916* family are beyond the scope of this review, but have been explored previously (98). The most common Tn*916*-like elements in *S. pneumoniae* containing erythromycin resistance cassettes include Tn*2009*, Tn*6002*, and Tn*2010* (96). Tn*2009* is a Tn*916*-like element with Mega inserted into orf6 of Tn*916* to provide macrolide resistance, the M phenotype (99). Tn6002 is also a Tn*916*-like element with macrolide resistance, MLS_B phenotype, due to the incorporation of an *erm*(B)-containing element into *orf20* of Tn*916* (100). The *erm*(B) gene may also be incorporated into Tn*916*. A Tn*917*, an *erm*(B)-containing transposon, insertion into *orf9* of Tn*916* creates Tn*3872* (100). *S. pneumoniae* with the dual macrolide resistance genotype contain Tn*2010* or the less common and newly described Tn*2017* (101). Tn*2010* is a Tn*916*-like element that with Mega in *orf6* and the *erm*(B) element in *orf20* of Tn*916* (102). Tn*2010* likely arose through the homologous recombination of Tn*2009* with Tn*6002*. A similar recombination event likely occurred with Tn*2009* and Tn*3872* to create Tn*2017*, which was found to be a Tn*916*-like element with a Mega insertion in *orf6* and Tn*917* in *orf9* of Tn*916* (101).

2. Interspecies Exchange of Macrolide Resistance

S. pneumoniae is naturally transformable. During its growth cycle, pneumococci develop a natural state of competence and acquire DNA from their environment. A mechanism of DNA repair allows for integration of new DNA through homologous recombination (103, 104). The human nasopharynx is the primary ecological niche for the pneumococcus during asymptomatic carriage that is a prerequisite for pneumococcal infections (16). In the nasopharynx, *S. pneumoniae* have the opportunity to acquire DNA from a wide diversity of commensal bacteria of the upper respiratory tract which may act as a reservoir for antibiotic resistance.

Bacteria other than *S. pneumoniae* that reside in the human upper respiratory tract also carry the macrolide resistance genes *erm*(B) and *mef*(E)/*mel* as Mega. Tn*6002* is the most common *erm*(B)-containing mobile genetic element of *S. pyogenes* (100). A recent study found Mega, Tn*2009*, Tn*6002*, and Tn*2010* in commensal viridans group streptococci isolated from the throats of patients with pharyngitis (105). In this study, *S. mitis* was the most commonly isolated streptococci and isolates were found with the macrolide resistance elements including Mega, Tn*2009*, Tn*6002*, and Tn*2010* (105). Various Gram-positive bacteria have been shown to carry *erm*(B) and/or *mef*(E) (106-108). The Tn*2009* element has also been found in the commensal, Gram-negative *Acinetobacter junii*, and the authors found evidence of this Mega-containing transposon in additional Gram-negative species including *E. coli*, *Enterobacter cloacae*, *Klebsiella* sp., *Proteus* sp., and *Pseudomonas* sp. (109). Interspecies dissemination of mobile genetic elements containing antibiotic resistance cassettes appears common.

Asymptomatic pneumococcal carriage occurs in children and adults with rates in children ranging from less than 15% to greater than 90% in developing countries and varies based on other factors include geography and socioeconomic class (16, 110). During nasopharyngeal carriage *S. pneumoniae* forms complex biofilm structures and enhance natural transformation (111). Genetic exchange during co-colonization by two pneumococcal strains is extremely efficient with transformation efficiencies of up to 10^{-2} (112). Therefore, nasopharyngeal carriage provides an opportunity for *S. pneumoniae* to acquire mobile genetic elements and macrolide resistance genes from co-colonizing pneumococci and commensal organisms. This environment may also have allowed for the assembly and selection of the dual macrolide resistance elements, Tn*2017* and the more common Tn*2010*.

V. Specific Aims

S. pneumoniae is an important obligate human pathogen with efficient mechanisms of horizontal genetic exchange. Two major selection pressures, new vaccines that impact pneumococcal biology and widespread antibiotic use have led to the emergence of adapted pneumococcal strains. In this dissertation, we focused on the emergence of macrolide resistance in pneumococci, the impact of new conjugate pneumococcal vaccines on macrolide resistance, the evolution of the genetic basis for macrolide resistance in pneumococci and the effects of macrolide resistance on pneumococcal fitness. We were fortunate to have used an established population-based surveillance program for this work. Invasive pneumococcal disease (IPD) has been assessed in Atlanta, Georgia since 1994 using prospective surveillance by the Georgia Emerging Infections Program as a part of the Centers for Disease Control and Prevention

(CDC) national Active Bacterial Core surveillance network (113-117). The initial impact of PCV-7 introduction on the incidence of IPD and the incidence of IPD caused by macrolide-resistant *S. pneumoniae* has been previously reported (115). The specific aims for this dissertation were:

1) To determine the molecular basis of macrolide resistance in invasive pneumococcal disease isolates from the Atlanta metropolitan area, during the PCV-7 era and after the introduction of PCV-13.
2) To determine the genetic basis responsible for and the biological advantage of efflux-mediated high-level macrolide resistance in *S. pneumoniae* and the emergence of *S. pneumoniae* with dual macrolide resistance determinants, *mef*(E)/*mel* and *erm*(B).

REFERENCES

1. **O'Brien KL, Wolfson LJ, Watt JP, Henkle E, Deloria-Knoll M, McCall N, Lee E, Mulholland K, Levine OS, Cherian T, Hib, Pneumococcal Global Burden of Disease Study T.** 2009. Burden of disease caused by *Streptococcus pneumoniae* in children younger than 5 years: global estimates. Lancet **374:**893-902.

2. **WHO.** 2007. Pneumococcal conjugate vaccine for childhood immunization—WHO position paper. Wkly Epidemiol Rec **82:**93-104.

3. **Geno KA, Gilbert GL, Song JY, Skovsted IC, Klugman KP, Jones C, Konradsen HB, Nahm MH.** 2015. Pneumococcal Capsules and Their Types: Past, Present, and Future. Clin Microbiol Rev **28:**871-899.

4. **Austrian R.** 2004. Forward, p xv-xxvii. *In* Tuomanen EI, Mitchell TJ, Morrison DA, Spratt BG (ed), The Pneumococcus. ASM Press, Washington, DC.

5. **Watson DA, Musher DM, Jacobson JW, Verhoef J.** 1993. A brief history of the pneumococcus in biomedical research: a panoply of scientific discovery. Clin Infect Dis **17:**913-924.

6. **Sternberg G.** 1881. A fatal form of septicemia in the rabbit, produced by the subcutaneous injection of human saliva. Reports of the National Board of Health **3:**87-92.

7. **Pasteur L.** 1881. Note sur la maladie mouvelle provoquee par la salive d'un enfant mort de la rage. Bulletin de l'Academie de Medicine (Paris) **10:**94-103.

8. **Stryker LM.** 1916. Variations in the Pneumococcus induced by growth in immune serum. J Exp Med **24:**49-68.

9. **Neufeld F.** 1900. Ueber ein specifische bacteriolytische Wirkung der Galle. Z Hyg Infektionskr **34:**454-464.

10. **Neufeld F.** 1902. Ueber die Agglutination der Pneumokokken and über die Theorieen der Agglutination. Z Hyg Infektionskr **40:**54-72.

11. **Jauneikaite E, Tocheva AS, Jefferies JM, Gladstone RA, Faust SN, Christodoulides M, Hibberd ML, Clarke SC.** 2015. Current methods for capsular typing of Streptococcus pneumoniae. J Microbiol Methods **113:**41-49.

12. **Satzke C, Dunne EM, Porter BD, Klugman KP, Mulholland EK.** 2015. The PneuCarriage Project: A Multi-Centre Comparative Study to Identify the Best Serotyping Methods for Examining Pneumococcal Carriage in Vaccine Evaluation Studies. PLoS Med **12:**e1001903; discussion e1001903.

13. **Griffith F.** 1928. The Significance of Pneumococcal Types. J Hyg (Lond) **27:**113-159.

14. **Avery OT, Macleod CM, McCarty M.** 1944. Studies on the chemical nature of the substance inducing transformation of pneumococcal types: induction of transformation by a desoxyribonucleic acid fraction isolated from pneumococcus type III. J Exp Med **79:**137-158.

15. **McCarty M.** 1985. The Transforming Principle: Discovering that Genes are Made of DNA. W. W. Norton & Company, Inc, New York, N.Y.

16. **Simell B, Auranen K, Kayhty H, Goldblatt D, Dagan R, O'Brien KL.** 2012. The fundamental link between pneumococcal carriage and disease. Expert Rev Vaccines **11:**841-855.

17. **Ramakrishnan K, Sparks RA, Berryhill WE.** 2007. Diagnosis and treatment of otitis media. Am Fam Physician **76:**1650-1658.

18. **Mattos JL, Colman KL, Casselbrant ML, Chi DH.** 2014. Intratemporal and intracranial complications of acute otitis media in a pediatric population. Int J Pediatr Otorhinolaryngol **78:**2161-2164.

19. **Mina MJ, Klugman KP, Rosch JW, McCullers JA.** 2015. Live attenuated influenza virus increases pneumococcal translocation and persistence within the middle ear. J Infect Dis **212:**195-201.

20. **Mina MJ, McCullers JA, Klugman KP.** 2014. Live attenuated influenza vaccine enhances colonization of *Streptococcus pneumoniae* and *Staphylococcus aureus* in mice. MBio **5**.

21. **Howard LS, Sillis M, Pasteur MC, Kamath AV, Harrison BD.** 2005. Microbiological profile of community-acquired pneumonia in adults over the last 20 years. J Infect **50:**107-113.

22. **Wang SA, Mantel CF, GacicDobo M, Dumolard L, Cherian T, Flannery B, Loo JD, Verani JR, Whitney CG.** 2013. Progress in introduction of pneumococcal conjugate vaccine - worldwide, 2000–2012 Morbidity and Mortality Weekly Report **62:**308-311.

23. **WHO.** 2015. Pneumonia: Fact Sheet.

24. **Short KR, Habets MN, Hermans PW, Diavatopoulos DA.** 2012. Interactions between *Streptococcus pneumoniae* and influenza virus: a mutually beneficial relationship? Future Microbiol **7:**609-624.

25. **Mina MJ, Klugman KP.** 2014. The role of influenza in the severity and transmission of respiratory bacterial disease. Lancet Respir Med **2:**750-763.

26. **Walters KA, D'Agnillo F, Sheng ZM, Kindrachuk J, Schwartzman LM, Kuestner RE, Chertow DS, Golding BT, Taubenberger JK, Kash JC.** 2016. 1918 pandemic influenza virus and *Streptococcus pneumoniae* co-infection results in activation of coagulation and widespread pulmonary thrombosis in mice and humans. J Pathol **238:**85-97.

27. **Zhou H, Haber M, Ray S, Farley MM, Panozzo CA, Klugman KP.** 2012. Invasive pneumococcal pneumonia and respiratory virus co-infections. Emerg Infect Dis **18:**294-297.

28. **Mahdi LK, Van der Hoek MB, Ebrahimie E, Paton JC, Ogunniyi AD.** 2015. Characterization of Pneumococcal Genes Involved in Bloodstream Invasion in a Mouse Model. PLoS One **10:**e0141816.

29. **Kuppermann N.** 1999. Occult bacteremia in young febrile children. Pediatr Clin North Am **46:**1073-1109.

30. **Weiser JN.** 2010. The pneumococcus: why a commensal misbehaves. J Mol Med (Berl) **88:**97-102.

31. **Metersky ML, Ma A, Houck PM, Bratzler DW.** 2007. Antibiotics for bacteremic pneumonia: Improved outcomes with macrolides but not fluoroquinolones. Chest **131:**466-473.

32. **Baddour LM, Yu VL, Klugman KP, Feldman C, Ortqvist A, Rello J, Morris AJ, Luna CM, Snydman DR, Ko WC, Chedid MB, Hui DS, Andremont A, Chiou CC.** 2004. Combination antibiotic therapy lowers mortality among

severely ill patients with pneumococcal bacteremia. Am J Respir Crit Care Med **170:**440-444.

33. **Panackal AA, Williamson KC, van de Beek D, Boulware DR, Williamson PR.** 2016. Fighting the Monster: Applying the Host Damage Framework to Human Central Nervous System Infections. MBio **7**.

34. **Chandran A, Herbert H, Misurski D, Santosham M.** 2011. Long-term sequelae of childhood bacterial meningitis: an underappreciated problem. Pediatr Infect Dis J **30:**3-6.

35. **Castelblanco RL, Lee M, Hasbun R.** 2014. Epidemiology of bacterial meningitis in the USA from 1997 to 2010: a population-based observational study. Lancet Infect Dis **14:**813-819.

36. **Iovino F, Seinen J, Henriques-Normark B, van Dijl JM.** 2016. How Does Streptococcus pneumoniae Invade the Brain? Trends Microbiol doi:10.1016/j.tim.2015.12.012.

37. **Bergman M, Huikko S, Huovinen P, Paakkari P, Seppala H.** 2006. Macrolide and azithromycin use are linked to increased macrolide resistance in *Streptococcus pneumoniae*. Antimicrob Agents Chemother **50:**3646-3650.

38. **Malhotra-Kumar S, Lammens C, Coenen S, Van Herck K, Goossens H.** 2007. Effect of azithromycin and clarithromycin therapy on pharyngeal carriage of macrolide-resistant streptococci in healthy volunteers: a randomised, double-blind, placebo-controlled study. Lancet **369:**482-490.

39. **McGuire JM, Bunch RL, Anderson RC, Boaz HE, Flynn EH, Powell HM.** 1952. 'Ilotycin,' a new antibiotic. Antibiotics and Chemotherapy **2:**281-283.

40. **Mazzei T, Mini E, Novelli A, Periti P.** 1993. Chemistry and mode of action of macrolides. J Antimicrob Chemother **31 Suppl C:**1-9.

41. **Pokkunuri I, Champney WS.** 2007. Characteristics of a 50S ribosomal subunit precursor particle as a substrate for *erm*E methyltransferase activity and erythromycin binding in *Staphylococcus aureus*. RNA Biol **4:**147-153.

42. **Weisblum B.** 1995. Insights into erythromycin action from studies of its activity as inducer of resistance. Antimicrob Agents Chemother **39:**797-805.

43. **Heffron R.** 1939. Pneumonia with special reference to pneumococcus lobar pneumonia. The Commonwealth Fund, New York, N.Y.

44. **Austrian R.** 2000. Pneumococcal otitis media and pneumococcal vaccines, a historical perspective. Vaccine **19 Suppl 1:**S71-77.

45. **Broome CV, Facklam RR.** 1981. Epidemiology of clinically significant isolates of Streptococcus pneumoniae in the United States. Rev Infect Dis **3:**277-281.

46. **CDC.** 1984. Update: Pneumococcal Polysaccharide Vaccine Usage-United States. Recommendations of the Immunization Practices Advisory Committee. Annals of Internal Medicine **101:**348-350.

47. **CDC.** 1997. Prevention of pneumococcal disease: recommendations of the Advisory Committee on Immunization Practices (ACIP). MMWR Recomm Rep **46:**1-24.

48. **Kobayashi M, Bennett NM, Gierke R, Almendares O, Moore MR, Whitney CG, Pilishvili T.** 2015. Intervals Between PCV13 and PPSV23 Vaccines: Recommendations of the Advisory Committee on Immunization Practices (ACIP). MMWR Morb Mortal Wkly Rep **64:**944-947.

49. **Advisory Committee on Immunization Practices.** 2000. Preventing pneumococcal disease among infants and young children. Recommendations of the Advisory Committee on Immunization Practices (ACIP). MMWR Recomm Rep **49:**1-35.

50. **Rodgers GL, Klugman KP.** 2011. The future of pneumococcal disease prevention. Vaccine **29S:**C43-C48.

51. **Beall B, McEllistrem MC, Gertz RE, Jr., Wedel S, Boxrud DJ, Gonzalez AL, Medina MJ, Pai R, Thompson TA, Harrison LH, McGee L, Whitney CG.** 2006. Pre- and postvaccination clonal compositions of invasive pneumococcal serotypes for isolates collected in the United States in 1999, 2001, and 2002. J Clin Microbiol **44:**999-1017.

52. **Mahjoub-Messai F, Doit C, Koeck JL, Billard T, Evrard B, Bidet P, Hubans C, Raymond J, Levy C, Cohen R, Bingen E.** 2009. Population snapshot of *Streptococcus pneumoniae* serotype 19A isolates before and after introduction of seven-valent pneumococcal vaccination for French children. J Clin Microbiol **47:**837-840.

53. **Li Y, Tomita H, Lv Y, Liu J, Xue F, Zheng B, Ike Y.** 2011. Molecular characterization of *erm*(B)- and *mef*(E)-mediated erythromycin-resistant *Streptococcus pneumoniae* in China and complete DNA sequence of Tn*2010*. J Appl Microbiol **110:**254-265.

54. **CDC.** 2010. Licensure of a 13-valent pneumococcal conjugate vaccine (PCV13) and recommendations for use among children - Advisory Committee on

Immunization Practices (ACIP), 2010. MMWR Morb Mortal Wkly Rep **59:**258-261.

55. **Desai AP, Sharma D, Crispell EK, Baughman W, Thomas S, Tunali A, Sherwood L, Zmitrovich A, Jerris R, Satola SW, Beall B, Moore MR, Jain S, Farley MM.** 2015. Decline in pneumococcal nasopharyngeal carriage of vaccine serotypes after the introduction of the 13-valent pneumococcal conjugate vaccine in children in Atlanta, Georgia. Pediatr Infect Dis J **34:**1168-1174.

56. **Pilishvili T, Lexau C, Farley MM, Hadler J, Harrison LH, Bennett NM, Reingold A, Thomas A, Schaffner W, Craig AS, Smith PJ, Beall BW, Whitney CG, Moore MR.** 2010. Sustained reductions in invasive pneumococcal disease in the era of conjugate vaccine. J Infect Dis **201:**32-41.

57. **Moore MR, Link-Gelles R, Schaffner W, Lynfield R, Lexau C, Bennett NM, Petit S, Zansky SM, Harrison LH, Reingold A, Miller L, Scherzinger K, Thomas A, Farley MM, Zell ER, Taylor TH, Jr., Pondo T, Rodgers L, McGee L, Beall B, Jorgensen JH, Whitney CG.** 2015. Effect of use of 13-valent pneumococcal conjugate vaccine in children on invasive pneumococcal disease in children and adults in the USA: analysis of multisite, population-based surveillance. Lancet Infect Dis **15:**301-309.

58. **Klugman KP.** 2002. Bacteriological evidence of antibiotic failure in pneumococcal lower respiratory tract infections. Eur Respir J Suppl **36:**3s-8s.

59. **Lonks JR, Garau J, Gomez L, Xercavins M, Ochoa de Echaguen A, Gareen IF, Reiss PT, Medeiros AA.** 2002. Failure of macrolide antibiotic treatment in

patients with bacteremia due to erythromycin-resistant *Streptococcus pneumoniae*. Clin Infect Dis **35:**556-564.

60. **Schentag JJ, Klugman KP, Yu VL, Adelman MH, Wilton GJ, Chiou CC, Patel M, Lavin B, Paladino JA.** 2007. *Streptococcus pneumoniae* bacteraemia: pharmacodynamic correlations with outcome and macrolide resistance--a controlled study. Int J Antimicrob Agents **30:**264-269.

61. **Keenan JD, Klugman KP, McGee L, Vidal JE, Chochua S, Hawkins P, Cevallos V, Gebre T, Tadesse Z, Emerson PM, Jorgensen JH, Gaynor BD, Lietman TM.** 2015. Evidence for clonal expansion after antibiotic selection pressure: pneumococcal multilocus sequence types before and after mass azithromycin treatments. J Infect Dis **211:**988-994.

62. **Farrell DJ, Couturier C, Hryniewicz W.** 2008. Distribution and antibacterial susceptibility of macrolide resistance genotypes in *Streptococcus pneumoniae*: PROTEKT Year 5 (2003-2004). International Journal of Antimicrobial Agents **31:**245-249.

63. **Weisblum B.** 1995. Erythromycin resistance by ribosome modification. Antimicrob Agents Chemother **39:**577-585.

64. **Skinner R, Cundliffe E, Schmidt FJ.** 1983. Site of action of a ribosomal RNA methylase responsible for resistance to erythromycin and other antibiotics. J Biol Chem **258:**12702-12706.

65. **Johnston NJ, De Azavedo JC, Kellner JD, Low DE.** 1998. Prevalence and characterization of the mechanisms of macrolide, lincosamide, and streptogramin

resistance in isolates of Streptococcus pneumoniae. Antimicrob Agents Chemother **42:**2425-2426.

66. **Chancey ST, Zhou X, Zähner D, Stephens DS.** 2011. Induction of efflux-mediated macrolide resistance in *Streptococcus pneumoniae*. Antimicrob Agents Chemother **55:**3413-3422.

67. **Chancey ST, Zähner D, Stephens DS.** 2012. Acquired inducible antimicrobial resistance in Gram-positive bacteria. Future Microbiology **7:**1-20.

68. **Gupta P, Sothiselvam S, Vazquez-Laslop N, Mankin A.** 2011. Why are *erm* genes inducible? 51st Interscience Conference on Antimicrobial Agents and Chemotherapy**:**abstr C1-1783.

69. **Min YH, Kwon AR, Yoon EJ, Shim MJ, Choi EC.** 2008. Translational attenuation and mRNA stabilization as mechanisms of *erm*(B) induction by erythromycin. Antimicrob Agents Chemother **52:**1782-1789.

70. **Wolter N, Smith AM, Farrell DJ, Northwood JB, Douthwaite S, Klugman KP.** 2008. Telithromycin resistance in *Streptococcus pneumoniae* is conferred by a deletion in the leader sequence of *erm*(B) that increases rRNA methylation. Antimicrob Agents Chemother **52:**435-440.

71. **Jenkins SG, Brown SD, Farrell DJ.** 2008. Trends in antibacterial resistance among *Streptococcus pneumoniae* isolated in the USA: update from PROTEKT US Years 1-4, p 1, Ann Clin Microbiol Antimicrob, vol 7, England.

72. **Chancey ST, Zähner D, Stephens DS.** 2012. Acquired inducible antimicrobial resistance in Gram-positive bacteria. Future Microbiology **7:**959-978.

73. **Ambrose KD, Nisbet R, Stephens DS.** 2005. Macrolide efflux in *Streptococcus pneumoniae* is mediated by a dual efflux pump (*mel* and *mef*) and is erythromycin inducible. Antimicrobial Agents and Chemotherapy **49:**4203-4209.

74. **Ambrose KD, Nisbet R, Stephens DS.** 2005. Macrolide efflux in *Streptococcus pneumoniae* is mediated by a dual efflux pump (*mel* and *mef*) and is erythromycin inducible. Antimicrob Agents Chemother **49:**4203-4209.

75. **Chancey ST, Bai X, Kumar N, Drabek EF, Daugherty SC, Colon T, Ott S, Sengamalay N, Sadzewicz L, Tallon LJ, Fraser CM, Tettelin H, Stephens DS.** 2015. Transcriptional attenuation controls macrolide inducible efflux and resistance in *Streptococcus pneumoniae* and in other Gram-positive bacteria containing *mef*/*mel*(*msr*(D)) elements. PLoS One **10:**e0116254.

76. **Gay K, Stephens DS.** 2001. Structure and dissemination of a chromosomal insertion element encoding macrolide efflux in *Streptococcus pneumoniae*. J Infect Dis **184:**56-65.

77. **Tait-Kamradt A, Clancy J, Cronan M, Dib-Hajj F, Wondrack L, Yuan W, Sutcliffe J.** 1997. *mefE* is necessary for the erythromycin-resistant M phenotype in *Streptococcus pneumoniae*. Antimicrob Agents Chemother **41:**2251-2255.

78. **Roberts MC, Sutcliffe J, Courvalin P, Jensen LB, Rood J, Seppala H.** 1999. Nomenclature for macrolide and macrolide-lincosamide-streptogramin B resistance determinants. Antimicrob Agents Chemother **43:**2823-2830.

79. **Nunez-Samudio V, Chesneau O.** 2013. Functional interplay between the ATP binding cassette Msr(D) protein and the membrane facilitator superfamily Mef(E)

transporter for macrolide resistance in *Escherichia coli*. Res Microbiol **164:**226-235.

80. **Wierzbowski AK, Boyd D, Mulvey M, Hoban DJ, Zhanel GG.** 2005. Expression of the *mef*(E) gene encoding the macrolide efflux pump protein increases in *Streptococcus pneumoniae* with increasing resistance to macrolides. Antimicrob Agents Chemother **49:**4635-4640.

81. **Zähner D, Zhou X, Chancey ST, Pohl J, Shafer WM, Stephens DS.** 2010. Human antimicrobial peptide LL-37 induces MefE/Mel-mediated macrolide resistance in *Streptococcus pneumoniae*. Antimicrob Agents Chemother **54:**3516-3519.

82. **Franceschi F, Kanyo Z, Sherer EC, Sutcliffe J.** 2004. Macrolide resistance from the ribosome perspective. Curr Drug Targets Infect Disord **4:**177-191.

83. **Vester B, Douthwaite S.** 2001. Macrolide resistance conferred by base substitutions in 23S rRNA. Antimicrob Agents Chemother **45:**1-12.

84. **Schuwirth BS, Borovinskaya MA, Hau CW, Zhang W, Vila-Sanjurjo A, Holton JM, Cate JH.** 2005. Structures of the bacterial ribosome at 3.5 A resolution. Science **310:**827-834.

85. **Chittum HS, Champney WS.** 1994. Ribosomal protein gene sequence changes in erythromycin-resistant mutants of *Escherichia coli*. J Bacteriol **176:**6192-6198.

86. **Wittmann HG, Stoffler G, Apirion D, Rosen L, Tanaka K, Tamaki M, Takata R, Dekio S, Otaka E.** 1973. Biochemical and genetic studies on two different types of erythromycin resistant mutants of *Escherichia coli* with altered ribosomal proteins. Mol Gen Genet **127:**175-189.

87. **Zaman S, Fitzpatrick M, Lindahl L, Zengel J.** 2007. Novel mutations in ribosomal proteins L4 and L22 that confer erythromycin resistance in *Escherichia coli*. Mol Microbiol **66:**1039-1050.

88. **Diner EJ, Hayes CS.** 2009. Recombineering reveals a diverse collection of ribosomal proteins L4 and L22 that confer resistance to macrolide antibiotics. J Mol Biol **386:**300-315.

89. **Corso A, Severina EP, Petruk VF, Mauriz YR, Tomasz A.** 1998. Molecular characterization of penicillin-resistant *Streptococcus pneumoniae* isolates causing respiratory disease in the United States. Microbial Drug Resistance **4:**325-337.

90. **Nishijima T, Saito Y, Aoki A, Toriya M, Toyonaga Y, Fujii R.** 1999. Distribution of *mefE* and *ermB* genes in macrolide-resistant strains of *Streptococcus pneumoniae* and their variable susceptibility to various antibiotics. Journal of Antimicrobial Chemotherapy **43:**637-643.

91. **Bowers JR, Driebe EM, Nibecker JL, Wojack BR, Sarovich DS, Wong AH, Brzoska PM, Hubert N, Knadler A, Watson LM, Wagner DM, Furtado MR, Saubolle M, Engelthaler DM, Keim PS.** 2012. Dominance of multidrug resistant CC271 clones in macrolide-resistant *streptococcus pneumoniae* in Arizona. BMC Microbiology **12:**12.

92. **Del Grosso M, Camilli R, Iannelli F, Pozzi G, Pantosti A.** 2006. The *mef*(E)-carrying genetic element (mega) of *Streptococcus pneumoniae*: insertion sites and association with other genetic elements. Antimicrobial Agents and Chemotherapy **50:**3361-3366.

93. **Del Grosso M, Northwood JG, Farrell DJ, Pantosti A.** 2007. The macrolide resistance genes *erm*(B) and *mef*(E) are carried by Tn2010 in dual-gene *Streptococcus pneumoniae* isolates belonging to clonal complex CC271. Antimicrobial Agents and Chemotherapy **51:**4184-4186.

94. **Moore MR, Gertz RE, Jr., Woodbury RL, Barkocy-Gallagher GA, Schaffner W, Lexau C, Gershman K, Reingold A, Farley M, Harrison LH, Hadler JL, Bennett NM, Thomas AR, McGee L, Pilishvili T, Brueggemann AB, Whitney CG, Jorgensen JH, Beall B.** 2008. Population snapshot of emergent *Streptococcus pneumoniae* serotype 19A in the United States, 2005. J Infect Dis **197:**1016-1027.

95. **Del Grosso M, Camilli R, Iannelli F, Pozzi G, Pantosti A.** 2006. The *mef*(E)-carrying genetic element (mega) of *Streptococcus pneumoniae*: insertion sites and association with other genetic elements. Antimicrob Agents Chemother **50:**3361-3366.

96. **Chancey ST, Agrawal S, Schroeder MR, Farley MM, Tettelin H, Stephens DS.** 2015. Composite mobile genetic elements disseminating macrolide resistance in *Streptococcus pneumoniae*. Front Microbiol **6:**26.

97. **Roberts AP, Mullany P.** 2011. Tn*916*-like genetic elements: a diverse group of modular mobile elements conferring antibiotic resistance. FEMS Microbiol Rev **35:**856-871.

98. **Roberts AP, Mullany P.** 2009. A modular master on the move: the Tn*916* family of mobile genetic elements. Trends Microbiol **17:**251-258.

99. **Del Grosso M, Scotto d'Abusco A, Iannelli F, Pozzi G, Pantosti A.** 2004. Tn*2009*, a Tn*916*-like element containing *mef*(E) in *Streptococcus pneumoniae*. Antimicrob Agents Chemother **48:**2037-2042.

100. **Brenciani A, Bacciaglia A, Vecchi M, Vitali LA, Varaldo PE, Giovanetti E.** 2007. Genetic elements carrying *erm*(B) in *Streptococcus pyogenes* and association with *tet*(M) tetracycline resistance gene. Antimicrob Agents Chemother **51:**1209-1216.

101. **Del Grosso M, Camilli R, Libisch B, Fuzi M, Pantosti A.** 2009. New composite genetic element of the Tn*916* family with dual macrolide resistance genes in a *Streptococcus pneumoniae* isolate belonging to clonal complex 271. Antimicrob Agents Chemother **53:**1293-1294.

102. **Del Grosso M, Northwood JG, Farrell DJ, Pantosti A.** 2007. The macrolide resistance genes *erm*(B) and *mef*(E) are carried by Tn*2010* in dual-gene *Streptococcus pneumoniae* isolates belonging to clonal complex CC271. Antimicrob Agents Chemother **51:**4184-4186.

103. **Havarstein LS, Coomaraswamy G, Morrison DA.** 1995. An unmodified heptadecapeptide pheromone induces competence for genetic transformation in *Streptococcus pneumoniae*. Proc Natl Acad Sci U S A **92:**11140-11144.

104. **Straume D, Stamsas GA, Havarstein LS.** 2015. Natural transformation and genome evolution in *Streptococcus pneumoniae*. Infect Genet Evol **33:**371-380.

105. **Brenciani A, Tiberi E, Tili E, Mingoia M, Palmieri C, Varaldo PE, Giovanetti E.** 2014. Genetic determinants and elements associated with antibiotic resistance in viridans group streptococci. J Antimicrob Chemother **69:**1197-1204.

106. **Luna VA, Coates P, Eady EA, Cove JH, Nguyen TT, Roberts MC.** 1999. A variety of gram-positive bacteria carry mobile *mef* genes. J Antimicrob Chemother **44:**19-25.

107. **Santoro F, Vianna ME, Roberts AP.** 2014. Variation on a theme; an overview of the Tn*916*/Tn*1545* family of mobile genetic elements in the oral and nasopharyngeal streptococci. Front Microbiol **5:**535.

108. **Seppala H, Haanpera M, Al-Juhaish M, Jarvinen H, Jalava J, Huovinen P.** 2003. Antimicrobial susceptibility patterns and macrolide resistance genes of viridans group streptococci from normal flora. J Antimicrob Chemother **52:**636-644.

109. **Ojo KK, Ruehlen NL, Close NS, Luis H, Bernardo M, Leitao J, Roberts MC.** 2006. The presence of a conjugative Gram-positive Tn*2009* in Gram-negative commensal bacteria. J Antimicrob Chemother **57:**1065-1069.

110. **O'Brien KL, Nohynek H.** 2003. Report from a WHO Working Group: standard method for detecting upper respiratory carriage of *Streptococcus pneumoniae*. Pediatr Infect Dis J **22:**e1-11.

111. **Chao Y, Marks LR, Pettigrew MM, Hakansson AP.** 2014. *Streptococcus pneumoniae* biofilm formation and dispersion during colonization and disease. Front Cell Infect Microbiol **4:**194.

112. **Marks LR, Reddinger RM, Hakansson AP.** 2012. High levels of genetic recombination during nasopharyngeal carriage and biofilm formation in *Streptococcus pneumoniae*. MBio **3**.

113. **Hofmann J, Cetron MS, Farley MM, Baughman WS, Facklam RR, Elliott JA, Deaver KA, Breiman RF.** 1995. The prevalence of drug-resistant *Streptococcus pneumoniae* in Atlanta. N Engl J Med **333:**481-486.

114. **Schuchat A, Hilger T, Zell E, Farley MM, Reingold A, Harrison L, Lefkowitz L, Danila R, Stefonek K, Barrett N, Morse D, Pinner R, Network ABCSTotEIP.** 2001. Active bacterial core surveillance of the emerging infections program network. Emerg Infect Dis **7:**92-99.

115. **Stephens DS, Zughaier SM, Whitney CG, Baughman WS, Barker L, Gay K, Jackson D, Orenstein WA, Arnold K, Schuchat A, Farley MM.** 2005. Incidence of macrolide resistance in *Streptococcus pneumoniae* after introduction of the pneumococcal conjugate vaccine: population-based assessment. Lancet **365:**855-863.

116. **Hyde TB, Gay K, Stephens DS, Vugia DJ, Pass M, Johnson S, Barrett NL, Schaffner W, Cieslak PR, Maupin PS, Zell ER, Jorgensen JH, Facklam RR, Whitney CG.** 2001. Macrolide resistance among invasive *Streptococcus pneumoniae* isolates. JAMA **286:**1857-1862.

117. **Gay K, Baughman W, Miller Y, Jackson D, Whitney CG, Schuchat A, Farley MM, Tenover F, Stephens DS.** 2000. The emergence of *Streptococcus pneumoniae* resistant to macrolide antimicrobial agents: a 6-year population-based assessment. J Infect Dis **182:**1417-1424.

Chapter 2: A population-based assessment of the impact of 7- and 13-valent pneumococcal conjugate vaccines on macrolide-resistant invasive pneumococcal disease: emergence and decline of *Streptococcus pneumoniae* serotype 19A (CC320) with dual macrolide resistance mechanisms

Max R. Schroeder[1,2], Scott T. Chancey[1,2], Stepy M. Thomas[2,3], Wan-Hsuan Kuo[4], Monica M. Farley[1,2,3], and David S. Stephens[1,2,3,4]

[1]Department of Medicine, Emory University School of Medicine, Atlanta, GA, USA; [2]Laboratories of Microbial Pathogenesis, Department of Veterans Affairs Medical Center, Atlanta, GA, USA; [3]Georgia Emerging Infections Program, Atlanta, GA, USA; [4]Rollins School of Public Health, Emory University, Atlanta, GA, USA

Paper in preparation

M.R.S. characterized resistance genes, analyzed the data, wrote and edited the paper.

RESEARCH IN CONTEXT

Evidence before this study

Streptococcus pneumoniae is a major cause of sepsis, meningitis, otitis media and pneumonia and is a leading cause of death among children and the elderly worldwide. Antibiotic resistance has emerged as a major concern in the treatment of *S. pneumoniae* infections. The emergence of penicillin resistant *S. pneumoniae* and the introduction of new synthetic macrolides led to the widespread use of macrolides for presumptive pneumococcal pneumonia and otitis media. However, in the 1990s the incidence of disease caused by macrolide-resistant *S. pneumoniae* began to increase worldwide.

The introduction of the heptavalent pneumococcal conjugate vaccines (PCV-7-containing serotypes 4, 6B, 9V, 14, 18C, 19F, and 23F) in pediatric populations reduced the incidence of pneumococcal disease by direct protection and by herd protection of unvaccinated individuals. However, "replacement" serotypes, especially serotype 19A, emerged following the introduction of PCV-7. In 2010, the US licensed the use of PCV-13 (containing the PCV-7 serotypes and serotypes 1, 3, 5, 6A, 7F, and 19A). Other countries have now incorporated PCV-13 or other expanded coverage pneumococcal conjugate vaccines.

Using an established population-based surveillance network, we investigated the impact of the 7- and 13-valent conjugate vaccine on macrolide resistant invasive pneumococcal disease in Atlanta, Georgia, USA. As background evidence for this study, we searched PubMed for publication for various combinations of "pneumococcal conjugate vaccine", "PCV-7", "PCV-13", "*Streptococcus pneumoniae*", "macrolide resistance", "*mef*(E)",

"*erm*(B)", "serotype 19A", "Tn*2010*", "serotype replacement", "pneumococcal carriage", "CC320", and "invasive pneumococcal disease". We focused on studies of invasive pneumococcal disease and pneumococcal carriage in the United States and other countries that had implemented PCV-7 and/or PCV-13 vaccination programs.

Added value of this study

The impact over two decades of PCV-7 and PCV-13 on macrolide-resistant invasive pneumococcal disease (MR-IPD) was assessed. The incidence and molecular basis of MR-IPD in the over three million population of metropolitan Atlanta, a mirror of the US population we determined. MR-IPD rapidly increased throughout the 1990s, due primarily to isolates containing *mef*(E)/*mel* carried on the genetic element Mega, which confers resistance through macrolide efflux. Following PCV-7 introduction in 2000, the incidence of MR-IPD rapidly declined (2000-2003) due to decreases in isolates with *mef*(E)/*mel* but also in isolates containing the gene for the ribosomal methylase *erm*(B). The incidence of MR-IPD stabilized from 2005-2009, but macrolide-resistant pneumococci, mostly serotype 19A CC320, with dual resistance mechanisms (*mef*(E)/*mel* and *erm*(B) contained on Tn*2010*), emerged, while the incidence of MR-IPD in PCV-7 serotypes continued to decline. Serotype 19A MR-IPD rapidly declined following PCV-13 introduction. However, increases in MR-IPD caused by serotypes 15A, 15B, 15C, 22F, 23A, and 35B, not currently represented in PCV formulations, were observed.

Implications of all the available evidence

Pneumococcal conjugate vaccine introductions not only reduce the burden of invasive pneumococcal disease but have had great impact on the incidence antibiotic-resistant

pneumococci. However, the selective pressures of continued macrolide use in populations and conjugate vaccine introduction can lead to the emergence and clonal expansion of new macrolide resistance genotypes. The study emphasizes the importance of continued surveillance of *S. pneumoniae* and the need for programs that emphasize the judicious use of antibiotics.

ABSTRACT

Background. Two major genetic determinants, *mef*(E)/*mel* and *erm*(B), encoding genes responsible for macrolide efflux and ribosomal methylation, respectively, confer most macrolide resistance in *Streptococcus pneumoniae*. The introduction of the heptavalent pneumococcal conjugate vaccine (PCV-7) in 2000 dramatically reduced macrolide-resistant invasive pneumococcal disease (MR-IPD) due to serotypes (6B, 9V, 14, 19F, and 23F) containing *mef*(E)/*mel* or *erm*(B). The continued impact of PCV-7 (2000-2009) and PCV-13 (2010-2013) on was prospectively assessed.

Methods. A twenty-year prospective study of invasive pneumococcal disease performed in Metropolitan Atlanta using population-based surveillance was the basis for this study. Genetic determinants of macrolide resistance were evaluated by established molecular techniques.

Findings. During the decade of PCV-7 use (2000-2009), MR-IPD decreased rapidly but then increased. In 2003, serotype 19A CC320 isolates containing both *mef*(E)/*mel* and *erm*(B) were observed and rapidly expanded in 2005-2009 peaking in 2010 (incidence 1.38 per 100,000 population), accounting for 36.1% of MR-IPD isolates and 11.7% of all IPD. The clonal expansion of 19A CC320 was greatest in the <2, 2-4, and 65+ year old populations. Following PCV-13 introduction, a 74.1% decrease in dual macrolide-resistant IPD was observed (incidence 0.32 per 100,000 in 2013).

Interpretation. The selective pressures of widespread macrolide use and PCV-7 introduction on *S. pneumoniae* were evident in our population. Serotype 19A (CC320) with dual macrolide resistance mechanisms emerged following PCV-7 but rapidly

declined after PCV-13 introduction. However, other macrolide-resistant serotypes not currently represented in current PCV formulations (15A, 15B, 15C, 22F, 23A, and 35B) have increased. Continued surveillance of IPD and the judicious use of antibiotics need to continue to be a focus public health strategy.

Funding. Work was supported by a VA Merit Grant and the CDC. The sponsors had no role in study design, data collection, or development of this report.

Running Title: PCV impact on macrolide-resistant invasive pneumococcal disease

Keywords: *Streptococcus pneumoniae*, pneumococcus, macrolide resistance, pneumococcal conjugate vaccines, PCV-7, PCV-13, invasive pneumococcal disease, molecular epidemiology

INTRODUCTION

Streptococcus pneumoniae is a commensal of the human nasopharynx and an opportunistic pathogen. The pneumococcus causes a range of diseases ranging from localized infections (e.g. otitis media and pneumonia) to severe invasive disease (sepsis and meningitis) with the highest burden of pneumococcal disease occurring in children less than five years old (1). β-lactam resistance emerged in the pneumococcus in the 1980s and 1990s, complicating the choice of treatment regimens. Macrolide antibiotics became a major alternative to the use of penicillins and cephalosporins for the treatment of suspected upper respiratory tract infections and community-acquired pneumonia caused by pneumococci. However, macrolide resistance rapidly emerged in *S. pneumoniae* following introduction and widespread use, especially, of new semisynthetic macrolides (e.g. azithromycin, clarithromycin) (2-4).

Two major macrolide resistance phenotypes are observed in pneumococci. An M phenotype and an MLS_B phenotype, mediated through macrolide efflux and ribosomal target site modification, respectively (5). The M phenotype results from the expression of the macrolide resistance efflux pump encoded by *mef*(E)/*mel*, two co-transcribed genes of the macrolide efflux genetic assembly (Mega), that confers moderate level resistance to 14- and 15-membered macrolides (6, 7). The MLS_B phenotype is due to the presence of the ribosomal methylase encoded by *erm*(B), which results in high level macrolide resistance as well as resistance to the chemically distinct lincosamides (clindamycin) and streptogramin B that target overlapping ribosomal sites (8). Throughout the 1990s, the expansion of macrolide-resistant invasive pneumococcal disease (MR-IPD) in the US was largely due to *mef*(E)/*mel*-mediated macrolide efflux (5, 9, 10). Both *mef*(E)/*mel* and

erm(B) are contained on conjugative transposable elements or smaller remnants of such elements. Horizontal gene transfer and clonal expansion contribute to the dissemination of macrolide resistance determinants in pneumococci (11, 12).

In 2000, the pneumococcal conjugate vaccine (PCV-7) containing seven capsular polysaccharides of serotypes 4, 6B, 9V, 14, 18C, 19F, and 23F conjugated to the CRM197 diphtheria protein was licensed for use in children under five years old in the United States (13, 14). However, serotype replacement was observed (15-17) and in 2010, an additional six serotypes (1, 3, 5, 6A, 7F, and 19A conjugated to CRM197) were added to the PCV-7 serotypes to create a 13-valent conjugate vaccine (PCV-13), which replaced PCV-7 in the US (14, 18). PCV-7 and PCV-13 vaccination also decrease pneumococcal upper respiratory carriage (19) and disease (20), "herd protection" due to the serotypes in the vaccines.

Using a well-established population-based surveillance network and molecular typing, we have followed MR-IPD in Atlanta for over twenty years. We documented the initial impact of PCV-7 on the incidence of macrolide resistant *S. pneumoniae* using population-based assessment (3). The aim of the current study was to investigate the incidence and molecular basis of macrolide resistance in invasive pneumococcal disease isolates in the Atlanta metropolitan area, during the PCV-7 era and after the introduction of PCV-13. The emergence and decline of MR-IPD due to serotype 19A belonging to clonal complex 320 (CC320) was defined. The clone contained dual macrolide resistance mechanisms (both *mef*(E)/*mel* and *erm*(B)). The emergence of MR-IPD due to serotypes 15A, 15B, 15C, 22F, 23A, 33F, and 35B was also observed.

MATERIALS AND METHODS

Surveillance. Invasive pneumococcal disease (IPD) has been tracked in Atlanta, Georgia since 1994 using prospective population-based surveillance (2, 9) as part of the Centers for Disease Control and Prevention (CDC) Active Bacterial Core Surveillance (ABCs) of the Georgia Emerging Infections Program (3, 21, 22). For this study, *S. pneumoniae* isolates from IPD were collected from all hospitals and laboratories within the Georgia Health District-3 (HD-3), which consists of the core metropolitan Atlanta counties (Clayton, Cobb, DeKalb, Douglas, Fulton, Gwinnett, Newton, and Rockdale) with a 2010 population of 3,682,873. Population census data (2000 and 2010) and post census estimates for the HD-3 population were obtained from the US Census Bureau each year.

Bacterial Strains. Each invasive *S. pneumoniae* isolate collected was serotyped and tested for antibiotic susceptibility at the CDC (7, 23). Serotyping was performed by standard Quellung reactions (21). Antibiotic minimum inhibitory concentrations (MIC) were determined by broth microdilution assays following Clinical and Laboratory Standards Institute guidelines (23). Isolates with an erythromycin MICs of $\geq$1 μg/ml were resistant, 0.5 μg/ml were intermediate-resistant, and <0.5 μg/ml were susceptible. All non-susceptible pneumococcal isolates, both resistant and intermediate-resistant, were then analyzed by PCR for the presence of macrolide resistance genetic determinants (3). Of 1170 macrolide non-susceptible isolates from 2003-2013, 1131 (96.6%) were available for the molecular determination of the macrolide resistance genotype.

Macrolide Resistance Gene Detection. Genomic DNA was isolated from erythromycin non-susceptible strains by either a crude lysis procedure (9) or the InstaGene™ Matrix (BioRad). One Taq® DNA polymerase and deoxynucleotide solution mix (New England Biolabs). PCR amplification of *erm*(B) of a 551 bp product was performed using primers KG1F (5'-TTGGAACAGGTAAAGGGCATT) and KG1R2 (5'-TTTGGCGTGTTTCATTGCTTG) (9). Detection of *mef*(E)/*mel* was determined by the presence of a 555 or 456 bp product from primers KG8 (5'-GTATCATGTCACTTGCTATGCC) (7) and KG10 (5'-ACACCTAGCTTGCCTACAAGTG). Whole genome sequences were available for 50 of the MR-IPD isolates (11, 24). The multilocus sequence type (MSLT) was determined for 35 dual macrolide resistant genotype isolates from the mid- and late-PCV-7 era through traditional methods and genomic sequence data using the pubmlst.org/spneumoniae database (25).

Statistical Analysis. Statistical analyses were performed using Prism® 5 (GraphPad). Chi Square analyses were used to compare proportions of cases and noncases as previously described (26). Population data was used to calculate incidence rates, which are reported as cases per 100,000 population (3).

RESULTS

Changes in Macrolide Resistant Invasive Pneumococcal Disease (1994-2013)

The emergence of MR-IPD cases in Georgia HD-3 between 1994 and 1999 and the initial impact of PCV-7 introduction 2000-2002 on MR-IPD have been previously reported (3). MR-IPD increased from 4.5 per 100,000 population in 1994 (16.3% of all IPD isolates) to 9.3 per 100,000 in 1999 (31.6% of all IPD isolates) (Figure 1). After PCV-7 introduction in 2000, the incidence of MR-IPD declined to 2.9 per 100,000 by 2002 (a 68.8% reduction, 22.1% of all IPD isolates) (Figure 1). From 2003-2005 to 2006-2009, the mean incidence of MR-IPD rose significantly from 3.64 to 3.85 per 100,000 ($p<0.0001$, 27.9% to 30.3% of all IPD isolates, Figure 1, Table 1). After introduction of PCV-13 in 2010, the incidence of MR-IPD decreased to 2.45 per 100,000 by 2013 ($p<0.0001$). Between 1999 and 2013 the MR-IPD incidence in our population decreased 73.7% (9.3 to 2.45 per 100,000).

Emergence of MR-IPD Due to erm(B) and the Dual Macrolide Resistance Genotype

In the pre-PCV-7 era (1994-1999) the increase in MR-IPD incidence was due to the emergence of *mef*(E)/*mel*-containing isolates (Figure 1), which expanded in particular in serotype 14 but also in serotypes 6B, 9V, 19F, and 23F (3). The incidence of MR-IPD with *erm*(B)-mediated macrolide resistance fluctuated between 1.5 and 2.3 per 100,000 from 1994-1999 (Figure 1) and was found predominantly in serotypes 6B, 14, 19F, and 23F (3). The rapid decline in MR-IPD following the introduction of PCV-7 in 2000-2002 (Figure 1) was due to a reduction of disease due to *mef*(E)/*mel*- and *erm*(B)-containing isolates of PCV-7 serotypes 14, 6B, 9V, 19F, and 23F (3). From 2003-2009, *mef*(E)/*mel*-

mediated MR-IPD continued to decline, from 3.49 to 1.64 per 100,000 ($p<0.0001$) (Figure 1, Table 1). However, this decline was offset by an emergence of isolates with *erm*(B)-mediated resistance after 2003. The incidence of isolates containing *erm*(B) alone significantly increased from the 2003-2009, from 0.22 to 0.87 per 100,000 ($p=0.0002$) (Figure 1, Table 1). Also noted was the emergence of isolates with a *mef*(E)/*mel* and *erm*(B) dual macrolide resistance genotype after 2003 (Figure 1, Table 1).

The dual macrolide resistance genotype was not observed prior to 2000 in our population but steadily increased from 0.19 per 100,000 in 2003 to 1.35 per 100,000 in 2010 ($p<0.0001$, Figure 1, Table 1). After introduction of PCV-13 in infants and young children in 2010, MR-IPD declined from 3.71 per 100,000 in 2009 to 2.45 per 100,000 by 2013 ($p=0.0103$) due to the significant reduction of MR-IPD with the dual macrolide resistance genotype, which declined from 1.11 per 100,000 in 2009 to 0.32 per 100,000 by 2013($p<0.0001$, Figure 1, Table 1). The incidence of MR-IPD with *mef*(E)/*mel* or *erm*(B) alone did not change significantly from 2009 to 2013 (Figure 1, Table 1).

Age Specific Changes in Macrolide-Resistant Invasive Pneumococcal Disease (MR-IPD)

In the <2 year old population, MR-IPD increased from 1994 to 1999 due to disease caused by isolates containing *mef*(E)/*mel* (incidence increased from 55.6 to 134.1 per 100,000) or *erm*(B) (incidence increased from 12.0 to 18.3 per 100,000) (3). MR-IPD incidence significantly declined from 2000 to 2002 following PCV-7 introduction, due to a marked reduction of isolates with *mef*(E)/*mel* or *erm*(B) (incidence decreased from 17.5 and 2.7 per 100,000, respectively, by 2002) (3). From 2003-2005 to 2006-2009, the mean

incidence of *erm*(B) alone or both *mef*(E)/*mel* and *erm*(B) increased from 0.00 and 2.48 to 2.13 and 5.72 per 100,000 in those <2 years (p=0.0077 and p=0.0106) respectively (Table 1, Figure 2A). Following PCV-13 introduction MR-IPD rapidly declined in <2 year olds, overall a 65.7% reduction in MR-IPD incidence was observed by 2013 (2006-2009 rate of 20.88 to 7.16 per 100,000 in 2013; p=0.0033) (Figure 2A, Table 1). Reductions were observed in the incidence of the three macrolide resistance genotypes in <2 year olds; MR-IPD caused by *mef*(E)/*mel* dropped 47.9% (2006-2009 mean incidence of 11.78 to 6.14 per 100,000 in 2013) and *erm*(B) dropped 51.2% (2006-2009 mean incidence of 2.09 to 1.02 per 100,000 in 2013) (Figure 2A, Table 1). After reaching an incidence of 10.92 per 100,000 in 2010, MR-IPD caused by the dual macrolide resistance genotype disappeared in the <2 years of age population by 2012 (Figure 2A, Table 1).

MR-IPD in the 2-4 year old population increased from 12.8 to 17.4 per 100,000 between 1994 and 1999, but after PCV-7 introduction declines by 2002 to 2.8 per 100,000 (3). From 2005 to 2009, the incidence of MR-IPD in this age group increased from 3.70 to 8.22 per 100,000. Following PCV-13 introduction, 2-4 year olds experienced a 68.5% reduction in MR-IPD cases (2006-2009 mean incidence of 6.45 to 2.03 per 100,000 in 2013, p=0.0254) (Figure 2B, Table 1). The *mef*(E)/*mel* genotype fell 43.6% (2007-2009 mean incidence of 3.60 to 2.03 per 100,000 in 2013) (Figure 2B, Table 1). After reaching peak rates of 1.55 per 100,000 for *erm*(B) in 2008 and 4.95 per 100,000 for the dual resistance genotype in 2010, neither genotype was observed in 2-4 year olds by 2013 (Figure 2B, Table 1).

In the ≥65 year old population, MR-IPD caused by isolates containing *mef*(E)/*mel* increased from 1994 to 1999 to an incidence of 18.3 per 100,000 (3). From 2000-2002,

following PCV-7 introduction, the incidence of *mef*(E)/*mel*-containing isolates decreased to 4.5 per 100,000 (3). From 2003-2009, MR-IPD incidence caused by isolates containing *erm*(B) increased from 1.02 to 3.31 per 100,000 and the dual macrolide resistance genotype increased significantly from 0.00 to 3.68 per 100,000 (p=0.0024), while the incidence of isolates containing *mef*(E)/*mel* declined from 13.76 to 6.26 per 100,000 (Table 1, Figure 2C). After the introduction of PCV-13, MR-IPD in the ≥65 year old population decreased 51.4% (2006-2009 mean incidence of 12.23 to 5.94 per 100,000 in 2013, p=0.0013) (Figure 2C, Table 1). The reduction after 2010 in MR-IPD cases was due to decreases in all resistance genotypes: 40.8% reduction of *mef*(E)/*mel* (2006-2009 mean incidence of 7.52 to 4.45 per 100,000 in 2013, p=0.0486), 49.1% reduction of *erm*(B) (2006-2009 mean incidence of 2.34 to 1.19 per 100,000 in 2013, p=0.0546), and 85.3% reduction of the dual resistance genotype (2006-2009 mean incidence of 2.04 to 0.30 per 100,000 in 2013, p=0.0169) (Figure 2C, Table 1). MR-IPD in other, lower risk age-groups (4-17, 18-39, and 40-64 year old populations) did not change significantly from 2006-2009 to 2013 (Table 1).

Macrolide Resistant Serotypes

PCV-7 or PCV-13 serotypes. MR-IPD caused by serotypes in PCV-7, and PCV-13 (4, 6B, 9V, 14, 18C, 19F, and 23F), continued to decline from 2003-2009 from 1.43 to 0.09 per 100,000 (p<0.0001) and, remarkably, by 2013 no cases of MR-IPD caused by PCV-7 serotypes were detected (Figure 3, Table S1). Of the additional six capsular serotypes contained in PCV-13 (1, 3, 5, 6A, 7F, and 19A), serotypes 1 and 5 did not cause MR-IPD and serotype 7F only caused 3 cases of MR-IPD in our population 2003-2013 (Figure 3, Table S1). MR-IPD caused by serotype 3 remained stable from 2003-

2013 at a mean incidence of 0.07 per 100,000 (Table S1). However, incidence of MR-IPD caused by serotype 19A significantly increased from 0.93 per 100,000 in 2003 to 2.15 per 100,000 in 2009 ($p=0.0001$) but, following PCV-13 introduction in 2010, sharply declined to 0.43 per 100,000 by 2013 ($p<0.0001$, Figure 3, Table S1). Interestingly, MR-IPD caused by serotype 6A declined from 0.57 per 100,000 in 2003 to 0.06 per 100,000 in 2009 ($p=0.0003$) and no cases occurred from 2010-2013 (Figure 3, Table S1).

Non-PCV-7 or PCV-13 serotypes. The incidence of MR-IPD cases due to serotype 33F remained stable with a mean incidence of 0.41 per 100,000 from 2003-2013, causing 9-15% of MR-IPD (Figure 3, Table S1). MR-IPD caused by three other serotypes significantly increased from 2003-2013: serotype 15A ($p=0.0033$), 22F ($p=0.0230$), and 23A ($p=0.0379$) (Figure 3, Table S1). From 2006-2009 to 2013, significant increases in MR-IPD caused by 15B ($p=0.0367$), 15C ($p=0.0047$), and 35B ($p<0.0001$) were also observed (Figure 3, Table S1).

Dual macrolide resistance serotypes. The dual macrolide resistance genotype (*mef*(E)/*mel* + *erm*(B)) was first identified in the Atlanta surveillance area in 2000 in three serotype 19F isolates (ST236, ST271, and ST3039), all belonging to the multi-locus sequence type clonal complex CC320 (11). In 2003, the first MR-IPD serotype 19A, ST320 isolate with the dual macrolide resistance genotype was identified (Figure 4). MR-IPD due to isolates with the dual resistance genotype significantly increased from the 2003-2009 ($p<0.0001$, Figure 1 and 4, Table 1). Dual macrolide resistant isolates from 2003-2005 belonged to CC320 (three 19F included ST271 and two ST3039, while 19A isolates were all ST320). All dual macrolide resistance isolates from 2007-2009 were also

found to belong to CC320, two 19F isolates (sequence types ST236 and ST3039), 23 19A, ST320 isolates and one 19A, ST1339 isolate. These isolates contain the newly recognized mobile genetic element Tn*2010* (12). The dual macrolide resistance genotype was also found in serotypes 3, 6C, 11A, 15A, 22F, 23A, 33F, 35B, and nontypeable *S. pneumoniae* (Figure 4). Following PCV-13 introduction in 2010, the number of isolates with the dual macrolide resistance genotype steadily declined (Figures 1 and 4).

Changes in Serotypes Causing Invasive Pneumococcal Disease (1994-2013)

As previously reported, IPD incidence in the Atlanta population ranged from 27.6 to 31.6 per 100,000 between 1994 and 1999 and dramatically decreased following PCV-7 introduction in 2000 to a rate of 13.0 per 100,000 by 2002, a 55.8% reduction from 1999 (Figure 5A) (3). IPD due to PCV-7 capsular serotypes fell dramatically (Figure 6). PCV-7 serotypes caused 18.1-22.0 cases per 100,000 from 1994-1999 but only 5.1 cases per 100,000 in 2002 (Figure 5A) (3). PCV-7 serotypes caused 62-70% of IPD from 1994-1999 but only 39% of IPD in 2002 (Figure 5B) (3).

From 2002 to 2009, IPD ranged between 11.0 and 14.1 cases per 100,000 (Figure 5A), but the proportion of disease caused by PCV-7 serotypes continued to decrease, 2.5% of IPD cases by 2009 (Figure 5B). After the introduction of PCV-13 in 2010, the incidence of IPD caused by PCV-7 serotypes declined to 0.1 per 100,000 by 2013. This represented a 99.5% reduction of cases (from 20.4 per 100,000 in 1999) caused by PCV-7 serotypes.

From 1994-2000, IPD caused by serotypes 1, 3, 5, 6A, 7F, and 19A, the six serotypes added to PCV-13 ranged between 3.2 and 5.6 per 100,000 (Figure 5A)

representing less than 15% of IPD cases (Figure 5B). Following PCV-7 introduction in 2000, IPD caused by these six serotypes ranged between 3.2 per 100,000 in 2000 and 5.9 per 100,000 in 2006, and remained between 4.7 and 6.2 per 100,000 from 2006-2009 (Figure 5A). IPD caused by serotypes 1, 3, 5, 6A, 7F, and 19A increased from 14.5% in 2000 to 48.9% in 2009 (Figure 5B). The incidence was due to both expansion of serotypes 7F and 19A, which increased dramatically from 1999 incidence of 0.2 and 0.9 per 100,000, respectively, to 2.1 and 3.0 per 100,000 in 2009 (Figure 7), and decreases in serotype 6A (see below). Interestingly, IPD caused by serotype 1 increased from 1994-1996, but then decreased from 1997-2004 and only occasionally caused disease afterwards (Figure 7). Serotype 5 rarely caused IPD in our population. IPD cases caused by serotype 6A decreased following the introduction of PCV-7 (Figure 7). IPD caused by serotype 3 was relatively consistent throughout the twenty-year study period (Figure 7). Though serotype 6A decreased serotype 6C, first observed in our population in 1999, emerged through 2010 (Figure 8). In 2010, of the six serotypes 1, 3 5, 6A, 7F, and 19A, only serotypes 3, 7F, and 19A caused IPD (Figure 7).

Following PCV-13 introduction, a 25.8% reduction of overall IPD from 12.0 per 100,000 in 2009 to 8.9 per 100,000 in 2013 was observed (Figure 5A). IPD caused by the six additional serotypes in PCV-13 decreased 74.8% from 5.9 per 100,000 in 2009 to 1.5 per 100,000 in 2013 (Figure 5A). The decline was due to reductions of IPD caused by serotypes 7F and 19A (Figure 7). Though not represented in PCV-13, IPD caused by serotype 6C also declined from 2010 through 2013, suggesting cross-reactivity with the serotypes 6A and 6B conjugates present in PCV-13 (Figure 8).

IPD caused by non-PCV-13 serotypes (non-vaccine serotypes) was 3.8-3.7 per 100,000 from 1994-1999 representing approximately 15% of IDP cases (Figure 5). After PCV-7 was introduced in 2000, non-vaccine IPD increased from 3.5 per 100,000 in 2000 to 7.1 cases per 100,000 in 2007 and remained between 5.8 and 7.3 per 100,000 from 2007-2013 (Figure 5A). Following the 2000 and 2010 introductions of PCV-7 and PCV-13, respectively, the proportion of IPD caused non-vaccine serotypes continued to increase from 15% before vaccination to 81.5% of IPD in 2013 (Figure 5B). The most prevalent non-vaccine serotypes causing IPD include serotype 12F, 15A, 22F, 23A, 33F, and 35B (Figure 9). Incidence of IPD caused by serotypes 12F and 22F fluctuated throughout the study period but remained between 0.2 and 1.4 per 100,000 (Figure 9). Following the PCV-7 introduction in 2000, IPD caused by serotypes 15A, 23A, 33F, and 35B emerged (Figure 9).

DISCUSSION

Pneumococcal conjugate vaccines (PCVs) have now been introduced into populations worldwide, and each time major reductions in the burden of pneumococcal disease have followed the introductions (14). PCVs provide individual protection and reduce transmission and asymptomatic nasopharyngeal carriage of the serotypes contained in PCVs (e.g. herd protection) (27, 28). PCVs also have reduced the incidence of antibiotic-resistant *S. pneumoniae* by decreasing the serotypes that often carry multiple, antibiotic resistant determinants (14). In a previous study, we found MR-IPD incidence decreased dramatically in the Atlanta population after the introduction of PCV-

7 in 2000, primarily due to the reduction of PCV-7 serotypes containing the *mef*(E)/*mel* efflux macrolide resistance determinants (3). A modest reduction of *erm*(B)-mediated resistance in pneumococci was also observed following PCV-7 introduction (3). The reductions of IPD and MR-IPD observed in metropolitan Atlanta, GA reflected those observed throughout the rest of the US (29).

However, as we report here, the incidence of MR-IPD stabilized in Atlanta from 2003-2005 and then increased to 2006-2009. The changes in incidence from 2003-2009 in IPD and MR-IPD were due to a continued decline in PCV-7 serotypes and "serotype replacement" by non-PCV-7 serotypes, especially 7F and 19A (Figures 3, 5, and 7). Specifically, a continued decrease in MR-IPD due to *mef*(E)/*mel*-containing isolates was observed 2003-2009 with PCV-7 use, but the MR-IPD increase was due to the re-emergence of *erm*(B)-only isolates and the rapid emergence of serotype 19A isolates containing both determinants (Figure 1). Introduction of PCV-13 in 2010 in the pediatric population decreased the incidence of MR-IPD caused by dual resistance (*mef*(E)/*mel* and *erm*(B)) isolates through the suppression of serotype 19A CC320. The greatest reductions in MR-IPD after PCV-13 were observed in the <2 (74%) and 2-4 year age groups (66%), and in unvaccinated ≥65 year old populations (51.4%). As of March 2012, only 56% of US children under five years old had been vaccinated with PCV-13, so the rapid decline in all age-groups may be attributed to both individual and herd protection (30). The data are consistent with overall IPD reductions seen throughout the US (20).

Older adults, ≥65 years of age, are at high risk of pneumococcal disease. Until recently, only the 23-valent pneumococcal polysaccharide vaccine (PPV23) was recommended for those ≥65 year old. PPV23 provides some protection against IPD but

does not impact pneumococcal carriage or transmission (14, 28). In August 2014, the US Advisory Committee on Immunization Practices (ACIP) recommended PCV-13 for routine use in the 65+ year old population (31, 32). This introduction should further reduce the incidence of IPD and MR-IPD in the ≥65 year old population.

The routine use of PCV-7 in children reduced cases of MR-IPD caused by PCV-7 serotypes but serotype replacement was observed (3, 15, 28, 33). In addition to 19A, the incidence MR-IPD caused by serotypes 15A, 22F, and 23A increased following PCV-7 introduction (Figures 3). These serotype replacement events were driven by the selective pressures of PCV-7 and continued high-level macrolide usage (4, 34). The introduction of PCV-13 was followed by decreased incidence of disease due to reduction in the additional serotypes of PCV-13, specifically 19A (20). MR-IPD due to serotypes 15B, 15C, and 35B increased after the introduction of PCV-13. Interestingly, MR-IPD caused by serotype 6A declined throughout the PCV-7 era despite a lack of coverage by PCV-7. Protection against serotype 6A by PCV-7 likely occurred through immunological cross-reaction with vaccine-induced antibodies to serotype 6B, which was included in PCV-7(35). The incidence of 6A was clarified by the discovery of serotype 6C, which was previously classified as serotype 6A (35). Continued monitoring of IPD and MR-IPD serotypes is important for future pneumococcal conjugate vaccine formulations (14).

S. pneumoniae containing both of the macrolide resistance determinants, *mef*(E)/*mel* and *erm*(B), were first noted in the late-1990s from the US and Japan (36-38). MR-IPD caused by dual macrolide-resistant serotype 19A *S. pneumoniae* belonging to CC320 (formerly CC271) (11, 12, 39) increased steadily from 2006-2010 in the Atlanta population and worldwide (10, 12, 17, 39). Dual macrolide-resistant isolates were found

to contain the mobile genetic element Tn*2010* (11) (Figure 4). Tn*2010* is a large 26.4-Kb element with Mega (*mef*(E)/*mel*) and Tn*917* (*erm*(B)) inserted at two distinct sites into a Tn*916*-like conjugative transposon (12). Tn*2010* likely arose from a recombination event between Tn*2009* [a Mega (*mef*(E)/*mel*)-containing Tn*916*-like transposon] and Tn*6002* [a Tn*917* (*erm*(B))-containing Tn*916*-like transposon] (11, 12). Introduction of PCV-13 in the US in 2010 was followed by a rapid decline in the incidence of IPD cases caused by the dual macrolide-resistant *S. pneumoniae*. By 2013, no invasive disease caused by dual macrolide resistant genotype isolates was detected in individuals under 18 years old in Atlanta.

The global use of macrolides is a selective pressure for the development and expansion of macrolide resistance in *S. pneumoniae* (4, 34). While PCVs have reduced the burden of MR-IPD (3, 10), macrolide resistance among the pneumococcus has continued to increase worldwide. In Atlanta less than 27.5% of IPD isolates from 2013 were macrolide resistant while in China over 90% of *S. pneumoniae* isolated are macrolide resistant (40, 41).

In summary, serotype 19A CC320 with dual macrolide resistant mechanisms emerged following PCV-7 introduction as a serotype replacement macrolide antibiotic resistant clone. The incidence of MR-IPD, due largely to the impact on serotype 19A, decreased dramatically among <2 year olds as well as in 2-4 year olds and 65+ year olds following the introduction of PCV-13 in 2010. PCVs can significantly reduce the incidence of antibiotic resistance in *S. pneumoniae*. Expanded pneumococcal conjugate vaccines continue to reduce the burden of IPD and are important tools in combating antibiotic resistance. Moreover, this study emphasizes the impact of ongoing surveillance

of *S. pneumoniae* and the need for programs that emphasize the judicious use of antibiotics.

Acknowledgements

We would like the thank Yih-Ling Tzeng and Sarah Satola for critical review of the paper, and Lillian Morgan, Wendy Baughman, and other members of the Georgia Emerging Infections Program. Also thanks to Bernard Beall and the CDC Streptococcus lab as well as Matthew Moore of the CDC Respiratory Disease Branch. This work was funded by the CDC as well as VA Merit Grant to DSS.

Table 1. Incidence of MR-IPD 2003-2013 in Atlanta, GA, by age-group, macrolide resistance, and macrolide resistance genotype. Incidence reported as cases per 100,000 population.

Incidence	**2003**	**2004**	**2005**	**2006**	**2007**	**2008**	**2009**	**2010**	**2011**	**2012**	**2013**
All Ages											
Overall IPD	14.02	12.29	12.89	13.50	13.23	12.02	11.99	11.51	9.46	8.03	8.90
Macrolide Resistance	4.09	3.36	3.48	4.34	3.46	3.88	3.71	3.82	2.62	2.72	2.45
mef(E)/*mel*	3.49	2.72	2.67	2.59	1.83	2.22	1.64	1.60	1.46	1.61	1.50
erm(B)	0.22	0.34	0.35	0.52	0.75	0.91	0.87	0.74	0.34	0.54	0.63
Dual Resistance	0.19	0.08	0.39	1.12	0.68	0.65	1.11	1.35	0.79	0.57	0.32
<2 years old											
Macrolide Resistance	23.82	14.74	16.21	18.79	18.88	25.48	20.36	18.57	16.80	5.28	7.16
mef(E)/*mel*	20.42	11.06	13.51	12.16	10.49	13.80	10.67	6.55	8.96	5.28	6.14
erm(B)	0.00	0.00	0.00	1.11	2.10	3.19	1.94	1.09	2.24	0.00	1.02
Dual Resistance	2.27	2.46	2.70	5.53	4.19	7.43	7.76	10.92	4.48	0.00	0.00
2-4 years old											
Macrolide Resistance	7.89	4.73	3.70	4.84	6.53	6.19	8.22	7.77	2.08	2.78	2.03
mef(E)/*mel*	7.89	3.94	1.48	3.45	4.35	1.55	5.06	2.12	0.69	1.39	2.03
erm(B)	0.00	0.00	0.74	0.69	0.73	1.55	1.27	0.71	0.69	0.00	0.00
Dual Resistance	0.00	0.00	1.48	0.69	1.45	3.09	1.27	4.95	0.69	1.39	0.00
5-17 years old											
Macrolide Resistance	0.36	0.36	0.39	0.61	0.48	0.60	0.48	0.67	0.00	0.48	0.31
mef(E)/*mel*	0.18	0.36	0.39	0.20	0.32	0.45	0.16	0.17	0.00	0.48	0.15
erm(B)	0.18	0.00	0.00	0.00	0.16	0.00	0.32	0.00	0.00	0.00	0.15
Dual Resistance	0.00	0.00	0.00	0.20	0.00	0.15	0.00	0.50	0.00	0.00	0.00
18-39 years old											
Macrolide Resistance	1.73	1.06	1.45	2.29	1.61	1.00	1.80	0.85	1.20	0.73	0.98
mef(E)/*mel*	1.62	0.82	1.32	1.72	0.80	0.78	0.54	0.53	0.65	0.27	0.45
erm(B)	0.11	0.23	0.00	0.11	0.57	0.11	0.45	0.21	0.09	0.09	0.45
Dual Resistance	0.00	0.00	0.00	0.46	0.23	0.00	0.81	0.00	0.46	0.36	0.09
40-64 years old											
Macrolide Resistance	4.17	4.34	4.54	5.08	3.63	4.13	2.80	3.85	3.30	4.03	3.70
mef(E)/*mel*	3.10	3.47	3.50	2.13	1.71	2.16	1.12	1.19	1.74	2.57	1.98
erm(B)	0.24	0.43	0.70	1.02	0.81	1.41	0.84	1.19	0.55	0.83	0.95
Dual Resistance	0.36	0.00	0.35	1.83	0.81	0.47	0.75	1.19	0.92	0.64	0.77
≥65 years old											
Macrolide Resistance	14.77	11.72	10.05	13.32	9.75	12.23	13.63	15.33	7.31	8.74	5.94
mef(E)/*mel*	13.76	9.96	7.18	10.36	5.32	8.15	6.26	8.82	4.52	4.21	4.45
erm(B)	1.02	1.76	0.96	0.99	2.22	2.85	3.31	2.68	0.35	2.59	1.19
Dual Resistance	0.00	0.00	1.44	1.48	1.77	1.22	3.68	3.83	2.09	1.94	0.30

FIGURE LEGENDS

Figure 1. The incidence (2003-2013) of macrolide-resistant invasive pneumococcal disease (MR-IPD) (black line) as cases per 100,000 population and incidence by macrolide resistance genotype: *mef*(E)/*mel* (white squares), *erm*(B) (white diamond), or the dual macrolide resistance genotype (*mef*(E)/*mel* and *erm*(B) (white triangles).

Figure 2. The incidence (2003-2013) of MR-IPD cases in individuals (A) <2 years, (B) 2-4 years, (C) ≥65 years. Incidence is shown as cases per 100,000 population with white bars for *mef*(E)/*mel* incidence, vertical striped bars for *erm*(B) incidence, and black bars for the dual macrolide resistance genotype (*mef*(E)/*mel* and *erm*(B)) incidence.

Figure 3. The *S. pneumoniae* serotype distribution of MR-IPD in (A) 2002 (two years after PCV-7 introduction), (B) 2003-2005, (C) 2006-2009, and (D) 2013 (three years after PCV-13 introduction). Size of pie charts are scaled to represent cases per year: Figure 3A (74%), 3B (100%), 3C (120%), 3D (86%). "Other" pneumococcal serotypes are non-vaccine serotypes that did not change over the study period. Serotypes contained in PCV-13 are underlined.

Figure 4. *S. pneumoniae* MR-IPD isolates with dual resistance genes (*mef*(E)/*mel* and *erm*(B)) were first observed in the surveillance area in 2000: 19F (black bars), 19A (white bars). Other serotypes (striped bars) with the dual macrolide resistance genotype first observed in 2006 (11A), 2008 (23A), 2009 (15A, 33F, and two nontypeable strains), 2010 (two 22F and one nontypeable), 2012 (6C and 35B), and 2013 (serotype 3).

Figure 5. The incidence (1994-2013) of invasive pneumococcal disease as cases per 100,000 population by capsular serotypes: serotypes contained in PCV-7 (black bars), additional six serotypes contained in PCV-13 not represented in PCV-7 (left strip bars), and non-vaccine serotypes (white bars).

Figure 6. The incidence (1994-2013) of invasive pneumococcal disease caused by PCV-7 serotypes as cases per 100,000 population. Incidence for each of the seven serotypes is presented: serotype 4 (black bars), 6B (left strip bars), 9V (black dots on white bars), 14 (horizontal strip bars), 18C (gray bars), 19F (right strip bars), and 23F (white bars).

Figure 7. The incidence (1994-2013) of invasive pneumococcal disease caused by the six PCV-13 serotypes not represented in PCV-7 as cases per 100,000 population. Incidence for each serotypes is presented: serotype 1 (black bars), 3 (left strip bars), 5 (black dots on white bars), 6A (horizontal strip bars), 7F (gray bars), and 19A (white bars).

Figure 8. Incidence of serogroup 6 IPD by serotype from 1994-2013. Incidence for 6B a PCV-7 serotype (black bars), 6A a PCV-13 serotype (left strip bars), and 6C a non-vaccine serotype (white bars) are presented.

Figure 9. The incidence (1994-2013) of invasive pneumococcal disease caused by non-vaccine serotypes as cases per 100,000 population. Incidence for each of the most prevalent serotypes in the Atlanta surveillance area is presented: serotype 12F (black bars), 15A (left strip bars), 22F (black dots on white bars), 23A (horizontal strip bars), 33F (gray bars), and 35B (right strip bars). “Other” serotypes are non-vaccine serotypes that caused less than 0.1 cases per 100,000 population and did not change dramatically during the course of the study (white bars).

Figure 1

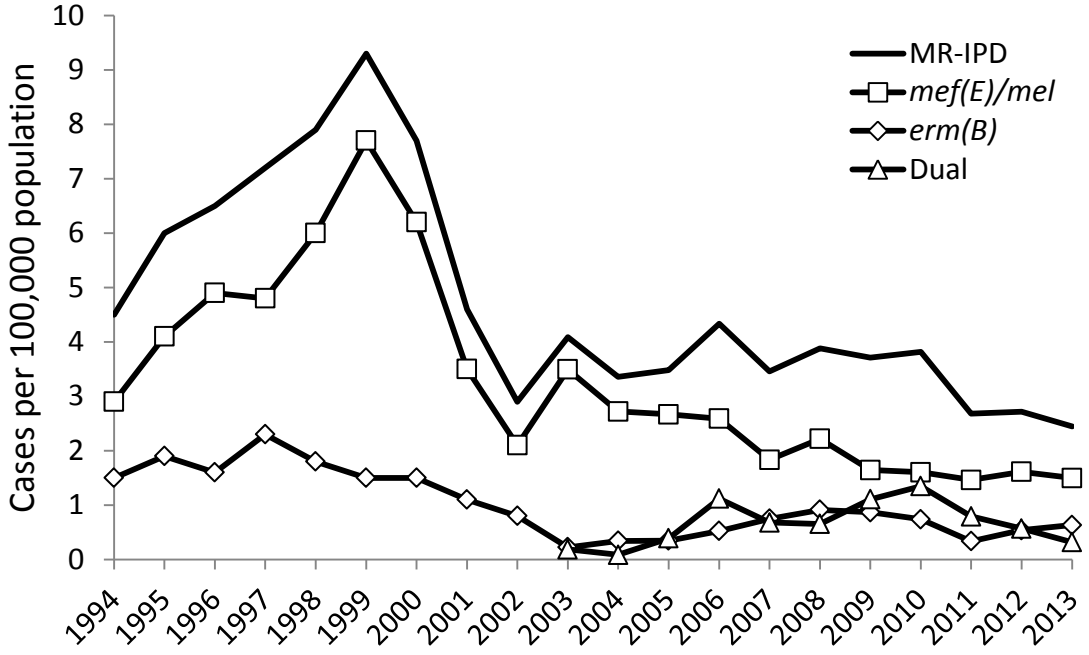
Cases per 100,000 population
10
9
8
7
6
5
4
3
2
1
0
1994
1995
1996
1997
1998
1999
2000
2001
2002
2003
2004
2005
2006
2007
2008
2009
2010
2011
2012
2013
MR-IPD
mef(E)/mel
erm(B)
Dual

Figure 2

A

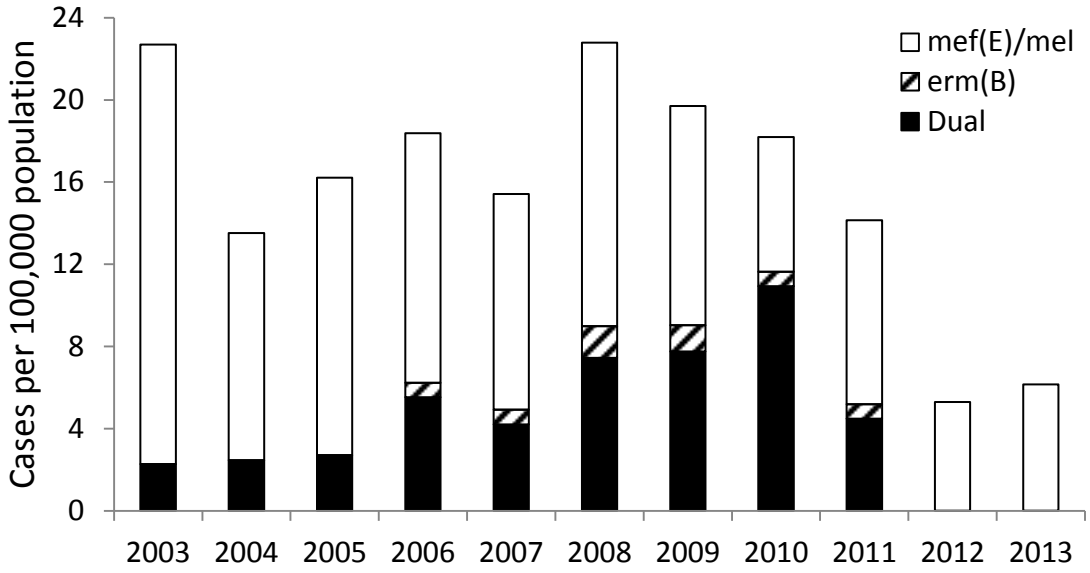
Cases per 100,000 population
24
20
16
12
8
4
0
2003
2004
2005
2006
2007
2008
2009
2010
2011
2012
2013
mef(E)/mel
erm(B)
Dual

B

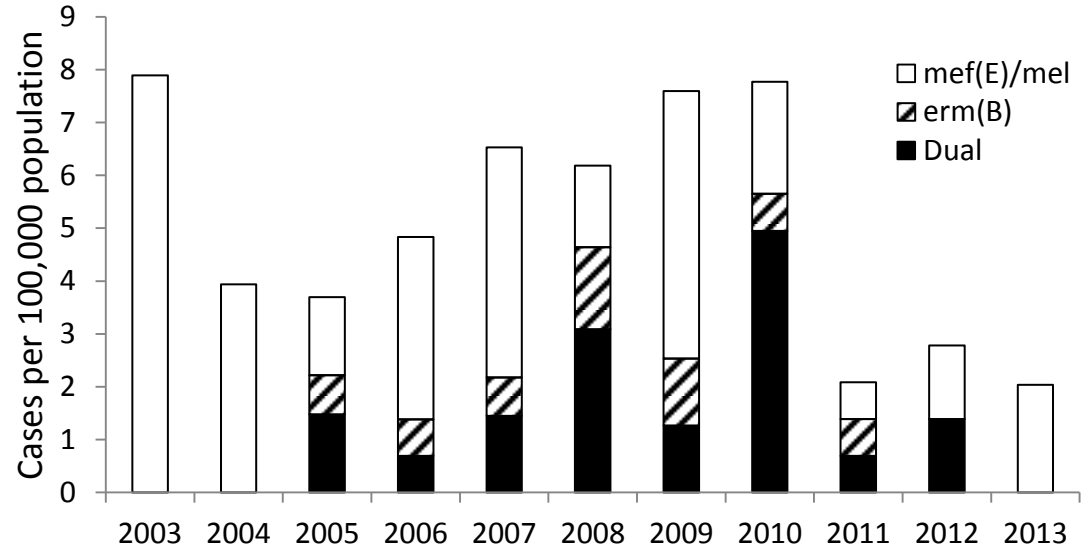
Cases per 100,000 population
9
8
7
6
5
4
3
2
1
0
2003
2004
2005
2006
2007
2008
2009
2010
2011
2012
2013
mef(E)/mel
erm(B)
Dual

C

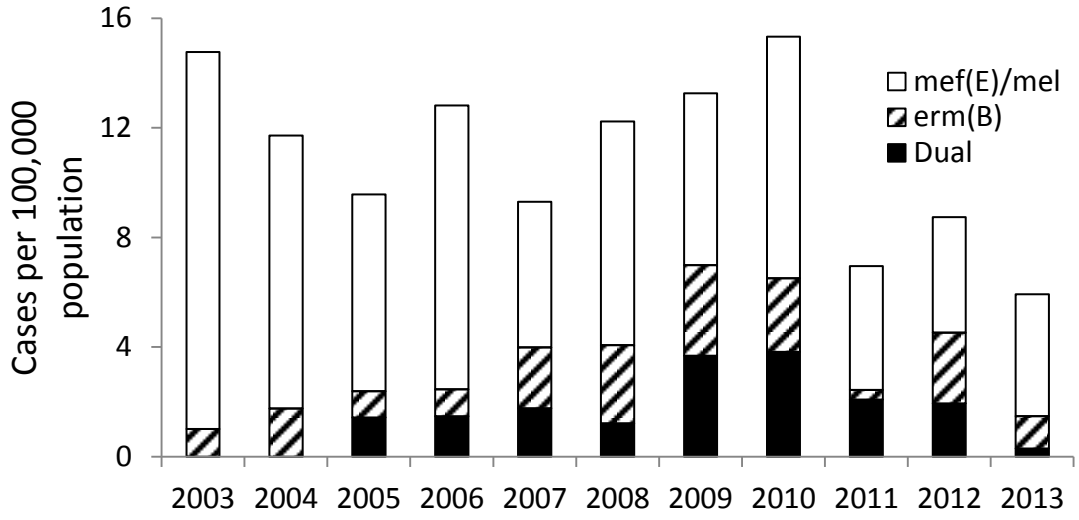
16
12
8
4
0
Cases per 100,000 population
2003
2004
2005
2006
2007
2008
2009
2010
2011
2012
2013
mef(E)/mel
erm(B)
Dual

Figure 3

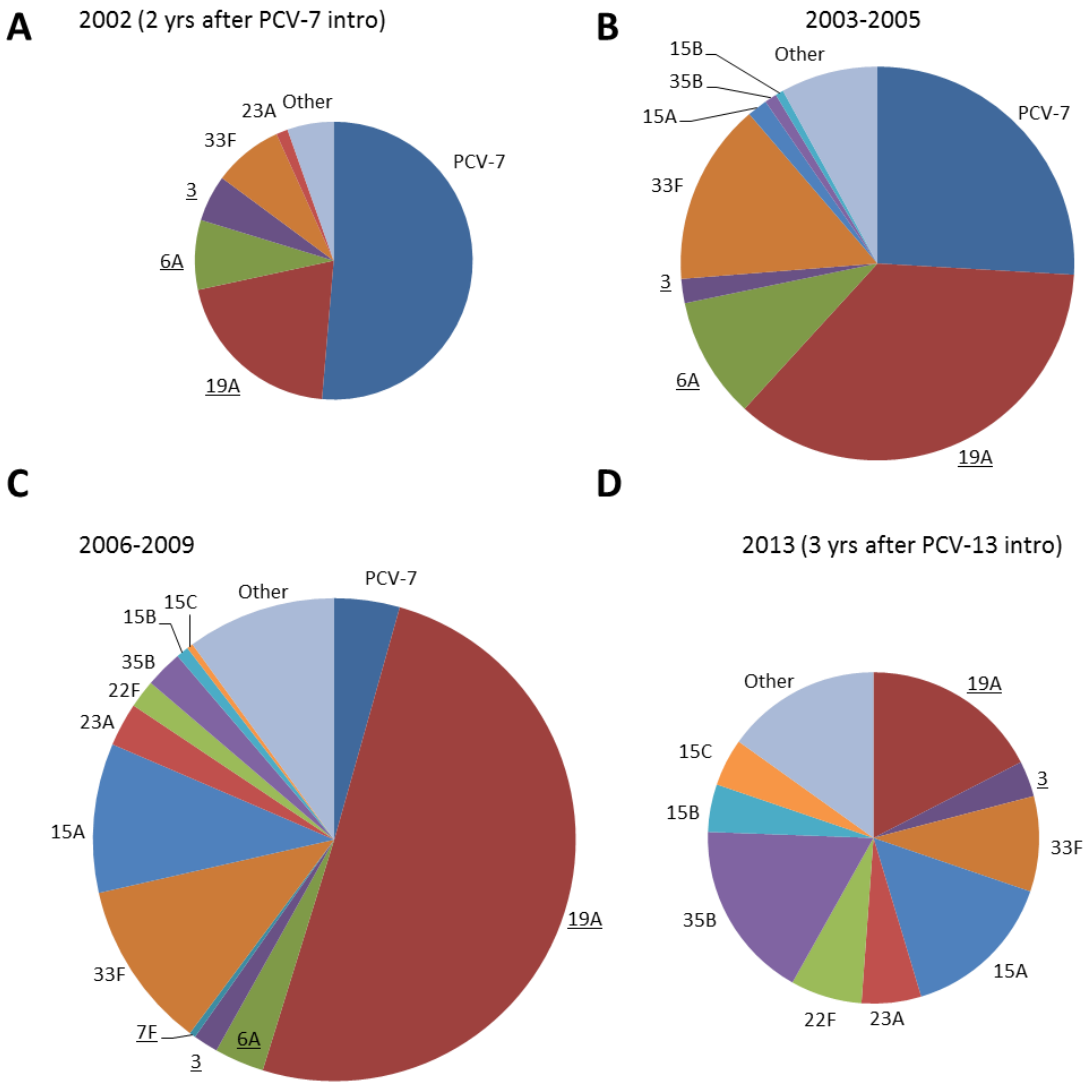
A
2002 (2 yrs after PCV-7 intro)
PCV-7
19A
6A
3
33F
23A
Other
B
2003-2005
PCV-7
19A
6A
3
33F
15A
35B
15B
Other
C
2006-2009
PCV-7
19A
6A
3
7F
33F
15A
23A
22F
35B
15B
15C
Other
D
2013 (3 yrs after PCV-13 intro)
19A
3
33F
15A
23A
22F
35B
15B
15C
Other

Figure 4

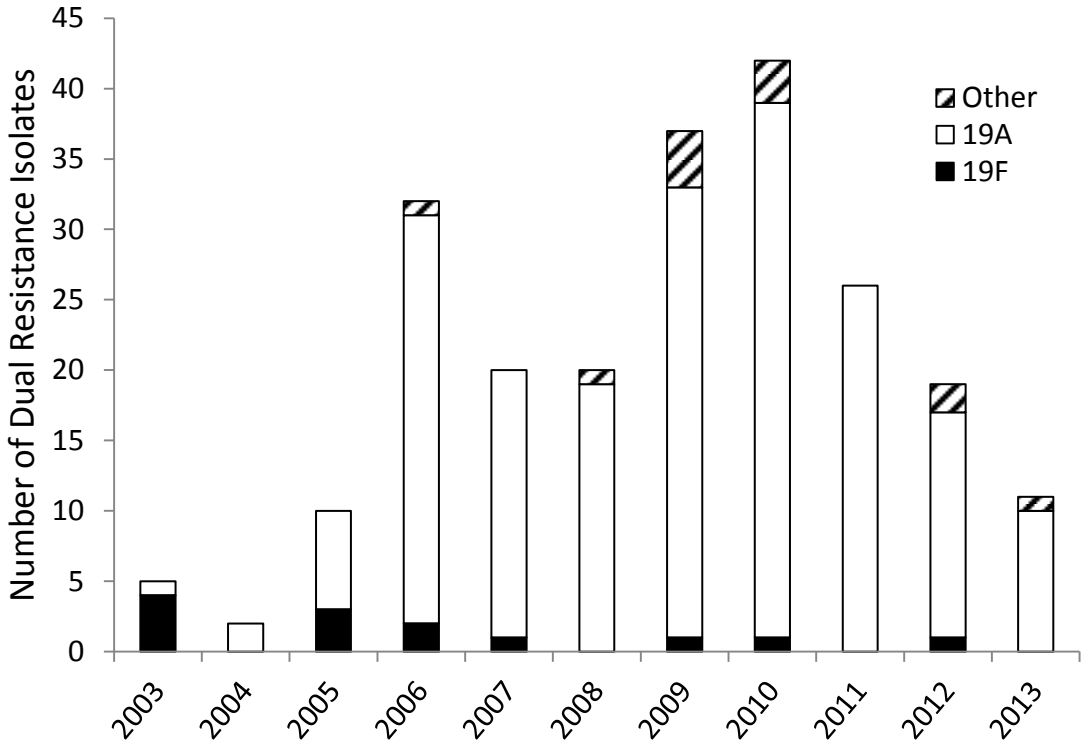
Number of Dual Resistance Isolates
45
40
35
30
25
20
15
10
5
0
2003
2004
2005
2006
2007
2008
2009
2010
2011
2012
2013
Other
19A
19F

Figure 5.

A

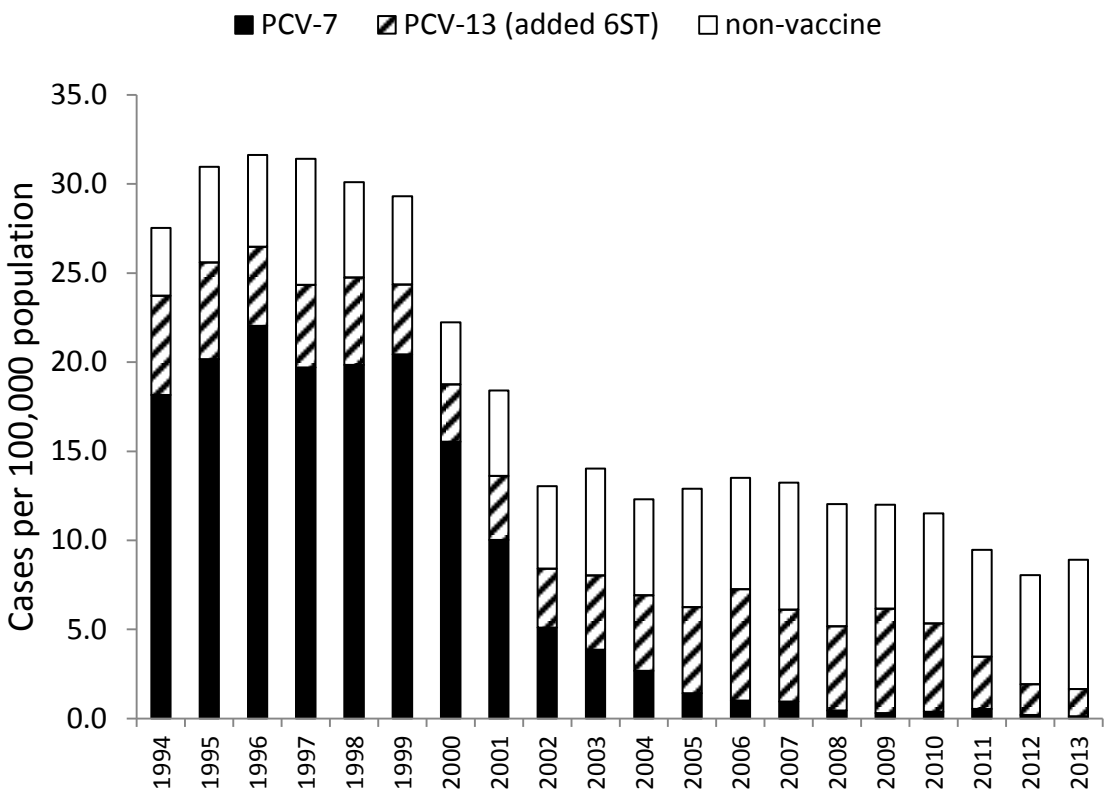
PCV-7
PCV-13 (added 6ST)
non-vaccine
Cases per 100,000 population
35.0
30.0
25.0
20.0
15.0
10.0
5.0
0.0
1994
1995
1996
1997
1998
1999
2000
2001
2002
2003
2004
2005
2006
2007
2008
2009
2010
2011
2012
2013

B

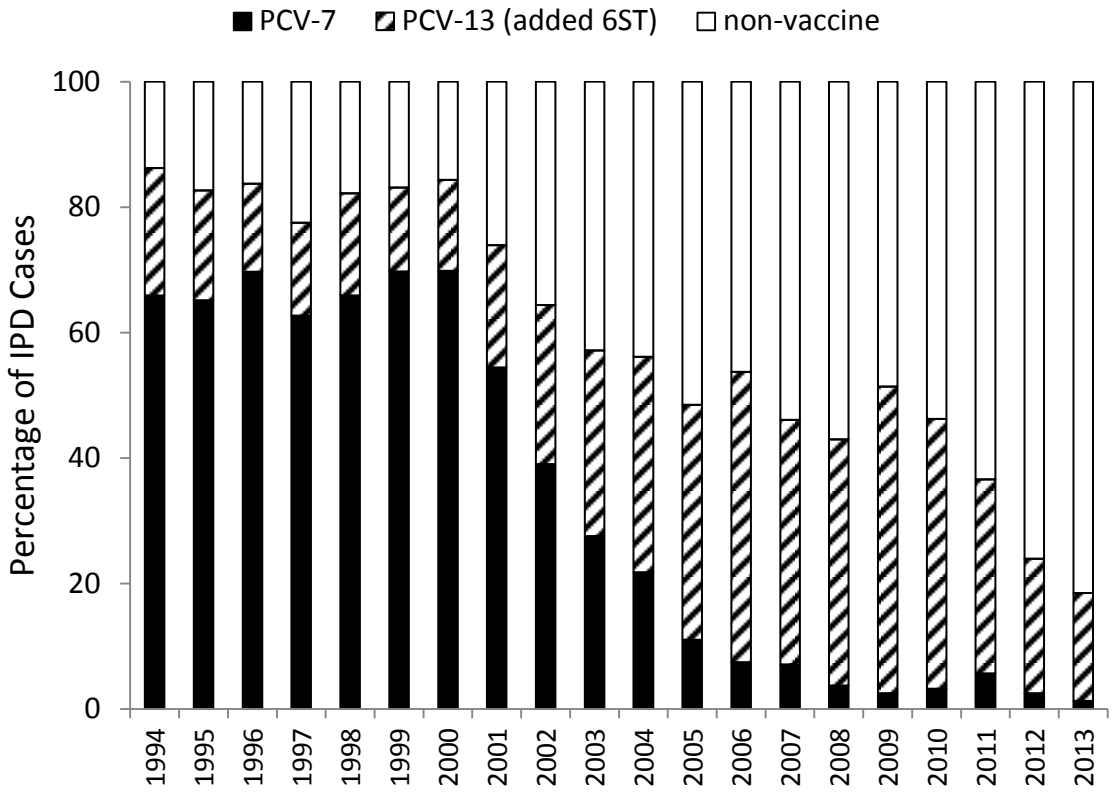
PCV-7
PCV-13 (added 6ST)
non-vaccine
Percentage of IPD Cases
100
80
60
40
20
0
1994
1995
1996
1997
1998
1999
2000
2001
2002
2003
2004
2005
2006
2007
2008
2009
2010
2011
2012
2013

Figure 6.

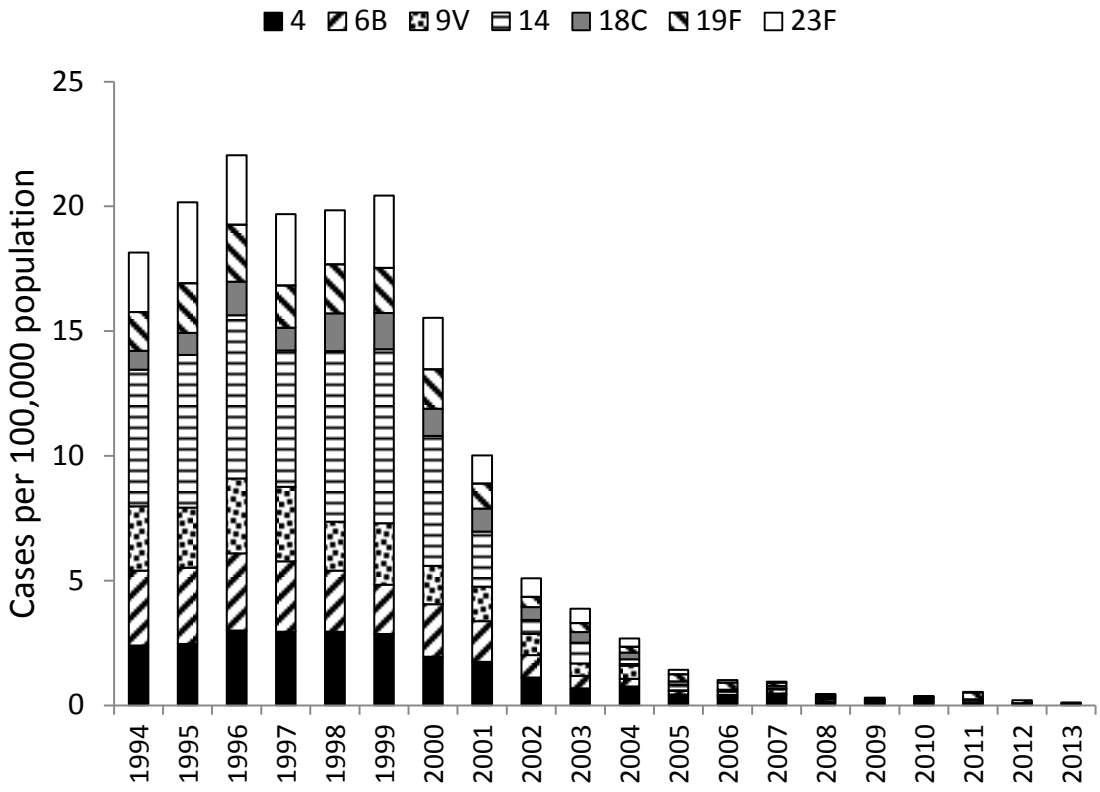
4
6B
9V
14
18C
19F
23F
Cases per 100,000 population
25
20
15
10
5
0
1994
1995
1996
1997
1998
1999
2000
2001
2002
2003
2004
2005
2006
2007
2008
2009
2010
2011
2012
2013

Figure 7.

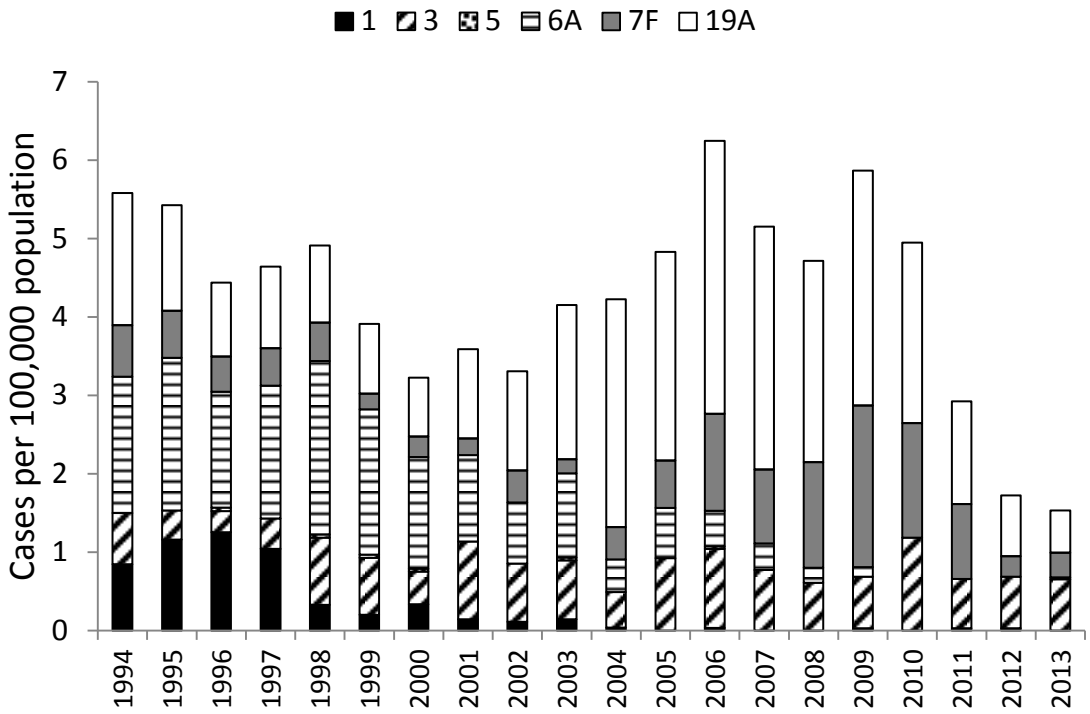
1
3
5
6A
7F
19A
Cases per 100,000 population
0
1
2
3
4
5
6
7
1994
1995
1996
1997
1998
1999
2000
2001
2002
2003
2004
2005
2006
2007
2008
2009
2010
2011
2012
2013

Figure 8.

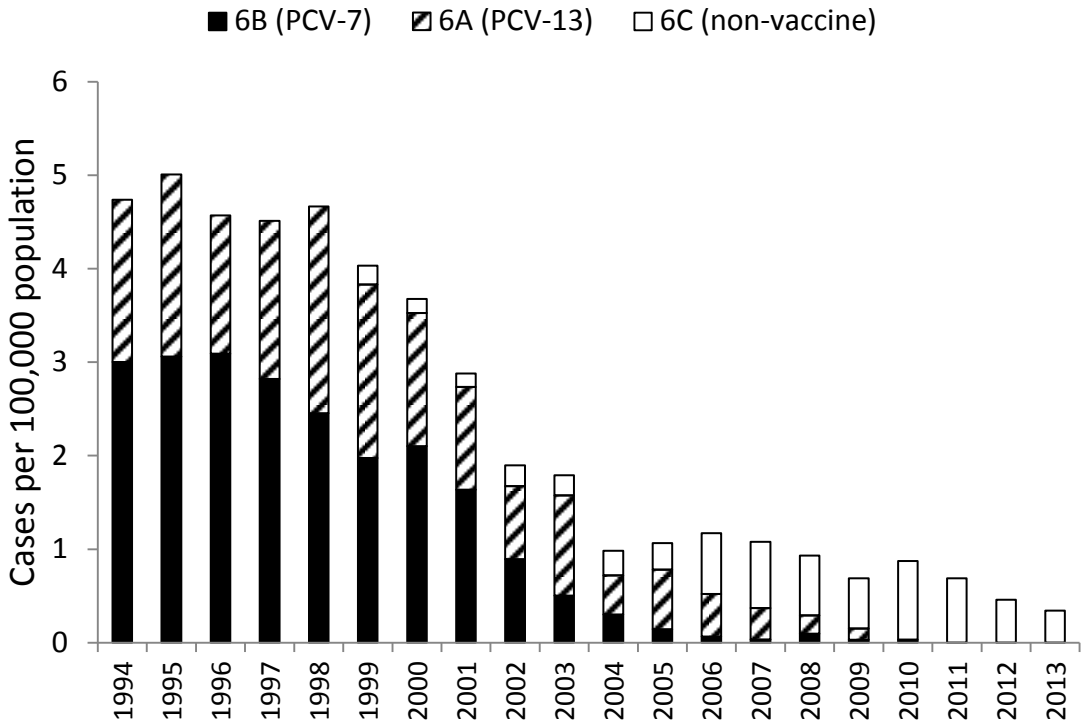
6B (PCV-7)
6A (PCV-13)
6C (non-vaccine)
Cases per 100,000 population
0
1
2
3
4
5
6
1994
1995
1996
1997
1998
1999
2000
2001
2002
2003
2004
2005
2006
2007
2008
2009
2010
2011
2012
2013

Figure 9.

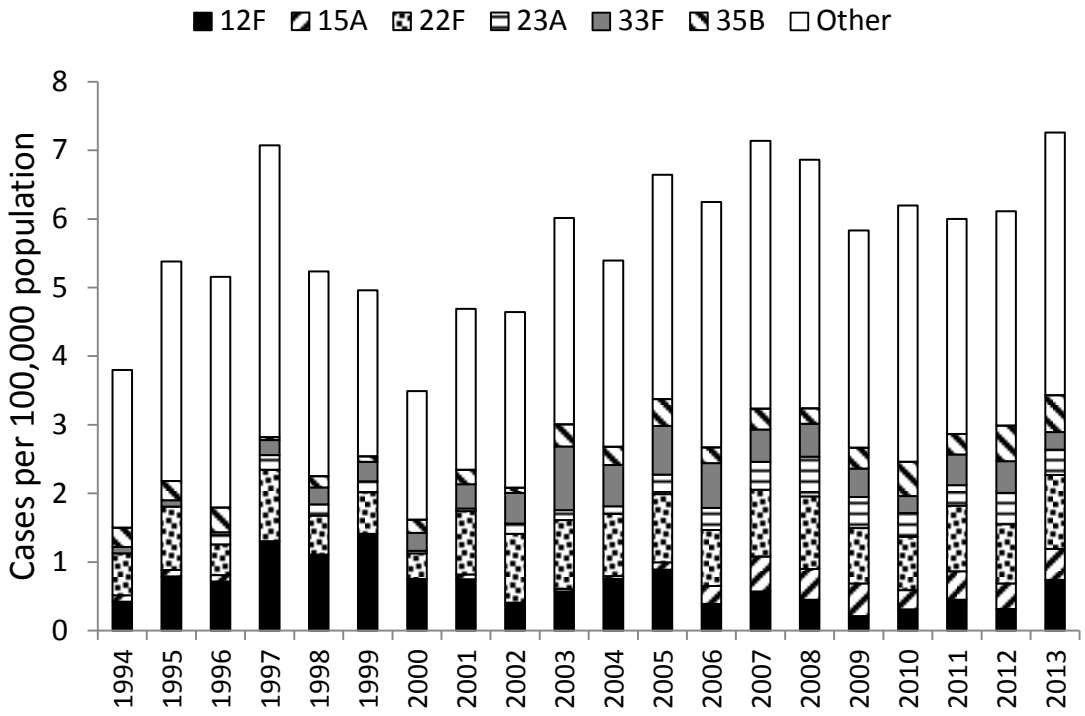
12F
15A
22F
23A
33F
35B
Other
Cases per 100,000 population
0
1
2
3
4
5
6
7
8
1994
1995
1996
1997
1998
1999
2000
2001
2002
2003
2004
2005
2006
2007
2008
2009
2010
2011
2012
2013

Table S1. Incidence of MR-IPD 2003-2013 in Atlanta, GA, by serotype. Incidence reported as cases per 100,000 population.

Incidence	2003	2004	2005	2006	2007	2008	2009	2010	2011	2012	2013
Overall IPD	14.02	12.29	12.89	13.50	13.23	12.02	11.99	11.51	9.46	8.03	8.90
MR-IPD	4.09	3.36	3.48	4.34	3.46	3.88	3.71	3.82	2.68	2.72	2.45
PCV-7 Serotypes	1.43	0.79	0.60	0.36	0.10	0.13	0.09	0.19	0.15	0.03	0.00
4	0.11	0.08	0.00	0.00	0.00	0.00	0.00	0.00	0.03	0.00	0.00
14	0.57	0.11	0.14	0.13	0.00	0.03	0.00	0.06	0.03	0.00	0.00
18C	0.00	0.00	0.00	0.00	0.00	0.00	0.00	0.00	0.00	0.00	0.00
19F	0.14	0.04	0.18	0.16	0.03	0.00	0.06	0.03	0.00	0.03	0.00
23F	0.25	0.15	0.14	0.03	0.00	0.00	0.03	0.03	0.00	0.00	0.00
6B	0.22	0.19	0.14	0.03	0.00	0.06	0.00	0.00	0.00	0.00	0.00
9V	0.14	0.23	0.00	0.00	0.07	0.03	0.00	0.06	0.09	0.00	0.00
PCV-13 Serotypes	1.61	1.73	1.88	2.51	1.83	1.92	2.30	1.88	1.08	0.77	0.51
1	0.00	0.00	0.00	0.00	0.00	0.00	0.00	0.00	0.00	0.00	0.00
3	0.11	0.08	0.04	0.13	0.03	0.00	0.09	0.16	0.00	0.15	0.09
5	0.00	0.00	0.00	0.00	0.00	0.00	0.00	0.00	0.00	0.00	0.00
19A	0.93	1.43	1.56	2.12	1.66	1.80	2.15	1.72	1.08	0.59	0.43
6A	0.57	0.23	0.28	0.23	0.10	0.13	0.06	0.00	0.00	0.00	0.00
7F	0.00	0.00	0.00	0.03	0.03	0.00	0.00	0.00	0.00	0.03	0.00
Non-vaccine Serotypes	1.04	0.83	0.99	1.47	1.53	1.83	1.32	1.75	1.39	1.92	1.93
12F	0.00	0.15	0.04	0.00	0.00	0.00	0.00	0.00	0.06	0.00	0.00
15A	0.04	0.04	0.11	0.26	0.51	0.42	0.36	0.28	0.33	0.35	0.37
15B	0.00	0.00	0.07	0.03	0.07	0.03	0.00	0.00	0.06	0.06	0.11
15B/C	0.00	0.00	0.00	0.00	0.00	0.00	0.03	0.19	0.03	0.00	0.00
15C	0.00	0.00	0.00	0.03	0.00	0.03	0.00	0.00	0.00	0.09	0.11
22F	0.00	0.00	0.00	0.07	0.00	0.13	0.09	0.13	0.03	0.15	0.17
23A	0.00	0.00	0.00	0.00	0.14	0.26	0.06	0.09	0.06	0.15	0.14
33F	0.68	0.34	0.60	0.55	0.41	0.45	0.33	0.19	0.27	0.44	0.23
35B	0.04	0.04	0.04	0.13	0.07	0.10	0.09	0.28	0.18	0.32	0.43
11A	0.07	0.08	0.00	0.10	0.03	0.10	0.03	0.19	0.09	0.12	0.17
6C	0.11	0.11	0.11	0.20	0.24	0.19	0.18	0.28	0.24	0.21	0.09
others	0.11	0.08	0.04	0.10	0.07	0.13	0.15	0.13	0.03	0.03	0.11

REFERENCES

1. **O'Brien KL, Wolfson LJ, Watt JP, Henkle E, Deloria-Knoll M, McCall N, Lee E, Mulholland K, Levine OS, Cherian T, Hib, Pneumococcal Global Burden of Disease Study T.** 2009. Burden of disease caused by *Streptococcus pneumoniae* in children younger than 5 years: global estimates. Lancet **374:**893-902.

2. **Hyde TB, Gay K, Stephens DS, Vugia DJ, Pass M, Johnson S, Barrett NL, Schaffner W, Cieslak PR, Maupin PS, Zell ER, Jorgensen JH, Facklam RR, Whitney CG.** 2001. Macrolide resistance among invasive *Streptococcus pneumoniae* isolates. JAMA **286:**1857-1862.

3. **Stephens DS, Zughaier SM, Whitney CG, Baughman WS, Barker L, Gay K, Jackson D, Orenstein WA, Arnold K, Schuchat A, Farley MM.** 2005. Incidence of macrolide resistance in *Streptococcus pneumoniae* after introduction of the pneumococcal conjugate vaccine: population-based assessment. Lancet **365:**855-863.

4. **Bergman M, Huikko S, Huovinen P, Paakkari P, Seppala H.** 2006. Macrolide and azithromycin use are linked to increased macrolide resistance in *Streptococcus pneumoniae*. Antimicrob Agents Chemother **50:**3646-3650.

5. **Hawkins PA, Chochua S, Jackson D, Beall B, McGee L.** 2015. Mobile elements and chromosomal changes associated with MLS resistance phenotypes of invasive pneumococci recovered in the United States. Microb Drug Resist **21:**121-129.

6. **Tait-Kamradt A, Clancy J, Cronan M, Dib-Hajj F, Wondrack L, Yuan W, Sutcliffe J.** 1997. *mefE* is necessary for the erythromycin-resistant M phenotype in *Streptococcus pneumoniae*. Antimicrob Agents Chemother **41:**2251-2255.

7. **Gay K, Stephens DS.** 2001. Structure and dissemination of a chromosomal insertion element encoding macrolide efflux in *Streptococcus pneumoniae*. J Infect Dis **184:**56-65.

8. **Weisblum B.** 1995. Erythromycin resistance by ribosome modification. Antimicrob Agents Chemother **39:**577-585.

9. **Gay K, Baughman W, Miller Y, Jackson D, Whitney CG, Schuchat A, Farley MM, Tenover F, Stephens DS.** 2000. The emergence of *Streptococcus pneumoniae* resistant to macrolide antimicrobial agents: a 6-year population-based assessment. J Infect Dis **182:**1417-1424.

10. **Rudolph K, Bulkow L, Bruce M, Zulz T, Reasonover A, Harker-Jones M, Hurlburt D, Hennessy T.** 2013. Molecular resistance mechanisms of macrolide-resistant invasive *Streptococcus pneumoniae* isolates from Alaska, 1986 to 2010. Antimicrob Agents Chemother **57:**5415-5422.

11. **Chancey ST, Agrawal S, Schroeder MR, Farley MM, Tettelin H, Stephens DS.** 2015. Composite mobile genetic elements disseminating macrolide resistance in *Streptococcus pneumoniae*. Front Microbiol **6:**26.

12. **Del Grosso M, Northwood JG, Farrell DJ, Pantosti A.** 2007. The macrolide resistance genes *erm*(B) and *mef*(E) are carried by Tn*2010* in dual-gene *Streptococcus pneumoniae* isolates belonging to clonal complex CC271. Antimicrob Agents Chemother **51:**4184-4186.

13. **Advisory Committee on Immunization Practices.** 2000. Preventing pneumococcal disease among infants and young children. Recommendations of the Advisory Committee on Immunization Practices (ACIP). MMWR Recomm Rep **49:**1-35.

14. **Rodgers GL, Klugman KP.** 2011. The future of pneumococcal disease prevention. Vaccine **29S:**C43-C48.

15. **Beall B, McEllistrem MC, Gertz RE, Jr., Wedel S, Boxrud DJ, Gonzalez AL, Medina MJ, Pai R, Thompson TA, Harrison LH, McGee L, Whitney CG.** 2006. Pre- and postvaccination clonal compositions of invasive pneumococcal serotypes for isolates collected in the United States in 1999, 2001, and 2002. J Clin Microbiol **44:**999-1017.

16. **Mahjoub-Messai F, Doit C, Koeck JL, Billard T, Evrard B, Bidet P, Hubans C, Raymond J, Levy C, Cohen R, Bingen E.** 2009. Population snapshot of *Streptococcus pneumoniae* serotype 19A isolates before and after introduction of seven-valent pneumococcal vaccination for French children. J Clin Microbiol **47:**837-840.

17. **Li Y, Tomita H, Lv Y, Liu J, Xue F, Zheng B, Ike Y.** 2011. Molecular characterization of *erm*(B)- and *mef*(E)-mediated erythromycin-resistant *Streptococcus pneumoniae* in China and complete DNA sequence of Tn*2010*. J Appl Microbiol **110:**254-265.

18. **CDC.** 2010. Licensure of a 13-valent pneumococcal conjugate vaccine (PCV13) and recommendations for use among children - Advisory Committee on

Immunization Practices (ACIP), 2010. MMWR Morb Mortal Wkly Rep **59:**258-261.

19. **Desai AP, Sharma D, Crispell EK, Baughman W, Thomas S, Tunali A, Sherwood L, Zmitrovich A, Jerris R, Satola SW, Beall B, Moore MR, Jain S, Farley MM.** 2015. Decline in pneumococcal nasopharyngeal carriage of vaccine serotypes after the introduction of the 13-valent pneumococcal conjugate vaccine in children in Atlanta, Georgia. Pediatr Infect Dis J **34:**1168-1174.

20. **Moore MR, Link-Gelles R, Schaffner W, Lynfield R, Lexau C, Bennett NM, Petit S, Zansky SM, Harrison LH, Reingold A, Miller L, Scherzinger K, Thomas A, Farley MM, Zell ER, Taylor TH, Jr., Pondo T, Rodgers L, McGee L, Beall B, Jorgensen JH, Whitney CG.** 2015. Effect of use of 13-valent pneumococcal conjugate vaccine in children on invasive pneumococcal disease in children and adults in the USA: analysis of multisite, population-based surveillance. Lancet Infect Dis **15:**301-309.

21. **Hofmann J, Cetron MS, Farley MM, Baughman WS, Facklam RR, Elliott JA, Deaver KA, Breiman RF.** 1995. The prevalence of drug-resistant *Streptococcus pneumoniae* in Atlanta. N Engl J Med **333:**481-486.

22. **Schuchat A, Hilger T, Zell E, Farley MM, Reingold A, Harrison L, Lefkowitz L, Danila R, Stefonek K, Barrett N, Morse D, Pinner R, Network ABCSTotEIP.** 2001. Active bacterial core surveillance of the emerging infections program network. Emerg Infect Dis **7:**92-99.

23. **CLSI.** 2012. Methods for dilution antimicrobial susceptibility tests for bacteria that grow aerobically; approved standard-Ninth Edition. CLSI document M07-A9. Clinical and Laboratory Standards Institute.

24. **Chancey ST, Bai X, Kumar N, Drabek EF, Daugherty SC, Colon T, Ott S, Sengamalay N, Sadzewicz L, Tallon LJ, Fraser CM, Tettelin H, Stephens DS.** 2015. Transcriptional attenuation controls macrolide inducible efflux and resistance in *Streptococcus pneumoniae* and in other Gram-positive bacteria containing *mef*/*mel*(*msr*(D)) elements. PLoS One **10:**e0116254.

25. **Jolley KA, Maiden MC.** 2010. BIGSdb: Scalable analysis of bacterial genome variation at the population level. BMC Bioinformatics **11:**595.

26. **Whitney CG, Farley MM, Hadler J, Harrison LH, Bennett NM, Lynfield R, Reingold A, Cieslak PR, Pilishvili T, Jackson D, Facklam RR, Jorgensen JH, Schuchat A, Active Bacterial Core Surveillance of the Emerging Infections Program N.** 2003. Decline in invasive pneumococcal disease after the introduction of protein-polysaccharide conjugate vaccine. N Engl J Med **348:**1737-1746.

27. **Simell B, Auranen K, Kayhty H, Goldblatt D, Dagan R, O'Brien KL.** 2012. The fundamental link between pneumococcal carriage and disease. Expert Rev Vaccines **11:**841-855.

28. **Lexau CA, Lynfield R, Danila R, Pilishvili T, Facklam R, Farley MM, Harrison LH, Schaffner W, Reingold A, Bennett NM, Hadler J, Cieslak PR, Whitney CG.** 2005. Changing epidemiology of invasive pneumococcal disease

among older adults in the era of pediatric pneumococcal conjugate vaccine. JAMA **294:**2043-2051.

29. **Rosen JB, Thomas AR, Lexau CA, Reingold A, Hadler JL, Harrison LH, Bennett NM, Schaffner W, Farley MM, Beall BW, Moore MR.** 2011. Geographic variation in invasive pneumococcal disease following pneumococcal conjugate vaccine introduction in the United States. Clin Infect Dis **53:**137-143.

30. **Schuck-Paim C, Taylor R, Lindley D, Klugman KP, Simonsen L.** 2013. Use of near-real-time medical claims data to generate timely vaccine coverage estimates in the US: the dynamics of PCV13 vaccine uptake. Vaccine **31:**5983-5988.

31. **Tomczyk S, Bennett NM, Stoecker C, Gierke R, Moore MR, Whitney CG, Hadler S, Pilishvili T.** 2014. Use of 13-valent pneumococcal conjugate vaccine and 23-valent pneumococcal polysaccharide vaccine among adults aged >/=65 years: recommendations of the Advisory Committee on Immunization Practices (ACIP). MMWR Morb Mortal Wkly Rep **63:**822-825.

32. **Bonten MJ, Huijts SM, Bolkenbaas M, Webber C, Patterson S, Gault S, van Werkhoven CH, van Deursen AM, Sanders EA, Verheij TJ, Patton M, McDonough A, Moradoghli-Haftvani A, Smith H, Mellelieu T, Pride MW, Crowther G, Schmoele-Thoma B, Scott DA, Jansen KU, Lobatto R, Oosterman B, Visser N, Caspers E, Smorenburg A, Emini EA, Gruber WC, Grobbee DE.** 2015. Polysaccharide conjugate vaccine against pneumococcal pneumonia in adults. N Engl J Med **372:**1114-1125.

33. **Albrich WC, Baughman W, Schmotzer B, Farley MM.** 2007. Changing characteristics of invasive pneumococcal disease in Metropolitan Atlanta, Georgia, after introduction of a 7-valent pneumococcal conjugate vaccine. Clin Infect Dis **44:**1569-1576.

34. **Malhotra-Kumar S, Lammens C, Coenen S, Van Herck K, Goossens H.** 2007. Effect of azithromycin and clarithromycin therapy on pharyngeal carriage of macrolide-resistant streptococci in healthy volunteers: a randomised, double-blind, placebo-controlled study. Lancet **369:**482-490.

35. **Park IH, Moore MR, Treanor JJ, Pelton SI, Pilishvili T, Beall B, Shelly MA, Mahon BE, Nahm MH.** 2008. Differential effects of pneumococcal vaccines against serotypes 6A and 6C. J Infect Dis **198:**1818-1822.

36. **Corso A, Severina EP, Petruk VF, Mauriz YR, Tomasz A.** 1998. Molecular characterization of penicillin-resistant *Streptococcus pneumoniae* isolates causing respiratory disease in the United States. Microb Drug Resist **4:**325-337.

37. **Luna VA, Coates P, Eady EA, Cove JH, Nguyen TT, Roberts MC.** 1999. A variety of gram-positive bacteria carry mobile *mef* genes. J Antimicrob Chemother **44:**19-25.

38. **Nishijima T, Saito Y, Aoki A, Toriya M, Toyonaga Y, Fujii R.** 1999. Distribution of *mefE* and *ermB* genes in macrolide-resistant strains of *Streptococcus pneumoniae* and their variable susceptibility to various antibiotics. J Antimicrob Chemother **43:**637-643.

39. **Bowers JR, Driebe EM, Nibecker JL, Wojack BR, Sarovich DS, Wong AH, Brzoska PM, Hubert N, Knadler A, Watson LM, Wagner DM, Furtado MR,**

Saubolle M, Engelthaler DM, Keim PS. 2012. Dominance of multidrug resistant CC271 clones in macrolide-resistant *Streptococcus pneumoniae* in Arizona. BMC Microbiol **12:**12.

40. **Pan F, Han L, Huang W, Tang J, Xiao S, Wang C, Qin H, Zhang H.** 2015. Serotype Distribution, Antimicrobial Susceptibility, and Molecular Epidemiology of *Streptococcus pneumoniae* Isolated from Children in Shanghai, China. PLoS One **10:**e0142892.

41. **Xiao Y, Wei Z, Shen P, Ji J, Sun Z, Yu H, Zhang T, Ji P, Ni Y, Hu Z, Chu Y, Li L.** 2015. Bacterial-resistance among outpatients of county hospitals in China: significant geographic distinctions and minor differences between central cities. Microbes Infect **17:**417-425.

Chapter 3: Composite mobile genetic elements disseminating macrolide resistance in *Streptococcus pneumoniae*

Scott T. Chancey[1,2], Sonia Agrawal[3], Max R. Schroeder[1,2], Monica M. Farley[1,2], Hervé Tettelin[3,4] and David S. Stephens[1,2]

[1]Division of Infectious Diseases, Department of Medicine, Emory University School of Medicine, Atlanta, GA, USA, [2]Laboratories of Microbial Pathogenesis, Department of Veterans Affairs Medical Center, Atlanta, GA, USA, [3]Institute for Genome Sciences, University of Maryland School of Medicine, Baltimore, MD, USA, [4]Department of Microbiology and Immunology, University of Maryland School of Medicine, Baltimore, MD, USA

Published in

Frontiers in Microbiology

February 2015 Volume 6 Article 26 pages 1-14

M.R.S. contributed to the data analysis and interpretation and assisted with writing and editing the paper.

frontiers in MICROBIOLOGY

ORIGINAL RESEARCH ARTICLE
published: 09 February 2015
doi: 10.3389/fmicb.2015.00026

Composite mobile genetic elements disseminating macrolide resistance in *Streptococcus pneumoniae*

Scott T. Chancey[1,2], Sonia Agrawal[3], Max R. Schroeder[1,2], Monica M. Farley[1,2], Hervé Tettelin[3,4†] and David S. Stephens[1,2*†]

[1] Division of Infectious Diseases, Department of Medicine, Emory University School of Medicine, Atlanta, GA, USA
[2] Laboratories of Microbial Pathogenesis, Department of Veterans Affairs Medical Center, Atlanta, GA, USA
[3] Institute for Genome Sciences, University of Maryland School of Medicine, Baltimore, MD, USA
[4] Department of Microbiology and Immunology, University of Maryland School of Medicine, Baltimore, MD, USA

Edited by:
Claudio Palmieri, Polytechnic University of Marche, Italy

Reviewed by:
Agnese Lupo, University of Bern, Switzerland
Kelly L. Wyres, IBM Research - Australia, Australia

***Correspondence:**
David S. Stephens, Division of Infectious Diseases, Department of Medicine, Emory University School of Medicine, Atlanta, GA, USA; Laboratories of Microbial Pathogenesis, Department of Veterans Affairs Medical Center, Atlanta, GA, USA
e-mail: dstep01@emory.edu

† These authors have contributed equally to this work.

Macrolide resistance in *Streptococcus pneumoniae* emerged in the U.S. and globally during the early 1990's. The RNA methylase encoded by *erm*(B) and the macrolide efflux genes *mef*(E) and *mel* were identified as the resistance determining factors. These genes are disseminated in the pneumococcus on mobile, often chimeric elements consisting of multiple smaller elements. To better understand the variety of elements encoding macrolide resistance and how they have evolved in the pre- and post-conjugate vaccine eras, the genomes of 121 invasive and ten carriage isolates from Atlanta from 1994 to 2011 were analyzed for mobile elements involved in the dissemination of macrolide resistance. The isolates were selected to provide broad coverage of the genetic variability of antibiotic resistant pneumococci and included 100 invasive isolates resistant to macrolides. Tn*916*-like elements carrying *mef*(E) and *mel* on the Macrolide Genetic Assembly (Mega) and *erm*(B) on the *erm*(B) element and Tn*917* were integrated into the pneumococcal chromosome backbone and into larger Tn*5253*-like composite elements. The results reported here include identification of novel insertion sites for Mega and characterization of the insertion sites of Tn*916*-like elements in the pneumococcal chromosome and in larger composite elements. The data indicate that integration of elements by conjugation was infrequent compared to recombination. Thus, it appears that conjugative mobile elements allow the pneumococcus to acquire DNA from distantly related bacteria, but once integrated into a pneumococcal genome, transformation and recombination is the primary mechanism for transmission of novel DNA throughout the pneumococcal population.

Keywords: mobile genetic elements, transposons, integrative and conjugative elements, macrolides, antibiotic resistance, *Streptococcus pneumoniae*

INTRODUCTION

Streptococcus pneumoniae, the pneumococcus, remains a significant risk to human health. Treatment of pneumococcal disease has been hindered by emergence of resistance to the key antibiotics (Klugman and Lonks, 2005). Macrolide resistance in pneumococci emerged throughout the 1990's, a process that has been documented in the Atlanta, Georgia, USA metropolitan area by an ongoing prospective-based surveillance of invasive pneumococcal disease by the Georgia Emerging Infections Program (Farley et al., 2002). A high incidence of efflux-mediated macrolide resistance was observed in serotypes prior to the introduction of the Seven-valent Pneumococcal Conjugate Vaccine (PCV7) in the Atlanta area in late 2000 (Gay et al., 2000; Stephens et al., 2005). PCV7 targets capsular polysaccharides of seven serotypes 4, 6B, 9V, 14, 18C, 19F, and 23F (Stephens et al., 2005). Expansion of these serotypes prior to PCV7 was a major driver of increased macrolide resistance in Atlanta (Stephens et al., 2005).

Most macrolide resistance in *S. pneumoniae* is conferred by the efflux genes *mef*(E) and *mel* or the target-modifying RNA methylase gene *erm*(B). The *mef*(E)/*mel* operon confers the M-phenotype, that is, resistance to 14- and 15-membered macrolides but not lincosamides or streptogramin B (Leclercq and Courvalin, 1991). Erm(B) confers resistance to macrolides, lincosamides and streptogramin B (MLS_B antibiotics) which is the MLS_B-phenotype (Syrogiannopoulos et al., 2003). The dissemination of macrolide resistance genes in pneumococci has been aided by mobile genetic elements (MGE). The *mef*(E) and *mel* genes are located on the Macrolide Genetic Assembly, Mega (Gay and Stephens, 2001). Mega can be 5.5 kb (Mega-1) or 5.4 kb (Mega-2) based on the size of the *mef*(E)/*mel* intergenic region. Expression of the *mef*(E)/*mel* operon is controlled by transcriptional attenuation and is inducible by 15- and 16-membered macrolides (Ambrose et al., 2005; Wierzbowski et al., 2005). Immediately downstream and convergent to the *mef*(E)/*mel* operon are four co-transcribed open reading frames, *orfs 3-6*. This operon has organization and sequence similarity to a SOS-responsive operon on the pneumococcal conjugative transposons Tn*5252* and Tn*5253* (Munoz-Najar and Vijayakumar, 1999; Gay

and Stephens, 2001). Tn*5253*, which is Tn*5252* with a Tn*916*-like insertion, is the prototype for a series of Tn*5253*-like integrative and conjugative element (ICE). It is one of two ICE demonstrated to carry macrolide resistance determinants in pneumococci (Ayoubi et al., 1991; Croucher et al., 2014; Mingoia et al., 2014). The other ICE commonly associated with macrolide resistance is ICE*Sp*23FST81 (Croucher et al., 2009).

The Mega element has integrated into at least four loci in the pneumococcal chromosome. Mega insertion classes I–IV were originally identified in US isolates (Gay and Stephens, 2001) and were also observed in Europe (Del Grosso et al., 2006). The class I Mega insertion site is in a homolog of the *S. pneumoniae* TIGR4 gene SP_1598 encoding a phosphomethylpyrimidine kinase predicted to be involved in thiamine biosynthesis (Gay and Stephens, 2001). Class II insertions are in a DNA-methyladenine glycosidase (SP_0180) and class III are in *capA* (SP_0103) located in the capsule biosynthesis locus. Class IV is in the RNA-methyltransferase *rumA* (SP_1029) located at the left flank of the pneumococcal pathogenicity island (PPI-1) (Brown et al., 2001).

In addition to the locations in the pneumococcal chromosome backbone, Mega has integrated into *orf6* of Tn*916*, a 18.0 kb conjugative transposon associated with tetracycline resistance due to the presence of *tet*(M) (Roberts and Mullany, 2011). Tn*916* has been enlisted to disseminate macrolide resistance in many forms. The Tn*916*-like element carrying Mega inserted into *orf6* is Tn*2009* (Del Grosso et al., 2004). A Tn*916*-like element with a 2.8 kb fragment carrying *erm*(B), named "*erm*(B) element," inserted into Tn*916 orf20* is Tn*6002* (Cochetti et al., 2007) (**Figure 1**). A Tn*916*-like element harboring both *orf6*::Mega and *orf20*::*erm*(B) is Tn*2010* (Del Grosso et al., 2007) (**Figure 1**). The fact that the two smaller cassettes are inserted into the same locations in the different Tn*916*-like elements suggests either a very specific target sequence leading to multiple identical insertions, or that Tn*2010* is linked to Tn*2009* and Tn*6002* through recombination of macrolide resistance-conferring MGE. The same is true for Tn*2009*, Tn*3872*, and Tn*2017*. Tn*3872* and Tn*2017* are Tn*916*-like elements with *orf9* disrupted by Tn*917*, a 5.3 kb transposon-related element carrying *erm*(B) (McDougal et al., 1998). Tn*2017* is nearly identical to Tn*3872*, but also contains Mega integrated into Tn*916 orf6* (Del Grosso et al., 2009). The apparent interchangeability of the smaller macrolide resistance elements raises a question regarding the relative roles of conjugation and recombination in the dissemination of macrolide resistance and the evolution in the pneumococcus. *S. pneumoniae* is a naturally competent bacterium and is extremely proficient at acquiring and incorporating exogenous DNA into its genome (Berge et al., 2002; Claverys et al., 2006; Prudhomme et al., 2006). On the other hand, macrolide resistance-encoding Tn*916*-like elements appear to be incapable of pneumococcus-to-pneumococcus conjugation (Del Grosso et al., 2004; Zhou et al., 2014). Tn*2009* and Tn*2010* are non-conjugative while Tn*6002* is conjugative but at very low frequencies (Del Grosso et al., 2004, 2007; Cochetti et al., 2007). Conjugative transfer of Mega from *S. salivarius*, however, has been observed, but only from a host strain with a co-resident conjugative transposon (Santagati et al., 2009). How important is DNA acquisition by conjugation in the pneumococcus, which is so proficient at transformation and recombination?

In the present study we utilized comparative genomics to identify the mobile elements involved in dissemination of macrolide resistance in a geographically defined population. We sequenced the genomes of 147 pneumococcal isolates, including 131 invasive and carriage isolates collected in Atlanta, Georgia over an 18 year period spanning the pre- and post-conjugative vaccine era (McDougal et al., 1998; Cochetti et al., 2008). The goal of this study was to make a broad survey of the genomic diversity in the pneumococcal clones circulating in the Atlanta metropolitan area in pre- and post-PCV7 eras, and to document the MGE

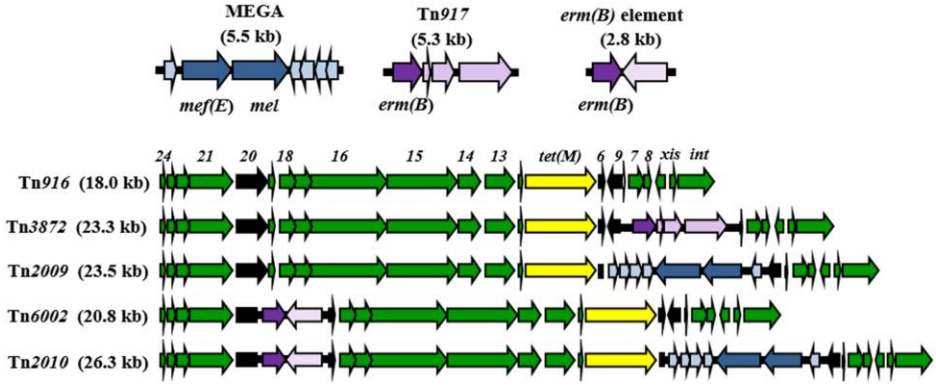

FIGURE 1 | Macrolide resistance determinants associated with mobile elements in pneumococci. Conjugative transposon Tn*916* and Tn*916*-like mosaic elements carrying Mega (blue), and *erm*(B) on the *erm*(B) element and Tn*917* (purple). The yellow arrows indicate *tet*(M) encoding tetracycline resistance. Black arrows indicate insertion sites.

that promoted the dissemination of macrolide resistance genes. By analyzing the genetic organization and the integration sites of the elements in relation to the clonal lineage and serotype of the isolates that harbor them, we hoped to gain a better understanding of the relative roles of conjugation and transformation in the evolution and dissemination of macrolide resistance in *S. pneumoniae*.

MATERIALS AND METHODS

BACTERIAL STRAINS

Atlanta invasive *S. pneumoniae* isolates were obtained from the Georgia Emerging Infections Program and were isolated from patients in Atlanta, Georgia as part of an ongoing, prospective, population-based surveillance study (Farley et al., 2002). Macrolide resistant isolates were assayed for the presence of macrolide resistance genes *mef*(E), *mel* and *erm*(B) by PCR as previously described (Stephens et al., 2005). One hundred and twenty one isolates recovered from patients between 1994 and 2011 were non-randomly selected for whole genome sequencing (Table S1). Selection criteria included capsule serotype, antibiotic resistance, macrolide resistance genes, and date of isolation. In addition to macrolide resistance, clindamycin, tetracycline, and chloramphenicol were considered indicators of mobile elements. Sequence type was also considered if available (see below). Thirteen invasive pneumococcal isolates from U.S. states other than Georgia were provided by the Antimicrobial Bacterial Core Surveillance Program and the Centers for Disease Control and Prevention (CDC) (McCormick et al., 2003). These included four isolates from Maryland, two each from Connecticut, Oregon, and Minnesota, and one each from California, New York, and Tennessee. Three invasive isolates, two from Europe and one from the North Carolina, were provided by the Pneumococcal Molecular Epidemiology Network (PMEN) (McGee et al., 2001). Finally, the study was supplemented with 10 carriage isolates collected from the Atlanta population; five each isolated pre-PCV7 (1995) and post-PCV7 (2009) (Sharma et al., 2013). Carriage isolates were collected from nasopharyngeal swabs of healthy children between the ages of 5 months and 5 years old (Sharma et al., 2013). The total number of sequenced pneumococcal genomes was 147 (Table S1).

CHARACTERIZATION OF ISOLATES

The capsule serotype of each isolate was determined by the institution from which it was acquired and verified by analyses of the capsule locus in the genome sequence. Minimal inhibitory concentrations (MIC) of erythromycin, clindamycin, tetracycline, and chloramphenicol were determined by microdilution or Etest (bioMerieux Inc., Durham, NC). The Multi Locus Sequence Type (MLST) of selected isolates was determined by Sanger nucleotide sequencing of PCR products with MLST allele-specific primers as previously described (Enright and Spratt, 1998). The sequence types of the remaining isolates were determined from allelic data extracted from their genomes. Isolates were assigned to a clonal complex based on eBURST analysis of the complete *S. pneumoniae* MLST database as of September, 2014 (http://pubmlst.org/spneumoniae/).

GENOME SEQUENCING

For each isolate sequenced, two shotgun libraries were constructed for 454 sequencing: one rapid non-paired-end library for coverage and one 3 kb paired-end library for assembly scaffolding. All isolates were sequenced using the 454 GS FLX Titanium to a depth of sequence coverage ranging from 16× to 57×. Shotgun reads were assembled into 4–32 contigs per isolate using Celera Assembler v6.1 (Myers et al., 2000). Genome sequences have been deposited in the GenBank Nucleotide Sequence Database (http://www.ncbi.nlm.nih.gov/) (Table S1) and the PathoSystems Resource Integration Center (PATRIC) (Wattam et al., 2014). Isolates are available through the American Type Culture Collection-managed Biodefense and Emerging Infections Resources repository (http://www.beiresources.org).

WHOLE GENOME ALIGNMENT AND PHYLOGENETIC TREE CONSTRUCTION

Two high throughput reference-based pipelines were used to perform single nucleotide polymorphism (SNP) discovery and validation in 166 genomes using the TIGR4 genome as a reference (Tettelin et al., 2001). The genomes included the 147 from the present project plus 15 publicly available, closed, pneumococcal genomes and four whole genome shotgun sequences from this project that were later excluded from this study due to the lack of associated meta-data (Table S1). The analysis pipelines made extensive use of Perl (https://www.perl.org) scripts and were implemented within the Ergatis framework (https://github.com/jorvis/ergatis) (Orvis et al., 2010). The alignment-based SNP discovery pipeline named Skirret mainly executes a series of utilities from the MUMmer 3.0 package (http://mummer.sourceforge.net/) (Kurtz et al., 2004) namely nucmer, delta-filter and show-SNPs to determine SNP positions. This pipeline was run on all 166 assembled genomes with a minimum alignment identity of 98%. A k-mer based algorithm called kSNP (http://sourceforge.net/projects/ksnp/) (Gardner and Hall, 2013) was also employed to identify SNPs in the assembled genomes using 41 bp as the length of the k-mer. Next, a BLAST-based validation pipeline was used to merge the SNP panels from the Skirret and kSNP pipelines and 41 bp sequence surrounding each SNP position was extracted from the reference TIGR4 genome. These short sequences were searched against all 166 genomes using all-vs.-all BLASTN searches (*e*-value cut-off 0.0001) to eliminate false positive SNP calls, only core SNPs in short sequences found in all 166 genomes were selected. Putative recombinogenic regions were not excluded. The set of 10,120 core SNP bases were concatenated from each of the input genomes to create a multi-FASTA file. This file was used for phylogenetic tree construction using the Geneious Basic software version 5.6.4 with neighbor-joining and the Hasegawa, Kishino and Yano (HKY) genetic distance model. The HKY model assumes that every base has a different equilibrium base frequency, and also assumes that transitions evolve at a different rate to transversions. A consensus tree was built based on 100 iterations to provide an estimate for the level of support for each clade in the final tree. We used a 100% consensus support threshold that resulted in a strict consensus tree where the clades included were those that were present in all the trees of the original set.

IDENTIFICATION AND CHARACTERIZATION OF MOBILE ELEMENTS

Mega and Mega insertion sites were located by comparing genomes with the 5,511 bp Mega element from strain GA17457 (Data File S1). ICE were identified by BLASTN (Altschul et al., 1997) search of the terminal direct repeats localized at the ends transposons ICE*Sp*23FST81 (81.0 kb; Accession no. FM211187), Tn*5253* (66.2 kb; Accession no. EU351020) (Iannelli et al., 2014), Tn*916* (18.0 kb; Accession no. U49939) and others. Elements were characterized by the *int* genes they carried. Integrase genes were identified by BLASTN search with query sequences from described ICE including those mentioned above. All query sequences used are supplied as supporting information (Data File S1). Comparisons of composite ICE were visualized with the Artemis Comparison Tool (Carver et al., 2005). Genomes were also searched for antibiotic resistance genes, including *mef*(E), *mef*(A), *mel*(*msr*(D)), *erm*(B), *erm*(A), *tet*(M) and *cat* (Data File S1). The nucleotide sequences of each Mega, Tn*916*-like and composite elements are provided as supporting information (Data Files S2, S3 and S4, respectively).

RESULTS

WHOLE GENOME COMPARISONS

Isolates of *S. pneumoniae* were selected from the >13,000 strain collection of the Georgia Emerging Infections Program. Isolates were collected as part of an ongoing, prospective, population-based surveillance of invasive pneumococcal disease (IPD) in the Atlanta metropolitan area (Farley et al., 2002). One hundred and twenty one invasive *S. pneumoniae* isolates from 1994 to 2011 were non-randomly selected for genome sequencing. Isolates were selected to provide broad coverage of the genotypes existing in the population during the surveillance period, but with a focus on macrolide resistance, with 100 resistant to erythromycin (MIC >1 μg/ml). 74 displayed the M-phenotype as indicated by susceptibility to the lincosamide clindamycin and 24 were also resistant to clindamycin (MLS_B-phenotype) (Table S1). In addition to the Atlanta invasive isolates, 10 carriage isolates from Atlanta were included. Also included were 16 strains not from Atlanta. For more detail, please see the Material Methods and supporting information (Table S1). In total 147 pneumococcal genomes were sequenced including 23 different serotypes, 77 multi-locus sequence types (ST), 24 clonal complexes (CC) and two singletons (Table S1).

The 147 isolates from this study and 15 publically available genomes were compared using whole genome single nucleotide polymorphism (SNP) analyses. The resulting phylogenetic tree is shown in **Figure 2**. The genomes clustered into MLST clonal complexes with the exception of CC156 which was divided into three clades (**Figure 2**). This may be an example of a limitation of MLST typing as the three clusters appear to be unrelated. CC156 is a large complex consisting of multiple subgroups thus not all were as closely related as the label CC156 implied (Figure S1). For example ST90 has only one allele in common with ST156. However, it was interesting to observe that two of the CC156 subgroups appear to be linked by a common Mega insertion event (see below). Further, the eBURST-predicted subgroups (SG90, SG124 and SG156) are well-established independent clonal complexes (CC90, CC124 and CC156, respectively) indicating that their inclusion into a single clonal complex is an artifact of eBURST and not a true indication of common ancestry.

DISTRIBUTION OF THE MACROLIDE RESISTANCE-ENCODING ELEMENT MEGA

Of the Atlanta invasive isolates, 86 contained Mega integrated into the pneumococcal chromosome backbone or nested within larger mobile elements. Mega was found in 17 serotypes, 16 clonal complexes and two singletons (**Table 1**). Of these, 48 carried the 5,511 kb Mega type 1 (Mega-1) with a 119 bp *mef*(E)/*mel* intergenic region and 38 carried the 5,412 kb Mega type 2 (Mega-2) with a 99 bp deletion in the intergenic region (**Table 1**). The genome of GA07643 contained a previously unidentified 5,617 bp Mega variant, designated Mega-3, characterized by a 107 bp tandem duplication that included the first 90 bp of *mel* and 23 bp upstream containing its ribosomal binding site (RBS). Analyses of the 454 raw reads revealed that both copies of the repeated sequence were contained on single reads and the tandem duplication region had greater than 40× sequence coverage. This confirmed that the duplication was not an assembly error. The authentic duplication resulted in an intergenic region that contained the 119 bp that immediately follows *mef*(E) in Mega-1, followed by a 38 codon ORF that includes the first 30 amino acids of Mel. The ORF had the *mel* RBS and appeared suitable for protein expression. Theoretically this could have a polar effect of *mel* translation, however, GA07643 had an erythromycin MIC of >16 μg/ml so it does not appear to have had a negative impact on resistance (Table S1). The full-length copy of *mel* overlapped the 3′ end of the duplicated ORF by 10 bp and maintained the native *mel* RBS. There was no correlation between the size of the *mef*(E)/*mel* intergenic region and the level of efflux-mediated erythromycin expressed by that strain (data not shown).

Mega was found inserted into each of the four previously identified insertion sites within the pneumococcal chromosome backbone (classes I-IV) (Gay and Stephens, 2001), in Tn*916*-like elements (class V), and in one novel site (**Table 1**). Six genomes contained Mega integrated into the class I insertion site, five of which were clonal (6A, CC2090) indicating clonal dissemination (**Figure 2**, light blue dots; **Table 1**). The exception was GA17457, a serotype 19A, CC199 isolate that has been used as the genetic background for studying the regulation of *mef*(E) and *mel* (Zähner et al., 2010; Chancey et al., 2011). GA17457 was closely related to four isolates in CC199 that contained Mega-1 in class III sites (Mega-1.III) and was the only CC199 strain to have Mega-1 integrated into class I (Mega-1.I) (**Figure 2**). Class II Mega insertions were identified in 38 genomes (**Table 1**). The elements inserted into this site include Mega-1 ($n = 2$), Mega-2 ($n = 35$) and the novel Mega-3 in strain GA07643 (**Table 1**). Mega-1.III was found in ten genomes in diverse backgrounds: five serotypes and four clonal complexes (**Table 1**). Mega class III insertions clustered mainly in CC199 but single isolates containing Mega-1.III were identified in CC156, CC81, and CC62 (**Figure 2**). Five genomes contained Mega-1 or Mega-2 inserted into the class IV site which was divided into three subclasses, IVa, IVb, and IVc (see below).

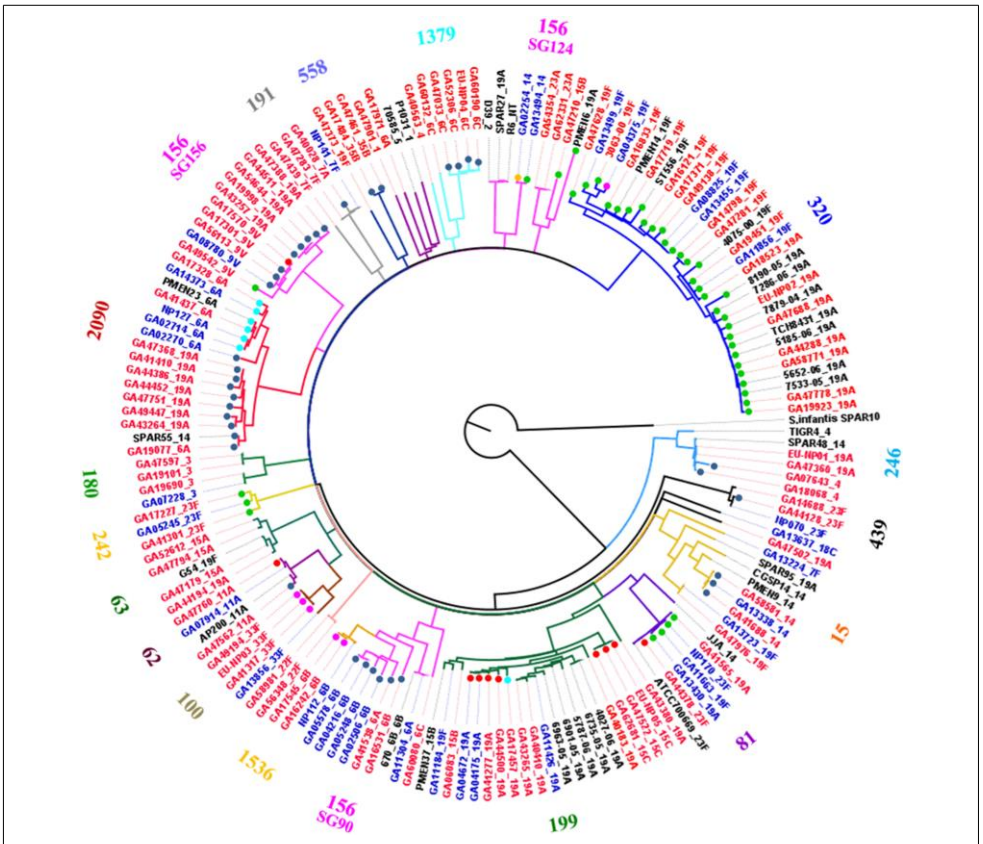

FIGURE 2 | Whole genome SNP-derived phylogenetic tree. Whole genome single nucleotide polymorphism analysis of 166 genomes, including 147 from the present study and nine publically available closed genomes, using the TIGR4 genome as reference. The tree was rooted using *S. infantis* SPAR10 as the outgroup. Numbers on the perimeter indicate the MLST clonal complex of the isolates and are colored the same as the branches leading to the isolates in each complex. The clonal complex of each sequence type was defined as the founder ST of a clonal group, as predicted by eBURST analyses of the entire *S. pneumoniae* MLST databased accessed in September, 2014 (http://pubmlst.org/spneumoniae/). Isolate names and serotype labels colored blue indicates that the strain was isolated prior to the introduction of PCV7 in 2000. Red colored names and serotypes indicate the strains were isolated in 2000 or later. Colored dots indicate a Mega insertion in the isolate and are color coded by Mega insertion site, light blue, class I; dark blue, class II; red, class III; pink, class IV; green, class V (Tn*916 orf6*); and gold, novel insertion site.

Comparison of the nucleotide sequences flanking Mega inserted into each site revealed conserved sequences upstream of the Mega insertion site that may indicate a target sequence (**Figure 3**). The potential consensus was 5′ TTTCCNCAA 3′ and was located approximately six bp upstream of Mega in all sites (**Figure 3**). The six base pairs flanking Mega on either side resembled coupling sequences as described for conjugative transposons such as Tn*916* (**Figure 3**). The coupling sequences and Mega flanking sequences illustrated in **Figure 3** were representative of all Mega elements inserted into the respective sites. This implies that the Mega integrated into each site were descended from a single, or very few, ancestral transposition event(s). An example of this can be seen in the whole genome phylogeny (**Figure 2**). The class II Mega insertion was present in almost all CC156 isolates (**Figure 2**, dark blue dots). Genomes from isolates of this large complex clustered into three clades correlating to CC156 subgroups 90, 124, and 156 (**Figure 2**). Almost all genomes in subgroups 90 and 156 contained Mega (**Figure 2**). All 10 subgroup

Table 1 | Insertion sites of Mega.

Element (no.)	Insert[a] (no.)	TIGR4 homolog[b]	Function	CC[c]	Serotype(s)[d] (no.)
Mega-1 (48)	I (6)	SP_1598	Phosphomethylpyrimidine kinase	2090	6A (5)
				199	19A (1)
	II (2)	SP_0180	DNA-3-methyladenine glycosylase	1379	6C (1)
				62	11A (1)
	III (10)	SP_0103	Capsule biosynthesis	156	9V (1)
				62	11A (1)
				199	15C (3), 19A (4)
				81	23F (1)
	IVb (2)	SP_1029	RNA methyltransferase	100	33F (2)
	V (27)	na	Transcriptional regulation	156	9V (1)
				124	14 (1)
				2218	15B (1)
				320	19A (6), 19F (15)
				242	23F (3)
	Novel (1)	*S. suis* element[e]			14 (1)
Mega-2 (38)	II (35)	SP_0180	DNA-3-methyladenine glycosylase	156	6A (1), 6B (5), 9V (2), 19A (5), 23A (2)
				2090	6A (2), 19A (5)
				15	14 (3)
				558	35B (2)
				62	11A (1)
				191	7A (1)
				66	4 (1)
				320	19F (1)
				433	22F (1)
				439	23F (1)
				singletons	19A (2)
	IVa/c (3)	SP_1029/SP_1067	Pneumococcal Pathogenicity Island 1	1536	6B (2)
				320	19F (1)
Mega-3 (1)	II (1)	SP_0180	DNA-3-methyladenine glycosylase	66	4 (1)

[a] *Class of Mega insertion site.*

[b] *Genes disrupted by Mega insertion. Classes I–IV are disrupted genes and are shown by S. pneumoniae TIGR4 locus tag.*

[c] *CC, clonal complex.*

[d] *PCV7 capsule serotypes are underlined.*

[e] *Integrative and conjugative element closely related to an element in Streptococcus suis 05HAS68 (Accession no. CP002007).*

156 genomes contained Mega; eight Mega-2, class II, one Mega-1 class III insertion and one integration into *orf6* of Tn*916* (**Table 1**; **Figure 2**). Further, CC2090, which branches from CC156, has two clades in one of which nine of nine isolates contain Mega class II. The other branch of CC2090 contains almost all isolates with Mega class I indicating a second conjugation event in this complex (**Figure 2**). Again this strongly implies that Mega inserted into the class II site early in the history of these lineages.

The Mega class IV insertion site, as previously described (Gay and Stephens, 2001), was near the 3′ end of *rumA* (SP_1029, TIGR4 annotation) that encoded a tRNA methyltransferase and was located at the left end of the Pneumococcal Pathogenicity Island-1 (PPI-1) (Brown et al., 2004) (**Figure 4**). Large deletions and multiple MGEs were associated with Mega integrated into this site, giving rise to the three class IV subclasses (**Table 1**). Starting with the simplest, the class IVb insertion contained Mega-1 integrated into *rumA* leaving Mega flanked by the fragments of the gene (**Figure 4**). Two class IVb isolates were identified, all serotype 33F, CC100 (**Table 1**). The class IVa insertion contained Mega-2 integrated into the same location in *rumA* and had an identical sequence to the left junction of Mega in class IVb (**Figure 4**). However, the downstream remnant of *rumA* was deleted along with the entire 30.7 kb PPI-1 (SP_1029 to SP_1067) (**Figure 4**). The island was replaced by Mega-2 and a 1,801 bp insertion sequence IS*Smi*2 found in *S. mitis* strain B6 (Accession no. FN568063.1) (**Figure 4**). The class IVc Mega-2 insertion was similar to class IVa in that PPI-1 was deleted and IS*Smi2* was located at the right junction with the chromosome (**Figure 4**). However, a 41,995 bp transposon-like sequence most closely related to ICE*Sz1* from *S. equi* subspecies *zooepidemicus* strain H70 (Accession no. FM204884) (Holden et al., 2009) was inserted between the *rumA* insertion site and the left end of Mega-2. Thus, the class IVc Mega site organization consists of, in tandem, a transposon previously undefined in pneumococci,

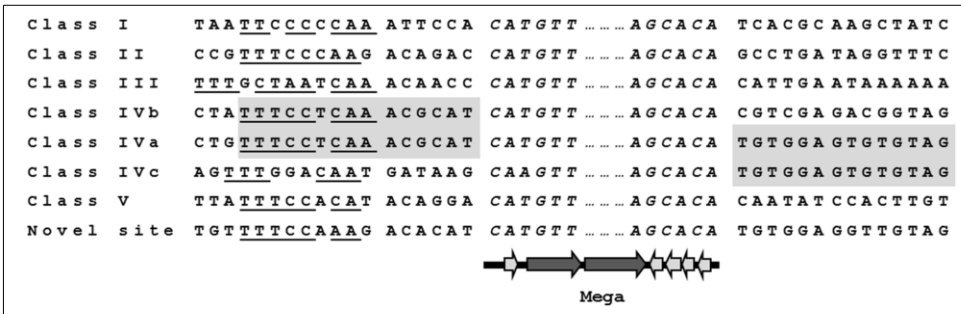

FIGURE 3 | Mega insertion sites. Target sites of the mobile element Mega encoding macrolide efflux genes *mef*(E) and *mel*. Putative six base coupling sequences (C.S.) are shown adjacent to both ends of Mega (italics). Underlined letters indicate conserved nucleotides that may be the consensus recognition sequence 5′ TTTCCNCAA 3′. Class IV was composed of three distinct, subclasses, IVa, IVb, and IVc. Class IVb and IVa share the same left junction and IVa and IVc same right junction (shaded).

Mega-2 and IS*Smi*2. The Atlanta invasive isolate GA17545 (6B, CC1536) contained the only class IVc Mega insertion identified (Tables S1, S2). Class IVa isolates are also typically 6B, CC100, however, a single Atlanta invasive isolate, GA04375, with serotype 19F, and in CC320 was also found to contain Mega-2.IVa (**Table 1**; Table S1). GA04375 was isolated in 1995 and was the earliest isolated CC320 in the genome collection and only one of two CC320 that contained Mega inserted into the pneumococcal chromosome backbone. The other was 3063-00, an invasive 19F, CC320 collected in 1999 in Tennessee (Table S1, S2). The serotype 14, CC156 isolate GA02254 from 1994 contained Mega-1 inserted into an unidentified transposon-like sequence and was most closely related to a sequence in *S. suis* 05HAS68 (Accession no. CP002007). Twenty-seven genomes contained Mega-1 inserted into *orf6* of a Tn*916*-like element (class V) (**Table 1**). Tn*916*-like elements are discussed further in the next section. These data suggest that PPI-1 is a hotspot for integration by recombination and conjugation. This locus could be an entry point for non-pneumococcal DNA to integrate into the pneumococcal genome. Conversely, the conservation of the target site in *rumA* across non-pneumococcal streptococci makes it possible that pneumococcus has been the donor and a non-pneumococcal streptococcus the recipient. The high degree of recombination in the pneumococcus makes it difficult to determine directionality of gene flow, but it likely can flow in both directions. With just these few isolates, we showed evidence for HGT with three non-pneumococcal streptococci; *S. equi*, *S. mitis*, and *S. suis*.

Tn*916*-LIKE ELEMENTS CARRYING MACROLIDE RESISTANCE DETERMINANTS

The genomes were searched for Tn*916*-like elements by BLASTN using the conserved ends of Tn*916* (Data File S1). Of the 86 macrolide resistant invasive isolates from Atlanta, 53 contained a full-length Tn*916*-like element (Table S3). A macrolide resistance determinant was nested within the Tn*916* element in all but six, which instead contained Tn*916* and an unlinked Mega-2.II ($n = 5$) or Mega-1.III ($n = 1$) (Table S3). Four distinct Tn*916*-like elements containing one or two macrolide resistance determinants were identified: Tn*2009*, Tn*2010*, Tn*6002*, and Tn*3872* (**Figure 1**; **Table 2**). Tn*2009* was found in 15 Atlanta invasive isolates spanning six CC and six serotypes (Table S3). Tn*6002* was carried by nine Atlanta invasive isolates including five CC (and a singleton) and seven serotypes (Table S3). Tn*2010* was found in 13 Atlanta invasive isolates, two Atlanta carriage isolates, and eight non-Atlanta invasive isolates (**Table 2**; Table S3).

To better understand the evolutionary relationships between these elements, the insertion site of each was determined. *Tn916*-like elements were integrated into four unique loci in the pneumococcal chromosome backbone and into several loci within Tn*5253*-like elements (**Figure 5**). Every Tn*2010* element discovered was inserted into SP_1947 (TIGR4 annotation) encoding a hypothetical secreted protein (**Table 2**; **Figure 5**). This is the same location where Tn*2010* has been previously reported to be integrated (Zhou et al., 2014). Six of 15 Tn*2009* elements and four of nine Tn*6002* elements found in invasive Atlanta isolates were inserted into the same locus as Tn*2010* (**Table 2**). The 6-base coupling sequences were identical for all elements in this locus suggesting that the elements found integrated into this locus were derived from a single transposition event (**Figure 5**). This further implies that the macrolide resistance elements Mega-1, Tn*917* and *erm*(B) were independently acquired by a Tn*916* residing in the SP_1947 locus. In addition, elements in this locus were identified in two clonal complexes (CC320, CC156) indicating transformation and recombination of the element in this locus between clonal complexes.

Tn*2009* was also identified integrated into SP_1638 (TIGR4), an iron-dependent transcriptional regulator, in a single serotype 9V, CC156 isolate from 2007. The fact that no element was identified in this locus from an earlier collected isolate may indicate that this integration event occurred more recently than the SP_1947 integration. Likewise, a single isolate (22F, CC433) from 2010 contained Tn*6002* integrated into the ABC transporter gene SP_1438. Five serotype 6B, CC384 isolates contained Tn*916* integrated into *lytA* (SP_1937) encoding an autolysin (**Table 2**). Each

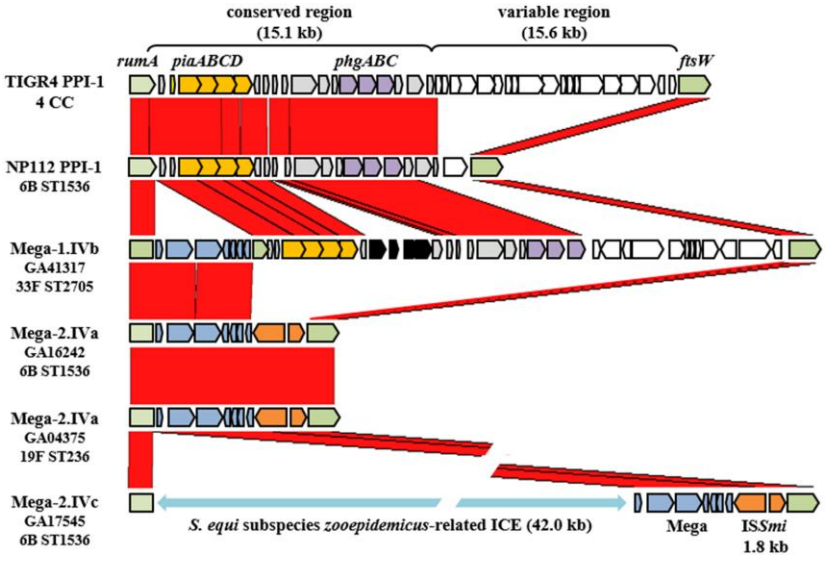

FIGURE 4 | Variations of the Pneumococcal Pathogenicity Island-1 associated with Mega. The Pneumococcal Pathogenicity Island-1 in TIGR4 extends from *rumA* (SP_1029) to *ftsW* (SP_1065). Strain NP112 is closely related to GA16242 and GA17545, the Mega-2.IVa and IVc strains, but contains the conserved region of PPI-1. Red blocks represent regions of homology. Arrows indicate genes. Green, PPI-1 borders; yellow, iron uptake operon *piaABCD*; purple, osmotic stress tolerance operon *phgABC*; gray, PPI-1 conserved region genes not otherwise labeled; white, PPI-1 variable region genes; blue, Mega; orange, IS*Smi*1. The light blue double arrow indicates the presence of an undefined transposon-like sequence from *S. equi* subspecies *zooepidemicus*.

Table 2 | Tn*916* and Tn*916*-like elements inserted directly into the chromosome backbone of invasive *S. pneumoniae* isolates from Atlanta, GA.

Element (no.)	Serotype (no.)	CC [a]	Insertion Sites [b] (no.)	Function	Resistance genes
Tn*916*-like	6B (5)	384	SP_1937	*lytA*, autolysin	*tet*(M)
Tn*6002*-like	22F (1)	433	SP_1438	ABC transporter/ATP-binding subunit	*erm*(B) *tet*(M)
Tn*6002*-like	15A (3) 19A (1)	63	SP_1947	Hypothetical protein	*erm*(B) *tet*(M)
Tn*2009*-like	9V (1)	156	SP_1638	Iron-dependent transcriptional regulator	*mef*(E) *mel tet*(M)
Tn*2009*-like	19F (6)	320	SP_1947	Hypothetical protein	*mef*(E) *mel tet*(M)
Tn*2010*-like	19A (6) 19F (7)	320	SP_1947	Hypothetical protein	*erm*(B) *mef*(E) *mel tet*(M)

[a] *Clonal complex as defined by eBURST analyses of multi-locus sequence type data.*

[b] *Chromosomal insertion sites are presented as the locus tag for homologous genes in S. pneumoniae TIGR4 (Tettelin et al., 2001).*

of these closely related isolates contained unlinked Mega-2.II (Table S2). The other Tn*916*-like elements identified were integrated into a composite ICE resembling Tn*5253* and are discussed below.

COMPOSITE ICE CONTAINING MACROLIDE RESISTANCE DETERMINANTS

Tn*916*-like elements with macrolide resistance determinants have been associated with large conjugative transposons also known as ICE (Henderson-Begg et al., 2009; Mingoia et al., 2014). To determine if ICE have been involved in macrolide resistance dissemination in Atlanta, the genomes of 100 macrolide resistant invasive pneumococcal isolates from Atlanta were searched by BLASTN for the conserved ends of known ICE (Data File S1). The genomes of 15 macrolide resistant isolates contained composite ICE-like elements that ranged in size from approximately 57 to 88 kb (**Table 3**). Comparison of the integrase genes encoded on the ICE revealed two distinct families of conjugative transposons. Nine belonged to the Tn*5253* family and six belonged to the ICE*Sp*23FST81 family (**Table 3**). Each

Tn*5253*	*orf43*	TATTTTTT	ATGGAT	AAAAA.....*TGTTT*	ACTGTTAA *orf20*
GA41301	*orf43*	AATATTTT	TATATG	AAAAA.....*TGTTT*	ACTGTTAA *orf20*
GA05245	*orf43*	AATATTTT	TATATG	AAAAA.....*TGTTT*	ACTGTTAA *orf20*
GA17227	*orf43*	AATATTTT	TATATG	AAAAA.....*TGTTT*	ACTGTTAA *orf20*
GA47502	*orf20*	CTGTTTTT	TTAGAA	AAAAA.....*TGTTT*	ACTGTTAA *orf20*
GA47597	*orf20*	CTGTTTTT	TTAGAA	AAAAA.....*TGTTT*	CAAATAAA *orf18*
GA60132 (R)	*orf43*	ATAAATTT	TATATA	AAAAA.....*TGTTT*	ATATGAAA *orf18*
GA11304 (R)	*orf43*	ATAAATTT	TATATA	AAAAA.....*TGTTT*	ATATGAAA *orf18*
GA40536 (R)	*orf20*	ATCTTTTT	TATATA	AAAAA.....*TGTTT*	TTCTAAAA *orf18*
GA19101 (R)	*orf20*	ATCTTTTT	TATATA	AAAAA.....*TGTTT*	ATTTGAAA *orf18*
GA47210	*orf20*	ATCTTTTT	TATTTG	AAAAA.....*TGTTT*	TTCTAAAA *orf18*
ICE*Sp*23FST81	*orf9*	AGTTTTTT	TAAAAT	AAAAA.....*TGTTT*	ATTTCAAA *orf8*
GA11663	*orf9*	AGTTTTTT	TAAAAT	AAAAA.....*TGTTT*	ATTTCAAA *orf8*
GA44378	*orf9*	AGTTTTTT	TAAAAT	AAAAA.....*TGTTT*	ATTTCAAA *orf8*
GA13430	*orf9*	AGTTTTTT	TAAAAT	AAAAA.....*TGTTT*	ATTTCAAA *orf8*
GA13494	*orf9*	AGTTTTTT	TAAAAT	AAAAA.....*TGTTT*	ATTTCAAA *orf8*
GA41565	*orf9*	AGTTTTTT	TAAAAT	AAAAA.....*TGTTT*	ATTTCAAA *orf8*

FIGURE 5 | Insertion sites of Tn*916*-like elements. Insertion sites within composite elements. The terminal sequences of Tn*916* are shown in italics. Coupling sequences are underlined. Plain text indicates the sequences of ICE flanking the Tn*916*-like element. (R) indicates that the Tn*916*-like element is in the reverse orientation. The ORFs that flank the Tn*916*-like elements are indicated adjacent to the ICE sequences on either side.

of the Tn*5253*-family transposons was inserted into the pneumococcal chromosome backbone in the gene for ribobiogenesis GTPase, *rbgA* (SP_1155, TIGR4 annotation) involved in assembly of 23S ribosomes. Downstream of Tn*5253*-like elements in this locus is the immunoglobulin A1 protease gene *iga* as has been described previously (Croucher et al., 2009). Each of the ICE*Sp*23FST81-like elements was inserted into the chromosome backbone gene *rplL* (SP_1354) which encodes ribosomal protein L7/L12 (Croucher et al., 2009). The correlation of ICE family and insertion sites reflects the specificity of the integrases Int_{Tn5253} and $Int_{ICESp23FST81}$ (Mingoia et al., 2007; Wyres et al., 2013).

The five ICE*Sp*23FST81-like elements contained Tn*916*-like insertions, including a Tn*916*-like, a Tn*3872*-like and four Tn*2009*-like elements (**Table 3**). Each of the smaller elements was integrated between *orf9* and *orf8* of *Tn5253* and contained identical flanking and coupling sequences, indicating that each was derived from a single conjugation event and subsequent transfer of Mega-1 between Tn*916* and Tn*2009* (**Figure 6**). GA44378 containing Tn*916* integrated into the ICE*Sp*23FST81-like element was macrolide resistant due to an unlinked Mega-1.III insertion (**Table 3**; Table S2). ICE*Sp*23FST81 was originally described in a 23F, ST81 isolate (Croucher et al., 2009). Five of six ICE*Sp*23FST81 family elements were also in CC81, however only two were serotype 23F (**Table 3**). The others were serotype 19A ($n = 1$) and 19F ($n = 2$) and represent capsule switching from a PCV7 vaccine serotype to a non-vaccine serotype and a different vaccine serotype, respectively. This conclusion is supported by the close relationship between the isolates, all but one of which was also serotype 23F and CC81 (**Figure 6**). The lone exception was GA13494, a serotype 14, CC156 isolate that contained Tn*2009*, indicating horizontal transfer of the composite element between the clones (**Figure 6**). These were isolated over a 9-year period spanning the pre-PCV7 and post-PCV7 eras (1995–2004). This demonstrated clonal expansion and the long-term stability of the clone and the Tn*5253*-like element harboring Tn*2009*.

In the other composites identified, the Tn*916*-like element was inserted between *orf43* and *orf20* of Tn*5253*. Tn*3872* was inserted in this locus in GA47597, a serotype 3, CC180 isolate from 2006 (**Table 3**). Tn*3872* was also inserted downstream of *orf20* and contained the same flanking DNA sequences, however, the right junction was flanked by *orf18*. This indicated that GA47597, a serotype 3, CC180 isolate from 2006, also contained Tn*3872* which had a sequence identical to GA47502 flanking the left junction of Tn*3872* (**Figure 6**). Tn*6002* was also found flanked by *orf20* on the left and *orf18* on the right in two isolates (**Table 3**; **Figure 5**). Like GA47597, GA19101 was a serotype CC180 isolate suggesting a common integration event for a Tn*916*-like element (**Figure 6**). However, Tn*6002* in both of these isolates was integrated in the opposite orientation from Tn*2009* and Tn*3872* (**Figure 6**). This suggests separate conjugation events (one for each orientation) followed by homologous recombination of one junction to create a chimeric insertion site (i.e., *orf20/orf18*). In both isolates with Tn*3872*, the element was integrated into *orf20/orf18* in the same orientation as Tn*2009* in this location (**Table 3**). Again, Tn*2009* and Tn*6002* in this location had identical coupling sequences indicating a single event integration event of a Tn*916*-like element followed by acquisition of nested macrolide resistance elements by homologous recombination. Finally, *orf43/orf18* was identified as the site of insertion of Tn*6002* in four isolates (**Table 2**).

Table 3 | Atlanta invasive isolates containing composite ICE encoding macrolide resistance.

Strain	Year	Type	CC[a]	Size (bp)	*Int* Family[b]	Tn*916*-like	Tn*916*-like I.S.[c]	Resistance genes[d]	Antibiogram[d]
GA05245	1995	23F	242	70,161	Tn*5253*	Tn*2009*-like	*orf43/orf20*	*mef*(E) *mel tet*(M)	ERY TET
GA11304	1999	06A	156	82,623	Tn*5253*	Tn*6002*-like	*orf43/orf18* (R)	*erm*(B) *tet*(M) *cat*	ERY CLI TET CHL
GA11663	1999	19F	81	86,725	ICE*Sp*23FST81	Tn*2009*-like	*orf9/orf8*	*mef*(E) *mel tet*(M) *cat*	ERY TET CHL
GA13430	1999	19F	81	86,674	ICE*Sp*23FST81	Tn*2009*-like	*orf9/orf8*	*mef*(E) *mel tet*(M) *cat*	ERY TET CHL
GA13494	1999	14	156	86,593	ICE*Sp*23FST81	Tn*2009*-like	*orf9/orf8*	*mef*(E) *mel tet*(M) *cat*	ERY TET CHL
GA17227	2000	23F	242	67,131	Tn*5253*	Tn*2009*-like	*orf43/orf20*	*mef*(E) *mel tet*(M)	ERY TET
GA19101	2002	03	180	67,673	Tn*5253*	Tn*6002*-like	*orf20/orf18* (R)	*erm*(B) *tet*(M) *cat*	ERY CLI TET CHL
GA40563	2003	04	S	60,190	Tn*5253*	Tn*6002*-like	*orf20/orf18* (R)	*erm*(B) *tet*(M) *cat*	ERY CLI TET CHL
GA41301	2004	23F	242	67,191	Tn*5253*	Tn*2009*-like	*orf43/orf20*	*mef*(E) *mel tet*(M)	ERY TET
GA41565	2004	19A	81	88,320	ICE*Sp*23FST81	Tn*2009*-like	*orf9/orf8*	*mef*(E) *mel tet*(M) *cat*	ERY TET CHL
GA44378	2005	23F	81	81,138	ICE*Sp*23FST81	Tn*916-like*	*orf9/orf8*	*mef*(E) *mel tet*(M) *cat*	ERY TET CHL
GA47210	2006	15B	156	56,904	Tn*5253*	Tn*2009*-like	*orf20/orf18*	*mef*(E) *mel tet*(M)	ERY TET
GA47502	2006	19A	S	70,931	ICE*Sp*23FST81	Tn*3872*-like	*orf9/orf8*	*erm*(B) *tet*(M) *cat*	ERY CLI TET CHL
GA47597	2006	03	180	67,106	Tn*5253*	Tn*3872*-like	*orf20/orf18*	*erm*(B) *tet*(M) *cat*	ERY CLI TET CHL
GA60132	2010	06C	1390	71,603	Tn*5253*	Tn*6002*-like	*orf43/orf18* (R)	*erm*(B) *tet*(M)	ERY CLI TET

[a] *CC, clonal complex. Clonal complex was defined as the predicted founder of a complex as predicted by eBURST analyses (default settings).*

[b] *Int, integrase gene.* int_{Tn5253} *(Accession no. EU351020);* $int_{ICESp23FST81}$, *(Accession no. FR671403).*

[c] *I.S., insertion site of Tn916-like element in the ICE. Orfs refer to the annotation of Tn5253. (R) indicates that the Tn916-like element is in the reverse orientation.*

[d] *Resistance to key antibiotics. ERY, erythromycin; CLI, clindamycin; TET, tetracycline; CHL, chloramphenicol. Minimum inhibitory concentrations for each isolate are provided as supporting information.*

The horizontal line divides the pre-and post-PCV7 isolate.

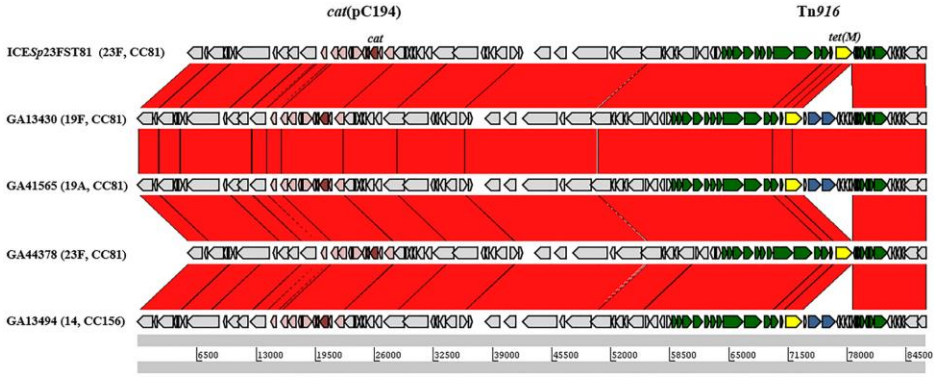

FIGURE 6 | Comparison of ICE*Sp*23FST81-like elements encoding macrolide resistance. The location of the Tn*916*-like element in each is indicated by the Tn*5253* genes shown as arrows above each track. Green arrows, Tn*916*-genes; Blue arrows, *mef*(E) and *mel*; yellow arrows, *tet*(M); pink arrows, integrated plasmid pC194; red arrows, *cat*.

Tn*5253* is also flanked by these genes and with conserved coupling sequences, indicating that each is descended from a single conjugation event followed by integration of the *erm*(B) element between *orf43* and *orf20*. These data suggest that *de novo* integration Tn*916*-like elements into pneumococcal chromosome backbones or ICE was infrequent relative to the rate of horizontal transfer by transformation and recombination.

DISCUSSION

The genome of *S. pneumoniae* is extremely plastic due to its natural competency and possession of numerous MGE. While transformation and conjugation are both involved in shaping the pneumococcal chromosome, the diversity of macrolide resistance elements, both independent and integrated into larger conjugative elements, raises the question of the relative role

of each mechanism in the dissemination of macrolide resistance in pneumococci. Recombination events involving various macrolide resistance determinants were evidenced by an apparent interchangeability of Mega, the *erm*(B) element and Tn*917* in Tn*916*-like elements. The conversion of Tn*6002* and Tn*6003* (containing aminoglycoside resistance gene *aphA-3*) has been reported (Palmieri et al., 2012). These elements in turn were integrated into the chromosome backbone or were inserted into larger integrative and conjugative transposons. In this study, comparative genomics were used to assess the elements existing in a geographically defined location before and after the introduction of PCV7, to better understand the complex history of macrolide dissemination.

We identified Mega inserted in the four previously described locations in the pneumococcal chromosome backbone (Gay and Stephens, 2001) and inserted into *orf6* of Tn*916*-like elements. We also found a novel insertion site within an undefined transposon-like sequence similar to an element in *S. suis*. It is not clear if Mega integrated into the element before or after it made the cross-species horizontal transfer into the pneumococcus. Either way, it is an apparent example of pneumococci acquiring novel DNA from a non-pneumococcal streptococci, likely by conjugation event introducing the *S. suis* element into pneumococci or by Mega inserting into a novel locus in pneumococci. We also identified a transposon-like element most closely related to ICE*Sz*1 from *S. equi* subsp. *zooepidemicus*. This element was located in the Pneumococcal Pathogenicity Island 1 (PPI-1) and was associated with Mega. However, the possibility of *S. suis* and *S. equi* having acquired these elements from the pneumococcus cannot be disregarded. In fact, there is no data to suggest that these elements cannot flow equally in both directions.

PPI-1 appears to be a hotspot for recombination and/or integration of MGE. Not only was Mega inserted in PPI-1 but it appeared that integration of Mega at this location created, or retained, target sites for mobile elements. The Mega class IVb insertion contains Mega with no deletion of the target site. This may have been the original integrated structure. Subsequently, each flank of Mega-1.IVb may have been dislocated by insertion of additional MGE. Downstream of Mega in classes IVa and IVc was an insertion sequence, IS*Sm1*, originally identified in *S. mitis* (Denapaite et al., 2010). Interestingly, IS*Smi* precisely replaced the variable region of the pathogenicity island, which was a remnant of a Tn*5252*-like ICE (Brown et al., 2001). The variability at this locus and the presence of multiple integrated MGE-related sequences suggested this to be a hotspot for recombination or a common target site for conjugative elements. Upstream of Mega in class IVc was a large unidentified conjugative transposon-like sequence related most closely to a transposon-like sequence from *S. equi* subspecies *zooepidemicus.* The undefined element was integrated into the exact location within *rumA* as Mega and was integrated immediately upstream of Mega resulting in three MGEs linked in tandem: the unidentified transposon, Mega, and IS*Smi*1. Both undefined pneumococcal transposons are currently under investigation to identify their origin, understand where they came from, how they moved, what cargo they carry and their ability to transfer by conjugation from pneumococci to pneumococci and non-pneumococcal streptococci.

Closed circle intermediates of excised Tn*916*-like elements are formed by binding of semi-complementary coupling sequences creating a heteroduplex. This process produces novel coupling sequences with each integration event. Based on the observation that coupling sequences are altered upon integration, we used predicted coupling sequences as indicators of unique integration events. Mega and *erm*(B) often integrate in Tn*916*-like elements (Del Grosso et al., 2004, 2007, 2011). In the present study we identified many of the previously reported macrolide resistant Tn*916*-like elements in the Atlanta population including Tn*2009*, Tn*2010*, Tn*6002*, and Tn*3872*. The mechanism of conjugation of Tn*916* is well-understood. The Tn*916* integrase is promiscuous, that is, targeting sequences that are A-T rich, but not sequence specific (Rudy et al., 1997; Rocco and Churchward, 2006). Tn*916*-like transposons excise imperfectly from a donor strain to carry some flanking genomic bases and create a closed-circle intermediate with a mismatched junction (Caparon and Scott, 1989). The resulting overlapping region is the coupling sequence for subsequent integration, and thus each transposition event may create a new coupling sequence (Lu and Churchward, 1995). These facts and the observation by our laboratory and others that Tn*916*-like elements are found integrated within relatively few sites in the pneumococcus and with little variation in the coupling sequences, suggest that conjugation into and between pneumococci is relatively infrequent compared to transformation and recombination events.

ICE appear to be well-established in the pneumococcal population. They were present during a rapid emergence of macrolide resistant invasive pneumococcal disease during the early to mid-1990's (Wyres et al., 2013) in the United States. In addition, ICE have been reported in isolates from the 1960's (Wyres et al., 2013). ICE were identified in invasive and carriage pneumococcal isolates in Atlanta (**Table 3**). The ICE carrying the shorter macrolide resistance elements were of two types as has been reported previously (Roberts and Kreth, 2014). The first was a group of Tn*5253*-like elements containing different combinations of Mega, the *erm*(B) element, and Tn*917* also carrying *erm*(B). All of these elements were integrated into the same location in the pneumococcal chromosome backbone: the ribobiogenesis GTPase, *rbgA*. The second group was similar to ICE*Sp*23FST81 and were all inserted into the ribosome protein encoding gene *rplL*. The conservation of insertion sites reflects the specificity of different integrases encoded on each element. Because of the specificity of these integrases, it is to be expected that they would integrate into the exact location repeatedly. Therefore, we can make no conclusions on the frequency of transfer of the element into or out of pneumococci.

Comparison of the sequence types and serotypes of the pneumococcal isolates carrying macrolide resistance determinants showed closely related isolates with variable macrolide resistance elements indicating horizontal transfer. For example, in **Figure 6** GA41565 and GA44378 are both CC81, but the former is serotype 19A and the latter is 23F. These isolates cluster together in the whole genome analyses further indicating their similarity. Both contain ICE*Sp*23FST81-like ICE that are nearly identical and both have a Tn*916*-like element with no macrolide resistance

determinant, while GA41565 contains Tn*2009*. This indicates the acquisition or loss of Mega by recombination. Analyses of the insertion sites suggested that conjugative insertion events of the elements into the pneumococcus are infrequent leading to the conclusion that these elements have been largely disseminated by lateral gene transfer through transformation and homologous recombination. Because homologous recombination requires homology between donor and host DNAs, gene flow between closely related isolates may occur more frequently than between distantly related clones. However, the presence of macrolide elements in composite transposons and the wide dissemination of composite transposons may aid in horizontal gene transfer between distant clones by creating 50–90 kb regions of homology that act as landing sites for the small nested elements carrying macrolide resistance determinants. These additional regions of homology may have aided in the dissemination of macrolide resistance not only because of the binding sites created by the composite elements, but also because of the multidrug resistance nature of the chimeric genetic elements. For example, macrolide resistance dissemination is aided by the non-macrolide antibiotic resistance determinants tetracycline and chloramphenicol due to soft selective sweeps of macrolide elements linked to *cat* and *tet*(M) genes carried on composite mobile elements.

The 7-valent Pneumococcal Conjugate Vaccine PCV7 was introduced into Atlanta in late 2000. We analyzed the genomic data in respect to the pre-vaccine and post-vaccine years. There appeared to be little effect on the types of elements harboring macrolide resistance determinants, however, the sequence types and serotypes harboring these elements were changed significantly. Some examples of this can be seen in the whole genome phylogenetic analyses where blue text indicated isolation in the pre-vaccine era and red indicated post-vaccine isolation (**Figure 2**). Note that in clonal complex 320, all isolates from before the vaccine were serotype 19F, a PCV7 serotype (**Figure 2**). After the vaccine was introduced serotype 19A, a non-PCV7 serotype, appeared. The shift to 19A was concomitant with the appearance of Tn*2010*, which was not detected in the pre-vaccine era. Interestingly, Tn*2010* was detected in only one chromosome backbone site and was not found in any ICE (**Table 2**). Likewise, CC2090 appears to have switched from the vaccine-associated serotype 6A to the non-vaccine serotype 19A (**Figure 2**). Every serotype 19A CC2090 strain was isolated after the introduction of the vaccine (**Figure 2**).

In conclusion, macrolide resistance dissemination in pneumococci has been greatly influenced by conjugation and transformation. Because Mega and Tn*916*-like element integration events appear infrequent, transformation and homologous recombination appear to be the primary means of horizontal transfer into the pneumococcus. With limited sites for insertion, the element has multiplied its capacity to disseminate throughout the pneumococcal population by co-opting the insertion sites of other elements. Thus, conjugation allows acquisition of DNA from more distantly related bacteria. Once in a pneumococcal genome, if beneficial and selected, the conjugated transposon is subsequently disseminated by transformation throughout the pneumococcal population.

ACKNOWLEDGMENTS

We are grateful to Wendy Baughman, Emily Crispell and the Georgia Emerging Infections Program for providing the invasive pneumococcal isolates from Georgia for genome sequencing. We are also grateful to Leslie McGee, the Pneumococcal Molecular Epidemiology Network and the Centers for Disease Control Streptococcus Laboratory for providing invasive isolates and Pekka Nourti and Shabnam Jain for providing nasopharyngeal isolates. This study was funded in part with an R01 grant from the National Institutes of Health (R01 AI070829 (to David S. Stephens) and with federal funds from the National Institute of Allergy and Infectious Diseases, National Institutes of Health, Department of Health and Human Services under contract number HHSN272200900009C. The funders had no role in study design, data collection and analysis, or preparation of the manuscript, but signed off on the publication after we sent them a copy for review.

SUPPLEMENTARY MATERIAL

The Supplementary Material for this article can be found online at: http://www.frontiersin.org/journal/10.3389/fmicb.2015.00026/abstract

REFERENCES

Altschul, S. F., Madden, T. L., Schäffer, A. A., Zhang, J., Zhang, Z., Miller, W., et al. (1997). Gapped BLAST and PSI-BLAST: a new generation of protein database search programs. *Nucleic Acids Res.* 25, 3389–3402. doi: 10.1093/nar/25.17.3389

Ambrose, K. D., Nisbet, R., and Stephens, D. S. (2005). Macrolide efflux in *Streptococcus pneumoniae* is mediated by a dual efflux pump (*mel* and *mef*) and is erythromycin inducible. *Antimicrob. Agents Chemother.* 49, 4203–4209. doi: 10.1128/AAC.49.10.4203-4209.2005

Ayoubi, P., Kilic, A. O., and Vijayakumar, M. N. (1991). Tn*5253*, the pneumococcal omega (*cat* tet) BM6001 element, is a composite structure of two conjugative transposons, Tn*5251* and Tn*5252*. *J. Bacteriol.* 173, 1617–1622.

Berge, M., Moscoso, M., Prudhomme, M., Martin, B., and Claverys, J.-P. (2002). Uptake of transforming DNA in Gram-positive bacteria: a view from *Streptococcus pneumoniae*. *Mol. Microbiol.* 45, 411–421. doi: 10.1046/j.1365-2958.2002.03013.x

Brown, J., Gilliland, S., and Holden, D. (2001). A *Streptococcus pneumoniae* pathogenicity island encoding an ABC transporter involved in iron uptake and virulence. *Mol. Microbiol.* 40, 572–585. doi: 10.1046/j.1365-2958.2001.02414.x

Brown, J. S., Gilliland, S. M., Spratt, B. G., and Holden, D. W. (2004). A locus contained within a variable region of pneumococcal pathogenicity Island 1 contributes to virulence in mice. *Infect. Immun.* 72, 1587–1593. doi: 10.1128/IAI.72.3.1587-1593.2004

Caparon, M. G., and Scott, J. R. (1989). Excision and insertion of the conjugative transposon Tn*916* involves a novel recombination mechanism. *Cell* 59, 1027–1034. doi: 10.1016/0092-8674(89)90759-9

Carver, T. J., Rutherford, K. M., Berriman, M., Rajandream, M.-A., Barrell, B. G., and Parkhill, J. (2005). ACT: the Artemis Comparison Tool. *Bioinformatics (Oxford, England)* 21, 3422–3423. doi: 10.1093/bioinformatics/bti553

Chancey, S. T., Zhou, X., Zähner, D., and Stephens, D. S. (2011). Induction of efflux-mediated macrolide resistance in *Streptococcus pneumoniae*. *Antimicrob. Agents Chemother.* 55, 3413–3422. doi: 10.1128/AAC.00060-11

Claverys, J.-P., Prudhomme, M., and Martin, B. (2006). Induction of competence regulons as a general response to stress in gram-positive bacteria. *Annu. Rev. Microbiol.* 60, 451–475. doi: 10.1146/annurev.micro.60.080805.142139

Cochetti, I., Tili, E., Mingoia, M., Varaldo, P. E., and Montanari, M. P. (2008). *erm*(B)-Carrying elements in tetracycline-resistant pneumococci and correspondence between Tn*1545* and Tn*6003*. *Antimicrob. Agents Chemother.* 52, 1285–1290. doi: 10.1128/AAC.01457-07

Cochetti, I., Tili, E., Vecchi, M., Manzin, A., Mingoia, M., Varaldo, P. E., et al. (2007). New Tn*916*-related elements causing *erm*(B)-mediated erythromycin

resistance in tetracycline-susceptible pneumococci. *J. Antimicrob. Chemother.* 60, 127–131. doi: 10.1093/jac/dkm120

Croucher, N. J., Hanage, W. P., Harris, S. R., McGee, L., van der Linden, M., de Lencastre, H., et al. (2014). Variable recombination dynamics during the emergence, transmission and 'disarming' of a multidrug-resistant pneumococcal clone. *BMC Biol.* 12:49. doi: 10.1186/1741-7007-12-49

Croucher, N. J., Walker, D., Romero, P., Lennard, N., Paterson, G. K., Bason, N. C., et al. (2009). Role of conjugative elements in the evolution of the multidrug-resistant pandemic clone *Streptococcus pneumoniae* Spain23F ST81. *J. Bacteriol.* 191, 1480–1489. doi: 10.1128/JB.01343-08

Del Grosso, M., Camilli, R., Barbabella, G., Blackman Northwood, J., Farrell, D. J., and Pantosti, A. (2011). Genetic resistance elements carrying *mef* subclasses other than *mef*(A) in *Streptococcus pyogenes*. *Antimicrob. Agents Chemother.* 55, 3226–3230. doi: 10.1128/AAC.01713-10

Del Grosso, M., Camilli, R., Iannelli, F., Pozzi, G., and Pantosti, A. (2006). The *mef*(E)-carrying genetic element (Mega) of *Streptococcus pneumoniae*: insertion sites and association with other genetic elements. *Antimicrob. Agents Chemother.* 50, 3361–3366. doi: 10.1128/AAC.00277-06

Del Grosso, M., Camilli, R., Libisch, B., Fuzi, M., and Pantosti, A. (2009). New composite genetic element of the Tn*916* family with dual macrolide resistance genes in a *Streptococcus pneumoniae* isolate belonging to clonal complex 271. *Antimicrob. Agents Chemother.* 53, 1293–1294. doi: 10.1128/AAC.01066-08

Del Grosso, M., Northwood, J. G. E., Farrell, D. J., and Pantosti, A. (2007). The macrolide resistance genes *erm*(B) and *mef*(E) are carried by Tn*2010* in dual-gene *Streptococcus pneumoniae* isolates belonging to clonal complex CC271. *Antimicrob. Agents Chemother.* 51, 4184–4186. doi: 10.1128/AAC.00598-07

Del Grosso, M., Scotto d'Abusco, A., Lannelli, F., Pozzi, G., and Pantosti, A. (2004). Tn*2009*, a Tn*916*-like element containing *mef*(E) in *Streptococcus pneumoniae*. *Antimicrob. Agents Chemother.* 48, 2037–2042. doi: 10.1128/AAC.48.6.2037-2042.2004

Denapaite, D., Bruckner, R., Nuhn, M., Reichmann, P., Henrich, B., Maurer, P., et al. (2010). The genome of *Streptococcus mitis* B6–what is a commensal? *PLoS ONE* 5:e9426. doi: 10.1371/journal.pone.0009426

Enright, M. C., and Spratt, B. G. (1998). A multilocus sequence typing scheme for *Streptococcus pneumoniae*: identification of clones associated with serious invasive disease. *Microbiology* 144, 3049–3060. doi: 10.1099/00221287-144-11-3049

Farley, M. M., Baughman, W., and Arnold, K. E. (2002). The Georgia emerging infections program: monitoring trends in invasive pneumococcal disease. *J. Med. Assoc. Ga.* 91, 20–23.

Gardner, S. N., and Hall, B. G. (2013). When whole-genome alignments just won't work: kSNP v2 software for alignment-free SNP discovery and phylogenetics of hundreds of microbial genomes. *PLoS ONE* 8:e81760. doi: 10.1371/journal.pone.0081760

Gay, K., Baughman, W., Miller, Y., Jackson, D., Whitney, C. G., Schuchat, A., et al. (2000). The emergence of *Streptococcus pneumoniae* resistant to macrolide antimicrobial agents: a 6-year population-based assessment. *J. Infect. Dis.* 182, 1417–1424. doi: 10.1086/315853

Gay, K., and Stephens, D. S. (2001). Structure and dissemination of a chromosomal insertion element encoding macrolide efflux in *Streptococcus pneumoniae*. *J. Infect. Dis.* 184, 56–65. doi: 10.1086/321001

Henderson-Begg, S. K., Roberts, A. P., and Hall, L. M. C. (2009). Diversity of putative Tn*5253*-like elements in *Streptococcus pneumoniae*. *Int. J. Antimicrob. Agents* 33, 364–367. doi: 10.1016/j.ijantimicag.2008.10.002

Holden, M. T. G., Heather, Z., Paillot, R., Steward, K. F., Webb, K., Ainslie, F., et al. (2009). Genomic evidence for the evolution of *Streptococcus equi*: host restriction, increased virulence, and genetic exchange with human pathogens. *PLoS Pathog.* 5:e1000346. doi: 10.1371/journal.ppat.1000346

Iannelli, F., Santoro, F., Oggioni, M. R., and Pozzi, G. (2014). Nucleotide sequence analysis of integrative conjugative element Tn*5253* of *Streptococcus pneumoniae*. *Antimicrob. Agents Chemother.* 58, 1235–1239. doi: 10.1128/AAC.01764-13

Klugman, K., and Lonks, J. (2005). Hidden epidemic of macrolide-resistant pneumococci. *Emerging Infect. Dis.* 11, 802–807. doi: 10.3201/eid1106.050147

Kurtz, S., Phillippy, A., Delcher, A. L., Smoot, M., Shumway, M., Antonescu, C., et al. (2004). Versatile and open software for comparing large genomes. *Genome Biol.* 5:R12. doi: 10.1186/gb-2004-5-2-r12

Leclercq, R., and Courvalin, P. (1991). Intrinsic and unusual resistance to macrolide, lincosamide, and streptogramin antibiotics in bacteria. *Antimicrob. Agents Chemother.* 35, 1273–1276. doi: 10.1128/AAC.35.7.1273

Lu, F., and Churchward, G. (1995). Tn*916* target DNA sequences bind the C-terminal domain of integrase protein with different affinities that correlate with transposon insertion frequency. *J. Bacteriol.* 177, 1938–1946.

McCormick, A. W., Whitney, C. G., Farley, M. M., Lynfield, R., Harrison, L. H., Bennett, N. M., et al. (2003). Geographic diversity and temporal trends of antimicrobial resistance in *Streptococcus pneumoniae* in the United States. *Nat. Med.* 9, 424–430. doi: 10.1038/nm839

McDougal, L. K., Tenover, F. C., Lee, L. N., Rasheed, J. K., Patterson, J. E., Jorgensen, J. H., et al. (1998). Detection of Tn*917*-like sequences within a Tn*916*-like conjugative transposon (Tn*3872*) in erythromycin-resistant isolates of *Streptococcus pneumoniae*. *Antimicrob. Agents Chemother.* 42, 2312–2318.

McGee, L., McDougal, L., Zhou, J., Spratt, B. G., Tenover, F. C., George, R., et al. (2001). Nomenclature of major antimicrobial-resistant clones of *Streptococcus pneumoniae* defined by the pneumococcal molecular epidemiology network. *J. Clin. Microbiol.* 39, 2565–2571. doi: 10.1128/JCM.39.7.2565-2571.2001

Mingoia, M., Morici, E., Morroni, G., Giovanetti, E., Del Grosso, M., Pantosti, A., et al. (2014). Tn*5253* Family Integrative and Conjugative Elements Carrying *mef*(I) and *catQ* Determinants in *Streptococcus pneumoniae* and *Streptococcus pyogenes*. *Antimicrob. Agents Chemother.* 58, 5886–5893. doi: 10.1128/AAC.03638-14

Mingoia, M., Vecchi, M., Cochetti, I., Tili, E., Vitali, L. A., Manzin, A., et al. (2007). Composite structure of *Streptococcus pneumoniae* containing the erythromycin efflux resistance gene *mef*(I) and the chloramphenicol resistance gene *catQ*. *Antimicrob. Agents Chemother.* 51, 3983–3987. doi: 10.1128/AAC.00790-07

Munoz-Najar, U., and Vijayakumar, M. (1999). An operon that confers UV resistance by evoking the SOS mutagenic response in streptococcal conjugative transposon Tn*5252*. *J. Bacteriol.* 181, 2782–2788.

Myers, E. W., Sutton, G. G., Delcher, A. L., Dew, I. M., Fasulo, D. P., Flanigan, M. J., et al. (2000). A whole-genome assembly of *Drosophila*. *Science* 287, 2196–2204. doi: 10.1126/science.287.5461.2196

Orvis, J., Crabtree, J., Galens, K., Gussman, A., Inman, J. M., Lee, E., et al. (2010). Ergatis: a web interface and scalable software system for bioinformatics workflows. *Bioinformatics (Oxford, England)* 26, 1488–1492. doi: 10.1093/bioinformatics/btq167

Palmieri, C., Mingoia, M., Massidda, O., Giovanetti, E., and Varaldo, P. E. (2012). *Streptococcus pneumoniae* transposon Tn*1545*/Tn6003 changes to Tn*6002* due to spontaneous excision in circular form of the *erm(B)*- and *aphA3*-containing macrolide-aminoglycoside-streptothricin (MAS) Element. *Antimicrob. Agents Chemother.* 56, 5994–5997. doi: 10.1128/AAC.01487-12

Prudhomme, M., Attaiech, L., Sanchez, G., Martin, B., and Claverys, J. P. (2006). Antibiotic stress induces genetic transformability in the human pathogen *Streptococcus pneumoniae*. *Science* 313, 89–92. doi: 10.1126/science.1127912

Roberts, A. P., and Kreth, J. (2014). The impact of horizontal gene transfer on the adaptive ability of the human oral microbiome. *Front. Cell. Infect. Microbiol.* 4:124. doi: 10.3389/fcimb.2014.00124

Roberts, A. P., and Mullany, P. (2011). Tn916-like genetic elements: a diverse group of modular mobile elements conferring antibiotic resistance. *FEMS Microbiol. Rev.* 35, 856–871. doi: 10.1111/j.1574-6976.2011.00283.x

Rocco, J. M., and Churchward, G. (2006). The integrase of the conjugative transposon Tn*916* directs strand- and sequence-specific cleavage of the origin of conjugal transfer, *oriT*, by the endonuclease Orf20. *J. Bacteriol.* 188, 2207–2213. doi: 10.1128/JB.188.6.2207-2213.2006

Rudy, C. K., Scott, J. R., and Churchward, G. (1997). DNA binding by the Xis protein of the conjugative transposon Tn*916*. *J. Bacteriol.* 179, 2567–2572.

Santagati, M., Lupo, A., Scillato, M., Di Martino, A., and Stefani, S. (2009). Conjugal mobilization of the Mega element carrying *mef(E)* from *Streptococcus salivarius* to *Streptococcus pneumoniae*. *FEMS Microbiol. Lett.* 290, 79–84. doi: 10.1111/j.1574-6968.2008.01408.x

Sharma, D., Baughman, W., Holst, A., Thomas, S., Jackson, D., Beall, B., et al. (2013). Pneumococcal carriage and invasive disease in children before introduction of the 13-valent conjugate vaccine: comparison with the era before 7-valent conjugate vaccine. *Pediatr. Infect. Dis. J.* 32, e45–e53. doi: 10.1097/INF.0b013e3182788fdd

Stephens, D. S., Zughaier, S. M., Whitney, C. G., Baughman, W. S., Barker, L., Gay, K., et al. (2005). Incidence of macrolide resistance in *Streptococcus pneumoniae*

after introduction of the pneumococcal conjugate vaccine: population-based assessment. *The Lancet* 365, 855–863. doi: 10.1016/S0140-6736(05)71043-6

Syrogiannopoulos, G. A., Grivea, I. N., Ednie, L. M., Bozdogan, B., Katopodis, G. D., Beratis, N. G., et al. (2003). Antimicrobial susceptibility and macrolide resistance inducibility of *Streptococcus pneumoniae* carrying *erm*(*A*), *erm*(*B*), or *mef*(*A*). *Antimicrob. Agents Chemother.* 47, 2699–2702. doi: 10.1128/AAC.47.8.2699-2702.2003

Tettelin, H., Nelson, K. E., Paulsen, I. T., Eisen, J. A., Read, T. D., Peterson, S., et al. (2001). Complete genome sequence of a virulent isolate of *Streptococcus pneumoniae*. *Science* 293, 498–506. doi: 10.1126/science.1061217

Wattam, A. R., Abraham, D., Dalay, O., Disz, T. L., Driscoll, T., Gabbard, J. L., et al. (2014). PATRIC, the bacterial bioinformatics database and analysis resource. *Nucleic Acids Res.* 42, D581–D591. doi: 10.1093/nar/gkt1099

Wierzbowski, A. K., Boyd, D., Mulvey, M., Hoban, D. J., and Zhanel, G. G. (2005). Expression of the *mef*(E) gene encoding the macrolide efflux pump protein increases in *Streptococcus pneumoniae* with increasing resistance to macrolides. *Antimicrob. Agents Chemother.* 49, 4635–4640. doi: 10.1128/AAC.49.11.4635-4640.2005

Wyres, K. L., van Tonder, A., Lambertsen, L. M., Hakenbeck, R., Parkhill, J., Bentley, S. D., et al. (2013). Evidence of antimicrobial resistance-conferring genetic elements among pneumococci isolated prior to 1974. *BMC Genomics* 14:500. doi: 10.1186/1471-2164-14-500

Zähner, D., Zhou, X., Chancey, S. T., Pohl, J., Shafer, W. M., and Stephens, D. S. (2010). Human antimicrobial peptide LL-37 induces *mefE/mel*-mediated macrolide resistance in *Streptococcus pneumoniae*. *Antimicrob. Agents Chemother.* 54, 3516–3519. doi: 10.1128/AAC.01756-09

Zhou, W., Yao, K., Zhang, G., Yang, Y., Li, Y., Lv, Y., et al. (2014). Mechanism for transfer of transposon Tn*2010* carrying macrolide resistance genes in *Streptococcus pneumoniae* and its effects on genome evolution. *J. Antimicrob. Chemother.* 69, 1470–1473. doi: 10.1093/jac/dku019

Conflict of Interest Statement: The authors declare that the research was conducted in the absence of any commercial or financial relationships that could be construed as a potential conflict of interest.

Received: 07 October 2014; accepted: 08 January 2015; published online: 09 February 2015.

Citation: Chancey ST, Agrawal S, Schroeder MR, Farley MM, Tettelin H and Stephens DS (2015) Composite mobile genetic elements disseminating macrolide resistance in Streptococcus pneumoniae. Front. Microbiol. ***6****:26. doi: 10.3389/fmicb.2015.00026*

This article was submitted to Antimicrobials, Resistance and Chemotherapy, a section of the journal Frontiers in Microbiology.

Figure S1. *S. pneumoniae* isolates clustered by MLST typing.

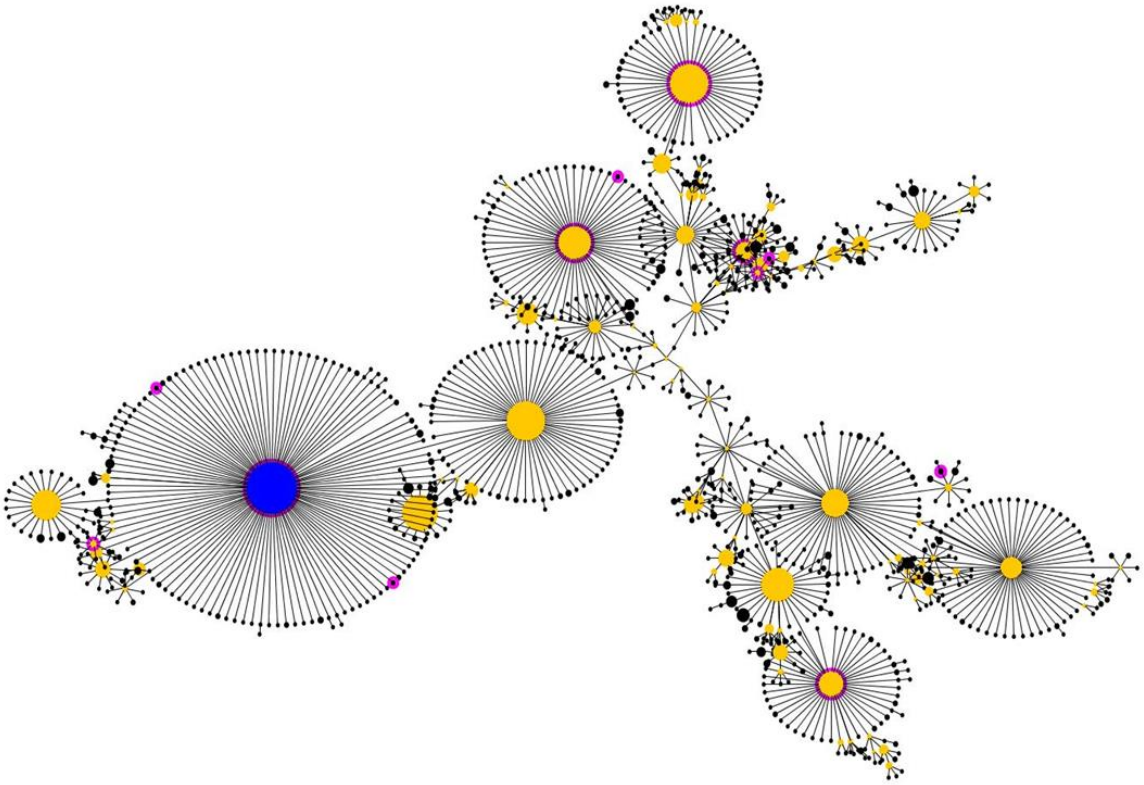

Table S1. Whole-genome sequenced *S. pneumoniae* isolates.

GenBank	Strain	Year	Serotype	ST	CC	Collection [a]	Source	MRME [b]	Resistance genes	CHL		CLI		ERY		TET		Syndromes
										MIC [c]	S/I/R [d]	MIC [c]	S/I/R [d]	MIC [c]	S/I/R [d]	MIC [c]	S/I/R [d]	
AIKK00000000	GA02714	1994	06A	376	2090	GA EIP	blood	Mega-1.I	*mef(E), mel*	=2	S	nd	nd	=4	R	<=0.25	S	healthy
AGQC00000000	NP127	1995	06A	376	2090	Nourti	carriage	Mega-1.I	*mef(E), mel*	dd	S	dd	S	dd	R	nd	S	pneumonia
AGQL00000000	N. carolina^{6A}-23	1997	06A	376	2090	PMEN	unknown	Mega-1.I	*mef(E), mel, cat*	=3	R	0.19	S	=4	R	=0.5	S	menigitis, sinusitis
AILN00000000	GA14373	2000	06A	376	2090	GA EIP	blood	Mega-1.I	*mef(E), mel*	=4	S	=0.12	S	=4	R	<=2	S	bacteremia
AGPH00000000	GA17328	2000	06A	376	2090	GA EIP	blood	Mega-1.I	*mef(E), mel*	<=2	S	<=0.06	S	2	R	<=2	S	bacteremia
AILS00000000	GA17457	2000	19A	199	199	GA EIP	blood	Mega-1.I	*mef(E), mel*	=4	S	=0.25	S	=32	R	<=2	S	pneumonia
AGPN00000000	GA41437	2004	06A	376	2090	GA EIP	blood	Mega-1.I	*mef(E), mel*	<=2	S	=0.06	S	=1	R	<=2	S	pneumonia
ALCQ01000001	GA58581	2010	14	13slv	15	GA EIP	blood	Mega-2.II	*mef(E), mel*	=4	S	=0.06	S	=8	R	<=2	S	pneumonia
AGOT00000000	GA07643	1998	04	695	66	GA EIP	blood	Mega-1.II	*mef(E), mel*	<=2	S	=0.12	S	>16	R	<=0.25	S	bacteremia
AGPZ00000000	GA52306	2007	06C	3676	1379	GA EIP	blood	Mega-1.II	*mef(E), mel*	=4	S	=0.06	S	=4	R	<=2	S	menigitis

GeneBank	Strain	Year	Serotype	ST	CC	Collection [a]	Source	MRME[b]	Resistance genes	CHL		CLI		ERY		TET		Syndromes
										MIC[c]	S/I/R[d]	MIC	S/I/R	MIC	S/I/R	MIC	S/I/R	
AIKH00000000	EU-NP04	2009	06C	1292	1379	Jain	carriage	Mega-1.II	*mef(E), mel*	dd	S	=0.06	S	=4	R	<=2	S	invasive
AIKL00000000	GA04175	1994	19A	199	199	GA EIP	blood	Mega-1.III	*mef(E), mel*	=2	S	<=0.06	S	=4	R	=0.5	S	healthy
ALCJ01000002	GA04672	1995	19A	199	199	GA EIP	blood	Mega-1.III	*mef(E), mel*	=2	S	<=0.06	S	=8	R	=0.5	S	bacteremia
ALCI01000002	GA17301	2000	09V	156	156	GA EIP	blood	Mega-1.III	*mef(E), mel*	<=2	S	<=0.06	S	=8	R	<=2	S	pneumonia
AFGB00000000	GA17570	2001	09V	156	156	GA EIP	blood	Mega-1.III	*mef(E), mel*	=4	S	=0.12	S	=8	R	<=2	S	n/a
AGPM00000000	GA41277	2004	19A	199	199	GA EIP	blood	Mega-1.III	*mef(E), mel*	<=2	S	=0.06	S	=4	R	<=2	S	pneumonia
AGOI00000000	GA44500	2005	19A	2269	199	GA EIP	blood	Mega-1.III	*mef(E), mel*	=4	S	=0.12	S	=16	R	<=2	S	bacteremia
AGOQ00000000	GA44378	2005	23F	81	81	GA EIP	blood	Mega-1.III	*mef(E), mel, tet(M) , cat*	>8	R	=0.06	S	=8	R	>8	R	bacteremia
ALCY01000001	GA47562	2006	11A	62	62	GA EIP	blood	Mega-1.III	*mef(E), mel*	=4	S	=0.12	S	=8	R	<=2	S	bacteremia
AILD00000000	GA47760	2006	11A	62	62	GA EIP	blood	Mega-1.III	*mef(E), mel*	=4	S	=0.06	S	=16	R	<=2	S	pneumonia

GeneBank	Strain	Year	Serotype	ST	CC	Collection [a]	Source	MRME[b]	Resistance genes	CHL		CLI		ERY		TET		Syndromes
										MIC[c]	S/I/R[d]	MIC	S/I/R	MIC	S/I/R	MIC	S/I/R	
AILA00000000	GA47522	2006	15C	199	199	GA EIP	blood	Mega-1.III	*mef(E), mel*	<=2	S	=0.12	S	=16	R	>8	R	menigitis, sinusitis, mastoiditis
AIJW00000000	EU-NP05	2009	15C	199	199	Jain	carriage	Mega-1.III	*mef(E), mel*	dd	S	=0.06	S	=8	R	<=2	S	invasive
AGQH00000000	EU-NP01	2009	19A	695	66	Jain	carriage	Mega-1.III	*mef(E), mel*	dd	S	=0.12	S	=16	R	<=2	S	invasive
ALCW01000001	GA62681	2011	15C	199	199	GA EIP	blood	Mega-1.III	*mef(E), mel*	=4	S	=0.06	S	=8	R	<=2	S	pneumonia
AFGT00000000	GA41317	2004	33F	2705	100	GA EIP	blood	Mega-1.IVb	*mef(E), mel*	=4	S	=0.12	S	=4	R	<=2	S	pneumonia
AILE00000000	GA49194	2006	33F	2705	100	GA EIP	blood	Mega-1.IVb	*mef(E), mel*	=4	S	=0.12	S	=8	R	<=2	S	pneumonia
AIKG00000000	EU-NP03	2009	33F	2705	100	Jain	carriage	Mega-1.IVb	*mef(E), mel*	dd	S	=0.06	S	=4	R	<=2	S	invasive
AIKI00000000	GA02254	1994	14	124	156	GA EIP	blood	Mega-1.Novel	*mef(E), mel*	=2	S	dd	S	=4	R	<=0.25	S	healthy
AGQG00000000	3063-00	1999	19F	652	320	EIP	blood	Mega-2.II	*mef(E), mel*	=4	S	dd	S	=4	R	=1	S	invasive
AIKJ00000000	GA02270	1994	06A	1339	2090	GA EIP	blood	Mega-2.II	*mef(E), mel*	=2	S	dd	S	=8	R	<=0.25	S	healthy

GeneBank	Strain	Year	Serotype	ST	CC	Collection [a]	Source	MRME[b]	Resistance genes	CHL		CLI		ERY		TET		Syndromes
										MIC[c]	S/I/R[d]	MIC	S/I/R	MIC	S/I/R	MIC	S/I/R	
AILJ00000000	GA02506	1994	06B	384	156	GA EIP	blood	Mega-2.II	*mef(E), mel, tet(M)*	=2	S	nd	nd	=4	R	=16	R	healthy
AIKM01000001	GA05248	1995	06B	384	156	GA EIP	blood	Mega-2.II	*mef(E), mel, tet(M)*	=2	S	<=0.06	S	=4	R	=1	S	bacteremia
ALCK01000002	GA04216	1995	06B	2150	156	GA EIP	blood	Mega-2.II	*mef(E), mel, tet(M)*	=2	S	<=0.06	S	=4	R	=1	S	bacteremia
AILH00000000	GA05578	1996	06B	2150	156	GA EIP	blood	Mega-2.II	*mef(E), mel, tet(M)*	=4	S	<=0.06	S	=4	R	=0.5	S	bronchitis
AGQJ00000000	GA08780	1997	09V	156	156	GA EIP	blood	Mega-2.II	*mef(E), mel*	<=2	S	=0.12	S	=16	R	<=0.25	S	pneumonia
AGOX00000000	GA13338	1999	14	13	15	GA EIP	blood	Mega-2.II	*mef(E), mel*	=4	S	=0.12	S	>16	R	<=1	S	bacteremia
ALCT01000001	GA17484	2000	35B	558	558	GA EIP	blood	Mega-2.II	*mef(E), mel*	<=2	S	=0.12	S	=32	R	<=2	S	pneumonia
AIKR00000000	GA18068	2001	04	695	66	GA EIP	blood	Mega-2.II	*mef(E), mel*	=4	S	=0.25	S	=32	R	<=2	S	pneumonia
AGOE00000000	GA16531	2001	06B	146	156	GA EIP	blood	Mega-2.II	*mef(E), mel*	=4	S	=0.12	S	=8	R	<=2	S	septic arthritis, knee
AGPK00000000	GA19077	2002	06A	1296	2090	GA EIP	blood	Mega-2.II	*mef(E), mel*	=4	S	=0.25	S	=32	R	<=2	S	menigitis

GeneBank	Strain	Year	Serotype	ST	CC	Collection [a]	Source	MRME[b]	Resistance genes	CHL		CLI		ERY		TET		Syndromes
										MIC[c]	S/I/R[d]	MIC	S/I/R	MIC	S/I/R	MIC	S/I/R	
AILP000 00000	GA40028	2002	07A	191	191	GA EIP	blood	Mega-2.II	*mef(E), mel*	=4	S	=0.25	S	=16	R	<=2	S	pneumonia
AGPP000 00000	GA41688	2004	14	13	15	GA EIP	blood	Mega-2.II	*mef(E), mel*	=4	S	=0.12	S	=32	R	<=2	S	menigitis
AGOL00 000000	GA41538	2004	06A	384	156	GA EIP	blood	Mega-2.II	*mef(E), mel*	<=2	S	=0.06	S	=4	R	<=2	S	pneumonia
ALCS000 00000	GA19998	2004	19A	156	156	GA EIP	blood	Mega-2.II	*mef(E), mel*	=4	S	=0.25	S	=16	R	<=2	S	pneumonia
AIKZ000 00000	GA41410	2004	19A	1339slv	2090	GA EIP	blood	Mega-2.II	*mef(E), mel*	<=2	S	<=0.03	S	=8	R	<=2	S	pneumonia
AGOA00 000000	GA47033	2005	06C	4150	1379	GA EIP	blood	Mega-2.II	*mef(E), mel*	=4	S	=0.06	S	=4	R	<=2	S	pneumonia
AIKU000 00000	GA43257	2005	19A	156	156	GA EIP	blood	Mega-2.II	*mef(E), mel*	<=2	S	=0.06	S	=4	R	<=2	S	pneumonia
AIJS0000 0000	GA43264	2005	19A	2270	2090	GA EIP	blood	Mega-2.II	*mef(E), mel*	<=2	S	=0.06	S	=8	R	<=2	S	pneumonia
AIKW00 000000	GA44386	2005	19A	2382	2090	GA EIP	blood	Mega-2.II	*mef(E), mel*	<=2	S	=0.06	S	=8	R	<=2	S	pneumonia
AGOC00 000000	GA44452	2005	19A	2541	single	GA EIP	blood	Mega-2.II	*mef(E), mel*	<=2	S	<=0.03	S	=8	R	<=2	S	pneumonia

GeneBank	Strain	Year	Serotype	ST	CC	Collection [a]	Source	MRME[b]	Resistance genes	CHL		CLI		ERY		TET		Syndromes
										MIC[c]	S/I/R[d]	MIC	S/I/R	MIC	S/I/R	MIC	S/I/R	
AGOR00000000	GA44511	2005	19A	4464	156	GA EIP	blood	Mega-2.II	*mef(E), mel*	<=2	S	=0.06	S	=4	R	<=2	S	menigitis
AIKV00000000	GA44128	2005	23F	37	439	GA EIP	blood	Mega-2.II	*mef(E), mel*	<=2	S	=0.06	S	=8	R	<=2	S	pneumonia
AFGS00000000	GA47368	2006	19A	1339	2090	GA EIP	blood	Mega-2.II	*mef(E), mel*	=4	S	=0.12	S	=32	R	<=2	S	pneumonia
AGQD00000000	GA47751	2006	19A	2268	2090	GA EIP	blood	Mega-2.II	*mef(E), mel*	=4	S	=0.12	S	=16	R	<=2	S	bacteremia
AGPU00000000	GA47388	2006	19A	4026	156	GA EIP	blood	Mega-2.II	*mef(E), mel*	=4	S	=0.12	S	=16	R	<=2	S	bacteremia
AGOK00000000	GA49447	2006	19A	4176	single	GA EIP	blood	Mega-2.II	*mef(E), mel*	=4	S	=0.12	S	=16	R	<=2	S	pneumonia
AIKZ00000000	GA47461	2006	35B	558	558	GA EIP	blood	Mega-2.II	*mef(E), mel*	=4	S	=0.06	S	=8	R	<=2	S	otitis
ALCP00000000	GA56113	2008	09V	156	156	GA EIP	blood	Mega-2.II	*mef(E), mel*	=4	S	=0.12	S	=16	R	<=2	S	pneumonia
AGQA00000000	GA54644	2008	19A	156	156	GA EIP	blood	Mega-2.II	*mef(E), mel*	=4	S	=0.12	S	=16	R	<=2	S	pneumonia
ALCN00000000	GA54354	2008	23A	338	156	GA EIP	CSF	Mega-2.II	*mef(E), mel*	=4	S	=0.12	S	>32	R	<=2	S	bacteremia

GeneBank	Strain	Year	Serotype	ST	CC	Collection [a]	Source	MRME[b]	Resistance genes	CHL		CLI		ERY		TET		Syndromes
										MIC[c]	S/I/R[d]	MIC	S/I/R	MIC	S/I/R	MIC	S/I/R	
ALCO01000002	GA56348	2009	22F	433	433	GA EIP	blood	Mega-2.II	*mef(E), mel*	<=2	S	=0.06	S	=16	R	<=2	S	bacteremia
ALCL01000001	GA60190	2010	06C	1292	1379	GA EIP	blood	Mega-2.II	*mef(E), mel*	=4	S	=0.06	S	=4	R	<=2	S	pneumonia
ALCU00000000	GA62331	2011	23A	338	156	GA EIP	blood	Mega-2.II	*mef(E), mel*	=4	S	=0.12	S	>32	R	<=2	S	otitis
AFAX00000000	GA04375	1995	19F	236	320	GA EIP	carriage	Mega-2.IVa	*mef(E), mel*	=2	S	<=0.06	S	=8	R	<=0.25	S	bacteremia
AGPE00000000	GA16242	2001	06B	1536	1536	GA EIP	blood	Mega-2.IVa	*mef(E), mel*	=4	S	=0.12	S	=64	R	<=2	S	pneumonia, fever
AFGA00000000	GA17545	2000	06B	1536slv	1536	GA EIP	CSF	Mega-2.IVc	*mef(E), mel*	=4	S	=0.12	S	>64	R	<=2	S	pneumonia
AGQB00000000	Netherlands^{15B}-37	1987	15C	199	199	PMEN	CSF	none	none	=0.19	S	0.19	S	0.13	S	=0.25	S	pneumonia
AGQF00000000	NP112	1995	06B	1536	1536	Nourti	carriage	none	none	dd	S	dd	S	dd	S	nd	S	pneumonia
AILG00000000	NP141	1995	07F	191	191	Nourti	carriage	none	none	dd	S	dd	S	dd	S	nd	S	menigitis
AGOH00000000	NP070	1995	23F	37	439	Nourti	carriage	none	none	dd	S	dd	S	dd	S	nd	S	pneumonia

GeneBank	Strain	Year	Serotype	ST	CC	Collection [a]	Source	MRME[b]	Resistance genes	CHL		CLI		ERY		TET		Syndromes
										MIC[c]	S/I/R[d]	MIC	S/I/R	MIC	S/I/R	MIC	S/I/R	
AIKN00000000	GA06083	1996	15B	199slv	199	GA EIP	blood	none	none	=2	S	=0.06	S	<=0.06	S	>16	R	invasive
AGQI00000000	GA07228	1997	03	180	180	GA EIP	blood	none	none	<=2	S	=0.12	S	=1	R	<=0.25	S	bacteremia
AIKO00000000	GA07914	1998	11A	62	62	GA EIP	blood	none	none	=4	S	=0.12	S	=0.12	S	<=1	S	invasive
AIKB00000000	GA13224	1999	07F	1791	single	GA EIP	blood	none	none	<=2	S	=0.12	S	=0.12	S	<=1	S	pneumonia
AGPA00000000	GA13637	1999	18C	3060	113	GA EIP	blood	none	none	<=2	S	=0.12	S	<=0.06	S	<=1	S	pneumonia
AGOV00000000	GA11426	1999	19A	1963	199	GA EIP	blood	none	none	<=2	S	=0.25	S	=0.12	S	<=1	S	bacteremia
AILM00000000	GA13723	1999	19F	43	15	GA EIP	blood	none	none	<=2	S	=0.12	S	=0.12	S	<=1	S	pneumonia
AIJZ00000000	GA13499	1999	19F	236	320	GA EIP	blood	none	none	<=2	S	=0.25	S	=0.12	S	<=1	S	bacteremia
AGNU00000000	GA11184	1999	19F	649	199	GA EIP	blood	none	none	<=2	S	=0.12	S	=0.12	S	<=1	S	invasive
AGPB00000000	GA13856	1999	33F	636	100	GA EIP	blood	none	none	<=2	S	<=0.06	S	<=0.06	S	<=1	S	bacteremia

GeneBank	Strain	Year	Serotype	ST	CC	Collection [a]	Source	MRME[b]	Resistance genes	CHL		CLI		ERY		TET		Syndromes
										MIC[c]	S/I/R[d]	MIC	S/I/R	MIC	S/I/R	MIC	S/I/R	
AIKQ00000000	GA14688	2000	23F	2745	single	GA EIP	blood	none	none	<=2	S	=0.12	S	<=0.06	S	<=2	S	bacteremia
AGPJ00000000	GA17971	2001	06A	1175	single	GA EIP	blood	none	none	<=2	S	=0.12	S	=0.06	S	<=2	S	bacteremia
AIJX00000000	GA40183	2002	19A	1341	199	GA EIP	blood	none	none	=4	S	=0.25	S	=0.12	S	<=2	S	bacteremia
AIKA00000000	GA40410	2003	19A	1963	15	GA EIP	blood	none	none	=4	S	=0.12	S	=0.12	S	<=2	S	bacteremia
AGQK00000000	GA19690	2004	03	180	180	GA EIP	blood	none	none	=4	S	>2	R	>32	R	>8	R	bacteremia
AGNW00000000	4027-06	2005	19A	2344	199	EIP	blood	none	none	=2	S	dd	S	=0.06	S	=2	S	pneumonia
AGNX00000000	6735-05	2005	19A	2344	199	EIP	PE	none	none	=2	S	dd	S	=0.03	S	=2	S	nd
AGPQ00000000	GA43380	2005	19A	2348	single	GA EIP	blood	none	none	<=2	S	=0.06	S	=0.06	S	<=2	S	pneumonia
AGOF00000000	6901-05	2005	19A	2381	199	EIP	blood	none	none	=2	S	dd	S	=0.03	S	=2	S	invasive
AGON00000000	6963-05	2005	19A	2392	199	EIP	blood	none	none	dd	S	dd	S	dd	S	nd	nd	invasive

GeneBank	Strain	Year	Serotype	ST	CC	Collection [a]	Source	MRME[b]	Resistance genes	CHL		CLI		ERY		TET		Syndromes
										MIC[c]	S/I/R[d]	MIC	S/I/R	MIC	S/I/R	MIC	S/I/R	
AGOM00000000	5787-06	2005	19A	2542	199	EIP	blood	none	none	=4	S	dd	S	=0.06	S	=2	S	bacteremia without focus
AGOB00000000	GA43265	2005	19A	2584	199	GA EIP	blood	none	none	<=2	S	=0.06	S	<=0.03	S	<=2	S	bacteremia
AFGR00000000	GA47901	2006	01	304	306	GA EIP	blood	none	none	=4	S	=0.06	S	=0.06	S	<=2	S	pneumonia, septic shock
AGPR00000000	GA47283	2006	07F	191	191	GA EIP	blood	none	none	<=2	S	=0.12	S	=0.06	S	<=2	S	pneumonia
AGPV00000000	GA47439	2006	07F	1176	218	GA EIP	blood	none	none	=4	S	=0.06	S	=0.06	S	<=2	S	pneumonia
AGPS00000000	GA47360	2006	19A	695	66	GA EIP	blood	none	none	=4	S	=0.12	S	=0.06	S	<=2	S	pneumonia
AGPY00000000	GA47976	2006	19F	43	15	GA EIP	blood	none	none	<=2	S	<=0.03	S	<=0.03	S	<=2	S	pneumonia
AGPT00000000	GA47373	2006	19F	654	251	GA EIP	blood	none	none	=4	S	=0.12	S	=0.12	S	<=2	S	pneumonia
ALCR01000002	GA60080	2010	06C	1092	66	GA EIP	blood	ribosomal mutatio	none	=4	S	>2	R	>32	R	<=2	S	pneumonia
AILI00000000	England[14]-9	1993	14	9	15	PMEN	nd	Tn*1207*	*mef(A), msr(D)*	=2	S	dd	S	=32	R	<1	S	invasive

GeneBank	Strain	Year	Serotype	ST	CC	Collection [a]	Source	MRME[b]	Resistance genes	CHL		CLI		ERY		TET		Syndromes
										MIC[c]	S/I/R[d]	MIC	S/I/R	MIC	S/I/R	MIC	S/I/R	
AGOS000000000	NP170	1995	23F	81	81	Nourti	carriage	Tn*2009*	*mef(E), mel,tet(M) , cat*	dd	R	dd	S	nd	R	nd	R	pneumonia
AILL010000001	GA05245	1995	23F	242	242	GA EIP	blood	Tn*2009*	*mef(E), mel, tet(M)*	=4	S	<=0.06	S	=4	R	=32	R	bacteremia
AILK000000000	GA08825	1998	19F	651	320	GA EIP	blood	Tn*2009*	*mef(E), mel, tet(M)*	<=2	S	=0.12	S	=4	R	=16	R	bacteremia
AGOZ00000000	GA13494	1999	14	656	156	GA EIP	blood	Tn*2009*	*mef(E), mel,tet(M) , cat*	=16	R	=0.12	S	=16	R	>8	R	bacteremia
AGOW00000000	GA11663	1999	19F	81	81	GA EIP	blood	Tn*2009*	*mef(E), mel,tet(M) , cat*	=16	R	<=0.06	S	=8	R	>8	R	bacteremia
AIKP000000000	GA13430	1999	19F	634	81	GA EIP	blood	Tn*2009*	*mef(E), mel,tet(M) , cat*	=16	R	=0.12	S	=8	R	>8	R	bacteremia
AGOY00000000	GA13455	1999	19F	651	320	GA EIP	blood	Tn*2009*	*mef(E), mel, tet(M)*	=4	S	=0.25	S	=8	R	>8	R	pneumonia
AGPI000000000	GA17371	2000	19F	8014	320	GA EIP	PE	Tn*2009*	*mef(E), mel, tet(M)*	=4	S	=0.25	S	=32	R	>8	R	bacteremia
AGPG000000000	GA17227	2000	23F	242	242	GA EIP	blood	Tn*2009*	*mef(E), mel, tet(M)*	<=2	S	=0.12	S	=2	R	>8	R	bacteremia
AILO000000000	GA17719	2001	19F	926	320	GA EIP	blood	Tn*2009*	*mef(E), mel, tet(M)*	=4	S	=0.12	S	=16	R	<=2	S	pneumonia

GeneBank	Strain	Year	Serotype	ST	CC	Collection [a]	Source	MRME[b]	Resistance genes	CHL		CLI		ERY		TET		Syndromes
										MIC[c]	S/I/R[d]	MIC	S/I/R	MIC	S/I/R	MIC	S/I/R	
AGPF000 00000	GA16833	2002	19F	5053	320	GA EIP	blood	Tn*2009*	*mef(E), mel, tet(M)*	<=2	S	=0.12	S	=16	R	>8	R	pneumonia
AGPO00 000000	GA41565	2004	19A	81	81	GA EIP	blood	Tn*2009*	*mef(E), mel,tet(M) , cat*	=8	R	<=0.03	S	=1	R	>8	R	menigitis
AFGD000 00000	GA41301	2004	23F	242	242	GA EIP	CSF	Tn*2009*	*mef(E), mel, tet(M)*	<=2	S	=0.06	S	=2	R	>8	R	pneumonia
AIKY000 00000	GA47210	2006	15B	3280	156	GA EIP	blood	Tn*2009*	*mef(E), mel, tet(M)*	=4	S	=0.12	S	=8	R	>8	R	pneumonia
AGOD00 000000	GA49138	2006	19F	651	320	GA EIP	blood	Tn*2009*	*mef(E), mel, tet(M)*	=4	S	=0.12	S	=8	R	>8	R	pneumonia
AILF000 00000	GA49542	2007	09V	3148	156	GA EIP	blood	Tn*2009*	*mef(E), mel, tet(M)*	=4	S	=0.12	S	=16	R	>8	R	pneumonia
AIKE000 00000	4075-00	1999	19F	635	320	EIP	blood	Tn*2010*	*mef(E), mel, erm(B),*	=4	S	dd	R	=16	R	=8	R	healthy
AGPD00 000000	GA16121	2000	19F	236	320	GA EIP	blood	Tn*2010*	*mef(E), mel, erm(B),*	<=2	S	>4	R	>64	R	=8	R	bacteremia, fever
AIJV0000 0000	GA11856	2000	19F	271	320	GA EIP	blood	Tn*2010*	*mef(E), mel, erm(B),*	=4	S	>4	R	>64	R	<=2	S	pneumonia
AGPC000 00000	GA14798	2000	19F	3039	320	GA EIP	blood	Tn*2010*	*mef(E), mel, erm(B),*	=4	S	>4	R	>64	R	>8	R	fever

GenBank	Strain	Year	Serotype	ST	CC	Collection [a]	Source	MRME[b]	Resistance genes	CHL		CLI		ERY		TET		Syndromes
										MIC[c]	S/I/R[d]	MIC	S/I/R	MIC	S/I/R	MIC	S/I/R	
AGOO00000000	GA18523	2001	19F	2476	320	GA EIP	blood	Tn*2010*	*mef(E), mel, erm(B),*	<=2	S	=0.5	I	>64	R	>8	R	pneumonia
AGPL00000000	GA19451	2003	19F	271	320	GA EIP	blood	Tn*2010*	*mef(E), mel, erm(B),*	=4	S	>4	R	>64	R	>8	R	pneumonia
AIKC00000000	GA19923	2004	19A	320	320	GA EIP	blood	Tn*2010*	*mef(E), mel, erm(B),*	<=2	S	>2	R	>32	R	>8	R	bacteremia
AIJT00000000	7533-05	2005	19A	320	320	EIP	blood	Tn*2010*	*mef(E), mel, erm(B),*	=4	S	dd	R	=32	R	=8	R	healthy
AGNY00000000	GA44288	2005	19A	320	320	GA EIP	CSF	Tn*2010*	*mef(E), mel, erm(B),*	=4	S	>2	R	>32	R	>8	R	pneumonia
AIJY00000000	8190-05	2005	19A	2347	320	EIP	blood	Tn*2010*	*mef(E), mel, erm(B),*	=4	S	dd	R	=32	R	=8	R	otitis media
AIKD00000000	7879-04	2005	19A	2383	320	EIP	blood	Tn*2010*	*mef(E), mel, erm(B),*	dd	S	dd	R	nd	R	nd	R	bacteremia
AGQE00000000	5185-06	2005	19A	2393	320	EIP	blood	Tn*2010*	*mef(E), mel, erm(B),*	=4	S	dd	R	=32	R	=8	R	healthy
AGOG00000000	7286-06	2005	19A	2514	320	EIP	blood	Tn*2010*	*mef(E), mel, erm(B),*	=4	S	dd	R	=32	R	=8	R	healthy
AIJU00000000	5652-06	2005	19A	2588	320	EIP	blood	Tn*2010*	*mef(E), mel, erm(B),*	=4	S	dd	R	=32	R	=8	R	healthy

GeneBank	Strain	Year	Serotype	ST	CC	Collection [a]	Source	MRME[b]	Resistance genes	CHL		CLI		ERY		TET		Syndromes
										MIC[c]	S/I/R[d]	MIC	S/I/R	MIC	S/I/R	MIC	S/I/R	
AGPW00000000	GA47688	2006	19A	320	320	GA EIP	blood	Tn*2010*	*mef(E), mel, erm(B),*	=8	R	>2	R	>32	R	>8	R	pneumonia
AGPX00000000	GA47778	2006	19A	320	320	GA EIP	blood	Tn*2010*	*mef(E), mel, erm(B),*	=4	S	>2	R	>32	R	>8	R	pneumonia, pancreatitis
AILC00000000	GA47628	2006	19F	236	320	GA EIP	joint	Tn*2010*	*mef(E), mel, erm(B),*	=4	S	>2	R	>32	R	>8	R	pneumonia
AGNZ00000000	GA47281	2006	19F	3039	320	GA EIP	CSF	Tn*2010*	*mef(E), mel, erm(B),*	=4	S	>2	R	>32	R	>8	R	bacteremia
AIKF00000000	EU-NP02	2009	19A	1451	320	Jain	carriage	Tn*2010*	*mef(E), mel, erm(B),*	S	S	>2	R	>32	R	>8	R	invasive
ALCM00000000	GA58771	2010	19A	320	320	GA EIP	blood	Tn*2010*	*mef(E), mel, erm(B),*	=4	S	>2	R	>32	R	>8	R	menigitis
AILB00000000	GA47597	2006	03	180	180	GA EIP	blood	Tn*3872*	*erm(B), tet(M), cat(pC194*	>8	R	>2	R	>32	R	>8	R	pneumonia, septic shock
AGNV00000000	GA47502	2006	19A	1374	single	GA EIP	blood	Tn*3872*	*erm(B), tet(M), cat(pC194*	=8	R	>2	R	>32	R	>8	R	pneumonia
AGOU00000000	GA11304	1999	06A	90	156	GA EIP	blood	Tn*6002*	*erm(B), tet(M), cat(pC194*	=16	R	>2	R	>16	R	>8	R	pneumonia
AIKS00000000	GA19101	2002	03	180	180	GA EIP	blood	Tn*6002*	*erm(B), tet(M), cat(pC194*	=16	R	=0.5	I	=2	R	>8	R	pneumonia

GeneBank	Strain	Year	Serotype	ST	CC	Collection [a]	Source	MRME[b]	Resistance genes	CHL		CLI		ERY		TET		Syndromes
										MIC[c]	S/I/R[d]	MIC	S/I/R	MIC	S/I/R	MIC	S/I/R	
AIKT00000000	GA40563	2003	04	5872	single	GA EIP	blood	Tn*6002*	*erm(B)*, *tet(M)*, *cat* (pC194	=16	R	>4	R	=64	R	>8	R	cellulitis
AGOP00000000	GA44194	2005	19A	2543	63	GA EIP	blood	Tn*6002*	*erm(B)*, *tet(M)*	=4	S	>2	R	>32	R	>8	R	pneumonia
AIKX00000000	GA47179	2006	15A	63	63	GA EIP	blood	Tn*6002*	*erm(B)*, *tet(M)*	=4	S	>2	R	>32	R	>8	R	pneumonia
AILQ01000002	GA47794	2006	15A	63	63	GA EIP	blood	Tn*6002*	*erm(B)*, *tet(M)*	=4	S	>2	R	>32	R	>8	R	septic arthritis
ALCG00000000	GA52612	2007	15A	5004	63	GA EIP	blood	Tn*6002*	*erm(B)*, *tet(M)*	=4	S	>2	R	>32	R	>8	R	pneumonia
ALCV00000000	GA60132	2010	06C	1390	1390	GA EIP	blood	Tn*6002*	*erm(B)*, *tet(M)*	=4	S	>2	R	>32	R	>8	R	pneumonia
ALCX00000000	GA58981	2010	22F	433	433	GA EIP	blood	Tn*6002*	*erm(B)*, *tet(M)*	=4	S	>2	R	>32	R	>8	R	pneumonia

[a] Collection, Isolates were provided by the following agencies: GEIP, EIP, Sharma, PMEN, Pneumococcal Molecular Epidemiology Network

[b] MRME, Macrolide Resistance Encoding Mobile Element

[C] MIC, Minimum inhibitory concentration, reported at µg/ml

[d] S/I/R, Sensitive/Intermediate/Resistant

Antibiotic abbreviations, ERY, erythromycin; CLI, clindamycin; TET, tetracycline

Supplemental Table S2. Macrolide resistance element insertion sites.

Isolate							ERY		CLI		TET	
Name	**Year**	**Serotype**		**CC**[a]	**Sequence name**	**Size (bp)**	**Insertion site**[b]	**MIC**[c]	**S/I/R**	**MIC**	**S/I/R**	**MIC**	**S/I/R**
3063-00	1999	19F	652	320	3063-00/Mega-2.II	5412	SP_0180	=4	R	dd	S	=1	S
4075-00	1999	19F	635	320	4075-00/Mega-1.V	5511	Tn*916 orf6*	=16	R	dd	R	=8	R
5185-06	2005	19A	2393	320	5185-06/Mega-1.V	5511	Tn*916 orf6*	=32	R	dd	R	=8	R
5652-06	2005	19A	2588	320	5652-06/Mega-1.V	5511	Tn*916 orf6*	=32	R	dd	R	=8	R
7286-06	2005	19A	2514	320	7286-06/Mega-1.V	5511	Tn*916 orf6*	=32	R	dd	R	=8	R
7533-05	2005	19A	320	320	7533-05/Mega-1.V	5511	Tn*916 orf6*	=32	R	dd	R	=8	R
7879-04	2005	19A	2383	320	7879-04/Mega-1.V	5511	Tn*916 orf6*	dd	R	dd	R	dd	R
8190-05	2005	19A	2347	320	8190-05/Mega-1.V	5511	Tn*916 orf6*	=32	R	dd	R	=8	R
EU-NP02	2009	19A	695	320	EU-NP02/Mega-1.V	5511	SP_0103	>32	R	>2	R	>8	R
EU-NP03	2009	33F	1451	100	EU-NP03/Mega-1.IVb	5511	SP_1029	=4	R	=0.06	S	<=2	S
EU-NP04	2009	06C	2705	1379	EU-NP04/Mega-1.II	5511	SP_0180	=4	R	=0.06	S	<=2	S
EU-NP05	2009	15C	1292	199	EU-NP05/Mega-1.III	5511	SP_0103	=8	R	=0.06	S	<=2	S
GA13338	1999	14	199	15	GA13338/Mega-2.II	5412	SP_0180	>16	R	=0.12	S	<=1	S
GA41688	2004	14	13	15	GA41688/Mega-2.II	5412	SP_0180	=32	R	=0.12	S	<=2	S
GA58581	2010	14	13	15	GA58581/Mega-2.II	5412	SP_0180	=8	R	=0.06	S	<=2	S
GA47562	2006	11A	62	62	GA47562/Mega-2.II	5412	SP_0180	=8	R	=0.12	S	<=2	S
GA47760	2006	11A	62	62	GA47760/Mega-1.III	5412	SP_0103	=16	R	=0.06	S	<=2	S
GA41565	2004	19A	81	81	GA41565/Mega-1.V	5511	Tn*916 orf6*	=1	R	<=0.03	S	>8	R
GA11663	1999	19F	81	81	GA11663/Mega-1.V	5511	Tn*916 orf6*	=8	R	<=0.06	S	>8	R
GA13430	1999	19F	634	81	GA13430/Mega-1.V	5511	Tn*916 orf6*	=8	R	=0.12	S	>8	R
NP170	1995	23F	81	81	NP170/Mega-1.V	5511	Tn*916 orf6*	dd	R	dd	S	nd	R
GA44378	2005	23F	81	81	GA44378/Mega-1.III	5511	SP_0103	=8	R	=0.06	S	>8	R
GA41317	2004	33F	2705	100	GA41317/Mega-1.IVb	5511	SP_1029	=4	R	=0.12	S	<=2	S
GA49194	2006	33F	2705	100	GA49194/Mega-1.IVb	5412	SP_1029	=8	R	=0.12	S	<=2	S
GA02254	1994	14	124	156	GA02254/Mega-1.novel	5511	novel	=4	R	dd	S	<=0.25	S
GA13494	1999	14	656	156	GA13494/Mega-1.V	5511	Tn*916 orf6*	=16	R	=0.12	S	>8	R
GA41538	2004	06A	384	156	GA41538/Mega-2.II	5412	SP_0180	=4	R	=0.06	S	<=2	S
GA02506	1994	06B	384	156	GA02506/Mega-2.II	5412	SP_0180	=4	R	dd	S	=16	R
GA04216	1995	06B	2150	156	GA04216/Mega-2.II	5412	SP_0180	=4	R	<=0.06	S	=1	S
GA05248	1995	06B	384	156	GA05248/Mega-2.II	5412	SP_0180	=4	R	<=0.06	S	=1	S
GA05578	1996	06B	2150	156	GA05578/Mega-2.II	5412	SP_0180	=4	R	<=0.06	S	=0.5	S
GA16531	2001	06B	146	156	GA16531/Mega-2.II	5412	SP_0180	=8	R	=0.12	S	<=2	S
GA08780	1997	09V	156	156	GA08780/Mega-2.II	5412	SP_0180	=16	R	=0.12	S	<=0.25	S
GA17301	2000	09V	156	156	GA17301/Mega-1.III	5511	SP_0103	=8	R	<=0.06	S	<=2	S

Isolate								ERY		CLI		TET	
Name	**Year**	**Serotype**		**CC[a]**	**Sequence name**	**Size (bp)**	**Insertion site[b]**	**MIC[c]**	**S/I/R**	**MIC**	**S/I/R**	**MIC**	**S/I/R**
GA17570	2001	09V	156	156	GA17570/Mega-1.III	5511	SP_0103	=8	R	=0.12	S	<=2	S
GA49542	2007	09V	3148	156	GA49542/Mega-1.V	5511	Tn*916 orf6*	=16	R	=0.12	S	>8	R
GA56113	2008	09V	156	156	GA56113/Mega-2.II	5412	SP_0180	=16	R	=0.12	S	<=2	S
GA47210	2006	15B	3280	156	GA47210/Mega-1.V	5511	Tn*916 orf6*	=8	R	=0.12	S	>8	R
GA19998	2004	19A	156	156	GA19998/Mega-2.II	5412	SP_0180	=16	R	=0.25	S	<=2	S
GA43257	2005	19A	156	156	GA43257/Mega-2.II	5412	SP_0180	=4	R	=0.06	S	<=2	S
GA44511	2005	19A	4464	156	GA44511/Mega-2.II	5412	SP_0180	=4	R	=0.06	S	<=2	S
GA47388	2006	19A	4026	156	GA47388/Mega-2.II	5412	SP_0180	=16	R	=0.12	S	<=2	S
GA54644	2008	19A	156	156	GA54644/Mega-2.II	5412	SP_0180	=16	R	=0.12	S	<=2	S
GA54354	2008	23A	338	156	GA54354/Mega-2.II	5412	SP_0180	>32	R	=0.12	S	<=2	S
GA62331	2011	23A	338	156	GA62331/Mega-2.II	5412	SP_0180	>32	R	=0.12	S	<=2	S
GA40028	2002	07A	191	191	GA40028/Mega-2.II	5412	SP_0180	=16	R	=0.25	S	<=2	S
GA47522	2006	15C	199	199	GA47522/Mega-1.III	5412	SP_0103	=16	R	=0.12	S	>8	R
GA04175	1994	19A	199	199	GA04175/Mega-1.III	5511	SP_0103	=4	R	<=0.06	S	=0.5	S
GA04672	1995	19A	199	199	GA04672/Mega-1.III	5511	SP_0103	=8	R	<=0.06	S	=0.5	S
GA17457	2000	19A	199	199	GA17457/Mega-1.I	5511	SP_1598	=32	R	=0.25	S	<=2	S
GA41277	2004	19A	199	199	GA41277/Mega-1.III	5511	SP_0103	=4	R	=0.06	S	<=2	S
GA44500	2005	19A	2269	199	GA44500/Mega-1.III	5511	SP_0103	=16	R	=0.12	S	<=2	S
GA05245	1995	23F	242	242	GA05245/Mega-1.V	5511	Tn*916 orf6*	=4	R	<=0.06	S	=32	R
GA17227	2000	23F	242	242	GA17227/Mega-1.V	5511	Tn*916 orf6*	=2	R	=0.12	S	>8	R
GA41301	2004	23F	242	242	GA41301/Mega-1.V	5511	Tn*916 orf6*	=2	R	=0.06	S	>8	R
GA19923	2004	19A	320	320	GA19923/Mega-1.V	5511	Tn*916 orf6*	>32	R	>2	R	>8	R
GA44288	2005	19A	320	320	GA44288/Mega-1.V	5511	Tn*916 orf6*	>32	R	>2	R	>8	R
GA47688	2006	19A	320	320	GA47688/Mega-1.V	5511	Tn*916 orf6*	>32	R	>2	R	>8	R
GA47778	2006	19A	320	320	GA47778/Mega-1.V	5511	Tn*916 orf6*	>32	R	>2	R	>8	R
GA58771	2010	19A	320	320	GA58771/Mega-1.V	5511	Tn*916 orf6*	>32	R	>2	R	>8	R
GA04375	1995	19F	236	320	GA04375/Mega-2.IVa	5412	SP_1029	=8	R	<=0.06	S	<=0.25	S
GA08825	1998	19F	651	320	GA08825/Mega-1.V	5511	Tn*916 orf6*	=4	R	=0.12	S	=16	R
GA13455	1999	19F	651	320	GA13455/Mega-1.V	5511	Tn*916 orf6*	=8	R	=0.25	S	>8	R
GA11856	2000	19F	271	320	GA11856/Mega-1.V	5511	Tn*916 orf6*	>64	R	>4	R	<=2	S
GA14798	2000	19F	3039	320	GA14798/Mega-1.V	5511	Tn*916 orf6*	>64	R	>4	R	>8	R
GA16121	2000	19F	236	320	GA16121/Mega-1.V	5511	Tn*916 orf6*	>64	R	>4	R	=8	R
GA17371	2000	19F	8014	320	GA17371/Mega-1.V	5511	Tn*916 orf6*	=32	R	=0.25	S	>8	R
GA17719	2001	19F	926	320	GA17719/Mega-1.V	5511	Tn*916 orf6*	=16	R	=0.12	S	<=2	S

Isolate								ERY		CLI		TET	
Name	**Year**	**Serotype**		**CC[a]**	**Sequence name**	**Size (bp)**	**Insertion site[b]**	**MIC[c]**	**S/I/R**	**MIC**	**S/I/R**	**MIC**	**S/I/R**
GA18523	2001	19F	2476	320	GA18523/Mega-1.V	5511	Tn*916 orf6*	>64	R	=0.5	I	>8	R
GA16833	2002	19F	5053	320	GA16833/Mega-1.V	5511	Tn*916 orf6*	=16	R	=0.12	S	>8	R
GA19451	2003	19F	271	320	GA19451/Mega-1.V	5511	Tn*916 orf6*	>64	R	>4	R	>8	R
GA47281	2006	19F	3039	320	GA47281/Mega-1.V	5511	Tn*916 orf6*	>32	R	>2	R	>8	R
GA47628	2006	19F	236	320	GA47628/Mega-1.V	5511	Tn*916 orf6*	>32	R	>2	R	>8	R
GA49138	2006	19F	651	320	GA49138/Mega-1.V	5511	Tn*916 orf6*	=8	R	=0.12	S	>8	R
GA56348	2009	22F	433	433	GA56348/Mega-2.II	5412	SP_0180	=16	R	=0.06	S	<=2	S
GA44128	2005	23F	37	439	GA44128/Mega-2.II	5412	SP_0180	=8	R	=0.06	S	<=2	S
GA17484	2000	35B	558	558	GA17484/Mega-2.II	5412	SP_0180	=32	R	=0.12	S	<=2	S
GA47461	2006	35B	558	558	GA47461/Mega-2.II	5412	SP_0180	=8	R	=0.06	S	<=2	S
GA47033	2005	06C	4150	1379	GA47033/Mega-1.II	5412	SP_0180	=4	R	=0.06	S	<=2	S
GA52306	2007	06C	3676	1379	GA52306/Mega-1.II	5412	SP_0180	=4	R	=0.06	S	<=2	S
GA60190	2010	06C	1292	1379	GA60190/Mega-1.II	5511	SP_0180	=4	R	=0.06	S	<=2	S
GA17545	2000	06B	1536slv	1536	GA17545/Mega-2.IVc	5412	SP_1029	>64	R	=0.12	S	<=2	S
GA16242	2001	06B	1536	1536	GA16242/Mega-2.IVa	5412	SP_1029	=64	R	=0.12	S	<=2	S
GA02270	1994	06A	1339	2090	GA02270/Mega-2.II	5412	SP_0180	=8	R	dd	S	<=0.25	S
GA02714	1994	06A	376	2090	GA02714/Mega-1.I	5511	SP_1598	=4	R	dd	S	<=0.25	S
NP127	1995	06A	376	2090	NP127/Mega-1.I	5511	SP_1598	dd	R	dd	S	nd	S
Northcarolina[6A]-23	1997	06A	376	2090	orthcarolina6A-23/Mega-	5511	SP_1598	=4	R	0.19	S	=0.5	S
GA14373	2000	06A	376	2090	GA14373/Mega-1.I	5511	SP_1598	=4	R	=0.12	S	<=2	S
GA17328	2000	06A	376	2090	GA17328/Mega-1.I	5511	SP_1598	2	R	<=0.06	S	<=2	S
GA19077	2002	06A	1296	2090	GA19077/Mega-2.II	5412	SP_0180	=32	R	=0.25	S	<=2	S
GA41437	2004	06A	376	2090	GA41437/Mega-1.I	5511	SP_1598	=1	R	=0.06	S	<=2	S
GA41410	2004	19A	1339slv	2090	GA41410/Mega-2.II	5412	SP_0180	=8	R	<=0.03	S	<=2	S
GA43264	2005	19A	2270	2090	GA43264/Mega-2.II	5412	SP_0180	=8	R	=0.06	S	<=2	S
GA44386	2005	19A	2382	2090	GA44386/Mega-2.II	5412	SP_0180	=8	R	=0.06	S	<=2	S
GA47368	2006	19A	1339	2090	GA47368/Mega-2.II	5412	SP_0180	=32	R	=0.12	S	<=2	S
GA47751	2006	19A	2268	2090	GA47751/Mega-2.II	5412	SP_0180	=16	R	=0.12	S	<=2	S
GA62681	2011	15C	199	199	GA62681/Mega-1.III	5511	SP_0103	=8	R	=0.06	S	<=2	S
GA07643	1998	04	695	246	GA07643/Mega-1.II	5511	SP_0180	>16	R	=0.12	S	<=0.25	S
GA18068	2001	04	695	246	GA18068/Mega-2.II	5412	SP_0180	=32	R	=0.25	S	<=2	S
GA44452	2005	19A	2541	single	GA44452/Mega-2.II	5412	SP_0180	=8	R	<=0.03	S	<=2	S
GA49447	2006	19A	4176	single	GA49447/Mega-2.II	5412	SP_0180	=16	R	=0.12	S	<=2	S

[a] CC, clonal complex

[b] TIGR4 annotation

[c] MIC, Minimum inhibitory concentration, reported at µg/ml

Antibiotic abbreviations, ERY, erythromycin; CLI, clindamycin; TET, tetracycline

Supplemental Table S3. Tn*916*-like elements in *S. pneumoniae*.

GenBank	Element	Size (bp)	Strain	Year	Type[a]	ST[b]	CC[c]	Sequence name	Gaps	Insertion	unlinked elements	Resistance gene	ERY		CLI		TET		CHL	
													MIC[d]	S/I/R	MIC[d]	S/I/R	MIC[d]	S/I/R	MIC[d]	S/I/R
AGOL00000000.1	Tn*2009*	23586	**GA49542**	2007	09V	3148	156	GA49542_Tn*2009*	1	SP_1638	null	*mef(E), mel, tet(M)*	=16	R	=0.12	S	>8	R	=4	S
AIJU00000000.1	Tn*2009*	23541	**GA08825**	1998	19F	651	320	GA08825_Tn*2009*	0	SP_1947	null	*mef(E), mel, tet(M)*	=4	R	=0.12	S	=16	R	<=2	S
AIKD00000000.1	Tn*2009*	23561	**GA13455**	1999	19F	651	320	GA13455_Tn*2009*	1	SP_1947	null	*mef(E), mel, tet(M)*	=8	R	=0.25	S	>8	R	=4	S
AGPC00000000.1	Tn*2009*	23560	**GA16833**	2002	19F	236slv	320	GA16833_Tn*2009*	1	SP_1947	null	*mef(E), mel, tet(M)*	=16	R	=0.12	S	>8	R	<=2	S
AGPD00000000.1	Tn*2009*	23561	**GA17371**	2000	19F	237slv	320	GA17371_Tn*2009*	1	SP_1947	null	*mef(E), mel, tet(M)*	=32	R	=0.25	S	>8	R	=4	S
AGPL00000000.1	Tn*2009*	23568	**GA17719**	2001	19F	926	320	GA17719_Tn*2009*	1	SP_1947	null	*mef(E), mel, tet(M)*	=16	R	=0.12	S	<=2	S	=4	S
AGOQ00000000.1	Tn*2009*	23591	**GA49138**	2006	19F	651	320	GA49138_Tn*2009*	1	SP_1947	null	*mef(E), mel, tet(M)*	=8	R	=0.12	S	>8	R	=4	S
AILC00000000.1	Tn*2009*	23539	**GA05245**	1995	23F	242	242	GA05245_Tn*2009*	1	Tn5252 *orf43*	null	*mef(E), mel, tet(M)*	=4	R	<=0.06	S	=32	R	=4	S
AGPO00000000.1	Tn*2009*	23533	**GA17227**	2000	23F	242	242	GA17227_Tn*2009*	0	Tn5252 *orf43*	null	*mef(E), mel, tet(M)*	=2	R	=0.12	S	>8	R	<=2	S
AIKP00000000.1	Tn*2009*	23481	**GA41301**	2004	23F	242	242	GA41301_Tn*2009*	1	Tn5252 *orf43*	null	*mef(E), mel, tet(M)*	=2	R	=0.06	S	>8	R	<=2	S

GenBank	Element	Size (bp)	Strain	Year	Type[a]	ST[b]	CC[c]	Sequence name	Gaps	Insertion	Linked elements	Resistance genes	ERY		CLI		TET		CHL	
													MIC[d]	S/I/R	MIC[d]	S/I/R	MIC[d]	S/I/R	MIC[d]	S/I/R
AIKF00000000.1	Tn*2009*	23571	**GA47210**	2006	15B	3280	156	GA47210_Tn*2009*	1	Tn*5253* *orf19*	null	*mef(E)*, *mel*, *tet(M)*	=8	R	=0.12	S	>8	R	=4	S
AFGD00000000.1	Tn*2009*	23527	**GA13494**	1999	14	656	156	GA13494_Tn*2009*	1	Tn*5253* *orf9*	null	*mef(E)*, *mel*, *tet(M)*	=16	R	=0.12	S	>8	R	=16	R
AGNZ00000000.1	Tn*2009*	23540	**GA41565**	2004	19A	81	81	GA41565_Tn*2009*	1	Tn*5253* *orf9*	null	*mef(E)*, *mel*, *tet(M)*	=1	R	<=0.03	S	>8	R	=8	R
AILB00000000.1	Tn*2009*	23545	**GA11663**	1999	19F	81	81	GA11663_Tn*2009*	1	Tn*5253* *orf9*	null	*mef(E)*, *mel*, *tet(M)*	=8	R	<=0.06	S	>8	R	=16	R
ALCK01000002.1	Tn*2009*	23571	**GA13430**	1999	19F	634	81	GA13430_Tn*2009*	1	Tn*5253* *orf9*	null	*mef(E)*, *mel*, *tet(M)*	=8	R	=0.12	S	>8	R	=16	R
AILH00000000.1	Tn*2009*	23565	**NP170**	1995	23F	81	81	NP170_Tn*2009*	1	Tn*5253* *orf9*	null	*mef(E)*, *mel*, *tet(M)*	nd	R	nd	S	nd	R	nd	S
AGOY00000000.1	Tn*2010*	26387	**7286_06**	2005	19A	2514	320	7286_06_Tn*2010*	0	SP_1947	null	*erm(B)*, *mef(E)*, *mel*,	=32	R	nd	R	=8	R	=4	S
AGOZ00000000.1	Tn*2010*	26394	**5185-06**	2005	19A	2393	320	5185_06_Tn*2010*	1	SP_1947	null	*erm(B)*, *mef(E)*, *mel*,	=32	R	nd	R	=8	R	=4	S
AGPF00000000.1	Tn*2010*	26397	**5652-06**	2005	19A	2588	320	5652_06_Tn*2010*	1	SP_1947	null	*erm(B)*, *mef(E)*, *mel*,	=32	R	nd	R	=8	R	=4	S
AGPG00000000.1	Tn*2010*	26393	**7533_05**	2005	19A	320	320	7533_05_Tn*2010*	1	SP_1947	null	*erm(B)*, *mef(E)*, *mel*,	=32	R	nd	R	=8	R	=4	S

GenBank	Element	Size (bp)	Strain	Year	Type[a]	ST[b]	CC[c]	Sequence name	Gaps	Insertion	Linked elements	Resistance genes	ERY		CLI		TET		CHL	
													MIC[d]	S/I/R	MIC[d]	S/I/R	MIC[d]	S/I/R	MIC[d]	S/I/R
AIKC00000000.1	Tn*2010*	26420	**7879_04**	2005	19A	2383	320	7879_04_Tn*2010*	1	SP_1947	null	*erm(B), mef(E), mel*,	nd	R	nd	R	nd	R	nd	S
ALCM00000000.1	Tn*2010*	26345	**8190_05**	2005	19A	2347	320	8190_05_Tn*2010*	1	SP_1947	null	*erm(B), mef(E), mel*,	=32	R	nd	R	=8	R	=4	S
AILQ01000002.1	Tn*2010*	26397	**EU-NP02**	2009	19A	1451	320	EU_NP02_Tn*2010*	1	SP_1947	null	*erm(B), mef(E), mel*,	>32	R	>2	R	>8	R	nd	-
ALCG00000000.1	Tn*2010*	26423	**GA19923**	2004	19A	320	320	GA19923_Tn*2010*	1	SP_1947	null	*erm(B), mef(E), mel*,	>32	R	>2	R	>8	R	<=2	S
AIKM01000001.1	Tn*2010*	26417	**GA44288**	2005	19A	320	320	GA44288_Tn*2010*	1	SP_1947	null	*erm(B), mef(E), mel*,	>32	R	>2	R	>8	R	=4	S
AIKT00000000.1	Tn*2010*	26407	**GA47688**	2006	19A	320	320	GA47688_Tn*2010*	1	SP_1947	null	*erm(B), mef(E), mel*,	>32	R	>2	R	>8	R	=8	R
AGOS00000000.1	Tn*2010*	26395	**GA47778**	2006	19A	320	320	GA47778_Tn*2010*	1	SP_1947	null	*erm(B), mef(E), mel*,	>32	R	>2	R	>8	R	=4	S
AGQE00000000.1	Tn*2010*	26426	**GA58771**	2010	19A	320	320	GA58771_Tn*2010*	1	SP_1947	null	*erm(B), mef(E), mel*,	>32	R	>2	R	>8	R	=4	S
AIKE00000000.1	Tn*2010*	26388	**4075-00**	1999	19F	635	320	4075_00_Tn*2010*	0	SP_1947	null	*erm(B), mef(E), mel*,	=16	R	nd	R	=8	R	=4	S
AIJT00000000.1	Tn*2010*	26423	**GA11856**	2000	19F	271	320	GA11856_Tn*2010*	1	SP_1947	null	*erm(B), mef(E), mel*,	>64	R	>4	R	<=2	S	=4	S

GenBank	Element	Size (bp)	Strain	Year	Type[a]	ST[b]	CC[c]	Sequence name	Gaps	Insertion	Linked elements	Resistance genes	ERY		CLI		TET		CHL	
													MIC[d]	S/I/R	MIC[d]	S/I/R	MIC[d]	S/I/R	MIC[d]	S/I/R
AIJY00000000.1	Tn*2010*	26404	**GA14798**	2000	19F	3039	320	GA14798_Tn*2010*	1	SP_1947	null	*erm(B), mef(E), mel*	>64	R	>4	R	>8	R	=4	S
AIJV00000000.1	Tn*2010*	26400	**GA16121**	2000	19F	236	320	GA16121_Tn*2010*	1	SP_1947	null	*erm(B), mef(E), mel*	>64	R	>4	R	=8	R	<=2	S
AIKS00000000.1	Tn*2010*	26364	**GA18523**	2001	19F	2476	320	GA18523_Tn*2010*	1	SP_1947	null	*erm(B), mef(E), mel*	>64	R	=0.5	I	>8	R	<=2	S
AIKX00000000.1	Tn*2010*	26430	**GA19451**	2003	19F	271	320	GA19451_Tn*2010*	1	SP_1947	null	*erm(B), mef(E), mel*	>64	R	>4	R	>8	R	=4	S
ALCV00000000.1	Tn*2010*	26397	**GA47281**	2006	19F	3039	320	GA47281_Tn*2010*	1	SP_1947	null	*erm(B), mef(E), mel*	>32	R	>2	R	>8	R	=4	S
AGNV00000000.1	Tn*2010*	26409	**GA47628**	2006	19F	236	320	GA47628_Tn*2010*	1	SP_1947	null	*erm(B), mef(E), mel*	>32	R	>2	R	>8	R	=4	S
AGOP00000000.1	Tn*3872*	23136	**GA47597**	2006	03	180	180	GA47597_Tn*3872*	1	Tn*5253 orf18*	null	*erm(B), tet(M)*	>32	R	>2	R	>8	R	>8	R
AGOO00000000.1	Tn*3872*	23392	**GA47502**	2006	19A	1374	singleton	GA47502_Tn*3872*	1	Tn*5253 orf18*	null	*erm(B), tet(M)*	>32	R	>2	R	>8	R	=8	R
AILF00000000.1	Tn*6002*	20879	**GA58981**	2010	22F	433	433	GA58981_Tn*6002*	0	SP_1438	null	*erm(B), tet(M)*	>32	R	>2	R	>8	R	=4	S
AGOD00000000.1	Tn*6002*	20923	**GA47179**	2006	15A	63	63	GA47179_Tn*6002*	2	SP_1947	null	*erm(B), tet(M)*	>32	R	>2	R	>8	R	=4	S
AGNY00000000.1	Tn*6002*	20923	**GA52612**	2007	15A	5004	63	GA52612_Tn*6002*	2	SP_1947	null	*erm(B), tet(M)*	>32	R	>2	R	>8	R	=4	S

GenBank	Element	Size (bp)	Strain	Year	Type[a]	ST[b]	CC[c]	Sequence name	Gaps	Insertion	Linked elements	Resistance genes	ERY		CLI		TET		CHL	
													MIC[d]	S/I/R	MIC[d]	S/I/R	MIC[d]	S/I/R	MIC[d]	S/I/R
AGOW00000000.1	Tn*6002*	20903	**GA47794**	2006	15A	63	63	GA47794_Tn*6002*	0	SP_1947	null	*erm(B)*, *tet(M)*	>32	R	>2	R	>8	R	=4	S
AILL01000001.1	Tn*6002*	20891	**GA44194**	2005	19A	2543	63	GA44194_Tn*6002*	1	SP_1947	null	*erm(B)*, *tet(M)*	>32	R	>2	R	>8	R	=4	S
AILO00000000.1	Tn*6002*	20924	**GA19101**	2002	03	180	180	GA19101_Tn*6002*	1	Tn*5253* *orf43* reverse	null	*erm(B)*, *tet(M)*	=2	R	=0.5	I	>8	R	=16	R
AIKY00000000.1	Tn*6002*	20917	**GA40563**	2003	04	5872	singleton	GA40563_Tn*6002*	1	Tn*5253* *orf43* reverse	null	*erm(B)*, *tet(M)*	=64	R	>4	R	>8	R	=16	R
AGPI00000000.1	Tn*6002*	20879	**GA11304**	1999	06A	90	156	GA11304_Tn*6002*	1	Tn*5253* *orf43* reverse	null	*erm(B)*, *tet(M)*	>16	R	>2	R	>8	R	=16	R
AGOG00000000.1	Tn*6002*	20892	**GA60132**	2010	06C	1390	63	GA60132_Tn*6002*	1	Tn*5253* *orf43* reverse	null	*erm(B)*, *tet(M)*	>32	R	>2	R	>8	R	=4	S
AILJ00000000.1	Tn*916*	17871	**GA41538**	2004	06A	384	156	GA41538_Tn*916*	0	SP_1937	Mega-2.II	*mef(E)*, *mel*, *tet(M)*	=4	R	=0.06	S	<=2	S	<=2	S
AGOU00000000.1	Tn*916*	17878	**GA02506**	1994	06B	384	156	GA02506_Tn*916*	0	SP_1937	Mega-2.II	*mef(E)*, *mel*, *tet(M)*	=4	R	nd	S	=16	R	=2	S
AGPX00000000.1	Tn*916*	17878	**GA05248**	1995	06B	384	156	GA05248_Tn*916*	0	SP_1937	Mega-2.II	*mef(E)*, *mel*, *tet(M)*	=4	R	<=0.06	S	=1	S	=2	S
AGPW00000000.1	Tn*916*	17878	**GA04216**	1995	06B	2150	156	GA04216_Tn*916*	0	SP_1937	Mega-2.II	*mef(E)*, *mel*, *tet(M)*	=4	R	<=0.06	S	=1	S	=2	S
AILK00000000.1	Tn*916*	17877	**GA05578**	1996	06B	2150	156	GA05578_Tn*916*	0	SP_1937	Mega-2.II	*mef(E)*, *mel*, *tet(M)*	=4	R	<=0.06	S	=0.5	S	=4	S
ALCX00000000.1	Tn*916*	18049	**GA44378**	2005	23F	81	81	GA44378_Tn*916*	1	Tn*5253* *orf9*	Mega-1.III	*mef(E)*, *mel*, *tet(M)*	=8	R	=0.06	S	>8	R	>8	R

[a] Type, serotype

[b] ST, Multilocus sequence type

[c] CC, Clonal complex

[d] MIC, Minimum inhibitory concentration, reported at µg/ml

Antibiotic abbreviations, ERY, erythromycin; CLI, clindamycin; CHL, chloramphenicol; TET, tetracycline

Chapter 4: High-level macrolide resistance in *Streptococcus pneumoniae*

Max R. Schroeder[1,2], Scott T. Chancey[1,2], and David S. Stephens[1,2,3]

[1]Department of Medicine, Emory University School of Medicine, Atlanta, GA, USA; [2]Laboratories of Microbial Pathogenesis, Department of Veterans Affairs Medical Center, Atlanta, GA, USA; [3]Rollins School of Public Health, Emory University, Atlanta, GA, USA

Paper in preparation

M.R.S. created deletion mutants, performed antibiotic susceptibility and competition assays, analyzed the data, wrote and edited the paper.

ABSTRACT

The explosive, widespread use of macrolides in the last thirty years has been a strong selective pressure contributing to the expansion of macrolide-resistant *Streptococcus pneumoniae*. Macrolide resistance in pneumococci is primarily due to ribosomal methylation by a methyltransferase encoded by *erm*(B) or due to efflux encoded by *mef*(E)/*mel*, an operon carried on the macrolide efflux genetic assembly (Mega) element. We have documented the recent clonal expansion of serotype 19A complex isolates that contain Tn*2010*, a new, emerging composite mobile genetic element with both *erm*(B) and Mega. In this study we, through creation of isogenic mutants, found that *erm*(B) was critical to confer high-level macrolide resistance in Tn*2010*-containing strains but that *mef*(E)/*mel*-mediated efflux remained functional. We also report new, high-level resistance (MIC >16 μg/ml) isolates containing Mega alone caused by specific genomic insertions, Mega-2.IVa and Mega-2.IVc, associated with the presence of IS*Smi*2 and deletions of the Pneumococcal Pathogenicity Island-1. Deletion of *mef*(E)/*mel* in these isolates completely eliminated macrolide resistance. Using *in vitro* competition experiments, we found that in the presence of erythromycin, high-level macrolide-resistant *S. pneumoniae* conferred by either *erm*(B) or Mega-2.IVa, have a growth fitness advantage over lower-level macrolide-resistant *S. pneumoniae* conferred by other Mega insertions. These data indicate that the ability of *S. pneumoniae* to generate high-level macrolide resistance by either ribosomal methylation or efflux affords a selective advantage for pneumococci in a macrolide environment, and that the efflux pump might have additional selective function(s).

Keywords: *Streptococcus pneumoniae*, pneumococcus, macrolide resistance, Mega, *mef*(E)/*mel*, *erm*(B), Tn*2010*

INTRODUCTION

Streptococcus pneumoniae, the pneumococcus, is an obligate commensal of the human nasopharynx and an opportunistic pathogen responsible for morbidity and mortality worldwide. *S. pneumoniae* causes non-invasive diseases such as acute otitis media, sinusitis, and pneumonia, as well as invasive diseases such as bacteremia and meningitis (1). Antibiotic therapy for community-associated upper respiratory tract bacterial infections often includes a macrolide (2, 3). However, the choice of a macrolide has been compromised by the rapid emergence of macrolide resistance in *S. pneumoniae*. Widespread use of macrolides has provided a strong selective pressure contributing to the expansion of macrolide-resistant *S. pneumoniae* (4). In the United States, macrolides are one of the most prescribed antibiotics with 190 prescriptions per 1000 people in 2011 (2). Macrolide resistance in *S. pneumoniae* rapidly emerged in the early-mid 1990s and increased throughout that decade (5, 6).

Macrolide resistance in *S. pneumoniae* is predominantly due to ribosomal modification or macrolide efflux (7). Macrolides bind to the 23S rRNA (A2058 for *Escherichia coli*) of the 50S ribosome to inhibit protein synthesis (8). A ribosomal methyltransferase, encoded by *erm*(B), prevents binding of macrolides by dimethylating the target site on the ribosome (9). Ribosomal methylation results in very high-level macrolide resistance (erythromycin MIC $\geq$256 μg/ml) as well as resistance to lincosamides and streptogramin B (the MLS_B phenotype). Macrolide efflux is mediated by *mef*(E) and *mel*, a dual efflux pump carried on the 5.5 kb or 5.4 kb genetic element Mega (10, 11). Mega is found in five locations in the pneumococcal genome and also as a component of a conjugative transposon or larger composite elements. The *mef*(E)/*mel*-

encoded macrolide efflux pump confers resistance to macrolides only (the M phenotype) and is inducible by 14- and 15-membered macrolide molecules (12, 13). In the United States, most pneumococcal macrolide resistance is due to efflux (14, 15). Efflux-mediated macrolide resistance has been generally reported as MICs of erythromycin as 1-16 µg/ml (12, 16), and the clinical significance of efflux-mediated resistance has been debated (17).

We have identified the mobile genetic elements disseminated macrolide resistance in our population and have documented the emergence and clonal expansion of macrolide-resistant serotype 19A clonal complex 320 isolates that contain Tn*2010*, with both *erm*(B) and *mef*(E)/*mel* (Chapter 2). In this study, we assessed the contribution of *erm*(B) and *mef*(E)/*mel* in Tn*2010* isolates Further, we have identified new high-level macrolide resistance of *S. pneumoniae* (MIC >16 µg/ml) with Mega alone. The genetic basis responsible for high-level macrolide resistance due to efflux in *S. pneumoniae* was investigated. We also found high-level macrolide resistance, regardless of mechanism, provided a competitive growth advantage during exposure to erythromycin.

RESULTS

Macrolide resistance in *S. pneumoniae* and the Mega element. To better understand the genetic basis for the wide variation in Mega-associated minimum inhibitory concentrations (MICs), a panel of 44 distinct, well-characterized macrolide-resistant clinical isolates was investigated (Table 1). This panel was selected from macrolide-resistant isolates collected through prospective population-based surveillance of invasive pneumococcal disease in Atlanta 1994-2011 (18). Strains represented

difference years of isolation, serotype, MLST, and clonal complex. The MICs to erythromycin of macrolide-resistant *S. pneumoniae* with the Mega element varied from 2 to ≥256 µg/ml (Figure 1). Erythromycin MICs of 1-16 µg/ml were classified as "resistant" and >16 µg/ml were classified as "high-level resistant."

The majority of these Mega-containing *S. pneumoniae* demonstrated typical resistant to erythromycin with MICs of 4-16 µg/ml (Table 1, Figure 1). However, after overnight growth with subinhibitory erythromycin (0.1 µg/ml), the erythromycin-induced MICs for these strains were 16-64 µg/ml (Table 1, Figure 1). These erythromycin MICs and induced-erythromycin MICs are representative of macrolide resistance caused by Mef(E)/Mel-mediated macrolide efflux previously reported (11-13). The relationship of MIC to the Mega promoter polymorphisms, the 99-bp difference in the *mef*(E)/*mel* intergenic region and the genomic sites of Mega insertion were assessed.

The *mef*(E)/*mel* promoter region is now well defined and is highly conserved (19). The single base pair change in the promoter sequence did not correlate with differences in MIC (Figure A1). Specifically, the consensus -19G to -19T found in four of the ten Mega classes did not correlate with the MIC.

Chromosomal insertion sites Mega-1.I, Mega-1.II, Mega-2.II, Mega-1.III, Mega-1.IVb, and Mega-1.VTn*2009* all have erythromycin MICs 2-16 µg/ml uninduced and 16-64 µg/ml induced (Table 1, Figure 1). These strains had the typical level of macrolide resistance associated with efflux for *S. pneumoniae*. These isolates were also susceptible to clindamycin and thus have an M phenotype. The newly described Mega-1.novel insertion (20), herein named Mega-1.VI, also exhibited an MIC of 4 µg/ml and an

induced-erythromycin MIC of 16 µg/ml. Mega type 1 (Mega-1) and Mega type 2 (Mega-2), due to a 99 bp insertion/deletion of the intergenic region between *mef*(E) and *mel* (11), did not contribute to macrolide resistance as both Mega-1.II and Mega-2.II were found to have the same erythromycin and induced-erythromycin MICs (Figure 1).

Mega-containing *S. pneumoniae* with high-level macrolide resistance. *S. pneumoniae* containing Mega-2.IVa, Mega-2.IVc, or Mega-1.V Tn*2010* were found to exhibit high-level macrolide resistance, e.g. uninduced MIC of >16 µg/ml and induced MIC of ≥64 µg/ml (Figure 1). Of the four *S. pneumoniae* isolates with Mega-2.IVa, the erythromycin MICs were 18-64 with induced-erythromycin MICs of 96 to ≥256 µg/ml. To date one *S. pneumoniae* Mega-2.IVc isolate has been identified (19, 20); this isolate has an erythromycin MIC of 64 µg/ml and is inducible to ≥256 µg/ml. Mega-2.IVa and Mega-2.IVc isolates were found to be clindamycin susceptible, e.g. M phenotype. No other macrolide resistant determinants were found in these isolates (see below). The Mega-1.V Tn*2010* isolates were found to have uninduced erythromycin MICs of ≥256 µg/ml, but this was due to the presence of *erm*(B) (see below). All *erm*(B)-containing isolates, including Tn*2010*-containing isolates, were clindamycin resistant, the MLS_B phenotype.

Macrolide resistance in dual *erm*(B) and *mef*(E)/*mel*, Tn*2010*-containing *S. pneumoniae*. To define high-level macrolide resistance phenotype observed for Tn*2010*-containing *S. pneumoniae*, isogenic deletion mutations were made in *erm*(B) or *mef*(E)/*mel* or both in strain GA44288, an invasive pneumococcal disease isolate (20). The deletion of *mef*(E)/*mel* from GA44288 (Tn*2010*), designated MS41, had no effect on MIC as MS41 (Tn*2010* Δ*mef*(E)/*mel*) had an erythromycin MIC of ≥256 µg/ml (Table 2).

The deletion of *erm*(B), in GA44288 designated MS32, lowered but did not eliminate macrolide resistance. MS32 (Tn*2010*Δ*erm*(B)) had an erythromycin MIC of 8 µg/ml and an induced erythromycin MIC of 64 µg/ml (Table 2). This MIC is similar to Tn*2009* Mega-containing isolates (Table 1, Figure 1). The deletion of both macrolide resistance determinants in GA44288 designated MS42 (Tn*2010* Δ*erm*(B)Δ*mef*(E)/*mel*) was found to be susceptible to erythromycin (MIC 0.125 µg/ml) (Table 2). This confirmed *erm*(B) and *mef*(E)/*mel* as the only macrolide resistance determinants in GA44288 and that high-level macrolide resistance of Tn*2010*-containing *S. pneumoniae* was due to the presence of *erm*(B).

In *S. pneumoniae* the expression of *mef*(E) and *mel* is controlled through transcriptional attenuation (12, 13, 19). Macrolide-induced ribosomal stalling results in deattenuation of *mef*(E)/*mel* to produce full-length polycistronic transcripts. In order to determine if *mef*(E)/*mel* were expressed in presence of *erm*(B), *mef*(E) expression was measured by qRT-PCR from GA44288 after a 15 min exposure to erythromycin. The expression of *mef*(E) was dose-dependent, and 0.5 µg/ml erythromycin was sufficient to induce expression in both the wild type (Figure 2) and Δ*erm*(B) background (data not shown). Thus in a dual macrolide resistance isolate, *mef*(E)/*mel* were expressed upon exposure to macrolides and as shown by MIC data above results in a functional efflux pump.

***mef*(E)/*mel*-encoded efflux alone is responsible for high-level macrolide resistance in Mega-2.IVa- and Mega-2.IVc-containing *S. pneumoniae*.** Isolates with Mega-2.IVa and Mega-2.IVc were found to have high-level macrolide resistance (Figure 1). To confirm the molecular basis for this high-level macrolide resistance,

mef(E)/*mel* was deleted from the high-level macrolide-resistant strain GA16242 with a Mega-2.IVa insertion (uninduced erythromycin MIC of 64 µg/ml) to create TS9001. TS9001 was susceptible to erythromycin at 0.125 µg/ml (Table 2). Similarly, deletion of *mef*(E)/*mel* from the high-level macrolide-resistant Mega-2.IVc strain GA17545 (uninduced erythromycin MIC of 64 µg/ml) resulted in susceptibility to macrolides as the erythromycin MIC of the mutant designated XZ8012-5 was 0.19 µg/ml (Table 2). Thus, *mef*(E)/*mel*-encoded efflux alone in this genomic location were responsible for high-level macrolide resistance in these *S. pneumoniae* isolates.

To further analyze the function of Mega in class IVa and IVc insertions and determine whether the high-level macrolide resistance phenotype of Mega was transferable, the Mega-2.IVa insertion was transformed into the erythromycin susceptible strain NP112 (MIC 0.19 µg/ml). The resulting NP112 Mega-2.IVa isolate (designated MS23) demonstrated high-level macrolide resistance with an erythromycin MIC of 32 µg/ml and was inducible up to ≥256 µg/ml (Table 2). The transfer of Mega-2.IVa included the adjacent IS*Smi*2 element and recreated the pneumococcal pathogenicity island (PPI-1) deletion found in Mega-2.IVa isolates (20). Deletion of *mef*(E)/*mel* from MS23 (MS30) restored macrolide susceptibility (Table 2). Efflux-mediated high-level macrolide resistance was also transferred to the GA17457 Δ*mef*(E)/*mel* deletion strain (XZ8009). After transformation with the Mega-2.IVa insertion, the strain designated MS27 was found to have an erythromycin MIC of 32 µg/ml inducible up to ≥256 µg/ml (Table 2). These data confirm that Mega-2.IVa insertions result in high-level macrolide resistance.

High-level macrolide resistance, regardless of mechanism, provides a growth competitive advantage during exposure to erythromycin. Unregulated *erm*(C) has been found through competitive growth assays to cause a growth defect in *S. aureus* after approximately 40 generations of growth (21). We first sought to determine whether *erm*(B) in *S. pneumoniae* resulted in a growth defect and whether such defect might be alleviated by the presence of *mef*(E)/*mel* in Tn*2010*-containing *S. pneumoniae*. Erythromycin-induced cultures of GA44288 and the isogenic mutants (MS32 and MS41) (Table 2) were used as the input for an *in vitro* competitive index (1:1 ratio), using a concentration of erythromycin known to be achieved in human serum during treatment (0.5 µg/ml) (22). There was no significant difference between MS41 (GA44288 Δ*mef*(E)/*mel*) and GA44288 in this assay (Figure 3A, p=0.5460). This suggested the presence of *mef*(E)/*mel* did not provide a growth advantage to an *erm*(B)-containing strain during exposure to erythromycin. When MS32 (GA44288 Δ*erm*(B)) was competed with GA44288 the competitive index decreased to approximately 0.01 after 50 generations (Figure 3B), which indicated a significant advantage for GA44288 (p=0.0012). Similarly, the competitive index of MS32 (GA44288 Δ*erm*(B)) versus MS41 (GA44288 Δ*mef*(E)/*mel*) dropped to approximately 0.01 by the endpoint 50 generations (Figure 3C, p<0.0001). When these experiments were performed without erythromycin, the competitive indexes remained at approximately 1 throughout the course of the experiments (Figure A2). In each of the erythromycin-induced competitive index experiments, an *erm*(B)-containing strain (GA44288 and MS41) had a competitive advantage over the *erm*(B) deletion stain (MS30) (Figure 3). The data suggest that

erm(B) provided a growth advantage during when *S. pneumoniae* is exposed to treatment-level concentrations of erythromycin.

To determine whether the competitive advantage for growth of *erm*(B) during erythromycin exposure was due Erm(B)-mediated ribosomal methylation or to the high-level macrolide resistance of the *erm*(B)-containing strains, we performed the competitive index assay with the GA44288 isogenic strains in competition with GA16242, a Mega-2.IVa strain that produces high-level macrolide resistance due to the presence of *mef*(E)/*mel* (Figure 1, Table 2). In the assay, the competitive index for GA44288 versus GA16242 remained ~1 throughout the course of the experiments (Figure 4A, p=0.3088). The competitive index for MS41 (GA44288 Δ*mef*(E)/*mel*) versus GA16242 also did not change throughout the experiments (Figure 4B, p=0.4397). These data suggest the growth advantage of *erm*(B) (Figure 3) was due to high-level macrolide resistance and was not specific to Erm(B)-mediated ribosomal methylation. Finally, we assayed MS32 (GA44288 Δ*erm*(B)) with GA16242 and found the competitive index decreased below 0.1 after 50 generations of growth (Figure 4C, p=0.0316). The competition advantage of high-level macrolide resistance strains (MS32 and GA16242) indicated that high-level macrolide resistance, regardless of mechanism, provided a growth competitive advantage during exposure to erythromycin.

DISCUSSION

High-level macrolide resistance due to efflux has previously been observed in a few clinical isolates (15) but not characterized at a molecular level. We found high-level macrolide resistance in *S. pneumoniae* is due to macrolide efflux caused by specific

(Mega-2.IVa and Mega-2.IVc) insertions that are linked to the presence of IS*Smi*2 and deletion of the Pneumococcal Pathogenicity Island-1 (PPI-1). We also defined the interesting dual macrolide resistance genotype of Tn*2010*-containing isolates, which emerged in the PCV-7 conjugate vaccine era (Chapter 2). Both *erm*(B) and *mef*(E)/*mel* are expressed and functional in these isolates. Further, high-level macrolide resistance, due to either ribosomal methylation or efflux, provided a growth competitive advantage during exposure to treatment levels of erythromycin.

The rise of macrolide resistance in the United States throughout the 1990s was largely attributed to the increased occurrence of isolates containing the Mega element encoding a two-component efflux pump (14, 15). Mega-containing isolates have been generally associated with lower levels of macrolide MICs (≤16 μg/ml erythromycin) compared to levels observed for *erm*(B) (≥64 μg/ml erythromycin) (15). Macrolide resistance in the pneumococcus, caused by *erm*(B) and *mef*(E)/*mel*, has been linked to treatment failures for lower respiratory tract infections and bacteremia (23-25).

The two most common Mega elements are type 1 and 2, which are distinguished by a 99-bp insertion/deletion (Mega-1 at 5.5-kb and Mega-2 at 5.4-kb) (11). Mega has inserted into the pneumococcal genome in six distinct sites, termed Mega classes (20). Insertion sites numbered I-IV were originally described (11). When inserted into Tn*916*-like elements, Mega is classified as insertion site V (26-28). Recently, we reported a novel chromosomal insertion site, VI (20).

Mega class IV has been further classified into three subclasses: Mega-2.IVa, Mega-1.IVb, and Mega-2.IVc (20) all of which are upstream of PPI-1. We found Mega-

2.IVa and Mega-2.IVc have high-level macrolide resistance while the Mega-1.IVb insertion has uninduced MICs of 2-16 µg/ml with induced MICs of 24-64 µg/ml (Table1). The 99-bp insertion/deletion in the intergenic region between *mef*(E) and *mel*, the distinguishing characteristic between Mega-1 from Mega-2, does not appear to affect the level of macrolide resistance.

The presence of IS*Smi*2 adjacent to Mega and the deletion of PPI-1 in Mega-IVa and Mega-IVc isolates should be investigated further to assess their roles in high-level macrolide resistance. The presence of IS*Smi*2 upstream of Mega *orf3-6* could cause upregulation of these genes leading to increased macrolide resistance. Alternatively, the deletion of the PPI-1 may result in high-level macrolide resistance of Mega-2.IVa/c isolates. The PPI-1 is comprised of a conserved region of 15.1-kb and a variable region of 15.6-kb (20, 29). Deletion of the *piaABCD* and *phgABC* operons of the conserved region of PPI-1 decrease virulence in mice (30, 31). Interestingly, the Mega-2.IVa/c isolates in this study were recovered from invasive pneumococcal disease patients, which suggest the strains have maintained virulence without the presence of the PPI-1.

In the mid-2000s after PCV-7 introduction, clonal expansion of macrolide-resistant serotype 19A *S. pneumoniae* with dual resistance determinants, Mega and *erm*(B), was observed worldwide (15, 27, 32, 33) (Chapter 2). This dual macrolide resistant genotype results in an MLS_B phenotype with high-level macrolide resistance (Table 2). The *mef*(E)/*mel* operon was inducible in the *erm*(B) background, which indicates co-expression of both macrolide resistance mechanisms. The high-level macrolide resistance of *S. pneumoniae* isolates with the dual macrolide resistance genotype, *mef*(E)/*mel* and *erm*(B) (Tn*2010*-containing), was due to *erm*(E), but

mef(E)/*mel* provided lower efflux-mediated resistance levels (Table 2) and may provide other selective advantages due to *mef*(E)/*mel* such as resistance to antimicrobial peptides (e.g. LL-37) (34). The introduction of PCV-13 has significantly decreased the incidence of serotype 19A and the dual macrolide resistance genotype especially in high-risk populations, <5 and ≥65 year old populations (Chapter 2).

Antibiotic resistance determinants are often inducible and provide a selective advantage over non-resistant organisms in an antibiotic-containing environment. However, expression of these determinants can be associated with a fitness cost when the selective pressure is absent (35). In the pneumococcus, *erm*(B) commonly is inducible and tightly regulated expressed through translational attenuation (36, 37). The *mef*(E)/*mel* operon is regulated through transcriptional attenuation (19). Overexpression of *erm*(B) in *S. pneumoniae* by a partial attenuator deletion did not cause a growth defect when the strain was grown *in vitro* as a pure culture (38). However, in *Staphylococcus aureus*, deregulation of *erm*(C), a homolog of *erm*(B), results in increased expression of a subset of the proteome that causes a 10-fold fitness defect *in vitro* (21). We found that *erm*(B) in *S. pneumoniae* did not cause a fitness defect and provided a competitive advantage up to 100-fold during macrolide exposure. Murine TLR13 is stimulated by a fragment of bacterial 23*S* rRNA but methylation of A2058, the target of *erm*(C) and *erm*(B), prevented TLR13 activation and prevented detection of the bacteria through this pathway (39). Humans do not have TLR13, and thus it is at present unclear if *erm*(B)-mediated ribosomal methylation has a protective effect against the human immune response.

The recent emergence of *S. pneumoniae* with dual macrolide resistance determinants is a novel event (Chapter 2). The dual macrolide resistance genotype may

have arisen by a *mef*(E)/*mel*-containing strain acquiring *erm*(B). A Tn*2009*-containing strain may have acquired *erm*(B) through homologous recombination of a Tn*6002* fragment with *erm*(B) flanked by Tn*916 orf20* to create Tn*2010*, which would convert the strain from an M phenotype with lower-level macrolide resistance to an MLS_B phenotype with high-level macrolide resistance. Alternatively, dual macrolide resistance genotype may have occurred through a Tn*6002*-containing strain becoming transformed with a Tn*2009* fragment with Mega flanked by Tn*916 orf6* to create Tn*2010*. During *in vitro* competitive growth assays, *erm*(B) provided a growth fitness advantage when subjected to erythromycin due to the high-level macrolide resistance conferred by *erm*(B) as *mef*(E)/*mel* did not contribute the *in vitro* survival benefit. The presence of *mef*(E)/*mel* has been found to enhance resistance to the human antimicrobial peptides LL-37 (34). The host immune response may have provided a selective pressure for the acquisition of *mef*(E)/*mel* by an *erm*(B)-containing *S. pneumoniae*. While it is not possible to determine the order of acquisition of the macrolide resistance determinants, the close genetic linkage of these resistance determinants and non-macrolide resistance determinants (i.e. tetracycline resistance) on Tn*2010* and Tn*2010*-like elements may result in a soft selective pressure for maintenance (40). With an undetectable fitness burden for maintenance of *mef*(E)/*mel* and/or *erm*(B) it is unlikely these determinants would be lost from the pneumococcal population, even with reduced use of macrolides in clinical settings (35).

The most effective measure to date in combating macrolide-resistant pneumococcal infections has been the introduction of pneumococcal conjugate vaccines (PCV). These vaccines provide individual protection for vaccinated individuals, reduce

transmission of vaccine serotypes leading to herd protection for unvaccinated individuals in the same population (41). PCV-7 containing capsular polysaccharides of serotypes 4, 6B, 9V, 14, 18C, 19F, and 23F conjugated to diphtheria protein CRM197 was introduced into the US pediatric population in 2000. Introduction of PCV-7 was followed by rapid decrease in the incidence of local and invasive pneumococcal disease caused by the vaccine serotypes; these vaccine serotypes also had the highest frequency of macrolide resistance determinants (14). Following serotype replacement by non-PCV-7 serotypes, PCV-13 containing capsular polysaccharides of serotypes from PCV-7 and serotypes 1, 3, 5, 6A, 7F, and 19A conjugated to CRM197 was introduced in the United States in 2010 and also resulted in decreased pneumococcal disease and macrolide-resistance due to the effects on vaccine serotypes (42) (Chapter 2). Overall macrolide-resistant invasive pneumococcal disease declined 70% in Atlanta since 1999 (Chapter 2). The dual macrolide resistance genotype (Tn*2010*-containing) has predominately been found in association with serotype 19F most commonly 19A, PCV-13 introduction decreased the incidence of invasive pneumococcal disease cause by isolates with the dual macrolide resistance genotype (Chapter 2).

In summary, high-level macrolide resistance in *S. pneumoniae* can result from efflux due to the *mef*(E)/*mel*-encoded two-component efflux pump, the specifically in the context of the Mega-2.IVa or Mega-2.IVc genomic insertions. Tn*2010*-containing *S. pneumoniae* isolates carry both *erm*(B) and *mef*(E)/*mel*, which are both functional in these strains. High-level macrolide resistance regardless of mechanism provides a competitive growth advantage during exposure to erythromycin.

MATERIALS and METHODS

Bacterial Strains, Media, and Growth Conditions. The characteristics of strains used are listed in Table 1 and 2. All *S. pneumoniae* strains were routinely grown on trypticase soy agar II containing 5% sheep's blood (blood agar) or in Todd-Hewitt broth containing 0.5% yeast extract broth (THY). Plate cultures were grown at 37°C with 5% CO_2 and broth cultures were grown in a 37°C water bath.

Antibiotic Susceptibility. Bacterial cultures were grown overnight on blood agar and subcultured onto blood agar or blood agar with erythromycin supplementation to induce resistance expression as a standard protocol in our laboratory (13, 34). These overnight cultures were suspended to a density approximately equal to a 0.5 McFarland standard and streaked onto Mueller-Hinton agar containing 5% sheep's blood. Erythromycin susceptibility tests were performed by applying an erythromycin Etest strips (bioMérieux). After an overnight incubation, erythromycin susceptibility was measured. Uninduced MICs of 1-16 μg/ml were classified as resistant and >16 μg/ml were classified as high-level resistant.

General DNA Manipulation. Primers sequences are listed in Table A1. PfuUltra II Fusion DNA polymerase (Agilent Technologies) or Q5 polymerase (New England Biolabs), restriction enzymes (New England Biolabs) and T4 DNA ligase (Invitrogen) was used for mutational cassette construction. Taq DNA polymerase (Applied Biosystems) or One Taq DNA polymerase (New England Biolabs) were used for screening putative mutants.

Transformations. *S. pneumoniae* was transformed by a standard method that utilized the competence-stimulating peptide 1 (CSP-1) for induction of competence(43).

CSP-1 was synthesized by Emory University Microchemical Facility. Transformations were performed using plasmid DNA or PCR products and selected on blood agar containing kanamycin at 400 µg/ml, erythromycin at 1 µg/ml, or chloramphenicol at 3.2 µg/ml as described below.

Mutants TS9001-3 and XZ8012-5 (Table 2)**.** Competent cells were transformed with a previously created plasmid that replaces *mef*(E) and *mel* with an *aphA-3* cassette and double crossover mutants were selected on kanamycin and confirmed by PCR and sequencing (34). This method was used to delete *mef*(E)/*mel* from GA16242 to create TS9001-3 and from GA17545 to create XZ8012-5.

Mutants MS23 and MS27 (Table 2)**.** A 10.9 kb PCR product containing Mega-2.IVa was amplified using primers SC173 and SC251 and purified using the QIAquick Gel Extraction kit. Purified PCR products were transformed into NP112 to create MS23 and XZ8009 to create MS27 and transformants were selected on erythromycin. Insertions were confirmed by PCR of the left and right junctions of Mega-2 in insertion site IVa with primers SC10 with SC173 and SC70 with SC251.

Mutant MS30 (Table 2)**.** Strain MS23 was transformed with BamHI digested *mef*(E)/*mel*::aphA-3 plasmid. The desired double crossover was selected on kanamycin. The insertion was confirmed by PCR amplification of a 1521 bp product with primers SC125 and kanA.

Mutant MS32 (Table 2)**.** From GA44288 genomic DNA, amplified upstream (primers MS34 and MS35) and downstream (primers MS36 and MS37) regions of *erm*(B) were spliced by overlapping extension (SOE) to create an internal XbaI site using the PCR amplified regions with primers MS34 and MS37. The resulting 1066 bp product

was digested with BamHI and PstI and cloned into double-digested pUC19 vector to create pMRS11. The kanamycin resistance cassette, *aphA-3* was PCR amplified from pSF151 (44) using primers MS53 and MS54 and the product was XbaI digested and cloned into pMRS11 to create pMRS13. The *aphA-3* cassette was confirmed to be in the forward direction by PCR with primers MS34 and MS54. Transformation of GA44288 cells with pMRS13 and selection on kanamycin to created strain MS32, which was confirmed by PCR amplification with primers MS27 and kanA as well as MS28 and kanC.

Mutant MS41 and MS42 (Table 2)**.** PCR amplification of the *mef*(E) upstream region by primers MS64 and MS72, the *mel* downstream region by primers MS63 and MS69, and the chloramphenicol cassette from pEVP3 (45) by primers MS70 and MS71. A single SOE PCR reaction with the three PCR products and primers MS63 and MS64 created a 2 kb Δ*mef*(E)/*mel*::cm^R cassette. This product was used for transformation and selection on chloramphenicol for GA44288 to create MS41 and MS32 to create MS42, which were confirmed by PCR amplification of a 2 kb product from primers MS63 and MS64.

qRT-PCR. Overnight blood agar cultures were suspended in THY and grown until to mid-log phase (OD_{600}=0.3-0.5). Each culture was diluted to OD_{600}=0.05 in prewarmed THY and grown to mid-log phase and cultures were divided into tube with or without erythromycin as indicated and continued to grow until desired treatment time was achieved. Culture aliquots were mixed with RNAprotect Bacterial Reagent (Qiagen) and RNA was isolated using the RNeasy Mini Kit (Qiagen). DNA was removed via the TURBO DNA-free (Applied Biosystems) and confirmed to be free of DNA by PCR

using primers for genes of interest (Table A2). QuantiTect Reverse Transcription Kit (Qiagen) was used to create cDNA from the purified RNA. qRT-PCR was performed using iQ SYBR Green Supermix (BioRad) with an iCycler iQ Real-Time Detection System (BioRad). qRT-PCR primers are listed in Table A2. The measured C_T values were averaged and wild type untreated condition was used to calculate the relative expression, $\Delta\Delta C_T$ value.

Competitive Index. Bacterial growth competitions were developed based on methods of Gupta *et al*. (21). Overnight blood agar cultures were subcultured onto blood agar with or without supplementation with erythromycin at 0.5 µg/ml. Each strain was suspended in THY broth with or without erythromycin (0.5 µg/ml) and grown to OD_{600}=0.5-0.7 and diluted to OD_{600}=0.050 in fresh media. Diluted cultures were mixed (1:1) for competition assays or grown independently as non-competition controls and grown to OD_{600}=0.5-0.7 and diluted 200-fold in fresh media. Cultures were subcultured three times allowing the cultures to grow for approximately 50 generations. Sampling of cultures was performed to monitor growth phase by OD_{600}. At T=0 and each time the cultures reached late-log/stationary phase, culture aliquots were collected, serially diluted in phosphate-buffered saline, and plated on blood agar without selection (total culture density) and selective blood agar (one of the mutants): kanamycin 400 µg/ml, erythromycin 1 µg/ml, chloramphenicol 3.2 µg/ml, or tetracycline 2 µg/ml. The competitive index (CI) was calculated as CI = (mutant CFU_{output}/wildtype CFU_{output})/ (mutant CFU_{input}/wildtype CFU_{input}) and a CI<1 indicates the mutant is less fit than then the wildtype.

Statistical analysis. Unpaired, two-tailed t tests with 95% confidence intervals were performed using Prism® 5 (GraphPad). For the growth competition experiments, the competitive index values of input were compared to the endpoint of 50 generations of growth.

FUNDING INFORMATION

The work was supported by a VA Merit Award grant, an HHS National Institutes of Health (NIH) grant (RO1 AI07829) to David S. Stephens, and with federal funds from the HHS NIH National Institute of Allergy and Infectious Diseases under contract number HHSN272200900009C.

ACKNOWLEDGEMENTS

We would like to thank Tammy Schwalm Tollison, Xiaoliu Zhou, and Aditya Gudlavalleti for assisting in laboratory work and creation of mutants. Strains were provided by the Georgia Emerging Infections Program and strain characterizations were aided by the CDC Streptococcus lab and CDC Respiratory Disease Branch.

TABLES

Table 1. *S. pneumoniae* isolates macrolide resistance gene classification and erythromycin minimum inhibitory concentrations (MICs).

Mega	*erm*(B)	Strain	MIC[a]	iMIC[a,b]	Isolation Year	Serotype	MLST	Clonal Complex	Source
Mega-1.I	None	GA17328	4	24	2000	6A	376	CC2090	(20)
		GA17457	8	48	2000	19A	199	CC199	(20, 34)
		GA16857	4-6	24-32	2002	6A	376	CC2090	GAEIP
		GA41348	6-8	32	2004	19A	199	CC199	GAEIP
		GA41437	3	24	2004	6A	376	CC2090	(20)
		GA41502	4	32	2004	19A	199	CC199	GAEIP
Mega-1.II	None	EU-NP04	4	16-24	2009	6C	2705	CC1379	(20)
		GA47033	4-6	16-24	2005	6C	4150	CC1379	(20)
		GA52306	4	12-24	2007	6C	3676	CC1379	(20)
		GA60190	8	16	2010	6C	1292	CC1379	(20)
Mega-2.II	None	GA11757	16	48	2000	14	13	CC15	GAEIP
		GA16531	8	48	2001	6B	146	CC156	(20)
		GA17530	16	48	2000	14	81slv	-	GAEIP
		GA41538	16	64	2004	6A	384	CC156	(20)
		GA41688	16	48	2004	14	13	CC15	(20)
Mega-1.III	None	GA17301	8	48	2000	9V	156	CC156	(20)
		GA17570	6	48	2001	9V	156	CC156	(20)
		GA18641	8-12	48-64	2002	9V	156	CC156	GAEIP
		GA41277	12-24	64	2004	19A	199	CC199	(20)
		GA47760	6-8	32	2006	11A	62	CC62	(20)
		GA62681	6-8	64	2011	15C	199	CC199	(20)
Mega-2.IVa	None	GA04375	18	96	1995	19F	236	CC320	(20)
		GA14846	64	≥256	2000	6B	1536	CC1536	GAEIP
		GA16242	64	≥256	2001	6B	1536	CC1536	(20)
		GA16374	64	≥256	2001	6B	1536	CC1536	GAEIP
Mega-2.IVc	None	GA17545	64	≥256	2000	6B	1536slv	CC1536	(19, 20)
Mega-1.IVb	None	GA17828	16	64	2001	33F	2705	CC100	GAEIP
		GA19795	4	24	2004	33F	2705	CC100	GAEIP
		GA40189	2-3	24	2002	33F	2705	CC100	GAEIP
		GA41317	8	24-32	2004	33F	2705	CC100	(20)
		GA41318	8	32	2004	33F	2705	CC100	GAEIP
Mega-1.V Tn*2009*	None	GA16833	4	32-48	2002	19F	5053	CC320	(20)
		GA17227	8-12	24	2000	23F	242	CC242	(20)
		GA17371	12	96	2000	19F	8014	CC320	(20)
		GA41301	12	32	2004	23F	242	CC242	(20)
		GA41565	3-4	32	2004	19A	81	CC81	(19, 20)
Mega-1.VI	None	GA02254	3-4	16	1994	14	124	CC156	(19, 20)
None	Tn*3872*	GA47597	≥256	≥256	2006	3	180	CC180	(20)
	Tn*6002*	GA44194	≥256	≥256	2005	19A	2543	CC63	(20)
Mega-2.V Tn*2010*	Tn*2010*	GA11856	≥256	≥256	2000	19F	271	CC320	(20)
		GA16121	≥256	≥256	2000	19F	236	CC320	(20)
		GA44288	≥256	≥256	2005	19A	320	CC320	(20)
		GA47688	≥256	≥256	2006	19A	320	CC320	(20)
		GA47778	≥256	≥256	2006	19A	320	CC320	(20)

[a] MICs determined by Etest in at least duplicate and reported as µg/ml. Ranges provided when replicates varied, and each range is within a two-fold dilution.

[b] Subinhibitory concentration used for induction: 0.1 µg/ml.

Table 2. Erythromycin minimum inhibitory concentrations (MICs) for *S. pneumoniae* strains and mutants (Mega insertion, serotype, MLST (clonal complex)) used in this study.

Strain	Uninduced MIC[a]	Induced MIC[a,b]	Relevant Genotype	Reference
GA44288	≥256	≥256	Mega-1.V Tn*2010*, 9A, ST320 (CC320)	(20)
MS32	8	64	GA44288 Δ*erm*(B)::*aphA-3*	This study
MS41	≥256	≥256	GA44288 Δ*mef*(E)/*mel*::cat^{R}	This study
MS42	0.125 ^{S}	*	GA44288 Δ*erm*(B)::*aphA-3*, Δ*mef*(E)/*mel*::cat^{R}	This study
GA16242	64	≥256	Mega-2.IVa, 6B, ST1536 (CC1536)	(20)
TS9001-3	0.125^{S}	*	GA16242 Δ*mef*(E)/*mel*::*aphA-3*	This study
GA17545	96	≥256	Mega-2.IVc 6B, ST1536slv (CC1536)	(19)
XZ8012-5	0.19 ^{S}	*	GA17545 Δ*mef*(E)/*mel*::*aphA-3*	This study
NP112	0.19 ^{S}	*	no macrolide resistance genes, 6B, ST1536 (CC1536)	(20)
MS23	32	≥256	NP112 +Mega-2.IVa	This study
MS30	0.19 ^{S}	*	MS23 Δ*mef*(E)/*mel*::*aphA-3*	This study
GA17457	8	64	Mega-1.I, 19A, ST199 (CC199)	(34)
XZ8009	0.125 ^{S}	*	GA17457 Δ*mef*(E)/*mel*::*aphA-3*	(34)
MS27	32	≥256	XZ8009 +Mega-2-IVa	This study

[a] MICs reported as µg/ml

[b] Subinhibitory concentration used for induction: 0.5 µg/ml

[S] Susceptible to erythromycin when MIC ≤ 0.5 µg/ml

* Susceptible strains were not tested for inducible MIC

FIGURE LEGENDS

Figure 1. Macrolide resistance phenotypes and genotypes of *S. pneumoniae*. Erythromycin minimum inhibitory concentrations (MICs) were determined from uninduced (black bars) and cultures induced with 0.1 μg/ml erythromycin (white bars). Each bar is the average MIC for a macrolide resistance genotype and strains are detailed in Table 1.

Figure 2. *mef*(E) expression in strain GA44288 after 15 min exposure to erythromycin. The data are normalized 1, to the expression of *mef*(E) without erythromycin (0 μg/ml) and error bars are the C_T value standard deviations of technical duplicates. The data presented are representative of experiments from at least three separate days.

Figure 3. The competitive index of isogenic GA44288 mutants grown *in vitro* with erythromycin (0.5 μg/ml) for approximately 50 generations: (A) MS41 (GA44288 Δ*mef*(E)/*mel*) versus GA44288, (B) MS32 (GA44288 Δ*erm*(B)) versus GA44288, and (C) MS32 (GA44288 Δ*erm*(B)) versus MS41 (GA44288 Δ*mef*(E)/*mel*).

Figure 4. The competitive index of high-level macrolide resistance strains with distinct mechanisms (*erm*(B) and Mega-2.IVa) *in vitro* with erythromycin (0.5 μg/ml) grown for approximately 50 generations: (A) GA44288 (*erm*(B)-and *mef*(E)/*mel*-containing) versus GA16242 (Mega-2.IVa-containing), (B) MS41 (GA44288 Δ*mef*(E)/*mel*, *erm*(B)-containing) versus GA16242 (Mega-2.IVa-containing), and (C) MS32 (GA44288 Δ*erm*(B)) versus GA16242 (Mega-2.IVa-containing)**.**

Figure 1

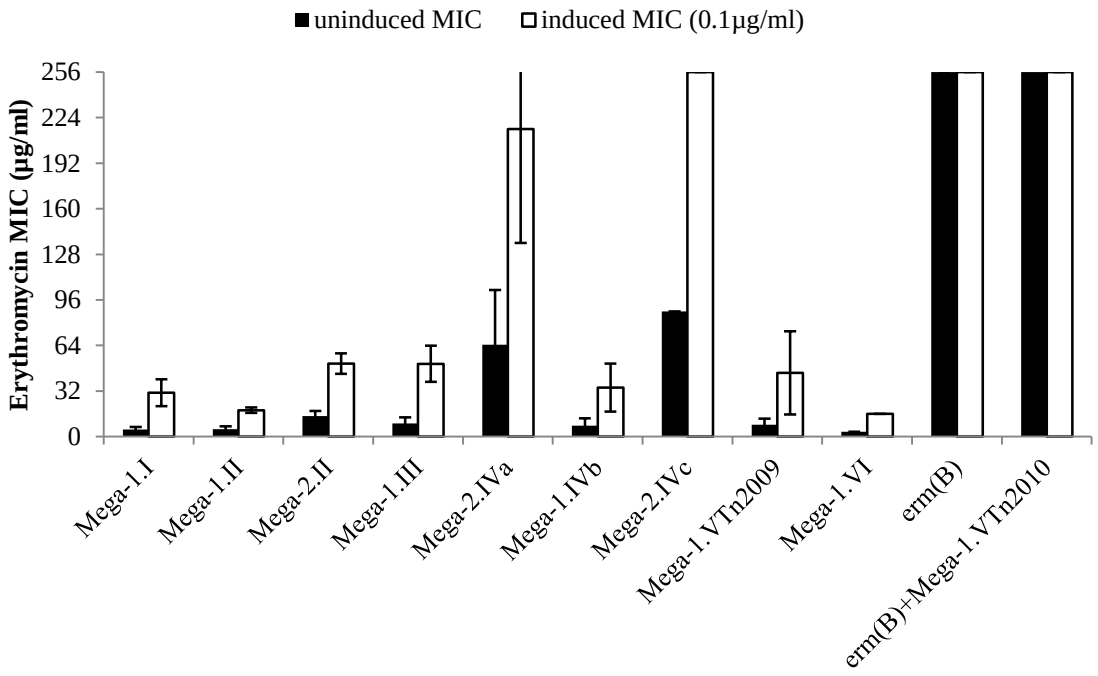
uninduced MIC
induced MIC (0.1µg/ml)
Erythromycin MIC (µg/ml)
256
224
192
160
128
96
64
32
0
Mega-1.I
Mega-1.II
Mega-2.II
Mega-1.III
Mega-2.IVa
Mega-1.IVb
Mega-2.IVc
Mega-1.VTn2009
Mega-1.VI
erm(B)
erm(B)+Mega-1.VTn2010

Figure 2

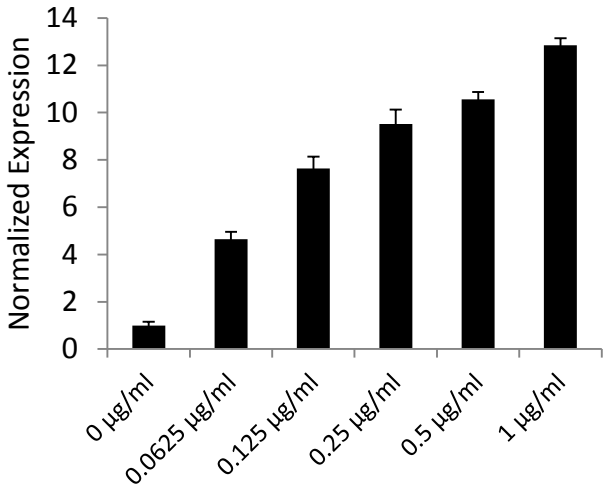
Normalized Expression
14
12
10
8
6
4
2
0
0 µg/ml
0.0625 µg/ml
0.125 µg/ml
0.25 µg/ml
0.5 µg/ml
1 µg/ml

Figure 3

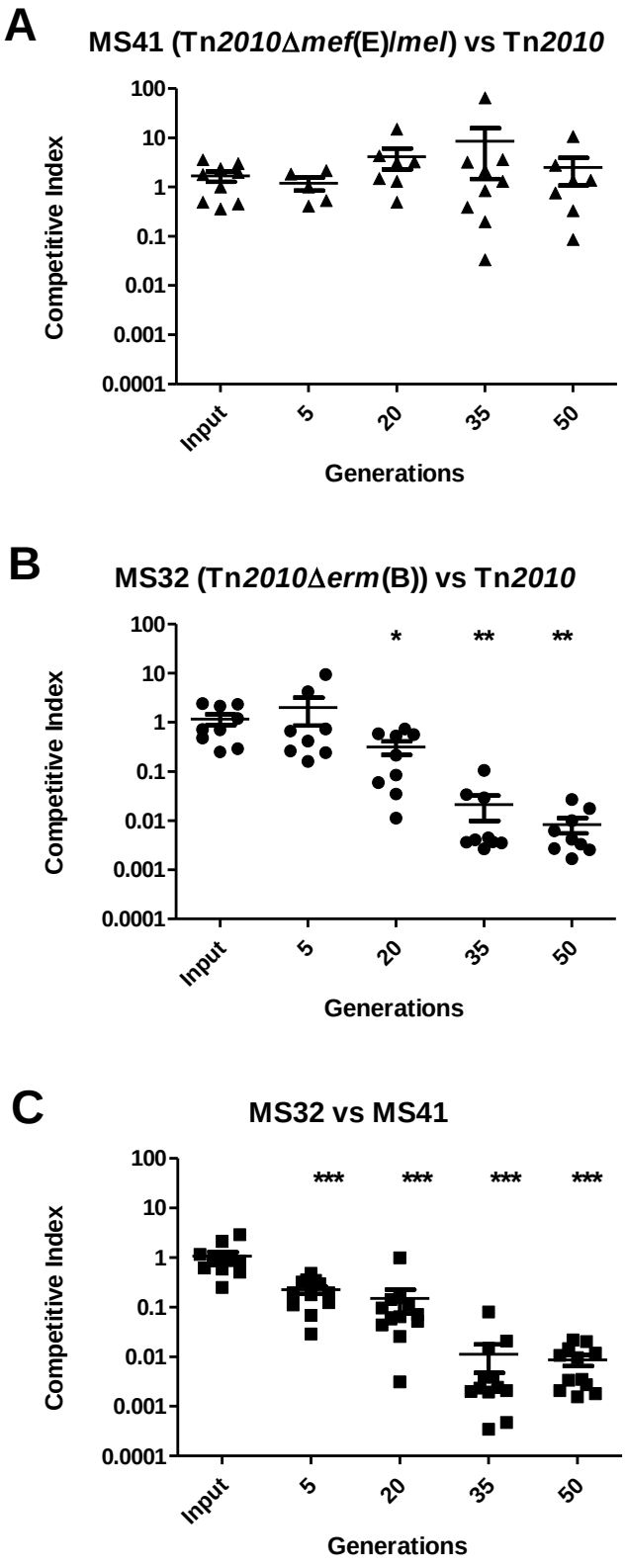
A
MS41 (Tn2010Δmef(E)/mel) vs Tn2010
Competitive Index
100
10
1
0.1
0.01
0.001
0.0001
Input
5
20
35
50
Generations
B
MS32 (Tn2010Δerm(B)) vs Tn2010
*
**
**
Competitive Index
Input
5
20
35
50
Generations
C
MS32 vs MS41
***
***
***
***
Competitive Index
Input
5
20
35
50
Generations

Figure 4

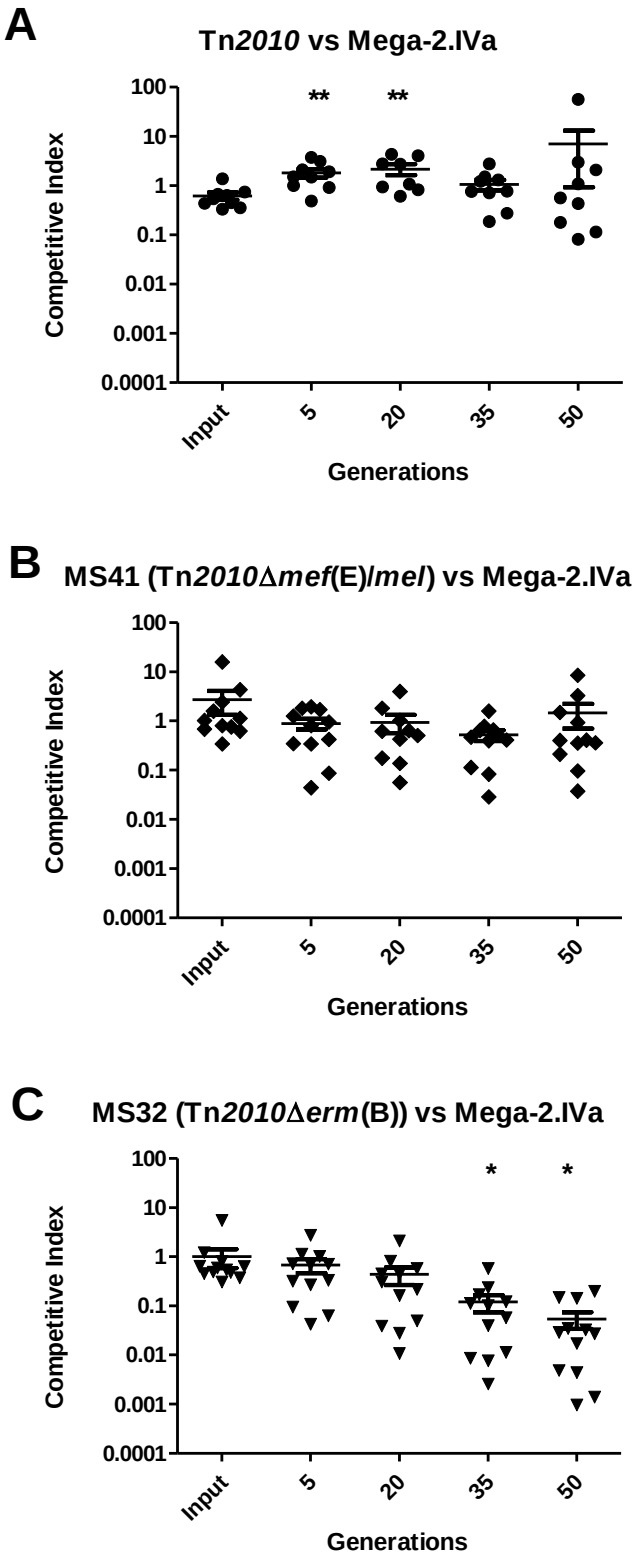
A
Tn2010 vs Mega-2.IVa
Competitive Index
100
10
1
0.1
0.01
0.001
0.0001
**
**
Input
5
20
35
50
Generations
B
MS41 (Tn2010Δmef(E)/mel) vs Mega-2.IVa
Competitive Index
100
10
1
0.1
0.01
0.001
0.0001
Input
5
20
35
50
Generations
C
MS32 (Tn2010Δerm(B)) vs Mega-2.IVa
Competitive Index
100
10
1
0.1
0.01
0.001
0.0001
*
*
Input
5
20
35
50
Generations

SUPPLEMENTAL MATERIALS

Supplemental Table A1. Primers used in the study.

Cloning Primers	**Sequence (5' to 3')**	**Restriction Site[a]**
SC173	CCAGAGATTGTGTCTGTCATGC	
SC251	GCTAGTCACTAGACGGTTTAGACC	
SC10	ACTTGTCAATCACGGACAGC	
SC70	GCAAGTTGCTGCTAGACACTG	
SC125	AGCAAGAGAGTACCAGGATAC	
kanA	CTTAGCAGGAGACATTCCTTCCG	
kanC	GTGGTATGACATTGCCTTCTGCG	
MS27	AGCGTGCCTATTATGCAGTC	
MS28	TCGCCAAAATGCTGTTGATC	
MS34	ATTAGGATCCTATCAATCGGTATATCCGTT	BamHI
	CGTGTAACTTTCCAAATTTATCTAGACTTAAGTT	XbaI
MS35	TGCTTCTAAGTC	
	GACTTAGAAGCAAACTTAAGTCTAGATAAATTT	XbaI
MS36	GGAAAGTTACACG	
MS37	TAATCTGCAGACTTACCAAGATATCACGAA	PstI
MS53	TATATCTAGACAGGACAATAACCTTATAGC	XbaI
MS54	TATATCTAGACCAACTTACTTCTGACAAC	XbaI
MS63	TATAGGATCCCATTTTGATAAAAACTACAACAG G	BamHI
MS64	TATACTGCAGAGCCTTGATTGCAAGGC	PstI
MS69	GCTTATCGATACCGTCGAATTTAAGGTAGTCGCT GG	
MS70	CCAGCGACTACCTTAAATTCGACGGTATCGATA AGC	
MS71	GGAAGTATGAGTCTCATTCCAGTTAGTGACATTA GAAAACCG	
MS72	CGGTTTTCTAATGTCACTAACTGGAATGAGACTC ATACTTCC	
qRT-PCR Primers	**Sequence (5' to 3')**	**Amplified Locus**
q16S_F2	CCAGATGGACCTGCGTTGTAT	16S rRNA
q16S_R2	TCCGTCCATTGCCGAAGATT	16S rRNA
qmef_F3	GTATTCCCGAAACGGCTAAACTG	*mef*(E)
qmef_R3	TGGAACGCCTGTGCATATTTC	*mef*(E)
qmel_F2	TTCTGCACCGACTATAGGGTATGG	*mel*
qmel_R2	AAACCCTAGAGCACAGGATTGC	*mel*
qerm_F2	CCGAACACTAGGGTTGCTCTT	*erm*(B)
qerm_R2	TGTGGTATGGCGGGTAAGTT	*erm*(B)

[a] Restriction sites are underlined.

Supplemental Figure A1. Clustal W alignment of *mef*(E) regulatory regions.

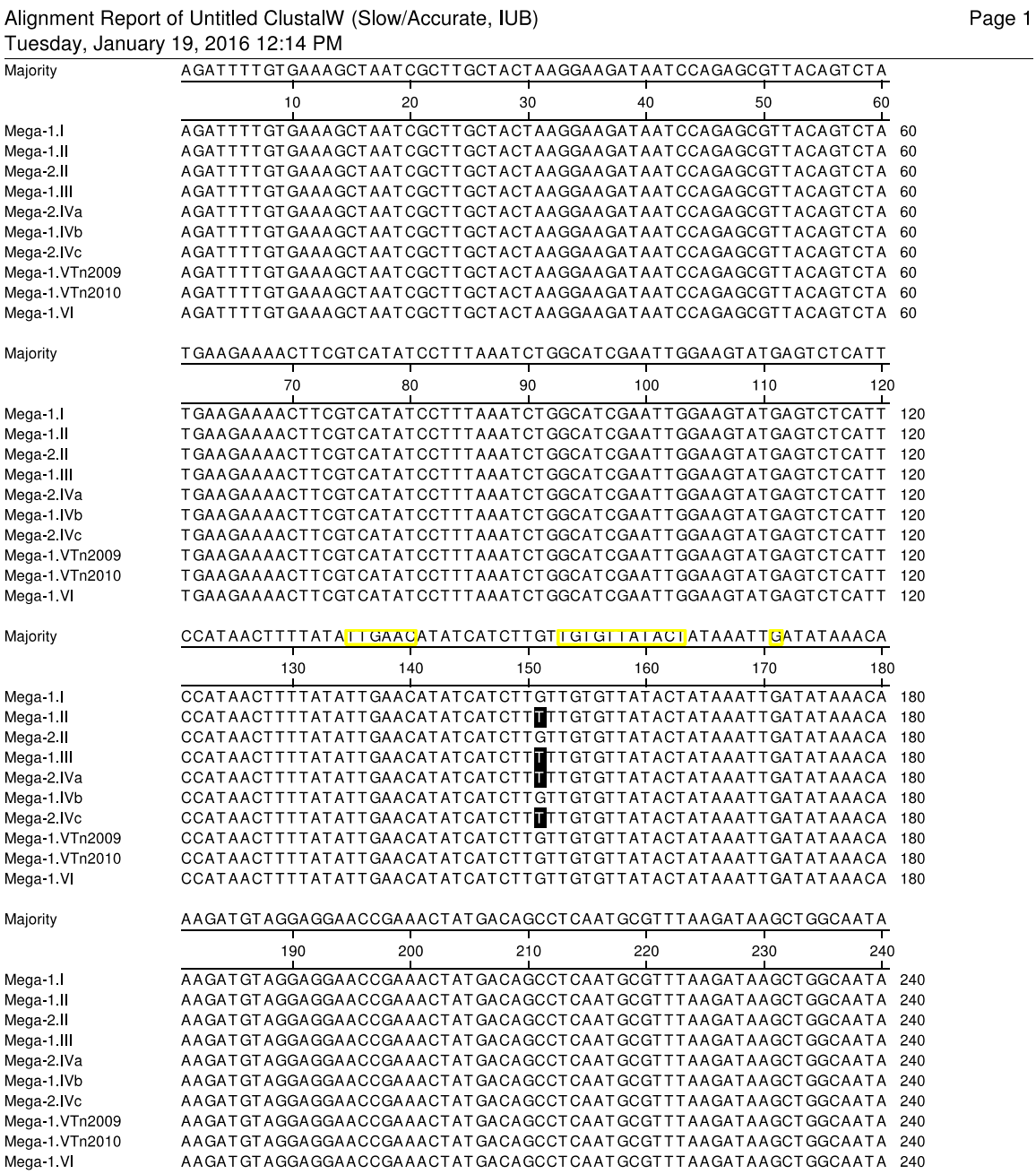

```
Majority          AAAAAAGCAGAATCTATACCCGATGATAGGCTTTTTTGTTGTGCTTATTTATACGATATT

                       250       260       270       280       290       300
Mega-1.I          AAAAAAGCAGAATCTATACCCGATGATAGGCTTTTTTGTTGTGCTTATTTATACGATATT 300
Mega-1.II         AAAAAAGCAGAATCTATACCCGATGATAGGCTTTTTTGTTGTGCTTATTTATACGATATT 300
Mega-2.II         AAAAAAGCAGAATCTATACCCGATGATAGGCTTTTTTGTTGTGCTTATTTATACGATATT 300
Mega-1.III        AAAAAAGCAGAATCTATACCCGATGATAGGCTTTTTTGTTGTGCTTATTTATACGATATT 300
Mega-2.IVa        AAAAAAGCAGAATCTATACCCGATGATAGGCTTTTTTGTTGTGCTTATTTATACGATATT 300
Mega-1.IVb        AAAAAAGCAGAATCTATACCCGATGATAGGCTTTTTTGTTGTGCTTATTTATACGATATT 300
Mega-2.IVc        AAAAAAGCAGAATCTATACCCGATGATAGGCTTTTTTGTTGTGCTTATTTATACGATATT 300
Mega-1.VTn2009    AAAAAAGCAGAATCTATACCCGATGATAGGCTTTTTTGTTGTGCTTATTTATACGATATT 300
Mega-1.VTn2010    AAAAAAGCAGAATCTATACCCGATGATAGGCTTTTTTGTTGTGCTTATTTATACGATATT 300
Mega-1.VI         AAAAAAGCAGAATCTATACCCGATGATAGGCTTTTTTGTTGTGCTTATTTATACGATATT 300

Majority          GAGCATTCATTAGTTACGGTGAGGATATTGGTTATTTAACTATACCTTTATTTAACTATG

                       310       320       330       340       350       360
Mega-1.I          GAGCATTCATTAGTTACGGTGAGGATATTGGTTATTTAACTATACCTTTATTTAACTATG 360
Mega-1.II         GAGCATTCATTAGTTACGGTGAGGATATTGGTTATTTAACTATACCTTTATTTAACTATG 360
Mega-2.II         GAGCATTCATTAGTTACGGTGAGGATATTGGTTATTTAACTATACCTTTATTTAACTATG 360
Mega-1.III        GAGCATTCATTAGTTACGGTGAGGATATTGGTTATTTAACTATACCTTTATTTAACTATG 360
Mega-2.IVa        GAGCATTCATTAGTTACGGTGAGGATATTGGTTATTTAACTATACCTTTATTTAACTATG 360
Mega-1.IVb        GAGCATTCATTAGTTACGGTGAGGATATTGGTTATTTAACTATACCTTTATTTAACTATG 360
Mega-2.IVc        GAGCATTCATTAGTTACGGTGAGGATATTGGTTATTTAACTATACCTTTATTTAACTATG 360
Mega-1.VTn2009    GAGCATTCATTAGTTACGGTGAGGATATTGGTTATTTAACTATACCTTTATTTAACTATG 360
Mega-1.VTn2010    GAGCATTCATTAGTTACGGTGAGGATATTGGTTATTTAACTATACCTTTATTTAACTATG 360
Mega-1.VI         GAGCATTCATTAGTTACGGTGAGGATATTGGTTATTTAACTATACCTTTATTTAACTATG 360

Majority          TCTTTAATATGAATGTTTCCAAATTGTATGTATGCAGACCAAAAGCCACATTGTGGGGTT

                       370       380       390       400       410       420
Mega-1.I          TCTTTAATATGAATGTTTCCAAATTGTATGTATGCAGACCAAAAGCCACATTGTGGGGTT 420
Mega-1.II         TCTTTAATATGAATGTTTCCAAATTGTATGTATGCAGACCAAAAGCCACATTGTGGGGTT 420
Mega-2.II         TCTTTAATATGAATGTTTCCAAATTGTATGTATGCAGACCAAAAGCCACATTGTGGGGTT 420
Mega-1.III        TCTTTAATATGAATGTTTCCAAATTGTATGTATGCAGACCAAAAGCCACATTGTGGGGTT 420
Mega-2.IVa        TCTTTAATATGAATGTTTCCAAATTGTATGTATGCAGACCAAAAGCCACATTGTGGGGTT 420
Mega-1.IVb        TCTTTAATATGAATGTTTCCAAATTGTATGTATGCAGACCAAAAGCCACATTGTGGGGTT 420
Mega-2.IVc        TCTTTAATATGAATGTTTCCAAATTGTATGTATGCAGACCAAAAGCCACATTGTGGGGTT 420
Mega-1.VTn2009    TCTTTAATATGAATGTTTCCAAATTGTATGTATGCAGACCAAAAGCCACATTGTGGGGTT 420
Mega-1.VTn2010    TCTTTAATATGAATGTTTCCAAATTGTATGTATGCAGACCAAAAGCCACATTGTGGGGTT 420
Mega-1.VI         TCTTTAATATGAATGTTTCCAAATTGTATGTATGCAGACCAAAAGCCACATTGTGGGGTT 420

Majority          TGGCCTGCATTTTTTATTGCCTAGAATGCTATTCAAAATAGAAATTCAAGCAAAATAATA

                       430       440       450       460       470       480
Mega-1.I          TGGCCTGCATTTTTTATTGCCTAGAATGCTATTCAAAATAGAAATTCAAGCAAAATAATA 480
Mega-1.II         TGGCCTGCATTTTTTATTGCCTAGAATGCTATTCAAAATAGAAATTCAAGCAAAATAATA 480
Mega-2.II         TGGCCTGCATTTTTTATTGCCTAGAATGCTATTCAAAATAGAAATTCAAGCAAAATAATA 480
Mega-1.III        TGGCCTGCATTTTTTATTGCCTAGAATGCTATTCAAAATAGAAATTCAAGCAAAATAATA 480
Mega-2.IVa        TGGCCTGCATTTTTTATTGCCTAGAATGCTATTCAAAATAGAAATTCAAGCAAAATAATA 480
Mega-1.IVb        TGGCCTGCATTTTTTATTGCCTAGAATGCTATTCAAAATAGAAATTCAAGCAAAATAATA 480
Mega-2.IVc        TGGCCTGCATTTTTTATTGCCTAGAATGCTATTCAAAATAGAAATTCAAGCAAAATAATA 480
Mega-1.VTn2009    TGGCCTGCATTTTTTATTGCCTAGAATGCTATTCAAAATAGAAATTCAAGCAAAATAATA 480
Mega-1.VTn2010    TGGCCTGCATTTTTTATTGCCTAGAATGCTATTCAAAATAGAAATTCAAGCAAAATAATA 480
Mega-1.VI         TGGCCTGCATTTTTTATTGCCTAGAATGCTATTCAAAATAGAAATTCAAGCAAAATAATA 480
```

Majority	TGCAGGAGATAATATAAATG	
	490 500	
Mega-1.I	TGCAGGAGATAATATAAATG	500
Mega-1.II	TGCAGGAGATAATATAAATG	500
Mega-2.II	TGCAGGAGATAATATAAATG	500
Mega-1.III	TGCAGGAGATAATATAAATG	500
Mega-2.IVa	TGCAGGAGATAATATAAATG	500
Mega-1.IVb	TGCAGGAGATAATATAAATG	500
Mega-2.IVc	TGCAGGAGATAATATAAATG	500
Mega-1.VTn2009	TGCAGGAGATAATATAAATG	500
Mega-1.VTn2010	TGCAGGAGATAATATAAATG	500
Mega-1.VI	TGCAGGAGATAATATAAATG	500

Decoration 'Decoration #1': Shade (with solid black) residues that differ from the Consensus.

Supplemental Figure A2.Competitive index of GA44288 mutants grown without erythromycin.

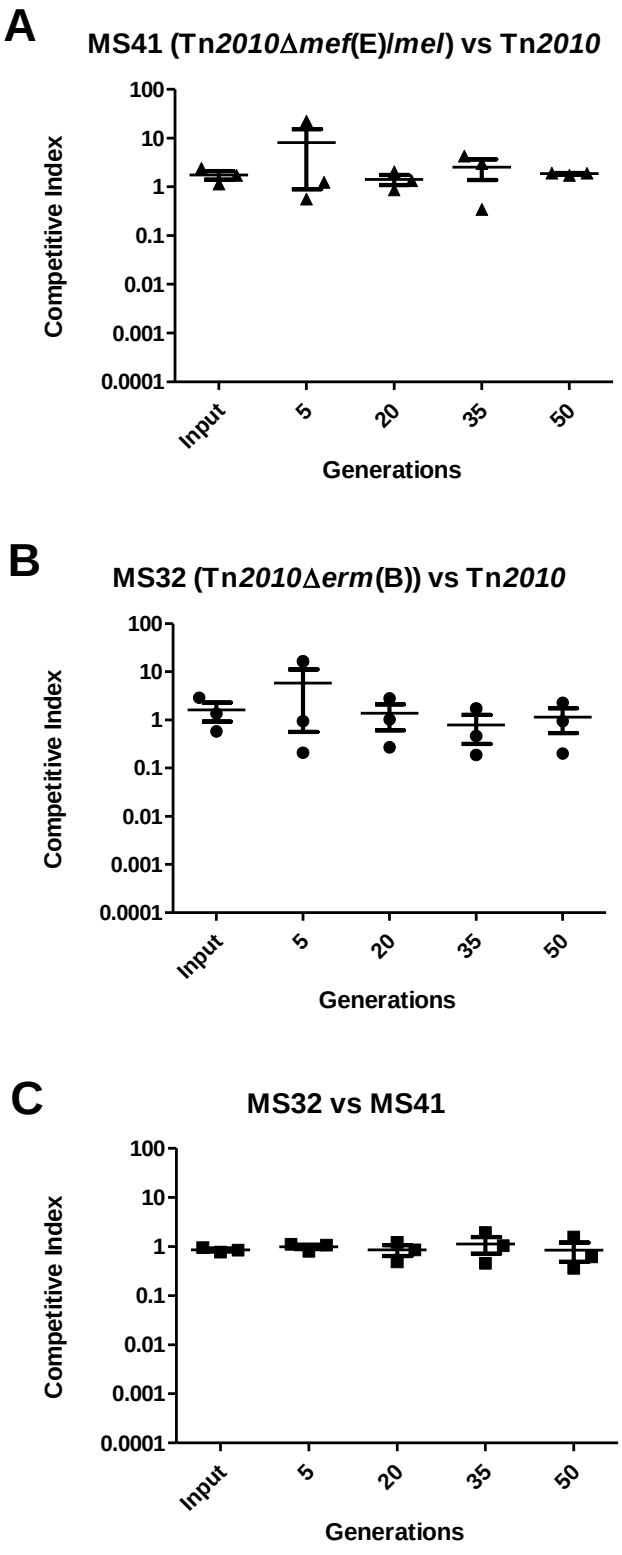

REFERENCES

1. **O'Brien KL, Wolfson LJ, Watt JP, Henkle E, Deloria-Knoll M, McCall N, Lee E, Mulholland K, Levine OS, Cherian T, Hib, Pneumococcal Global Burden of Disease Study T.** 2009. Burden of disease caused by *Streptococcus pneumoniae* in children younger than 5 years: global estimates. Lancet **374:**893-902.

2. **Hicks LA, Bartoces MG, Roberts RM, Suda KJ, Hunkler RJ, Taylor TH, Jr., Schrag SJ.** 2015. US outpatient antibiotic prescribing variation according to geography, patient population, and provider specialty in 2011. Clin Infect Dis **60:**1308-1316.

3. **Suda KJ, Hicks LA, Roberts RM, Hunkler RJ, Taylor TH.** 2014. Trends and seasonal variation in outpatient antibiotic prescription rates in the United States, 2006 to 2010. Antimicrob Agents Chemother **58:**2763-2766.

4. **Appelbaum PC.** 2002. Resistance among *Streptococcus pneumoniae*: Implications for drug selection. Clin Infect Dis **34:**1613-1620.

5. **Gay K, Baughman W, Miller Y, Jackson D, Whitney CG, Schuchat A, Farley MM, Tenover F, Stephens DS.** 2000. The emergence of *Streptococcus pneumoniae* resistant to macrolide antimicrobial agents: a 6-year population-based assessment. J Infect Dis **182:**1417-1424.

6. **Hyde TB, Gay K, Stephens DS, Vugia DJ, Pass M, Johnson S, Barrett NL, Schaffner W, Cieslak PR, Maupin PS, Zell ER, Jorgensen JH, Facklam RR, Whitney CG.** 2001. Macrolide resistance among invasive *Streptococcus pneumoniae* isolates. JAMA **286:**1857-1862.

7. **Roberts MC, Sutcliffe J, Courvalin P, Jensen LB, Rood J, Seppala H.** 1999. Nomenclature for macrolide and macrolide-lincosamide-streptogramin B resistance determinants. Antimicrobial Agents and Chemotherapy **43:**2823-2830.

8. **Weisblum B.** 1995. Insights into erythromycin action from studies of its activity as inducer of resistance. Antimicrobial Agents and Chemotherapy **39:**797-805.

9. **Weisblum B.** 1995. Erythromycin resistance by ribosome modification. Antimicrob Agents Chemother **39:**577-585.

10. **Tait-Kamradt A, Clancy J, Cronan M, Dib-Hajj F, Wondrack L, Yuan W, Sutcliffe J.** 1997. *mefE* is necessary for the erythromycin-resistant M phenotype in *Streptococcus pneumoniae*. Antimicrob Agents Chemother **41:**2251-2255.

11. **Gay K, Stephens DS.** 2001. Structure and dissemination of a chromosomal insertion element encoding macrolide efflux in *Streptococcus pneumoniae*. J Infect Dis **184:**56-65.

12. **Ambrose KD, Nisbet R, Stephens DS.** 2005. Macrolide efflux in *Streptococcus pneumoniae* is mediated by a dual efflux pump (*mel* and *mef*) and is erythromycin inducible. Antimicrob Agents Chemother **49:**4203-4209.

13. **Chancey ST, Zhou X, Zähner D, Stephens DS.** 2011. Induction of efflux-mediated macrolide resistance in *Streptococcus pneumoniae*. Antimicrob Agents Chemother **55:**3413-3422.

14. **Stephens DS, Zughaier SM, Whitney CG, Baughman WS, Barker L, Gay K, Jackson D, Orenstein WA, Arnold K, Schuchat A, Farley MM.** 2005. Incidence of macrolide resistance in *Streptococcus pneumoniae* after introduction

of the pneumococcal conjugate vaccine: population-based assessment. Lancet **365:**855-863.

15. **Rudolph K, Bulkow L, Bruce M, Zulz T, Reasonover A, Harker-Jones M, Hurlburt D, Hennessy T.** 2013. Molecular resistance mechanisms of macrolide-resistant invasive *Streptococcus pneumoniae* isolates from Alaska, 1986 to 2010. Antimicrob Agents Chemother **57:**5415-5422.

16. **Chancey ST, Zähner D, Stephens DS.** 2012. Acquired inducible antimicrobial resistance in Gram-positive bacteria. Future Microbiology **7:**959-978.

17. **Cilloniz C, Albert RK, Liapikou A, Gabarrus A, Rangel E, Bello S, Marco F, Mensa J, Torres A.** 2015. The Effect of Macrolide Resistance on the Presentation and Outcome of Patients Hospitalized for *Streptococcus pneumoniae* Pneumonia. Am J Respir Crit Care Med **191:**1265-1272.

18. **Schuchat A, Hilger T, Zell E, Farley MM, Reingold A, Harrison L, Lefkowitz L, Danila R, Stefonek K, Barrett N, Morse D, Pinner R, Network ABCSTotEIP.** 2001. Active bacterial core surveillance of the emerging infections program network. Emerg Infect Dis **7:**92-99.

19. **Chancey ST, Bai X, Kumar N, Drabek EF, Daugherty SC, Colon T, Ott S, Sengamalay N, Sadzewicz L, Tallon LJ, Fraser CM, Tettelin H, Stephens DS.** 2015. Transcriptional attenuation controls macrolide inducible efflux and resistance in *Streptococcus pneumoniae* and in other Gram-positive bacteria containing *mef*/*mel*(*msr*(D)) elements. PLoS One **10:**e0116254.

20. **Chancey ST, Agrawal S, Schroeder MR, Farley MM, Tettelin H, Stephens DS.** 2015. Composite mobile genetic elements disseminating macrolide resistance in *Streptococcus pneumoniae*. Front Microbiol **6:**26.

21. **Gupta P, Sothiselvam S, Vazquez-Laslop N, Mankin AS.** 2013. Deregulation of translation due to post-transcriptional modification of rRNA explains why *erm* genes are inducible. Nat Commun **4:**1984.

22. **Metzler K, Drlica K, Blondeau JM.** 2013. Minimal inhibitory and mutant prevention concentrations of azithromycin, clarithromycin and erythromycin for clinical isolates of *Streptococcus pneumoniae*. J Antimicrob Chemother **68:**631-635.

23. **Lonks JR, Garau J, Gomez L, Xercavins M, Ochoa de Echaguen A, Gareen IF, Reiss PT, Medeiros AA.** 2002. Failure of macrolide antibiotic treatment in patients with bacteremia due to erythromycin-resistant *Streptococcus pneumoniae*. Clin Infect Dis **35:**556-564.

24. **Schentag JJ, Klugman KP, Yu VL, Adelman MH, Wilton GJ, Chiou CC, Patel M, Lavin B, Paladino JA.** 2007. *Streptococcus pneumoniae* bacteraemia: pharmacodynamic correlations with outcome and macrolide resistance--a controlled study. Int J Antimicrob Agents **30:**264-269.

25. **Klugman KP.** 2002. Bacteriological evidence of antibiotic failure in pneumococcal lower respiratory tract infections. Eur Respir J Suppl **36:**3s-8s.

26. **Del Grosso M, Camilli R, Iannelli F, Pozzi G, Pantosti A.** 2006. The *mef*(E)-carrying genetic element (mega) of *Streptococcus pneumoniae*: insertion sites and

association with other genetic elements. Antimicrob Agents Chemother **50:**3361-3366.

27. **Del Grosso M, Northwood JG, Farrell DJ, Pantosti A.** 2007. The macrolide resistance genes *erm*(B) and *mef*(E) are carried by Tn*2010* in dual-gene *Streptococcus pneumoniae* isolates belonging to clonal complex CC271. Antimicrob Agents Chemother **51:**4184-4186.

28. **Del Grosso M, Scotto d'Abusco A, Iannelli F, Pozzi G, Pantosti A.** 2004. Tn*2009*, a Tn*916*-like element containing *mef*(E) in *Streptococcus pneumoniae*. Antimicrob Agents Chemother **48:**2037-2042.

29. **Brown JS, Gilliland SM, Holden DW.** 2001. A *Streptococcus pneumoniae* pathogenicity island encoding an ABC transporter involved in iron uptake and virulence. Mol Microbiol **40:**572-585.

30. **Brown JS, Gilliland SM, Basavanna S, Holden DW.** 2004. phgABC, a three-gene operon required for growth of *Streptococcus pneumoniae* in hyperosmotic medium and *in vivo*. Infect Immun **72:**4579-4588.

31. **Brown JS, Gilliland SM, Spratt BG, Holden DW.** 2004. A locus contained within a variable region of pneumococcal pathogenicity island 1 contributes to virulence in mice. Infect Immun **72:**1587-1593.

32. **Li Y, Tomita H, Lv Y, Liu J, Xue F, Zheng B, Ike Y.** 2011. Molecular characterization of *erm*(B)- and *mef*(E)-mediated erythromycin-resistant *Streptococcus pneumoniae* in China and complete DNA sequence of Tn*2010*. J Appl Microbiol **110:**254-265.

33. **Bowers JR, Driebe EM, Nibecker JL, Wojack BR, Sarovich DS, Wong AH, Brzoska PM, Hubert N, Knadler A, Watson LM, Wagner DM, Furtado MR, Saubolle M, Engelthaler DM, Keim PS.** 2012. Dominance of multidrug resistant CC271 clones in macrolide-resistant *Streptococcus pneumoniae* in Arizona. BMC Microbiol **12:**12.

34. **Zähner D, Zhou X, Chancey ST, Pohl J, Shafer WM, Stephens DS.** 2010. Human antimicrobial peptide LL-37 induces MefE/Mel-mediated macrolide resistance in *Streptococcus pneumoniae*. Antimicrob Agents Chemother **54:**3516-3519.

35. **Andersson DI, Hughes D.** 2010. Antibiotic resistance and its cost: is it possible to reverse resistance? Nat Rev Microbiol **8:**260-271.

36. **Min YH, Kwon AR, Yoon EJ, Shim MJ, Choi EC.** 2008. Translational attenuation and mRNA stabilization as mechanisms of *erm*(B) induction by erythromycin. Antimicrob Agents Chemother **52:**1782-1789.

37. **Montanari MP, Mingoia M, Giovanetti E, Varaldo PE.** 2001. Differentiation of resistance phenotypes among erythromycin-resistant pneumococci. Journal of Clinical Microbiology **39:**1311-1315.

38. **Wolter N, Smith AM, Farrell DJ, Northwood JB, Douthwaite S, Klugman KP.** 2008. Telithromycin resistance in *Streptococcus pneumoniae* is conferred by a deletion in the leader sequence of *erm*(B) that increases rRNA methylation. Antimicrob Agents Chemother **52:**435-440.

39. **Oldenburg M, Kruger A, Ferstl R, Kaufmann A, Nees G, Sigmund A, Bathke B, Lauterbach H, Suter M, Dreher S, Koedel U, Akira S, Kawai T, Buer J,**

Wagner H, Bauer S, Hochrein H, Kirschning CJ. 2012. TLR13 recognizes bacterial 23S rRNA devoid of erythromycin resistance-forming modification. Science **337:**1111-1115.

40. **Croucher NJ, Chewapreecha C, Hanage WP, Harris SR, McGee L, van der Linden M, Song JH, Ko KS, de Lencastre H, Turner C, Yang F, Sa-Leao R, Beall B, Klugman KP, Parkhill J, Turner P, Bentley SD.** 2014. Evidence for soft selective sweeps in the evolution of pneumococcal multidrug resistance and vaccine escape. Genome Biol Evol **6:**1589-1602.

41. **Rodgers GL, Klugman KP.** 2011. The future of pneumococcal disease prevention. Vaccine **29S:**C43-C48.

42. **Moore MR, Link-Gelles R, Schaffner W, Lynfield R, Lexau C, Bennett NM, Petit S, Zansky SM, Harrison LH, Reingold A, Miller L, Scherzinger K, Thomas A, Farley MM, Zell ER, Taylor TH, Jr., Pondo T, Rodgers L, McGee L, Beall B, Jorgensen JH, Whitney CG.** 2015. Effect of use of 13-valent pneumococcal conjugate vaccine in children on invasive pneumococcal disease in children and adults in the USA: analysis of multisite, population-based surveillance. Lancet Infect Dis **15:**301-309.

43. **Havarstein LS, Coomaraswamy G, Morrison DA.** 1995. An unmodified heptadecapeptide pheromone induces competence for genetic transformation in *Streptococcus pneumoniae*. Proc Natl Acad Sci U S A **92:**11140-11144.

44. **Tao L, LeBlanc DJ, Ferretti JJ.** 1992. Novel streptococcal-integration shuttle vectors for gene cloning and inactivation. Gene **120:**105-110.

45. **Claverys JP, Dintilhac A, Pestova EV, Martin B, Morrison DA.** 1995. Construction and evaluation of new drug-resistance cassettes for gene disruption mutagenesis in *Streptococcus pneumoniae*, using an *ami* test platform. Gene **164:**123-128.

Chapter 5: Final Discussion

I. The Pneumococcus

Streptococcus pneumoniae is an opportunistic pathogen that causes non-invasive (acute otitis media and pneumonia) and invasive disease such as bacteremia and meningitis. As a common commensal of the human nasopharynx, the pneumococcus is often carried by young children, less than five years of age (1, 2). Each year approximately 1.6 million people die from pneumococcal infections; one million are children under the age of five (3). During the mid-1990s, the high prevalence of penicillin resistance among *S. pneumoniae* resulted in a shift from β-lactam to macrolide antibiotics for non-invasive pneumococcal diseases and upper respiratory infections. Widespread use of macrolides contributed to the expansion of macrolide-resistant *S. pneumoniae*. Globally, erythromycin resistance among *S. pneumoniae* is geographically variable and ranges from <10% to >50% (4).

II. Invasive Pneumococcal Disease (IPD) Serotypes

S. pneumoniae serotypes 4, 6B, 9V, 14, 18C, 19F, and 23F were the most common serotypes causing invasive pneumococcal disease (IPD) worldwide through 2000 (5). This was despite the inclusion of these serotypes in the 23-valent pneumococcal polysaccharide vaccine (PPSV-23) which was licensed in 1984. In 2000, a heptavalent pneumococcal conjugate vaccine (PCV-7) was licensed for use in children under five years old in the United States (6, 7). PCV-7 contains the capsular polysaccharides of serotypes 4, 6B, 9V, 14, 18C, 19F, and 23F conjugated to the CRM197 diphtheria

protein. With the rise in IPD from non-PCV-7 serotypes, PCV-13 was licensed in 2010 for use in the pediatric population as a replacement for PCV-7 (7, 8). PCV-13 contains serotypes from PCV-7 with the addition of serotypes 1, 3, 5, 6A, 7F, and 19A conjugated to the CRM197 diphtheria protein.

We investigated the impact of PCV-7 and PCV-13 on invasive pneumococcal disease. In Atlanta, from 1994-1999 the incidence of IPD averaged 30.2 cases per 100,000 population (9). Pediatric (children <2 years old) vaccination with PCV-7 began in Atlanta in 2000 and by 2002 IPD was reduced 57% (9). Worldwide reductions of IPD were also observed following PCV-7 introductions in other countries, attributed both individual protection and herd protection (10-16). Vaccination with pneumococcal conjugate and other bacterial meningitis conjugate vaccines reduces nasopharyngeal carriage of vaccine serotypes in populations (7, 17), which protects non-vaccinated individuals through interference with human-to-human transmission (12, 18). In Chapter 2, we determined the effect of PCV-7 and PCV-13 on the incidence of IPD from 2002 through 2013 as a result of continued vaccine pressure within the population. Although IPD caused by PCV-7 serotypes continued to decline following PCV-7 introduction, the rate of IPD remained constant at ~12 per 100,000 from 2002-2009 due to serotype replacement. “Serotype replacement” following PCV-7 introduction has been observed worldwide (10, 11). The expansion of non-vaccine serotypes such as 7F and selection of capsule switching events (e.g. a capsule switch event in a highly successful serotype 19F led to the expansion of this clone as serotype 19A, which is not represented in PCV-7 (19, 20), both contributed to “serotype replacement.” Unlike PCV-7, successful conjugate

vaccines against other respiratory and meningitis pathogens, *Haemophilus influenza* and *Neisseria meningitides*, have not resulted in serotype replacement (21-23).

As shown in Chapter 2, PCV-13 introduction in Atlanta in 2010 was followed by a further decline in incidence of IPD, which by 2013 was 8.8 cases per 100,000 population. Overall, IPD in Atlanta was reduced 71% from 1994-1999 to 2013 due to PCV-7 and PCV-13 introduction. Reduction of IPD in Atlanta following PCV-13 was largely due to reductions of IPD caused by serotypes 7F and 19A: worldwide PCV-13 has led to reductions in IPD due to each of the six additional serotypes (1, 3, 5, 6A, 7F, and 19A) (17, 24-27). In Atlanta, IPD caused by serotype 3 was consistent but at low incidence throughout the twenty-year study period, while serotypes 1 and 5 infrequently caused IPD in this population. Following the 2000 and 2010 introductions of PCV-7 and PCV-13, respectively, the proportion of IPD caused by vaccine serotypes continued to decline and by 2013 accounted for only 18.5% of IPD in Atlanta. As young children were initial target of vaccination, the overall decreased rates of IPD in all age populations highlights the success of PCV-7 and PCV-13 vaccine interventions in reducing the burden of disease in vaccination and non-vaccinated individuals by herd protection (7, 10, 13, 14, 25, 28, 29).

III. Macrolide-Resistant Invasive Pneumococcal Disease (MR-IPD)

Macrolide resistance rapidly emerged in *S. pneumoniae* in the early-1990s (9, 30, 31). The introduction and widespread use of semisynthetic macrolides including azithromycin and clarithromycin was an important driver. Macrolides reversibly at a site near the peptidyl transferase center of the 50S ribosomal subunit on the 23S rRNA, which

inhibits protein synthesis (32, 33). Macrolide resistance in *S. pneumoniae* is predominantly due to two mechanisms: target site modification and macrolide efflux (34). The ribosomal methylation by the gene product encoded by *erm*(B) confers high-level resistance to macrolide as well as resistance to lincosamide and streptogramin B (MLS_B phenotype) (35). Pneumococcal macrolide efflux occurs through a yet-undefined mechanism by the presence of *mef*(E)/*mel* of the transposable genetic element Mega (36), confers resistance to 14- and 15-membered macrolides while remaining susceptible to lincosamides and streptogramin B (37, 38).

Between 1994 and 1999, MR-IPD rapidly emerged in Atlanta, GA, largely due to an increase in cases caused by isolates containing *mef*(E)/*mel* (9, 39). PCV-7 introduction reduced the incidence of MR-IPD. The highest rates of macrolide resistance were present in PCV-7 vaccine serotypes (9, 40-42). In Chapter 2, we noted the stabilization of the incidence of MR-IPD from 2002 through 2009 due to the continued decline of macrolide-resistant PCV-7 serotypes that was offset by the rapid emergence of macrolide-resistant serotypes not covered by PCV-7 specifically serotype 19A. This serotype replacement event was largely caused by clonal expansion of a serotype 19A, ST320, clone that belongs to clonal complex 320 (formerly CC271) (43-45). The clone arose from a capsule switch event where a 19F strain was transformed to 19A. Interestingly, many macrolide-resistant serotype 19A CC320 isolates were found to contain both *erm*(B) and *mef*(E)/*mel*.

The incidence of MR-IPD caused by isolates with the dual macrolide resistance phenotype (both *erm*(B) and *mef*(E)/*mel*) rapidly increased from 2003 through 2010 and expanded worldwide (2, 45-49). Selective pressure by PCV-7 and the frequent use of

macrolides clinically provided an opportunity for this clone to become quite successful. The introduction of PCV-13, which includes serotype 19A, was successful in reducing IPD caused by macrolide-resistant serotype 19A isolates in Atlanta. By 2013, there were no cases of MR-IPD caused by isolates from CC320 vaccine-targeted age-groups (those <5 years old) and disease due to this clone was greatly reduced in non-vaccinated individuals in Atlanta (Chapter 2). Despite challenges with serotype replacement, PCVs were an effective intervention in reducing the incidence of disease caused by vaccine serotypes with high rates of macrolide resistance. From 1999 to 2013, PCVs decreased MR-IPD 74% in the Atlanta population.

IV. Macrolide Resistance Elements

Following the observation that the emergence of MR-IPD in the late-1990s was caused by isolates containing *mef*(E)/*mel* (39), our lab identified the Macrolide Efflux Genetic Assembly (Mega) as the insertion element in *S. pneumoniae* that carries *mef*(E) and *mel* under control of a single promoter (50, 51). Mega is related to the Tn*916* family of conjugative transposons, but due to its lack of transposition genes, Mega is most efficiently transferred horizontally through transformation and homologous recombination between pneumococci (50). In Chapter 3, we investigated the composite mobile genetic elements in *S. pneumoniae* responsible for macrolide resistance through genomic sequencing of 147 isolates, 131 of which were collected from the Atlanta population-based surveillance. In addition to the five previously reported Mega insertion sites (50, 52), we identified a novel Mega insertion site, now termed the class VI insertion site. We found that all Mega insertion sites had putative six base coupling sequences at each end of Mega (left junction 5'-CATGTT-3' and right junction 5'-AGCACA) as well

as a consensus recognition sequence of 5'-TTTCCNCAA-3'. These data resemble insertion sites of conjugative transposons and suggest conjugative transposition specific machinery have facilitated insertion of Mega in to these specific genetic regions. The conserved insertion sites suggest very few transposition events may have occurred leading to Mega insertion into these genetic contexts.

Also, In Chapter 3, we reported the macrolide resistance elements of *S. pneumoniae* detected in our collection of sequenced genomes. In 2004 del Grosso and colleagues described the insertion of Mega into *orf*6 of Tn*916* (52), i.e. class V insertion. We found this Mega insertion commonly within the sequenced genomes. The presence of Mega in a Tn*916*-like element was identified as Tn*2009* (47, 52) while the presence of both Mega and *erm*(B) in a Tn*916*-like element was identified as Tn*2010* (44, 46) Only Tn*2010* was found within the Atlanta population isolates. Tn*6002* and Tn*3872*, which contain *erm*(B) on Tn*916*-like elements, were also found in macrolide-resistant *S. pneumoniae* (43). Another dual macrolide resistance element, Tn*2017* was not identified in the sequenced genomes (53). Tn*2017* isolate have been reported in serotype 19F, and may not be present in the United States due to vaccine pressure by PCV-7 and PCV-13. The Tn*2010*-containing serotype 19A ST320 clone emerged in the PCV-7 era as a vaccine replacement serotype and spread worldwide as both a carriage isolate and as a cause IPD (44-46).

V. High-Level Macrolide Resistance

The emergence of the Tn*2010*-containing serotype 19A ST320 clone was of interest due to the presence of dual macrolide resistance determinants. In Chapter 4,

through creation of a series of isogenic mutants, we found the presence of *erm*(B) in Tn*2010* was critical in conferred a high-level macrolide resistance phenotype similar to *S. pneumoniae* with *erm*(B) at other sites. The *mef*(E)/*mel* operon did not contribute to the high-level macrolide resistance or enhance survival *in vitro* in the presence or absence of erythromycin. In *Staphylococcus aureus*, *erm*(C)-mediated resistance has been shown to exert a fitness cost due to ribosomal methylation (54). However, we concluded that expression of *erm*(B) in *S. pneumoniae* did not produce a fitness defect for which the presence of *mef*(E)/*mel* would alleviate. A recent study also found Tn*2010* does not confer a fitness cost in the pneumococcus (55). Previous research found that *S. pneumoniae* isolates that contained both *erm*(B) and *mef*(E)/*mel* had high rates of recombination (56). This may suggest that the ancestor clone was created Tn*2010* through a recombination event wherein Tn*2009* acquired *erm*(B) or Tn*6002* acquired Mega. A potential explanation for the maintenance of Mega in Tn*2010* is discussed later.

Mega can be found as two isoforms Mega-1 (5.4-kb) and Mega-2 (5.5-kb) due to a 99 bp insertion between *mef*(E) and *mel*. We investigated the level (MIC) of macrolide resistance of six Mega insertion sites and found high-levels (≥32 μg/ml) of macrolide resistance were conferred by Mega-2.IVa and Mega-2.IVc insertions (Chapter 4). The 99-bp intergenic region between *mef*(E) and *mel* of Mega-2 was not the cause of high-level resistance because Mega-2.II displayed lower levels of macrolide resistance, MICs 1-16 μg/ml. In addition, we showed that Mega-2.IVa and Mega-2.IVc have a downstream deletion of the adjacent Pneumococcal Pathogenicity Island-1 (PPI-1) (Chapter 3), which has a conserved 15.1-kb region and a variable 15.6-kb region (43, 57). The elimination of certain genetic regions of this island may be involved in up-regulation of *mef*(E) and *mel*.

Deletion of the *piaABCD* and *phgABC* operons of the conserved region and deletion of different variable regions has been associated with decreased virulence in mice (58-60). Although predicted to be less virulent, all five high-level *mef*(E)/*mel* strains were invasive isolates.

Through our competition experiments, we found that high-level macrolide-resistant *S. pneumoniae* have a growth fitness advantage over lower-level macrolide-resistant *S. pneumoniae* in the presence of selection. This difference was found to be independent of macrolide resistance mechanism causing high-level resistance as either high-level *erm*(B) or a high-level Mega-containing isolate outcompetes a lower-level Mega strain. Strains with either high-level macrolide resistance mechanism were equally fit in competition with each other under erythromycin pressure. The concentration of erythromycin used was the same as is achieved in serum during erythromycin treatment (0.5 μg/ml). The presence of *mef*(E)/*mel* did not enhance fitness during the competition assays, the contribution of *mef*(E)/*mel* in dual macrolide resistance isolates is still unclear.

VI. Future Directions

Surveillance programs such as the one essential for this work are critical in monitoring the epidemiology of pneumococcal disease including antibiotic resistant IPD and pneumococcal carriage. As part of the Active Bacterial Core surveillance (ABCs) program the Emerging Infections Program in Atlanta has tracked IPD and collected *S. pneumoniae* isolates for over twenty years. This long-term surveillance program observed the emergence of MR-IPD in the late-1990s and was among the first to report on the remarkable success of PCV-7 in reducing IPD and MR-IPD in populations and that

significant herd protection was resulting from vaccination of young children. As of 2015, the Centers for Disease Control and Prevention (CDC) is now performing genomic sequencing of all IPD isolates collected from the 10 sites in the United States as part of the ABCs program that has a *S. pneumoniae* surveillance population of over 31 million people (Atlanta, GA; Baltimore, MD; Connecticut state; Denver, CO; Minnesota state; New Mexico state; Oregon state; Rochester and Albany, NY; San Francisco, CA; Tennessee state). Continued prospective population-based surveillance is critical in providing data on the incidence of IPD, the serotypes involved and antibiotic resistance.

After PCV-7 introduction, serotype replacement and clonal expansion of capsule switch clones stalled reductions of pneumococcal disease. Following the introduction of PCV-13 IPD and MR-IPD decreased within three years. Continued surveillance is needed to determine if these decreases will be sustained and if serotype replacement again appeared.

As discussed in Chapter 3, the non-vaccine serotypes 12F, 15A, 22F, 23A, 33F, and 35B are now the most prevalent IPD serotypes and non-vaccine serotypes 15A, 15B, 15C, 23A, 22F, 33F, and 35B are the most prevalent MR-IPD serotypes. In less than four years following PCV-13 introduction, carriage of serotype 35B *S. pneumoniae* significantly increased and 15B, 15C, and 11A remained common carriage serotypes (1). With the well documented link between nasopharyngeal carriage and pneumococcal disease (61), serotype 35B, 15B, 15C, and 11A are important serotypes to monitor during PCV-13 implementation.

The rapid emergence of the serotype 19A CC320 clone containing Tn*2010*, with both *erm*(B) and *mef*(E)/*mel*, as a replacement serotype was observed worldwide. With the higher-level macrolide resistance and broader range of antibiotic resistance conferred by the presence of *erm*(B) compared to *mef*(E)/*mel*, the presence of *mef*(E)/*mel* in dual macrolide resistance strains appears functionally redundant. We did not find a macrolide resistance or fitness benefit of the presence of *mef*(E)/*mel* in a strain containing *erm*(B). However, previous works by our group showed that expression of *mef*(E)/*mel* are inducible by the human antimicrobial peptide LL-37 and the presence of *mef*(E)/*mel* enhances resistance to LL-37 (62). Thus *mef*(E)/*mel* may be maintained and selected for in strains containing *erm*(B) to enhance protection against host antimicrobial peptides at mucosal membranes. Future studies should focus on the role of *mef*(E)/*mel* during *in vivo* colonization, where they may be induced and expressed and provide initial protection during macrolide treatment before *erm*(B) is expressed. Recently, macrolide-induced expression of *mef*(E)/*mel* was shown to occur through a tightly controlled regulation system of transcriptional attenuation (51). Expression of *mef*(E)/*mel* may occur through an additional mechanism as LL-37 induction of *mef*(E)/*mel* was not due to the same induction mechanism as macrolides (Chancey, unpublished data).

The mechanism of macrolide efflux in *S. pneumoniae* has yet to be fully elucidated (37). Efflux is mediated by the gene products of *mef*(E) and *mel* for macrolide resistance in *S. pneumoniae*: *mef*(E) encodes a major facilitator superfamily protein and *mel* encodes an ATP-binding cassette (ABC) transporter protein but lacks a hydrophobic, membrane-binding domain (36, 63). While it is thought that Mef(E) and Mel cooperate to expel macrolides, a direct interaction of these two proteins has yet to be demonstrated.

High-level macrolide resistance is most commonly due to the presence of *erm*(B); but in Chapter 4, we showed Mega in some genetic locations will confer similar high-level macrolide resistance. As Mega-2.IVa and Mega-2.IVc insertions coincided with a unique deletion of PPI-1, this region should be further probed to determine if a product(s) of this region is(are) involved in the regulation of *mef*(E)/*mel*. Expression of *mef*(E)/*mel* may be affected by osmotic stress or iron levels that are controlled by the PPI-1 operons *phg*ABC and *pia*ABCD, respectively (57, 59), both of which are missing in these high-level macrolide-resistant Mega-only isolates. Alternatively, a protein or RNA regulator encoded on PPI-1 may be involved in suppression of *mef*(E)/*mel* expression to levels observed in all Mega-containing isolates with an intact PPI-1. These high-level expressing Mega isolates are not commonly found but enhanced expression of *mef*(E)/*mel* may also lead to higher levels of resistance to LL-37 and promote enhanced survival during colonization. Additional surveillance for these high-level macrolide-resistant Mega stains is important during genomic analysis of IPD isolates.

Pneumococcal conjugate vaccines are widely used now in developed countries are of increasing focus in developing countries, which should continue to decrease the burden of pneumococcal disease worldwide especially toward reducing the rates of childhood mortality. In the United States, PCV-7 and PCV-13 have been successful in reducing the incidence of IPD and continued use of PCV-13 is needed to sustain the lower incidence of disease. In August 2014, the Advisory Committee on Immunization Practices (ACIP) recommended PCV-13 for routine use in the 65+ year old population (64, 65), which should further reduce the incidence of IPD and MR-IPD in this high-risk population. Some vaccine efforts also seek to target pneumococcal surface proteins that

would lead to the eradication of the pneumococcus from the human nasopharynx, but such efforts should be pursued with caution as complete elimination from the microbiome of children may lead to imbalances and niche availability for another prominent opportunistic pathogen with high rates of antibiotic resistance, such as *S. aureus*. Future pneumococcal vaccine development efforts should seek to increase the number of serotypes in PCVs to further reduce the incidence of pneumococcal disease.

References

1. **Desai AP, Sharma D, Crispell EK, Baughman W, Thomas S, Tunali A, Sherwood L, Zmitrovich A, Jerris R, Satola SW, Beall B, Moore MR, Jain S, Farley MM.** 2015. Decline in pneumococcal nasopharyngeal carriage of vaccine serotypes after the introduction of the 13-valent pneumococcal conjugate vaccine in children in Atlanta, Georgia. Pediatr Infect Dis J **34:**1168-1174.

2. **Sharma D, Baughman W, Holst A, Thomas S, Jackson D, da Gloria Carvalho M, Beall B, Satola S, Jerris R, Jain S, Farley MM, Nuorti JP.** 2013. Pneumococcal carriage and invasive disease in children before introduction of the 13-valent conjugate vaccine: comparison with the era before 7-valent conjugate vaccine. Pediatr Infect Dis J **32:**e45-53.

3. **WHO.** 2007. Pneumococcal conjugate vaccine for childhood immunization—WHO position paper. Wkly Epidemiol Rec **82:**93-104.

4. **Farrell DJ, Couturier C, Hryniewicz W.** 2008. Distribution and antibacterial susceptibility of macrolide resistance genotypes in *Streptococcus pneumoniae*: PROTEKT Year 5 (2003-2004). International Journal of Antimicrobial Agents **31:**245-249.

5. **Hausdorff WP, Bryant J, Paradiso PR, Siber GR.** 2000. Which pneumococcal serogroups cause the most invasive disease: implications for conjugate vaccine formulation and use, part I. Clin Infect Dis **30:**100-121.

6. **Advisory Committee on Immunization Practices.** 2000. Preventing pneumococcal disease among infants and young children. Recommendations of

the Advisory Committee on Immunization Practices (ACIP). MMWR Recomm Rep **49:**1-35.

7. **Rodgers GL, Klugman KP.** 2011. The future of pneumococcal disease prevention. Vaccine **29S:**C43-C48.

8. **CDC.** 2010. Licensure of a 13-valent pneumococcal conjugate vaccine (PCV13) and recommendations for use among children - Advisory Committee on Immunization Practices (ACIP), 2010. MMWR Morb Mortal Wkly Rep **59:**258-261.

9. **Stephens DS, Zughaier SM, Whitney CG, Baughman WS, Barker L, Gay K, Jackson D, Orenstein WA, Arnold K, Schuchat A, Farley MM.** 2005. Incidence of macrolide resistance in *Streptococcus pneumoniae* after introduction of the pneumococcal conjugate vaccine: population-based assessment. Lancet **365:**855-863.

10. **Miller E, Andrews NJ, Waight PA, Slack MP, George RC.** 2011. Herd immunity and serotype replacement 4 years after seven-valent pneumococcal conjugate vaccination in England and Wales: an observational cohort study. Lancet Infect Dis **11:**760-768.

11. **Sahni V, Naus M, Hoang L, Tyrrell GJ, Martin I, Patrick DM.** 2012. The epidemiology of invasive pneumococcal disease in British Columbia following implementation of an infant immunization program: increases in herd immunity and replacement disease. Can J Public Health **103:**29-33.

12. **Haber M, Barskey A, Baughman W, Barker L, Whitney CG, Shaw KM, Orenstein W, Stephens DS.** 2007. Herd immunity and pneumococcal conjugate vaccine: a quantitative model. Vaccine **25:**5390-5398.

13. **Albrich WC, Madhi SA, Lafond KE, Klugman KP.** 2007. Herd immunity after pneumococcal conjugate vaccination. Lancet **370:**218-219; author reply 219-220.

14. **Nurhonen M, Cheng AC, Auranen K.** 2013. Pneumococcal transmission and disease *in silico*: a microsimulation model of the indirect effects of vaccination. PLoS One **8:**e56079.

15. **Beall B, McEllistrem MC, Gertz RE, Jr., Wedel S, Boxrud DJ, Gonzalez AL, Medina MJ, Pai R, Thompson TA, Harrison LH, McGee L, Whitney CG.** 2006. Pre- and postvaccination clonal compositions of invasive pneumococcal serotypes for isolates collected in the United States in 1999, 2001, and 2002. J Clin Microbiol **44:**999-1017.

16. **Elberse KE, van der Heide HG, Witteveen S, van de Pol I, Schot CS, van der Ende A, Berbers GA, Schouls LM.** 2012. Changes in the composition of the pneumococcal population and in IPD incidence in The Netherlands after the implementation of the 7-valent pneumococcal conjugate vaccine. Vaccine **30:**7644-7651.

17. **Gounder PP, Bruce MG, Bruden DJ, Singleton RJ, Rudolph K, Hurlburt DA, Hennessy TW, Wenger J.** 2014. Effect of the 13-valent pneumococcal conjugate vaccine on nasopharyngeal colonization by *Streptococcus pneumoniae*--Alaska, 2008-2012. J Infect Dis **209:**1251-1258.

18. **Lexau CA, Lynfield R, Danila R, Pilishvili T, Facklam R, Farley MM, Harrison LH, Schaffner W, Reingold A, Bennett NM, Hadler J, Cieslak PR, Whitney CG.** 2005. Changing epidemiology of invasive pneumococcal disease among older adults in the era of pediatric pneumococcal conjugate vaccine. JAMA **294:**2043-2051.

19. **Moore MR, Gertz RE, Jr., Woodbury RL, Barkocy-Gallagher GA, Schaffner W, Lexau C, Gershman K, Reingold A, Farley M, Harrison LH, Hadler JL, Bennett NM, Thomas AR, McGee L, Pilishvili T, Brueggemann AB, Whitney CG, Jorgensen JH, Beall B.** 2008. Population snapshot of emergent *Streptococcus pneumoniae* serotype 19A in the United States, 2005. J Infect Dis **197:**1016-1027.

20. **Mahjoub-Messai F, Doit C, Koeck JL, Billard T, Evrard B, Bidet P, Hubans C, Raymond J, Levy C, Cohen R, Bingen E.** 2009. Population snapshot of *Streptococcus pneumoniae* serotype 19A isolates before and after introduction of seven-valent pneumococcal vaccination for French children. J Clin Microbiol **47:**837-840.

21. **Alonso JM, Gilmet G, Rouzic EM, Nassif X, Plotkin SA, Ramsay M, Siegrist CA, Stephens DS, Teyssou R, Vogel U.** 2007. Workshop on vaccine pressure and *Neisseria meningitidis*, Annecy, France, 9-11 March 2005. Vaccine **25:**4125-4129.

22. **Stephens DS.** 2011. Protecting the herd: the remarkable effectiveness of the bacterial meningitis polysaccharide-protein conjugate vaccines in altering transmission dynamics. Trans Am Clin Climatol Assoc **122:**115-123.

23. **Stephens DS.** 2008. Vaccines for the unvaccinated: protecting the herd. J Infect Dis **197:**643-645.

24. **Moore MR, Link-Gelles R, Schaffner W, Lynfield R, Lexau C, Bennett NM, Petit S, Zansky SM, Harrison LH, Reingold A, Miller L, Scherzinger K, Thomas A, Farley MM, Zell ER, Taylor TH, Jr., Pondo T, Rodgers L, McGee L, Beall B, Jorgensen JH, Whitney CG.** 2015. Effect of use of 13-valent pneumococcal conjugate vaccine in children on invasive pneumococcal disease in children and adults in the USA: analysis of multisite, population-based surveillance. Lancet Infect Dis **15:**301-309.

25. **Patrzalek M, Kotowska M, Gorynski P, Albrecht P.** 2015. Indirect effects of a seven-year PCV7/PCV13 mass vaccination programme in children on the incidence of pneumonia among adults: a comparative study based on two Polish cities. Curr Med Res Opin doi:10.1185/03007995.2015.1119676**:**1-25.

26. **Richter SS, Diekema DJ, Heilmann KP, Dohrn CL, Riahi F, Doern GV.** 2014. Changes in pneumococcal serotypes and antimicrobial resistance after introduction of the 13-valent conjugate vaccine in the United States. Antimicrob Agents Chemother **58:**6484-6489.

27. **Waight PA, Andrews NJ, Ladhani NJ, Sheppard CL, Slack MP, Miller E.** 2015. Effect of the 13-valent pneumococcal conjugate vaccine on invasive pneumococcal disease in England and Wales 4 years after its introduction: an observational cohort study. Lancet Infect Dis **15:**629.

28. **Scarbrough Lefebvre CD, Terlinden A, Standaert B.** 2015. Dissecting the indirect effects caused by vaccines into the basic elements. Hum Vaccin Immunother **11:**2142-2157.

29. **O'Brien KL, Dagan R.** 2003. The potential indirect effect of conjugate pneumococcal vaccines. Vaccine **21:**1815-1825.

30. **Hyde TB, Gay K, Stephens DS, Vugia DJ, Pass M, Johnson S, Barrett NL, Schaffner W, Cieslak PR, Maupin PS, Zell ER, Jorgensen JH, Facklam RR, Whitney CG.** 2001. Macrolide resistance among invasive *Streptococcus pneumoniae* isolates. JAMA **286:**1857-1862.

31. **Bergman M, Huikko S, Huovinen P, Paakkari P, Seppala H.** 2006. Macrolide and azithromycin use are linked to increased macrolide resistance in *Streptococcus pneumoniae*. Antimicrob Agents Chemother **50:**3646-3650.

32. **Pokkunuri I, Champney WS.** 2007. Characteristics of a 50S ribosomal subunit precursor particle as a substrate for *erm*E methyltransferase activity and erythromycin binding in *Staphylococcus aureus*. RNA Biol **4:**147-153.

33. **Weisblum B.** 1995. Insights into erythromycin action from studies of its activity as inducer of resistance. Antimicrob Agents Chemother **39:**797-805.

34. **Roberts MC, Sutcliffe J, Courvalin P, Jensen LB, Rood J, Seppala H.** 1999. Nomenclature for macrolide and macrolide-lincosamide-streptogramin B resistance determinants. Antimicrobial Agents and Chemotherapy **43:**2823-2830.

35. **Weisblum B.** 1995. Erythromycin resistance by ribosome modification. Antimicrob Agents Chemother **39:**577-585.

36. **Ambrose KD, Nisbet R, Stephens DS.** 2005. Macrolide efflux in *Streptococcus pneumoniae* is mediated by a dual efflux pump (*mel* and *mef*) and is erythromycin inducible. Antimicrob Agents Chemother **49:**4203-4209.

37. **Chancey ST, Zähner D, Stephens DS.** 2012. Acquired inducible antimicrobial resistance in Gram-positive bacteria. Future Microbiology **7:**959-978.

38. **Tait-Kamradt A, Clancy J, Cronan M, Dib-Hajj F, Wondrack L, Yuan W, Sutcliffe J.** 1997. *mefE* is necessary for the erythromycin-resistant M phenotype in *Streptococcus pneumoniae*. Antimicrob Agents Chemother **41:**2251-2255.

39. **Gay K, Baughman W, Miller Y, Jackson D, Whitney CG, Schuchat A, Farley MM, Tenover F, Stephens DS.** 2000. The emergence of *Streptococcus pneumoniae* resistant to macrolide antimicrobial agents: a 6-year population-based assessment. J Infect Dis **182:**1417-1424.

40. **Hawkins PA, Chochua S, Jackson D, Beall B, McGee L.** 2015. Mobile elements and chromosomal changes associated with MLS resistance phenotypes of invasive pneumococci recovered in the United States. Microb Drug Resist **21:**121-129.

41. **Rudolph K, Bulkow L, Bruce M, Zulz T, Reasonover A, Harker-Jones M, Hurlburt D, Hennessy T.** 2013. Molecular resistance mechanisms of macrolide-resistant invasive *Streptococcus pneumoniae* isolates from Alaska, 1986 to 2010. Antimicrob Agents Chemother **57:**5415-5422.

42. **Kuo W-H.** 2012. Population-based assessment of invasive disease and macrolide resistance from *Streptococcus pneumoniae* in Atlanta from 2007-2010. Master of Science in Public Health. Emory University.

43. **Chancey ST, Agrawal S, Schroeder MR, Farley MM, Tettelin H, Stephens DS.** 2015. Composite mobile genetic elements disseminating macrolide resistance in *Streptococcus pneumoniae*. Front Microbiol **6:**26.

44. **Del Grosso M, Northwood JG, Farrell DJ, Pantosti A.** 2007. The macrolide resistance genes *erm*(B) and *mef*(E) are carried by Tn*2010* in dual-gene *Streptococcus pneumoniae* isolates belonging to clonal complex CC271. Antimicrob Agents Chemother **51:**4184-4186.

45. **Bowers JR, Driebe EM, Nibecker JL, Wojack BR, Sarovich DS, Wong AH, Brzoska PM, Hubert N, Knadler A, Watson LM, Wagner DM, Furtado MR, Saubolle M, Engelthaler DM, Keim PS.** 2012. Dominance of multidrug resistant CC271 clones in macrolide-resistant *Streptococcus pneumoniae* in Arizona. BMC Microbiol **12:**12.

46. **Li Y, Tomita H, Lv Y, Liu J, Xue F, Zheng B, Ike Y.** 2011. Molecular characterization of *erm*(B)- and *mef*(E)-mediated erythromycin-resistant *Streptococcus pneumoniae* in China and complete DNA sequence of Tn*2010*. J Appl Microbiol **110:**254-265.

47. **Quintero B, Araque M, van der Gaast-de Jongh C, Hermans PW.** 2011. Genetic diversity of Tn*916*-related transposons among drug-resistant *Streptococcus pneumoniae* isolates colonizing healthy children in Venezuela. Antimicrob Agents Chemother **55:**4930-4932.

48. **Lyu S, Yao KH, Dong F, Xu BP, Liu G, Wang Q, Shi W, Tong JJ, Shen KL, Yang YH.** 2015. Vaccine Serotypes of *Streptococcus pneumoniae* with High-

Level Antibiotic Resistance Isolated More Frequently 7 Years After the Licensure of PCV7 in Beijing. Pediatr Infect Dis J doi:10.1097/inf.0000000000001000.

49. **Pan F, Han L, Huang W, Tang J, Xiao S, Wang C, Qin H, Zhang H.** 2015. Serotype Distribution, Antimicrobial Susceptibility, and Molecular Epidemiology of *Streptococcus pneumoniae* Isolated from Children in Shanghai, China. PLoS One **10:**e0142892.

50. **Gay K, Stephens DS.** 2001. Structure and dissemination of a chromosomal insertion element encoding macrolide efflux in *Streptococcus pneumoniae*. J Infect Dis **184:**56-65.

51. **Chancey ST, Bai X, Kumar N, Drabek EF, Daugherty SC, Colon T, Ott S, Sengamalay N, Sadzewicz L, Tallon LJ, Fraser CM, Tettelin H, Stephens DS.** 2015. Transcriptional attenuation controls macrolide inducible efflux and resistance in *Streptococcus pneumoniae* and in other Gram-positive bacteria containing *mef*/*mel*(*msr*(D)) elements. PLoS One **10:**e0116254.

52. **Del Grosso M, Scotto d'Abusco A, Iannelli F, Pozzi G, Pantosti A.** 2004. Tn*2009*, a Tn*916*-like element containing *mef*(E) in *Streptococcus pneumoniae*. Antimicrob Agents Chemother **48:**2037-2042.

53. **Del Grosso M, Camilli R, Libisch B, Fuzi M, Pantosti A.** 2009. New composite genetic element of the Tn*916* family with dual macrolide resistance genes in a *Streptococcus pneumoniae* isolate belonging to clonal complex 271. Antimicrob Agents Chemother **53:**1293-1294.

54. **Gupta P, Sothiselvam S, Vazquez-Laslop N, Mankin AS.** 2013. Deregulation of translation due to post-transcriptional modification of rRNA explains why *erm* genes are inducible. Nat Commun **4:**1984.

55. **Zhou W, Yao K, Zhang G, Yang Y, Li Y, Lv Y, Feng J.** 2014. Mechanism for transfer of transposon Tn*2010* carrying macrolide resistance genes in *Streptococcus pneumoniae* and its effects on genome evolution. J Antimicrob Chemother **69:**1470-1473.

56. **Lee JY, Song JH, Ko KS.** 2010. Recombination rates of *Streptococcus pneumoniae* isolates with both *erm*(B) and *mef*(A) genes. FEMS Microbiology Letters **309:**163-169.

57. **Brown JS, Gilliland SM, Holden DW.** 2001. A *Streptococcus pneumoniae* pathogenicity island encoding an ABC transporter involved in iron uptake and virulence. Mol Microbiol **40:**572-585.

58. **Harvey RM, Stroeher UH, Ogunniyi AD, Smith-Vaughan HC, Leach AJ, Paton JC.** 2011. A variable region within the genome of *Streptococcus pneumoniae* contributes to strain-strain variation in virulence. PLoS One **6:**e19650.

59. **Brown JS, Gilliland SM, Basavanna S, Holden DW.** 2004. phgABC, a three-gene operon required for growth of *Streptococcus pneumoniae* in hyperosmotic medium and *in vivo*. Infect Immun **72:**4579-4588.

60. **Brown JS, Gilliland SM, Spratt BG, Holden DW.** 2004. A locus contained within a variable region of pneumococcal pathogenicity island 1 contributes to virulence in mice. Infect Immun **72:**1587-1593.

61. **Simell B, Auranen K, Kayhty H, Goldblatt D, Dagan R, O'Brien KL.** 2012. The fundamental link between pneumococcal carriage and disease. Expert Rev Vaccines **11:**841-855.

62. **Zähner D, Zhou X, Chancey ST, Pohl J, Shafer WM, Stephens DS.** 2010. Human antimicrobial peptide LL-37 induces MefE/Mel-mediated macrolide resistance in *Streptococcus pneumoniae*. Antimicrob Agents Chemother **54:**3516-3519.

63. **Ambrose KD, Nisbet R, Stephens DS.** 2005. Macrolide efflux in *Streptococcus pneumoniae* is mediated by a dual efflux pump (*mel* and *mef*) and is erythromycin inducible. Antimicrobial Agents and Chemotherapy **49:**4203-4209.

64. **Tomczyk S, Bennett NM, Stoecker C, Gierke R, Moore MR, Whitney CG, Hadler S, Pilishvili T.** 2014. Use of 13-valent pneumococcal conjugate vaccine and 23-valent pneumococcal polysaccharide vaccine among adults aged >/=65 years: recommendations of the Advisory Committee on Immunization Practices (ACIP). MMWR Morb Mortal Wkly Rep **63:**822-825.

65. **Bonten MJ, Huijts SM, Bolkenbaas M, Webber C, Patterson S, Gault S, van Werkhoven CH, van Deursen AM, Sanders EA, Verheij TJ, Patton M, McDonough A, Moradoghli-Haftvani A, Smith H, Mellelieu T, Pride MW, Crowther G, Schmoele-Thoma B, Scott DA, Jansen KU, Lobatto R, Oosterman B, Visser N, Caspers E, Smorenburg A, Emini EA, Gruber WC, Grobbee DE.** 2015. Polysaccharide conjugate vaccine against pneumococcal pneumonia in adults. N Engl J Med **372:**1114-1125.

Appendix A: Subversion of host recognition and defense systems by *Francisella* spp.

Crystal L. Jones,[a] Brooke A. Napier,[a] Timothy R. Sampson,[a] Anna C. Llewellyn,[a] Max R. Schroeder,[a] and David S. Weiss[b,c]

Department of Microbiology and Immunology, Microbiology and Molecular Genetics Program,[a] Emory Vaccine Center,[b] and Division of Infectious Diseases, Department of Medicine,[c] Emory University, Atlanta, Georgia, USA

Published in

Microbiology and Molecular Biology Reviews

June 2012 Volume 76 Number 2 pages 383-404

M.R.S. contributed to the development of the review and wrote the introduction and assisted in editing of the paper.

MMBR
Journals.ASM.org

Subversion of Host Recognition and Defense Systems by *Francisella* spp.

Crystal L. Jones,[a] Brooke A. Napier,[a] Timothy R. Sampson,[a] Anna C. Llewellyn,[a] Max R. Schroeder,[a] and David S. Weiss[b,c]

Department of Microbiology and Immunology, Microbiology and Molecular Genetics Program,[a] Emory Vaccine Center,[b] and Division of Infectious Diseases, Department of Medicine,[c] Emory University, Atlanta, Georgia, USA

INTRODUCTION

Francisella tularensis was first identified as the causative agent of a fatal plague-like disease in a population of ground squirrels in Tulare County, CA, in 1911 (147). Originally called *Bacterium tularense*, it was later renamed *Francisella tularensis* in honor of Edward Francis, who spent his career extensively studying and characterizing the transmission and growth of this bacterium (209). Although it causes disease in squirrels, rabbits, and numerous other mammals, no animal has been identified as a reservoir. Instead, the reservoir may be freshwater or amoebae living therein. As there is no person-to-person spread, *F. tularensis* is acquired primarily by humans via arthropod vectors or zoonotic transmission, though it can also be transmitted by inhalation of aerosolized bacteria or ingestion of contaminated food or water (2). Inhalation of *F. tularensis* causes the most severe infections, and only 10 bacteria can lead to a potentially fatal disease. This high infectivity, along with its ease of aerosolization, have led to its history of weaponization (209).

Francisella species are endemic only in the Northern Hemisphere. *F. tularensis* subsp. *tularensis* (*F. tularensis*) is the most virulent etiologic agent of tularemia in humans and is the primary disease-causing *Francisella* species in North America. *Francisella tularensis* subsp. *holarctica* (*F. holarctica*) is responsible for the majority of reported cases of tularemia in Europe and Asia. The current vaccine is an attenuated live vaccine strain (LVS) derived from virulent *F. holarctica* by serial passage. LVS causes a very mild infection in humans but can cause a lethal infection in mice and is therefore commonly used as a model to study *Francisella* pathogenesis. The closely related *Francisella novicida* species rarely causes disease in humans, though some cases have been documented (31, 125). However, *F. novicida* is highly virulent in mice, has over 98% identity to *F. tularensis* at the DNA level (188), shares many of the same virulence genes (43), and is also used as a model system to study *Francisella* virulence. Finally, *Francisella tularensis* subsp. *mediasiatica* is a species of intermediate virulence in humans and is found in Central Asia, while *Francisella philomiragia* and *Francisella noatunensis* can cause infections in aquatic organisms, including wild and farmed fish (57). Throughout this paper we will refer to "*Francisella*" when discussing general characteristics shared by numerous species and subspecies and will otherwise refer to specific species and subspecies by name. It is important to note that there are significant differences between highly virulent and less pathogenic strains in terms of the requirements of genes for pathogenesis, susceptibilities to host defenses, and the types of immune responses induced. Therefore, caution must be used when interpreting results from experiments using less pathogenic species and drawing conclusions about the characteristics of highly virulent species.

F. tularensis subspecies are the etiological agents of the disease tularemia, also known as rabbit fever. Tularemia is characterized by a 3- to 5-day incubation period (209) during which the bacteria replicate almost "silently" in macrophages and other types of host cells. The eventual release of bacteria from these cells may coincide with the presentation of flu-like symptoms. There are several manifestations of tularemia, each dependent on the route of acquisition (159). The most common form of tularemia is ulceroglandular disease, which can result from insect bites or from contact with infected animal tissues following mechanical damage to the skin. A cutaneous ulcer develops at the site of infection, and

Address correspondence to David S. Weiss, david.weiss@emory.edu.
C.L.J., B.A.N., and T.R.S. contributed equally to this article.

doi:10.1128/MMBR.05027-11

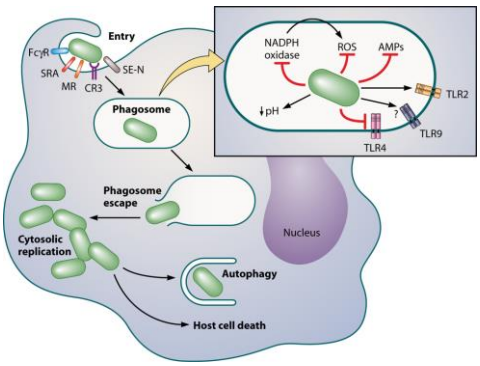

FIG 1 Stages of *Francisella* pathogenesis in the macrophage. *Francisella* can be detected by multiple macrophage receptors (see "Mechanisms of Entry and Fate of Intracellular *Francisella*" below) and is engulfed by a unique pseudopod loop mechanism. It then traffics to an early phagosome called the *Francisella*-containing phagosome (FCP). *Francisella* uses multiple mechanisms to evade host defenses in this harsh environment (inset). *Francisella* blocks the NADPH oxidase and also detoxifies reactive oxygen species (ROS). It can also resist the action of antimicrobial peptides (AMPs). *Francisella* does not signal through TLR4 but does activate TLR2 and may induce TLR9 signaling. *Francisella* then escapes the FCP to replicate within the cytosol. Subsequently, *Francisella* associates with autophagosomes, although the outcome of this interaction is unknown. *Francisella* can also induce host cell death.

bacteria drain to lymph nodes, subsequently causing a systemic infection. Less common forms of the disease include pneumonic, oculoglandular, and oropharyngeal tularemia. Streptomycin or doxycycline is indicated for treatment. Tularemia may be fatal; however, survivors gain robust immunity that has been found to last for up to 30 years (79).

Upon infection, *Francisella* initially comes into contact with extracellular defenses such as complement, antibody, and cationic antimicrobial peptides (28, 29, 51, 190). Binding of these components to bacteria directly or indirectly leads to lysis and killing (189). Therefore, *Francisella* uses multiple surface structures and outer membrane modifications (capsule, lipopolysaccharide [LPS] O antigen, modifications that increase surface charge, etc.) to resist these components and block killing. In addition, this prevents structural damage that would release proinflammatory bacterial components capable of initiating a strong immune response. *Francisella* also enters host cells as an efficient way of evading extracellular defenses.

After engulfment by phagocytic cells, including macrophages, *Francisella* is taken up into phagosomes that contain an array of toxic antimicrobials aimed at degrading the bacteria (Fig. 1). However, this pathogen has an equally diverse cache of defenses to counteract host antimicrobials. These once again prevent not only killing but also the release of proinflammatory bacterial components that could be recognized by host innate immune receptors (including Toll-like receptors [TLRs]) that stimulate inflammatory responses. Furthermore, similarly to entering host cells to avoid extracellular antimicrobials, *Francisella* escapes the phagosome to avoid phagosomal antimicrobials and, importantly, reach the cytosol, where it can replicate (Fig. 1). The cytosol is also, however, guarded by innate recognition and defense systems (including the inflammasome) with which the bacteria must contend. In order to replicate in this host compartment, *Francisella* must also obtain the nutrients required to sustain its rapid cell division and actively counteract host defenses aimed at limiting nutrient availability.

In addition to subverting extracellular and intracellular defenses to facilitate replication, *Francisella* suppresses the activation of adaptive immune defenses that have the capability of destroying infected host cells. For example, CD8 T cells can directly lyse infected host cells, clearing these havens for bacterial replication. They and other cells also secrete the cytokine gamma interferon (IFN-γ), which can activate strong defenses in host cells, allowing them to resist *Francisella* replication. Therefore, *Francisella* uses several strategies to skew adaptive responses and block IFN-γ signaling to help preserve its replication niche in infected host cells (35, 119, 166, 189). Here we review the multitude of ways in which *Francisella* subverts host defenses at each of the stages of intracellular infection as well as its effects on adaptive immune responses.

SUBVERSION OF HOST DEFENSES

Following its transmission, *Francisella* must resist extracellular host defenses prior to entry into host cells. Furthermore, there is evidence that a potentially important extracellular phase exists after the initial stage of infection (87, 136, 239). Up to 75% of viable LVS and *F. tularensis* SchuS4 bacteria in the blood are present extracellularly at multiple time points following intranasal and intradermal murine infection (87). This finding was confirmed in studies with *F. novicida* in which ~80% of viable bacteria in the blood were present extracellularly in serum (239). Of important note, these extracellular *Francisella* organisms are still infectious, suggesting that this extracellular phase may play an important role in dissemination from the site of infection (239). These data highlight the fact that *Francisella* must subvert extracellular host defenses to initiate infection and likely to spread and cause disease at later stages as well.

Complement and Antibody

During extracellular phases of infection, *Francisella* must be able to subvert, resist, or evade killing by a plethora of antimicrobial defenses. One major extracellular defense is the complement system that is present and active in mammalian blood. The complement system consists of an intricately regulated cascade of extracellular signaling proteins that can be triggered by the recognition of a microbe, ultimately leading to its lysis by a pore-forming complex or promoting uptake and killing by phagocytes (190). Throughout the process of complement activation, host signaling molecules which act to promote inflammation and recruit phagocytes and T cells to the site of infection are formed. Furthermore, inhibition of complement activation is necessary to maintain the integrity and viability of the pathogen, as well as to prevent the release of immunostimulatory bacterial components (pathogen-associated molecular patterns [PAMPs]) that would activate an enhanced immune response.

Complement activation is a complex process and is described in detail in a number of reviews (88, 190). Briefly, this process is initiated by the binding of lectins or antibodies to bacteria, which subsequently promote the recruitment and activation of the complement factors C1 through C4. This leads to the generation of the C3 convertase, a central signaling molecule in the complement cascade. When C3 is cleaved to C3a (an anaphylatoxin) and C3b,

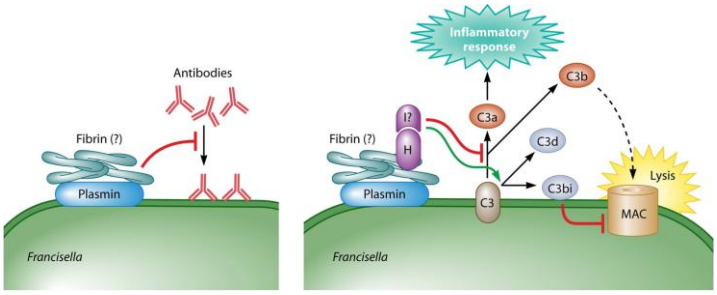

FIG 2 Complement Evasion by *Francisella*. Antibodies (Abs) can bind to the bacterial surface (left panel), leading to binding of complement component C3 (right panel), triggering activation of the complement cascade and generation of C3a, an inflammatory anaphylatoxin, and C3b. C3b ultimately leads to the formation of the membrane attack complex (MAC) and lysis of the bacterial cell. *Francisella* counteracts these defenses by binding host plasmin, which inhibits antibody binding (left panel) and thus complement activation. *Francisella* also binds host factor H, which inhibits C3 cleavage to C3a and C3b and instead acts with host factor I to create the complement-inhibitory molecules C3d and C3bi. This skews the complement cascade from promoting MAC formation and lysis to facilitating phagocytosis. Factor H binding may be promoted by fibrinogen, which is converted to fibrin and is known to bind plasmin, but this has yet to be demonstrated.

the canonical complement cascade continues, ultimately leading to bacterial lysis (Fig. 2). Briefly, lysis occurs when C3b, bound to the bacterial envelope, interacts with other complement factors to signal for the formation of the membrane attack complex (MAC). The MAC forms a pore in the bacterial envelope, leading to loss of membrane integrity and osmotic potential, in turn leading to lysis of the bacterium.

Although C3 binds to the bacteria, *Francisella* blocks complement activation by cleaving this protein into the smaller inhibitory fragments C3bi and C3d (Fig. 2) (28, 29, 51). Generation of these fragments prevents the ability of C3 to signal toward MAC formation. The exact mechanism of C3 inactivation on the *Francisella* surface is not yet known; however, host factor H readily binds the *Francisella* cell surface (29) and can inhibit formation of the C3 convertase (Fig. 2). Importantly, factor H can also serve as a cofactor for host factor I-mediated cleavage of C3b to C3bi and C3d. Despite the evidence that factor H binds *Francisella*, factor I (which is necessary for C3b cleavage) has not yet been shown to interact directly with the bacterial surface. Factor I may interact only transiently, or if it does not bind, a *Francisella*-encoded factor may be responsible for C3b cleavage to C3bi and C3d.

Generation of C3bi and C3d is not only responsible for inhibiting subsequent MAC formation but is also important in promoting opsonophagocytosis. By binding complement receptor 3 (CR3) on host phagocytes, C3bi and C3d allow *Francisella* to enter host cells, further promoting escape from extracellular antimicrobials such as complement, antibody, and antimicrobial peptides (20, 28) and facilitating entry of the bacteria into an intracellular replicative niche. It should be noted, however, that uptake mediated by C3bi/C3d and CR3 leads to limited *Francisella* replication compared to uptake by nonopsonic receptors (see "Mechanisms of Entry and Fate of Intracellular *Francisella*" below for a more detailed discussion). Therefore, *Francisella* encounters complement upon infection and can prevent complement-mediated lysis by converting C3 into C3bi and C3d. This routes *Francisella* to a nonoptimal replicative pathway within host cells, but it is nonetheless an effective way to subvert extracellular antimicrobials and promote intracellular replication.

Francisella's complement-inhibiting activity is highly dependent on the O-antigen oligosaccharide present on LPS on the surface of the bacterial cell (51, 192, 211). Mutants lacking O antigen, either by random selection for rough or gray variants or by targeting *wbt* locus genes necessary for O-antigen production, are significantly more sensitive to complement than their wild-type counterparts (51, 192, 211). Interestingly, the relative importance of O antigen in complement resistance differs between *F. novicida* and *F. tularensis*. *F. novicida wbt* mutants are more than 2,000-fold more sensitive to serum than wild-type bacteria, while *F. tularensis* mutants are only 4-fold more sensitive (221). This may be due to the structural differences in O-antigen tetrasaccharide oligomers between these species (221) and/or additional O-antigen-independent mechanisms of complement resistance in *F. tularensis* that have not yet been elucidated.

The sensitivity of *Francisella* O-antigen mutants to complement is due to increased binding of complement factors compared to that in the wild type and an inability to catalyze the cleavage of C3 to C3bi (51, 192, 211). This results in the binding of complement factors C5 to C9, which form the MAC and do not bind wild-type *Francisella*, ultimately causing lysis of the mutant bacteria and decreased survival in serum (29, 51, 192, 211). Therefore, the presence of the O antigen is vital not only for regulating the quantity of complement factors which bind to the *Francisella* envelope but also for subverting the ability of bound complement components to mediate lysis of the bacteria.

The importance of maintaining resistance to complement lysis is demonstrated by the fact that complement-sensitive mutants are also severely attenuated *in vivo*. *Francisella* strains with mutations in the *wbt* locus are attenuated during infection of both macrophages (130, 135, 221) and mice (129, 153, 204, 221, 232). Furthermore, mutants lacking genes necessary for O-antigen production that are outside the *wbt* locus are also attenuated for intracellular replication and *in vivo* virulence compared to the wild type (130).

Additionally, strains with mutations in genes predicted to be important for capsule production are also significantly attenuated *in vitro* and *in vivo* (throughout this paper, "*in vitro*" refers to

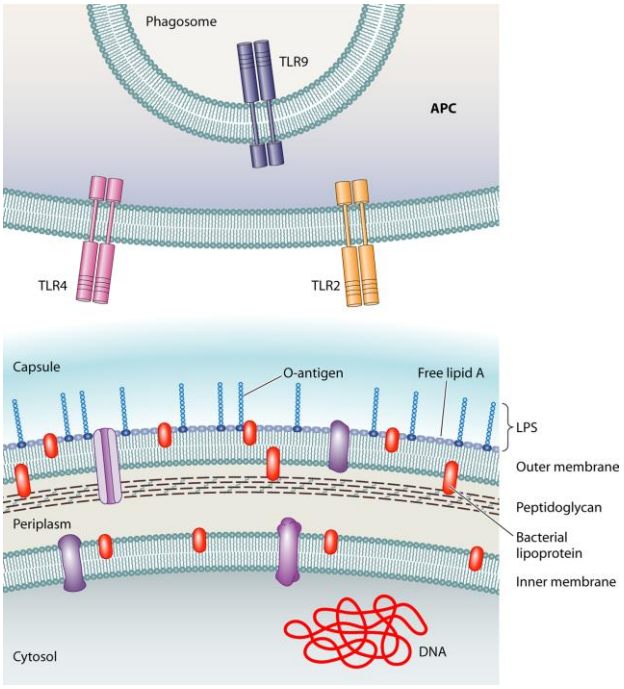

FIG 3 Shielding of inflammatory PAMPs in *Francisella*. *Francisella* modifies and limits the release of its inflammatory components (PAMPs) that can be recognized by pattern recognition receptors, such as TLRs, expressed by antigen-presenting cells (APC). *Francisella* bacterial lipoproteins (BLPs) and DNA (shown in red) are PAMPs with inflammatory activity, while the capsule, LPS, free lipid A, and membrane phospholipids do not elicit an inflammatory response. *Francisella* modifies its LPS and free lipid A such that these PAMPs do not activate host TLR4. It is unclear whether *Francisella* peptidoglycan (PGN) has inflammatory activity (represented in brown). Membrane proteins that are not BLPs and are not as a class considered PAMPs are shown in purple. The capsule and LPS O antigen provide resistance to antimicrobials such as complement and antimicrobial peptides, preventing damage to the bacterial membranes, which would result in the release of immunostimulatory BLPs and DNA. In addition to providing resistance to the damaging effects of antimicrobials, the capsule and O antigen may also serve as physical barriers to the release of PAMPs into the environment.

infection of host cells in culture, while "*in vivo*" refers to infection of mammalian hosts such as mice) (110, 130, 153, 232). This is important to note, since recent evidence has suggested that the O antigen and capsule of *Francisella* are structurally similar, with the capsule consisting of a polymer of O-antigen tetrasaccharide subunits (9) as well as a glycoprotein component termed a "capsule-like complex" (18). As such, some mutants deficient in LPS O-antigen production are also impaired in the production of capsule (9, 130), including specific *wbt* operon mutants (*wbtA*, *wbtC*, *wbtM*, and *wbtI*). *wbtK* and *lpxL* mutants lose the ability to synthesize LPS O antigen but maintain the polysaccharide capsule (9). Conversely, the *F. tularensis* genes *FTT_0673* and *FTT_0674* are necessary for capsule production but dispensable for O-antigen production (9). However, to the best of our knowledge, the ability of these mutants to resist complement has not been established. Testing the level of complement resistance in these mutants would allow the elucidation of which structure(s) is required. Thus, the current literature suggests that complement resistance in *Francisella* depends on O antigen, an O-antigen polysaccharide capsule, or both, as well as other potential factors that have yet to be elucidated.

Interestingly, the *Francisella* genome is known to contain an operon with similarity to the *Bacillus* species *capBCA* genes necessary for the production of a poly-D-glutamic acid capsule (71, 110, 153). However, to date, no poly-D-glutamic acid has been identified in *Francisella*. Although *Francisella capB* mutants are attenuated during murine infection, an LVS *capB* mutant did not exhibit increased sensitivity to serum (110, 213). Furthermore, it is not known whether CapB is required for production of the O-antigen capsule, the glycoprotein capsule-like complex, or a different bacterial envelope structure.

In addition to their sensitivity to complement, recent work has demonstrated that LPS O-antigen and capsule mutants are significantly more proinflammatory than wild-type cells (153, 171). An important, but perhaps overlooked, aspect of O-antigen and capsule function may be the ability of these large surface structures to mask and prevent the release of PAMPs on the *Francisella* surface (Fig. 3). In support of this hypothesis, LPS O-antigen mutants

release more DNA into the cytosol of host cells during infection, leading to an increase in host inflammation and proinflammatory cell death (discussed further in "Cytosolic Defenses" below) (171). However, it is unclear whether this release of bacterial DNA (a PAMP) is due to a general instability of the *Francisella* envelope or an increased sensitivity to serum components and/or other antimicrobials. Taken together, these data highlight the important role that polysaccharide surface structures play in preventing host recognition of *Francisella* and virulence.

In addition to the strategies described above, some bacteria use additional mechanisms to inhibit complement activation. For example, *Streptococcus pneumoniae* uses its surface M protein to bind host fibrinogen, a protein that can bind the complement inhibitor factor H, thus allowing fibrinogen-coated bacteria to inhibit complement activation (233). To our knowledge, no study to date has demonstrated that *Francisella* is capable of binding fibrinogen. However, recent work has shown that *Francisella* binds host plasminogen on its surface, which is in turn converted to plasmin (54), which can bind fibrinogen (137). Thus, although not yet directly demonstrated, this may be the mechanism used by *Francisella* to bind and sequester factor H, contributing to complement resistance (Fig. 2). Plasmin can also degrade soluble antibody, allowing *Francisella* to prevent antibody-mediated complement activation (59). Highlighting the potential importance of plasmin binding in pathogenesis, *F. tularensis* binds plasmin while the attenuated LVS strain does not, and LVS is therefore unable to evade this pathway. Together, *Francisella* utilizes LPS O antigen, its O-antigen polysaccharide capsule, and plasmin in order to subvert complement activation, promoting extracellular bacterial survival and preventing the release of proinflammatory PAMPs that would subsequently initiate a strong host immune response leading to clearance of the infection.

Antimicrobial Peptides

In addition to complement, the host produces a variety of other antimicrobials, most notably cationic antimicrobial peptides such as defensins and cathelicidins (42). Positively charged antimicrobial peptides, capable of disrupting the negatively charged bacterial membrane, are present extracellularly on mucosal surfaces as well as within macrophages and neutrophils. Upon infection, the bacteria first encounter either the epithelium of the lungs (after inhalation) or the skin (upon arthropod bites or contact with infected animal tissue). Subsequently, macrophages and neutrophils are among the first cell types the bacteria enter. Therefore, resistance to cationic antimicrobial peptides is likely a critical component of early pathogenesis.

Three defensin antimicrobial peptides (hBD-1, hBD-2, and hBD-3) are present in the human airway mucosa (42). The 50% effective concentration (EC_{50}) (the concentration that kills 50% of the bacteria) for hBD-1 and hBD-2 against *F. novicida* is higher than that against other bacteria such as *Pseudomonas*, *Staphylococcus*, and *Escherichia coli* (roughly 100-fold greater for hBD-1 and 10-fold greater for hBD-2) (108). Accordingly, hBD-1 and hBD-2 are ineffective at killing *F. novicida* (98), and at sites of infection, it is estimated that hBD-1 and hBD-2 concentrations are below the levels required for killing (198). It is likely that even though *in vitro* infection of lung epithelial cells with *F. novicida* induces the expression of hBD-1 and hBD-2 (10- and 40-fold, respectively), these levels are still too low to effectively kill the bacteria. hBD-3, however, is effective at killing *F. novicida* (in broth culture) (98), but it is present at levels only about 2-fold higher than the EC_{50} (198), and infection does not further induce its expression (98). Therefore, it is likely that defensins play very little role in host defense against *Francisella*, due to its high resistance to hBD-1 and hBD-2 as well as its lack of induction of hBD-3 during infection.

Similar to the case for hBD-1 and hBD-2, *F. novicida* significantly induces the production of the cathelicidin LL-37 in lung epithelial cells *in vitro* (5). Furthermore, it is estimated that at sites of infection, LL-37 peptide concentrations average approximately 25 μg/ml (198), about 100-fold higher than the EC_{50} for *F. novicida* (5). Similar to its evasion of complement, *Francisella* must likely resist the action of LL-37 and presumably other host antimicrobials (such as hBD-1 and hBD-2) to prevent not only lysis and death but also the release of PAMPs that would subsequently trigger a proinflammatory response.

The literature to date has described at least two different mechanisms by which *Francisella* can either resist or evade the action of host antimicrobials: (i) by altering the charge of its surface and thus being able to use electrostatic interactions to repel cationic antimicrobial peptides and (ii) by encoding a number of efflux systems that are necessary for resistance to antimicrobials as well as for virulence *in vivo*.

Francisella modifies its lipid A, an outer membrane glycolipid structure that is a component of LPS but is also present in *Francisella* in a "free" form which lacks the canonical LPS core and O-antigen sugars (discussed in greater detail in "Toll-Like Receptors" below) (230). The bacteria remove the negatively charged phosphate groups from the 1 and 4′ positions of the lipid A portion of complete LPS (Fig. 4), which serves to increase the overall charge of the bacterial surface and repel cationic antimicrobials (94). Mutants that do not remove the 4′ phosphate are much more sensitive to cationic antimicrobial peptides and are highly attenuated *in vivo* (229). This attenuation is attributed to the increased susceptibility to cationic antimicrobials, which leads to membrane damage and the release of higher levels of PAMPs, resulting in a greater proinflammatory response, including increased neutrophil recruitment that results in clearance of the bacteria (210, 229).

Preventing interactions with cationic host antimicrobials is one of *Francisella*'s first lines of defense against the host immune response. However, increased surface charge does not prevent all antimicrobials from acting on the bacterial cell, particularly uncharged or negatively charged antimicrobials that could potentially be attracted more efficiently. *Francisella*, like many other bacteria, including *Neisseria* (95), *Pseudomonas* (179), and *Salmonella* (23), encodes at least one known multidrug efflux pump that allows resistance to a number of different antimicrobials and detergents, the AcrAB/TolC efflux pump. In addition, other predicted efflux pump proteins have been identified in screens for *Francisella* virulence genes, including *FTN_1066*, *FTN_1217*, *FTN_1277*, *FTN_1654*, and *FTN_1657* (130, 140, 232). While the exact functions of these predicted efflux proteins are unknown, they may play a role complementary to the known functions of the AcrAB/TolC efflux pump.

The AcrAB inner membrane efflux platform (30), coupled with the TolC outer membrane transporter (91, 178), forms a pump that facilitates the active efflux of toxic compounds and detergents from the bacteria, preventing their antimicrobial action. This multidrug efflux pump is important for *Francisella* resistance to β-lactams, tetracyclines, aminoglycosides, quinolones, detergents

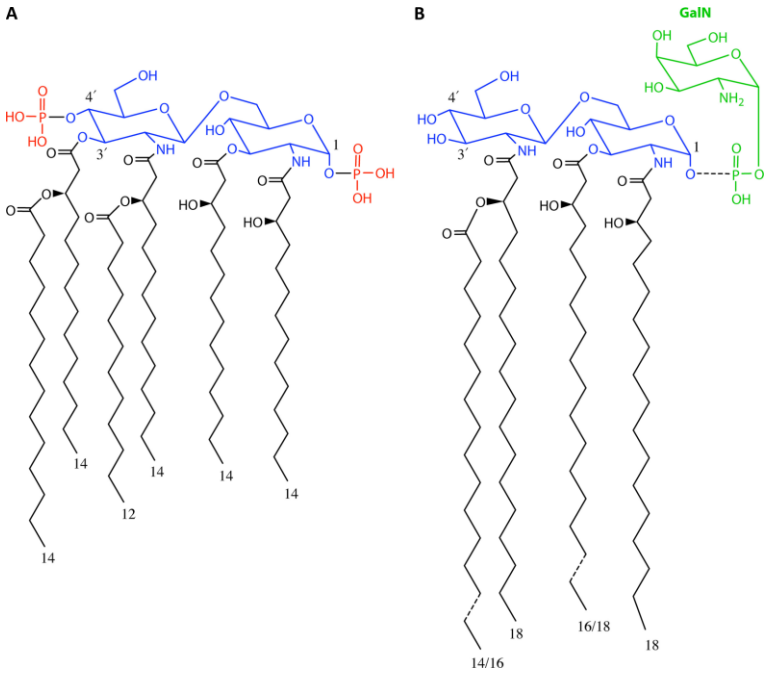

FIG 4 *E. coli* and *Francisella* lipid A structures. The structures of the *E. coli* lipid A moiety (A) and free lipid A from *Francisella* species (B) are shown. For both structures, the sugar backbone is highlighted in blue and acyl chains are represented in black, with numbers denoting length. Phosphate groups at the *E. coli* lipid A 4′ and 1 positions (absent from lipid A of full-length *Francisella* LPS) are highlighted in red. *Francisella* free lipid A contains the phosphate at the 1 position and is modified with galactosamine (GalN) (in green).

(notably bile salts), and antimicrobial dyes (30, 91). Highlighting the importance of this system in pathogenesis, mutants with mutations in pump components are severely attenuated *in vivo* (30, 91, 178). While the AcrAB/TolC system is known to provide resistance against host antimicrobial peptides in bacteria (95) and it is assumed that *Francisella* mutants would be more sensitive to host-derived antimicrobials during infection, to the best of our knowledge this has not been directly tested.

Interestingly, TolC mutants stimulate an increased proinflammatory response compared to that of wild-type *Francisella* (178). This may be due to increased sensitivity to antimicrobials *in vivo* leading to increased PAMP release or to a general membrane instability defect eventually leading to PAMP release. Furthermore, since TolC has been shown to be involved in the secretion of virulence factors in other bacteria such as *Pseudomonas* (100) and *E. coli* (227), it cannot be ruled out that it may play a similar role in *Francisella* pathogenesis, accounting for some of the virulence defects exhibited by mutants lacking this protein.

Another important aspect of antimicrobial peptide resistance in *Francisella* is the potential contribution of the O antigen and/or capsule. The *Klebsiella* capsule prevents interaction with antimicrobial peptides (39), and the O antigen of *Salmonella* has been shown to act similarly (212). However, to the best of our knowledge, whether these systems contribute to *Francisella* resistance is not yet known. Together, the ability of *Francisella* to resist and evade the action of complement, antibody, and antimicrobial peptides within the host allows it not only to survive but also to maintain the integrity of its envelope, preventing the release of proinflammatory molecules that would induce a host response and promoting its virulence.

Mechanisms of Entry and Fate of Intracellular *Francisella*

As mentioned above, one mechanism used by bacteria to evade extracellular defenses is simply to enter host cells. Macrophages are sentinels of infection and are one of the first cell types to encounter *Francisella* (97). Upon initial contact with macrophages, *Francisella* binds to host receptors and is taken up via spacious, asymmetrical protrusions called pseudopod loops (52). Ultrastructural analyses have shown that pseudopod loops are formed during uptake of unopsonized and opsonized *Francisella* and are present in multiple cell types (52). This novel phenomenon differs from other described bacterial uptake mechanisms, including coiling phagocytosis seen at the surface of phagocytes during *Legionella pneumophila* infection and conventional phagocytosis observed during infection with multiple bacterial and viral species (102, 103, 199, 200).

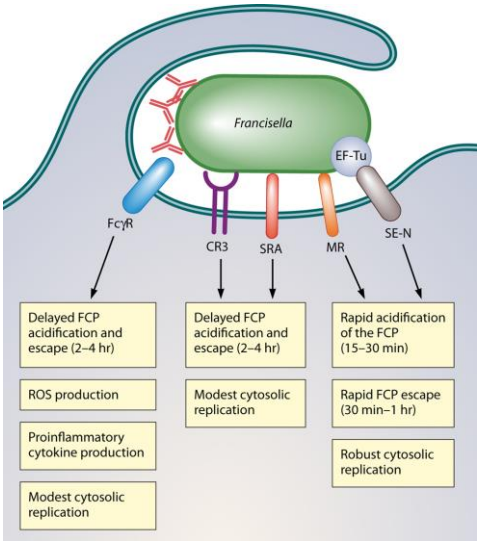

FIG 5 Intracellular fates of *Francisella* after uptake by different macrophage receptors. Antibody-opsonized *Francisella* is taken up via the FcγR, leading to increased ROS production and induction of proinflammatory cytokines, delayed FCP acidification and bacterial escape (2 to 4 h) from the phagosome, and only moderate levels of cytosolic replication. Uptake of serum (complement)-opsonized *Francisella* is mediated mainly by complement receptor 3 (CR3) and scavenger A receptors (SRA), which lead to slowed FCP acidification and phagosomal escape (2 to 4 h) and result in modest cytosolic replication. Lastly, uptake of unopsonized *Francisella* is mediated by the mannose receptor (MR) and surface-exposed nucleolin (SE-N), leading to rapid acidification (15 to 30 min) and escape from the FCP (30 min to 1 h) and robust cytosolic replication.

Furthermore, *Francisella* LVS can recruit host cell membrane cholesterol-rich lipid domains, or "lipid rafts," with caveolin-1 for successful entry into macrophages (217). Depletion of plasma membrane cholesterol or removal of glycosylphosphatidylinositol (GPI)-anchored proteins results in a severe decrease in *Francisella* uptake and subsequent intracellular replication (217). Interestingly, in nonphagocytic cells such as hepatocytes, LVS and *F. novicida* use cholesterol-rich lipid domains dependent on clathrin, not caveolin-1, for entry (123). Thus, *Francisella* uses multiple mechanisms for uptake into phagocytic and nonphagocytic cells.

The efficiency of *Francisella* uptake by macrophages depends in large part on whether the bacteria are opsonized, since serum- or antibody-opsonized bacteria are taken up by macrophages at 10-fold-higher levels than unopsonized bacteria (90). While this increased efficiency of uptake helps the bacteria evade extracellular defenses, it comes at a cost since the intracellular fates of opsonized and unopsonized bacteria are different (Fig. 5). Opsonized bacteria escape the phagosome with delayed kinetics and replicate modestly in the host cell cytosol (28, 90, 176, 202). In contrast, unopsonized *Francisella* escapes the phagosome rapidly and replicate robustly in the cytosol (17, 202). Therefore, the route of uptake has a profound impact on the outcome of infection, and as discussed below, *Francisella* uses several strategies to promote entry mechanisms that favor its survival and replication.

Uptake of unopsonized *Francisella* depends largely on the mannose receptor (MR). When the MR is blocked with antibody or mannan, uptake of unopsonized *Francisella* decreases by more than 50% (17, 202). Unopsonized *Francisella* taken up by the MR escapes the phagosome rapidly and replicate to high numbers. In addition, the MR is known to induce relatively weak inflammatory responses compared to those induced by other phagocytic receptors (225). All of these outcomes favor the bacteria, and therefore, MR-mediated uptake makes host cells more permissive for *Francisella* replication, similar to what is observed during uptake of *Mycobacterium tuberculosis* (113).

In contrast, serum-opsonized bacteria are bound by complement, leading to uptake mediated in large part by complement receptor 3 (CR3). Ablation of CR3 ($CR3^{-/-}$ macrophages) results in at least a 50% decrease in uptake of serum-opsonized LVS (202). The scavenger A receptor (SRA), although traditionally known to play a role in uptake of unopsonized bacteria, contributes to the uptake of serum-opsonized *Francisella*, since $SRA^{-/-}$ macrophages exhibit a 20% reduction in the uptake of serum-opsonized LVS (176). Macrophage cell surface-exposed nucleolin has also been implicated in uptake of serum-opsonized *Francisella* by binding the bacterial membrane protein EF-Tu (19). Finally, MR-mediated uptake also plays a role in uptake of serum-opsonized *Francisella* (roughly 30% decreased uptake when blocked) (90). As mentioned above, this multireceptor uptake pathway predominated by CR3 results in delayed phagosomal escape and replication and is therefore nonoptimal for *Francisella*.

Opsonization with antibody, specifically IgG, leads to FcγR-mediated uptake of *Francisella*. $Fc\gamma R^{-/-}$ macrophages exhibit a 90% reduction in uptake of IgG-opsonized *Francisella*, although they have no defect in the uptake of unopsonized or serum-opsonized bacteria (90). FcγR-mediated uptake leads to increased activation of the NADPH oxidase, a phagosomal enzyme complex that produces toxic reactive oxygen species (ROS) and is discussed in greater detail below. This activation results in a more inhospitable environment for the bacteria in the phagosome, acting to delay phagosomal escape and severely limit subsequent bacterial replication. The efficacy of this host defense is revealed when ROS production is abrogated by genetic deletion of an NADPH oxidase component (using $gp91^{phox-/-}$ macrophages), since IgG-opsonized *Francisella* bacteria are rescued and can replicate to high levels (90).

Binding of plasmin by *Francisella* (mentioned in "Complement and Antibody" above) leads to degradation of soluble antibody at the bacterial surface (Fig. 2) (59), which limits uptake by the FcγR pathway and therefore subversion of this pathway, facilitating higher levels of intracellular replication. *Francisella* also subverts the CR3-mediated pathway using LPS O antigen and capsule, which inhibit binding of complement factors. It should be noted that when complement binding does occur, the bacteria alter the complement pathway to prevent MAC formation and lysis (Fig. 2). However, the alternate complement fragments generated actually promote phagocytosis via CR3. While uptake via this pathway is not optimal, it does still support bacterial replication and is a much better outcome for the bacteria than complement-mediated lysis. The most optimal entry pathway, however, is mediated via the MR. Therefore, *Francisella* uses the aforementioned subversion mechanisms to promote uptake by the more favorable

MR-mediated pathway, facilitating the highest levels of intracellular replication.

Phagosomal Acidification

After uptake by the macrophage, *Francisella* resides within the *Francisella*-containing phagosome (FCP) and subsequently escapes into the cytosol, where it can replicate (Fig. 1) (184). The brief time spent in the FCP is a dynamic step in infection during which *Francisella* must actively evade host antimicrobial defenses, including acidification of the FCP, reactive oxygen species, and antimicrobial peptides. Acidification of the phagosome is a defense mechanism that lowers the pH in this compartment, preventing many types of bacteria from efficiently replicating. Many intracellular pathogens must subvert this host defense mechanism by either blocking it, escaping the phagosome, or maintaining intracellular pH in spite of the lowered pH in the environment (184). It is interesting to note that acidification is actually required for the rapid phagosomal escape of the intracellular pathogen *Listeria monocytogenes* (27). Studies with *Francisella* have shown a brief acidification of the FCP that is dependent on the route of uptake, although there has been debate about whether this step is required for rapid escape and about its effect on the outcome of infection, as detailed below (49, 52, 53, 194).

Uptake of unopsonized *Francisella* leads to transient acidification of the FCP and rapid escape (49, 194). Santic et al. reported acidification of the phagosome at 15 to 30 min postinfection of human monocyte-derived macrophages (MDM) with unopsonized *F. novicida*, followed by escape at 30 min to 1 h postinfection (194). Interestingly, they showed that inhibition of the vacuolar proton ATPase (vATPase) pump by bafilomycin A (BFA) does not block escape but results in delayed escape (6 to 12 h). These results suggest that acidification is required for rapid escape from the FCP (194). Additionally, Chong et al. observed brief acidification of the FCP in macrophages infected with unopsonized *F. tularensis* (49). Similarly, BFA did not inhibit phagosomal escape or cytosolic replication but slowed infection kinetics (49). Together these data show that acidification of the FCP ensures rapid escape and robust replication of unopsonized *Francisella*; however, it is not required for these processes.

Concurrently, it has been reported that uptake of serum-opsonized *Francisella* results in acidification of a modest 20% to 30% of phagosomes containing serum-opsonized LVS and that it is not required for escape or replication (53). Additionally, the authors found that the maturing FCP does not acquire high levels of the acid hydrolase cathepsin D, which is a cellular marker of acidification, or the endosomal-lysosomal markers CD63, LAMP1, and LAMP2, which are cellular markers of phagosomal maturation (52, 53). In contrast to the previously mentioned work using unopsonized bacteria, BFA did not significantly delay infection kinetics in these experiments using serum-opsonized bacteria (53). These data demonstrate that acidification of the FCP is not required for escape and replication of unopsonized or serum-opsonized *Francisella* but is required for rapid escape of unopsonized *Francisella*. The fact that *Francisella* does not exhibit a significant survival or replication defect in the presence or absence of acidification demonstrates that this pathogen has devised ways to efficiently resist this host defense. This resistance is mediated in part by physically escaping the FCP, where acidification takes place (discussed in "*Francisella* Escape from the Phagosome" below). It is also likely that *Francisella* has evolved mechanisms to maintain intracellular pH while in the acidified environment of the FCP.

Inhibition of Reactive Oxygen Species

In addition to subverting the potentially toxic effect of acidification of the FCP, *Francisella* must contend with reactive oxygen species (ROS) produced in this compartment. ROS are produced by the NADPH oxidase, a membrane-bound multicomponent enzyme system that converts molecular oxygen into toxic superoxide anions (161). In a resting phagocyte, NADPH oxidases are unassembled, with the gp91^{phox} and p22^{phox} (also called flavocytochrome b_{558}) components localizing to the plasma membrane and p47^{phox}, p40^{phox}, p67^{phox}, and Rac2 to the cytosol (145, 161). Upon phagocytosis of a microbe, the cytosolic subunits traffic to the phagosome and assemble with the membrane subunits to create the active NADPH oxidase that then produces ROS. Similar to the case for numerous extracellular and intracellular bacterial species, including *Helicobacter pylori* and *Salmonella* spp., multiple *Francisella* species block NADPH oxidase assembly in neutrophils and macrophages (4, 89, 145, 156, 203).

Francisella species use several approaches to inhibit ROS, including blocking initial assembly of NADPH oxidase components at the phagosomal membrane, blocking ROS production in complexes that have assembled, and detoxifying ROS that are generated. *F. novicida* requires four putative acid phosphatases (AcpA, AcpB, AcpC, and Hap) for inhibition of NADPH oxidase assembly (155, 186). AcpA colocalizes with the cytosolic NADPH oxidase component p47^{phox} during infection, and purified AcpA dephosphorylates p47^{phox} and p40^{phox} (155). Without phosphorylated membrane-bound components, the cytosolic NADPH oxidase components are not recruited and assembly cannot occur (14). These data suggest that AcpA interacts directly with NADPH oxidase components to block complex assembly.

While AcpA plays a role in limiting the oxidative burst, its relative contribution to virulence is unclear. Two studies found that AcpA is required for replication of *F. novicida* in human macrophage-like cells, indicating that blocking the NADPH oxidase is an important factor in facilitating replication (11, 155). In contrast, another study using *F. novicida* determined that AcpA did not play a role in replication in murine macrophages (22). In *F. tularensis*, deletion of *acpA*, or even of *acpA*, *acpB*, and *acpC* together, did not influence virulence in murine macrophages or human monocytes (48, 146). These conflicting data indicate that AcpA is not required for *Francisella* replication under all conditions tested. Its requirement may depend on the species or host cells used and the specific infection conditions.

In addition to blocking assembly, *F. tularensis* can also inhibit the generation of ROS when NADPH oxidase assembly is induced by exogenous stimuli (146). In spite of the formation of this complex, *F. tularensis* can inhibit the production of ROS. These data show that *F. tularensis* can block NADPH oxidase-dependent ROS production postassembly (146), although the mechanism by which this occurs has not yet been elucidated.

Although *Francisella* uses the mechanisms described above to significantly suppress activation of the NADPH oxidase, low levels of ROS are produced in the phagosome during infection (203). Like many pathogens, *Francisella* can directly detoxify ROS using proteins, including catalase (134, 151, 214) and superoxide dismutases (15, 16, 151), whose specific mechanisms of action are reviewed extensively elsewhere (135). In addition to these well-

known mechanisms of ROS resistance, we identified a previously uncharacterized protein, FTN_1133, that is required for virulence and resistance to organic hydroperoxides (135). FTN_1133 has sequence similarity to Ohr proteins, which are involved in resistance to organic hydroperoxides created during the interaction of ROS with lipids of the bacterial cell membrane (135). The *FTN_1133* mutant was attenuated for replication, although this could be restored in gp91$^{phox-/-}$ macrophages and mice (135). These data together indicate that *Francisella* has numerous overlapping mechanisms with which to subvert the NADPH oxidase and ROS, facilitating pathogenesis.

Francisella Escape from the Phagosome

Phagosomal escape is the last step in *Francisella*'s subversion of the phagocytic pathway, allowing it to escape the toxic phagosome and reach the cytosol, where it can replicate. The timing of escape has been a topic of debate and, as mentioned above, is largely dependent on the route of *Francisella* uptake by host cells. Unopsonized *Francisella* escapes the phagosome rapidly (within 1 h) whereas opsonized *Francisella* exhibits delayed escape (2 to 4 h) (92).

The exact mechanism of escape is not yet known; however, the proteins encoded in the *Francisella* pathogenicity island (FPI) are absolutely required. The FPI encodes a putative type VI secretion system (T6SS) that is essential for *Francisella* replication and pathogenesis (21; reviewed in reference 160). The requirement of a specialized secretion system for phagosomal escape would be in line with the situation in many intracellular bacteria, including *Shigella flexneri* (T3SS), *Listeria monocytogenes* (Sec pathway), and *Burkholderia* spp. (T3SS) (70, 168, 177, 193, 197). Briefly, the FPI proteins IglA and IglB share homology with proteins encoded in T6SS clusters in multiple bacterial species, are required for phagosomal escape, and may form the putative outer tube of the T6SS "needle" (64, 65). IglC has been proposed to form the inner tube (64), while IglI and VgrG are secreted and therefore may interact with host proteins during infection (21). In addition, numerous proteins that are not encoded in the FPI have also been implicated in phagosome escape and are reviewed elsewhere (11, 49).

To facilitate phagosomal escape, *Francisella* must subvert the action of host factors that have evolved to slow or block this process in order to control infection. Activation of the phosphatidylinositol 3-kinase (PI3K)/Akt pathway by bacteria leads to production of proinflammatory cytokines, increased ROS production, and retention of bacteria in the phagosome (61, 104, 181). In accordance, activation of the PI3K/Akt pathway during *F. novicida* infection blocks phagosomal escape and cytosolic replication (181). Interestingly, *F. novicida* infection of macrophages activates the SH2 domain-containing inositol phosphatase (SHIP) by an unknown mechanism that is dependent on live bacteria (167). SHIP antagonizes activation of the PI3K/Akt pathway, leading to rapid escape from the phagosome and robust cytosolic replication (167). Additionally, the PI3K/Akt pathway can be activated by cell surface receptors, including FcγR (143) and TLRs (121). Therefore, *Francisella* mechanisms to evade these receptors (discussed in "Complement and Antibody" above and in "Toll-Like Receptors" below) may also function to block activation of the PI3K/Akt pathway and ensure rapid phagosomal escape.

Toll-Like Receptors

Upon contact with host cells, extracellular and intracellular microbes encounter host pathogen recognition receptors (PRRs) that are capable of detecting conserved microbial components (PAMPs) (109). These receptors can then trigger multiple pathways, including phagocytosis and inflammatory signaling (109) (115). Toll-like receptors (TLRs) are important PRRs that can recognize PAMPs outside the host cell and in the endosome/phagosome (115, 216). TLR signaling is mediated by TIR domain-containing adaptor proteins, including MyD88, TRIF, and TIRAP, that activate transcription factors such as NF-κB and IRF3 (115). These transcriptional regulators induce the expression of inflammatory cytokines and type I interferons, resulting in the activation of innate and adaptive immune cells (109, 115). Numerous TLRs recognize bacterial PAMPs, including TLR2, which senses bacterial lipoproteins (BLPs) and peptidoglycan (PGN) (12, 73), TLR4, which signals in response to LPS from Gram-negative bacteria, TLR5, which recognizes flagellin, and TLR9, which senses bacterial CpG DNA (115).

A central component of *Francisella*'s success as a pathogen is its ability to avoid recognition and subvert the host inflammatory response, particularly in the early stages of infection. Indeed, *Francisella* can likely evade or suppress inflammatory signaling by all of the aforementioned bacterium-sensing TLRs. For example, *Francisella* does not encode flagellin, and therefore TLR5 is not activated in response to infection (128). Though TLR recognition of *Francisella* DNA has been suggested (77), TLR9 (present in the membranes of endosomes and phagosomes) was shown to be unimportant for the host response to *Francisella* infection *in vivo* (56). This suggests that *Francisella* may subvert TLR9 activation, possibly by limiting the release of its DNA through resistance to damaging antimicrobial agents (see "Complement and Antibody" and "Antimicrobial Peptides" above) and/or by directly modulating TLR9 signaling. In support of the idea that *Francisella* maintains strong structural integrity to prevent DNA release, Peng et al. have shown that some hyperinflammatory *F. novicida* mutants exhibit increased bacteriolysis and DNA release during *in vitro* infection (171). Though *Francisella* rapidly escapes the phagosome (see "*Francisella* Escape from the Phagosome" above), it is intuitive that bacterial damage or killing and resulting DNA release during the time within this compartment would activate TLR9. It would be interesting to determine the extent of bacterial damage in the phagosome, whether phagosomal bacteria can trigger TLR9 signaling, and whether *Francisella* DNA is capable of acting as a TLR9 activator.

While TLR4 is considered a primary sensor of Gram-negative bacteria, *Francisella* LPS does not efficiently activate TLR4 compared to LPS from *E. coli* and other Gram-negative pathogens (180). Many Gram-negative bacteria that elicit robust TLR4 signaling synthesize a hexa-acylated lipid A portion of LPS with acyl chains of 12 to 14 carbons and phosphate groups at the 1 and 4′ positions (Fig. 4) (180). However, *Francisella* modifies or removes these important signaling structures. For example, *Francisella* lipid A acyl chains are two to six carbons longer than those in *E. coli* LPS (180). In addition, *Francisella* lipid A is tetra-acylated, as it lacks the canonical 3′ double acyl chain, and both the 1 and 4′ phosphate groups are absent (Fig. 4) (180). These modifications are critical for virulence, since an *F. novicida* mutant lacking the *lpxF* gene and producing a penta-acylated lipid A containing the 4′

phosphate group is rapidly cleared in a mouse infection model (229). This mutant exhibits hypersensitivity to the cationic antimicrobial peptide polymyxin B and elicits an increased local cytokine response and increased neutrophil recruitment *in vivo*. TLR4 is not involved in this response, suggesting that the attenuation is not due to an increase in the signaling capacity of the mutant LPS. Instead, it is likely that the observed attenuation is due to the mutant's increased sensitivity to antimicrobial peptides that lead to outer membrane damage and leakage of other bacterial PAMPs, such as BLPs and DNA, within the phagosome, where they could trigger TLR2- or TLR9-dependent inflammatory responses.

Unlike in other bacteria, between 70% and 90% of total *Francisella* lipid A exists as "free lipid A" that does not contain core polysaccharides or O antigen (Fig. 4) (230, 243). Similar to the case for the complete LPS, free lipid A is tetra-acylated with elongated acyl chains and lacks the 4′ phosphate group. However, instead of being removed as it is in complete LPS, the phosphate at the 1 position is present and modified with galactosamine (230, 243). This modification to free lipid A alone is critical for pathogenesis, since an *flmK* mutant that does not add the galactosamine to free lipid A is highly attenuated *in vivo* (114). To the best of our knowledge, free lipid A is unique to *Francisella* and could represent a novel mechanism of virulence that might be involved in strengthening the outer membrane. However, it is somewhat counterintuitive that *Francisella* would produce free lipid A without O antigen, since O antigen is so critical for virulence (see "Complement and Antibody" above). Further studies of the role of *Francisella*'s free lipid A during host interactions will elucidate its contribution to virulence.

Since *Francisella* LPS (and likely free lipid A) is a poor TLR4 activator, it is expected that TLR4 would not play a critical role in host defense against this pathogen. Most reports support this conclusion, although some disagree as to the magnitude of TLR4 signaling that *Francisella* LPS can elicit as well as whether TLR4 plays a minor role or no role in host defense. For example, studies have reported that, *in vitro*, LPS from *F. novicida* triggers a low level inflammatory response (96, 116) while LVS LPS does not, even at high concentrations (5 μg/ml) (6, 116, 219). However, other studies reported that LVS LPS can induce TLR4 signaling in both transiently transfected HEK293 cells and human monocytes, but only when added at high doses that are likely not biologically relevant (≥2.5 μg/ml) (72). The varied LPS signaling responses may be due to differences in the cell types used or slight structural variations, such as the 6′ glucose addition to *F. novicida* LPS or the 4′ or 6′ hexose modifications of the LVS LPS (25, 94). Overall, these data show that the LPS from the *Francisella* species tested is markedly less inflammatory than LPS from other Gram-negative organisms such as *E. coli*, *Salmonella*, or *Bordetella* (6, 72, 96, 219). This finding is in agreement with the general lack of TLR4 activation during *in vivo Francisella* infections, as discussed below.

Though early reports indicated that TLR4-deficient mice exhibit increased sensitivity to LVS infection (8, 138), the bulk of the current evidence suggests that TLR4 is not essential for the host response to infection. For example, TLR4-deficient mice are not more susceptible than wild-type mice to low-dose *F. tularensis* or LVS aerosol challenge (46), LVS low-dose intradermal (i.d.) infection (47), or intranasal inoculation with either LVS or *F. novicida* (1). However, the 50% lethal dose (LD_{50}) for LVS is 1 log lower in TLR4-deficient mice than in wild-type mice after high-dose i.d. infection (10^6 to 10^7 CFU) (47). Therefore, TLR4 may play a minor role in the host response to high-dose infections, though doubts remain about whether such a high inoculum is physiologically relevant. Even if TLR4 does play a minor role in host defense, it is not nearly as important as other innate defense proteins (tumor necrosis factor alpha [TNF-α], IFN-γ, or MyD88) that are critically required for resistance to infection as judged by the susceptibility to infection of mice lacking these proteins (1, 126). Overall, *Francisella* LPS is a poor TLR4 ligand, and TLR4 does not appear to play an important role in the host response to infection *in vitro* or *in vivo*.

TLR2 is the primary TLR involved in the inflammatory response to *Francisella* infection (1). Known *Francisella* TLR2 agonists include the uncharacterized lipoproteins LpnA/Tul4 and FTT_1103 (86, 220). To our knowledge, TLR2 recognition of *Francisella* PGN has not been reported, and the status of PGN as a TLR2 ligand is still under debate (12, 73, 222). Several reports have shown that TLR2 is essential for the early inflammatory response to *Francisella* infection in macrophages *in vitro*, as well as a critical component of the host response to *in vivo Francisella* infection as demonstrated by its requirement for control of pulmonary and intradermal infection (1, 16, 55).

However, while *Francisella* elicits TLR2-dependent signaling, it can also dampen this response. Specific *Francisella* genes that play a role in this suppression of the host inflammatory response have been identified. For example, a strain with a mutation in the FPI gene *iglC* not only failed to escape the phagosome or replicate in macrophages but also was unable to suppress TNF-α production and other inflammatory responses (64, 131, 196, 219). In addition, infection of macrophages with wild-type LVS blocked TLR2 and TLR4 activation in response to the addition of *E. coli* BLP and LPS, respectively, while the *iglC* mutant could not block this signaling (219). Further supporting the attenuation of TLR2 signaling by *Francisella*, infection with *F. tularensis* has been shown to reduce TLR2 expression (38). Mechanisms that the bacteria use to resist damage by antimicrobials, and therefore the release of BLPs, are also an indirect way of evading TLR2 signaling. It has been reported that high-molecular-weight (HMW) carbohydrates from "host-adapted" LVS and *F. tularensis* capsules impede TLR2-dependent cytokine production in murine macrophages (240), possibly by shielding the bacteria from antimicrobials. Taken together, these data indicate that *Francisella* is capable of subverting TLR2 signaling, while the host uses this pathway as a mechanism of innate defense.

Preliminary evidence suggests that highly virulent *F. tularensis* is able to suppress host recognition and inflammatory signaling even further. Melillo et al. recently reported that *F. tularensis* strain SchuS4 has a greater ability to prevent proinflammatory cytokine production than LVS during infection of murine macrophages (150). Indeed, 2 days after pulmonary infection, *F. tularensis* replicates to high numbers in the lungs of mice but does not induce inflammatory signaling and in fact triggers an increase in anti-inflammatory signaling (7, 34, 35). In addition, *F. tularensis* infection of dendritic cells (DC) suppresses the response of both infected and bystander cells to TLR agonists, due at least in part to a heat-stable bacterial component (44). Taken together, these findings suggest that *F. tularensis* is able to suppress the host inflammatory response to an even greater degree than other *Francisella* species, correlating with its heightened virulence. Further studies querying the role of TLR signaling in response to *F. tular-*

ensis infection could shed light on the mechanisms of inflammatory subversion utilized by this pathogen.

Finally, Collazo et al. demonstrated that mice lacking the adaptor MyD88, but not those lacking TLR2, TLR4, or TLR9, had greatly increased susceptibility to LVS infection (56). This indicates that multiple TLRs may play overlapping roles in resistance to infection, such that no one TLR knockout displays highly enhanced susceptibility (56). Alternatively, Medina et al. propose that an unknown MyD88-dependent PRR may be involved in the host response to LVS infection (148). Overall, *Francisella* species are able to largely evade recognition by TLRs as well as to suppress TLR2 signaling, significantly contributing to virulence.

Cytosolic Defenses

When *Francisella* reaches the cytosol, it has trafficked past TLRs and phagosomal defenses. It is nonetheless faced with a formidable challenge: replicate to high numbers without triggering an effective immune response. This is all the more challenging since the process of bacterial replication results in the release of PAMPs that can be recognized by cytosolic PRRs. Like the cell surface and the phagosome, the cytosol is equipped with numerous PRRs that recognize an array of bacterial products and elicit an immune response aimed at clearing the invaders. One large family of cytosolic PRRs is the Nod-like receptor (NLR) family, whose 22 members respond to a diverse set of PAMPs, including PGN (Nod1 and Nod2), flagellin (NLRC4, NAIP5, and NAIP6) (118), components of bacterial type III secretion systems (NLRC4), and damage induced by pore-forming toxins (NLRP3) (152). Nod1 and Nod2 are membrane-associated NLRs that detect muropeptide subunits of PGN and induce NF-κB activation and proinflammatory cytokine production (174). A role for Nods during *Francisella* infection has yet to be described, but these receptors may recognize and respond to PGN from this pathogen. Alternatively, *Francisella* may subvert Nods by modifying its PGN (similar to the case for *Listeria monocytogenes*, which *N*-deacetylates its PGN [33]) or by suppressing the Nod signaling pathway.

Other cytosolic PRRs, such as RIG-I and MDA-5, bind bacterial or viral nucleic acids and induce the production of type I interferons (IFNs) (157). The type I IFN family includes numerous IFN-α proteins, a single IFN-β protein, and other IFNs (66). These secreted cytokines have a well-established role in interfering with viral replication but can also be induced in response to bacterial infection (157). *F. novicida* induces type I IFN production independently of TLRs, Nod1/2, RIG-I, or MDA-5 (99). The cytosolic PRR that induces type I IFN production in response to *F. novicida* is currently unknown. However, the adaptor protein STING (stimulator of interferon genes) is required for type I IFN production during *F. novicida* infection and is speculated to act downstream of the yet-to-be-identified cytosolic PRR (112). STING is known to induce type I IFN production in response to cytosolic double-stranded DNA (dsDNA) derived from transfected plasmids, viruses, and some bacteria (107). Therefore, it is likely that *Francisella* DNA, which has been observed in the host cytosol by confocal microscopy (112), is the ligand that activates this cytosolic defense system.

It is not clear how *Francisella* DNA reaches the cytosol to trigger type I IFN, but bacterial escape from the phagosome is required for induction of this host response (99, 112). Perhaps damage incurred by *Francisella* in phagosomes allows for the release of DNA from ruptured phagosomes following escape. Interestingly, an auxotrophic mutant of LVS that escapes the phagosome but cannot replicate in the cytosol failed to trigger cytosolic defense pathways (169), suggesting that bacterial replication might be required to increase the amount of DNA to a threshold level to which the host responds. In this context, mechanisms of maintaining structural integrity (LPS modifications, O antigen, and capsule; see "Complement and Antibody" and "Toll-Like Receptors" above) may prevent damage to the bacteria and the release of DNA in the cytosol and therefore would be hypothesized to promote subversion of these cytosolic defenses.

In addition to triggering the type I IFN pathway, cytosolic DNA released during *Francisella* infection can also be recognized by the PRR absent in melanoma 2 (AIM2) (82, 183), whose expression is upregulated by IFN-β (112). AIM2 is a member of the PYHIN (pyrin and HIN-200) family of proteins that binds dsDNA through a HIN-200 domain (81, 101, 187). AIM2 contributes to host defense by initiating the formation of a multiprotein complex called the inflammasome that is comprised of a PRR (from the NLR or PYHIN families), the scaffolding protein ASC, and the cysteine protease caspase-1 (144). Inflammasome activation causes infected cells to undergo an inflammatory form of programmed cell death called pyroptosis (84). This cell death may release bacteria into the extracellular environment, where they can easily be taken up by cells such as neutrophils that are not permissive for replication (210). Additionally, pyroptosis is accompanied by the release of the proinflammatory cytokines interleukin-1β (IL-1β) and IL-18 from dying cells, serving to recruit and activate other immune cells and further promote bacterial clearance. AIM2 inflammasome activation is essential for controlling *F. novicida* infection, since mice lacking components of this defense system succumb to infection much more rapidly than their wild-type counterparts (81, 141). The murine NLRC4 and NLRP3 inflammasomes do not play an obvious role in combating *F. novicida* during infection of macrophages or mice (141, 142). However, the NLRP3 inflammasome, along with the AIM2 inflammasome, is activated during *Francisella* infection of human epithelial cells and monocytes/macrophages (13). The mechanism underlying NLRP3 activation in human cells is not clear, since *Francisella* does not express known NLRP3 ligands.

Unlike the less virulent *F. novicida*, highly virulent *F. tularensis* fails to efficiently activate the inflammasome (234). Macrophages and dendritic cells infected with *F. tularensis* secrete very low levels of the inflammasome-dependent cytokine IL-18 *in vitro*, and there is very little caspase-1 activation induced in the spleens and livers of infected mice (234). As mentioned, microarray analysis of human monocytes infected with *F. tularensis* revealed that this pathogen downregulates the expression of several genes belonging to the TLR and type I IFN pathways (38, 60). TLR2 signaling is necessary for the expression of IL-1β and increases the rate of inflammasome activation during *F. novicida* infection (111), while type I IFN is essential for inflammasome activation (99). Therefore, hampering TLR2 and IFN signaling, two major host defense pathways that contribute to inflammasome activation, could lead to a lack of activation of this complex during *F. tularensis* infection. It is likely that highly virulent *F. tularensis* also has additional ways by which to limit inflammasome activation.

Several *Francisella* genes have been implicated in modulating inflammasome activation (82, 106, 224, 232). However, Peng et al. recently showed that these genes were not important for actively modulating the inflammasome (171). Instead, the increased induction of

macrophage death triggered by a panel of mutants lacking genes encoding membrane-associated proteins was due to increased bacteriolysis in the cytosol that allowed for the leakage of DNA and increased inflammasome activation. This study suggests that maintenance of membrane integrity is critical for *Francisella* to prevent the release of PAMPs and induction of the inflammasome. *F. tularensis* may also directly suppress inflammasome activation; however, genes important for direct suppression of the inflammasome complex by *F. tularensis* have not been identified. The presence of such genes in *F. tularensis* but not less virulent *Francisella* species could explain the divergence in activation of this complex.

During the latter stages of *F. tularensis* infection, infected cells undergo caspase-3-dependent programmed cell death or apoptosis. Unlike pyroptosis, this form of cell death is noninflammatory (120). Wickstrum et al. observed a significant increase in apoptosis in the livers and spleens of *F. tularensis*-infected mice between days 3 and 4 postinfection. This spike in apoptosis was preceded by an exponential increase in bacteria and antigen distribution in the infected organs (234). *F. tularensis* may direct host cells to undergo apoptosis instead of pyroptosis following cytosolic replication, facilitating dissemination to neighboring cells without triggering a strong inflammatory response. Additionally, phagocytosis of apoptotic bodies by activated macrophages impairs the ability of these cells to produce proinflammatory cytokines (80). In the context of an *F. tularensis* infection, these macrophages that have been rendered immunologically suppressed by taking up bacterium-containing apoptotic bodies could serve as reservoirs for further replication. Interestingly, it is not clear how *Francisella* egresses from infected cells and disseminates throughout the host. These impaired macrophages could also serve as Trojan horses, trafficking the bacteria systemically.

Another strategy commonly used by viruses and some pathogenic bacteria to exit host cells is to hijack the autophagic pathway (69). Autophagy is a process carried out by eukaryotic cells in which cytoplasmic material is engulfed into double-membrane-bound vacuoles called autophagosomes that subsequently fuse with lysosomes for degradation (127). This pathway was originally described as being important for maintaining cellular homeostasis, but it is now evident that it is also important for host defense. Following cytosolic replication, some *Francisella* organisms reside inside autophagosomes (45), although it is not clear whether this is a host-induced response to control infection or a pathogen-induced mechanism to promote virulence. *Francisella* autophagosomes contain major histocompatibility complex (MHC) class II (105), suggesting that the host might induce autophagy to degrade bacteria and present their antigens to activate the immune system and control bacterial replication. However, *F. tularensis* modulates the expression of *atg5*, *beclin 1*, and several other autophagy-related genes (60) during macrophage infection, supporting the notion that *Francisella* may act to subvert this host defense system. Furthermore, autophagy was recently shown to regulate the level of AIM2 inflammasome activation by targeting these complexes for lysosomal degradation (206). Therefore, hijacking the autophagic pathway could serve as a critical step in *F. tularensis* pathogenesis by hampering inflammasome-mediated bacterial clearance and providing this pathogen with a method by which to escape from host cells.

Replicating in the cytosol of host cells without inducing an inflammatory response is one of the most challenging yet critical immune subversion tactics employed by *F. tularensis* during infection. Although many of the virulence determinants that aid in evasion of cytosolic defenses are not currently known, it is likely that there are numerous genes necessary to subvert recognition by multiple PRRs, activation of cell death pathways, and killing via autophagy.

Nutritional Defenses

Although subverting host defenses in the cytosol is essential to facilitate intracellular replication and virulence, *Francisella* must also ensure that it can acquire sufficient nutrients in this host cell compartment to sustain its high growth rate. The host, however, has developed mechanisms that limit the availability of specific nutrients, providing a "nutritional" defense against pathogens. The fight over nutrients highlights another critical aspect of host-pathogen interactions.

Many *Francisella* genes annotated as being involved in metabolism, for both energy production and biosynthesis of macromolecules, have been identified in screens for genes important in intracellular replication and *in vivo* virulence (130, 135, 140, 214, 232). These screens identified genes required for growth during infection but not in rich media, and they therefore suggest that *Francisella* must utilize distinct metabolic pathways in order to successfully survive and replicate within the host, compared to those required for growth in broth. Mapping the genes identified in these screens onto predicted pathways has highlighted specific metabolic pathways critical to *Francisella* replication in the host, such as the biosynthesis of purines and pyrimidines as well as gluconeogenesis and glycolysis. The importance of these pathways in *Francisella* intracellular replication has recently been reviewed by Meibom and Charbit (149). We will focus on the mechanisms utilized by *Francisella* to directly access nutrients, such as iron and tryptophan, which are actively limited by the host during infection.

Iron, one of the most thoroughly studied nutrients in terms of host-pathogen interactions, is necessary for a variety of enzymatic functions in bacteria and is a vital component of various redox reactions that take place during growth. Within the host, nearly 99.9% of total iron is intracellular (37). Extracellular iron is highly insoluble, which thus represents a barrier to its uptake (36). Therefore, the little iron present outside host cells is associated with iron storage molecules such as heme, transferrin, and lactoferrin (36, 228). *Francisella* can overcome this first barrier to iron acquisition by entering host cells, where the iron content is substantially higher. However, even within host cells, iron is often sequestered by iron-containing redox enzymes and iron storage proteins such as ferritin and lactoferrin, making its acquisition by the bacteria challenging (36, 228).

Furthermore, the host has additional mechanisms to try to sequester iron away from pathogens as it responds to infection. Past work has demonstrated that when macrophages sense LPS or are stimulated with IFN-γ, the host cells respond by decreasing expression of the transferrin receptor (TfR) that shuttles iron-bound transferrin into the cell (158). These signs of infection also signal the host to increase production of ferritin, which binds and sequesters free iron within host cells (185). Together, these host strategies decrease the availability of free iron both extracellularly and intracellularly.

Due in part to these mechanisms, serum iron concentrations significantly decrease in otherwise healthy human volunteers during *F. tularensis* SchuS4 inhalational infection (170), as occurs during other microbial infections (231). This can be correlated

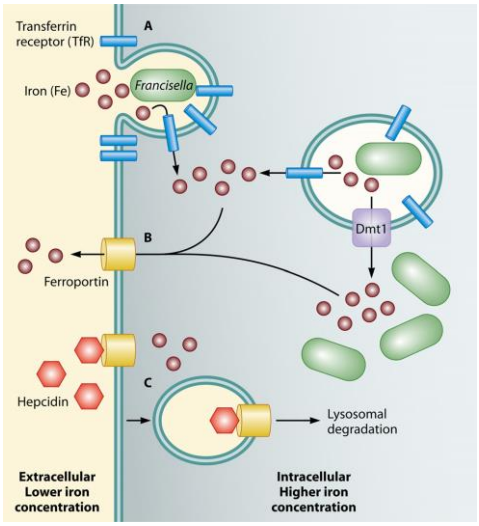

FIG 6 Competition for iron during *Francisella* infection. (A) Upon infection of macrophages, *Francisella* induces the upregulation and relocalization of the transferrin receptor (TfR) to the forming phagosome, facilitating an influx of iron into the host cell. (B) The host counteracts this by upregulating Dmt1 and ferroportin, which export iron from the phagosome to the cytosol and from the cytosol to the extracellular space, respectively. (C) *Francisella*, however, counters this by inducing host hepcidin, which binds ferroportin and causes it to be degraded. In total, this leads to an increase of intracellular iron available in the cytosol for *Francisella* replication.

with the fact that instead of the decrease in TfR expression typically observed in response to infection, TfR is significantly upregulated during LVS infection (165) and even colocalizes with the early *Francisella*-containing phagosome (FCP) (165). Interestingly, TfR localization does not occur with killed bacteria, indicating that LVS actively alters host TfR localization through an unknown mechanism (165). Increases in TfR would lead to increased intracellular pools of iron, while decreasing serum iron levels. Also, unlike stimulation with IFN-γ and/or LPS, LVS infection does not induce expression of ferritin (165). Therefore, LVS may also actively prevent the host from sequestering the intracellular iron brought in by TfR, allowing the bacteria to utilize the increased iron pool. Together, these changes in host expression of TfR and ferritin, as well as TfR localization to the FCP, cause a significant increase in usable intracellular iron that can enhance *Francisella* replication (Fig. 6).

Further highlighting the tug-of-war between host and pathogen, the host counters the influx of iron due to increased TfR expression during LVS infection by increasing expression of Dmt1, a phagosomal membrane protein which transports iron from phagosomes into the cytosol, as well as ferroportin, which shuttles iron from the cytosol out of the cell (Fig. 6) (165). The combined action of these proteins would limit the amount of intracellular iron available to replicating *Francisella* in the cytosol. Countering this restriction, LVS infection induces the production of hepcidin, an antimicrobial peptide secreted by hepatic cells (165). Hepcidin binds to ferroportin on the host cell surface, causing it to become internalized and subsequently be degraded (162). Thus, hepcidin induction and subsequent inhibition of efflux of cytosolic iron appear to be one strategy employed by LVS to maintain intracellular iron pools at levels permissive for replication. However, whether LVS actively induces hepcidin production to specifically inhibit ferroportin or whether hepcidin's antiferroportin action is an unintentional consequence to the host and secondary to its antimicrobial activity is not known. The exact mechanisms by which *Francisella* promotes the expression of hepcidin and TfR, while simultaneously preventing ferritin expression, are unknown.

Further contributing to its ability to capture and acquire iron, *Francisella* utilizes a rhizoferrin-like siderophore (215). Siderophores are small molecules that selectively bind iron at a significantly higher affinity than host iron-sequestering compounds, creating a biochemical flux in favor of the siderophore-producing organism (154). This allows *Francisella* to outcompete the host for available iron. The *Francisella* locus necessary for production and utilization of its siderophore is *fslABCDE* (also termed *figABCDE*) (117, 215). *fslABCD* are directly involved in the production and/or export of the *Francisella* siderophore (117, 215). *fslE*, on the other hand, is not necessary for production or export, but instead is required for the utilization of the siderophore, through either siderophore binding or import (117, 182). *Francisella* lacks genes with significant similarity to the known (and typically highly conserved) siderophore receptor and importer genes *tonB*, *exbB*, and *exbD* (122). It is therefore hypothesized that *fslE*, or one of the two *fslE* orthologs present in the genome, may act as a novel siderophore importer (182). The two *fslE*-like genes, termed *fupAB* (encoded in LVS by a single protein fusion of these two paralogs, named *fupA/B*) (132, 205), are important for siderophore uptake, particularly in LVS compared to *F. tularensis*, which relies more heavily on *fslE* for siderophore import (132, 182, 205).

In the context of an infection, siderophore production and iron acquisition proteins are a vital component of *Francisella*'s ability to maintain iron homeostasis and ultimately survive and replicate in the host. *fslABC* and *feoB*, encoding a ferrous iron importer utilized by other bacteria to directly import free iron (41, 122, 215), have each been identified in *in vivo* virulence screens (214, 232). *fslABC* have also been shown to be necessary for replication in macrophages (135). Furthermore, *fupAB* are required for full virulence in mice during LVS (205) and *F. tularensis* (223) infection and for LVS replication in macrophages (140, 205). Interestingly, while unable to produce siderophores, an *fslA* mutant of *F. tularensis* SchuS4 is not attenuated during infection of mice, suggesting that other iron acquisition pathways, such as the *feoB* importer or the *fupAB* system, may be playing a parallel role. On the other hand, while not identified in previous screens for virulence factors, we have identified *fslE* in a negative selection screen in *F. tularensis* for genes necessary for survival in mice (D. S. Weiss et al., unpublished observation).

Although iron acquisition may play an important role in pathogenesis, recent work has demonstrated that *Francisella* must also limit its total intracellular iron concentration (133). Increased intracellular iron concentrations can lead to increased susceptibility to oxygen radical damage within the bacteria. In fact, more virulent strains, such as *F. tularensis* SchuS4, have lower levels of intracellular iron than the less virulent LVS, which correlates with increased resistance to oxygen radical-mediated stresses (133). It is important to note that these studies were performed using bacteria grown on agar plates. It would

be interesting to measure the iron content of each strain during infection to see if the differences mentioned above are maintained. Overall, these data suggest that *Francisella* maintains homeostasis of intracellular iron, importing enough to promote survival while preventing excessively high and toxic concentrations.

Although it is the most thoroughly studied, iron is not the only nutrient whose availability is actively limited by the host. The intracellular concentration of the amino acid tryptophan is significantly decreased during infection (218) due to an increase in the expression of indoleamine 2,3-dioxygenase (IDO), which initiates the tryptophan catabolic pathway by converting tryptophan to kynurenine (218). IDO is expressed in nearly every cell type, excluding hepatic cells, and is particularly highly expressed in the lungs and placenta (218). Infection by *Chlamydia* (26) or *Streptococcus* (172), as well as stimulation with IFN-γ (238) or LPS (237), induces IDO expression and results in decreased tryptophan levels. This is an important defensive mechanism, as it creates an innate nutritional barrier that limits the ability of microbes to replicate.

Upon intranasal infection with *Francisella*, IDO is significantly upregulated in the lung (172). *Francisella* is capable of overcoming this host defense by maintaining the ability to synthesize tryptophan *de novo*, although this process is very energy intensive (241). The importance of tryptophan prototrophy is exemplified by the fact that strains with mutations in *trpB*, which is necessary for the final step of tryptophan biosynthesis, are significantly attenuated during intranasal infection (50, 172) and that this attenuation can be overcome in $IDO^{-/-}$ mice (172). *trpB* mutants are capable of limited intracellular replication in macrophages and show decreased survival in IFN-γ-stimulated macrophages compared to wild-type *Francisella* (50). As IDO expression is induced by IFN-γ, the attenuation of the *trpB* mutant is also rescued upon infection of IFN-γ receptor (IFNGR)-deficient mice (50). These data indicate that tryptophan prototrophy is a necessary attribute of *Francisella* pathogenesis, allowing the bacterium to overcome an aspect of the nutritional barrier induced by IFN-γ and IDO upon infection of the lung.

While it can produce tryptophan, *Francisella* is auxotrophic for 13 amino acids which it cannot synthesize *de novo*, likely because it does not encode some or all of the enzymes required for their biosynthetic pathways (122, 149, 188). Therefore, it is intuitive that being able to acquire these essential amino acids within the host is a necessary component of *Francisella* pathogenesis. *Francisella* is predicted to lack all of the biosynthetic enzymes for arginine, histidine, lysine, methionine, and tyrosine (122). Interestingly, a putative methionine uptake transporter (*FTN_1107/FTT1125*) (140, 214), lysine importer (*FTN_0296/FTT1633c*) (232), and tyrosine permease (*FTN_1711/FTT1732c*) (11) have all been identified in virulence screens, suggesting that they are necessary for pathogenesis. Furthermore, amino acid importers with no predicted substrate (*FTN_0097/FTT1688* and *FTN_0848/FTT0968c*) have been identified as well (130, 135, 140, 214, 232). This suggests that *Francisella* may have developed strategies to scavenge from the host those amino acids which it cannot synthesize *de novo*.

Other than tryptophan restriction, to the best of our knowledge, we do not know of another example of active host depletion of an amino acid that is important during *Francisella* infection. While numerous biosynthetic and metabolic pathways have been lost during the reductive evolution of the more recently evolving *F. tularensis* and *F. holarctica* subspecies, *Francisella* species are capable of *de novo* biosynthesis of alanine, glutamate, glutamine, asparagine, glycine, phenylalanine, and tryptophan (122, 149, 188). In fact, pathways for the synthesis of glutamate, glycine, and phenylalanine are redundantly represented. This suggests that the ability to synthesize these amino acids is essential for pathogenesis and could potentially counter active host restriction mechanisms, similar to the way *Francisella* counters tryptophan depletion as described above. In further support of this idea, asparagine synthase (*FTN_1421/FTT1456c*) which is necessary for asparagine prototrophy (130, 135, 232), and a number of enzymes utilized for the creation of aromatic amino acid precursors have been identified in virulence screens (149).

Another well-known example of *Francisella* auxotrophy is the requirement for cysteine, which serves as a necessary source of sulfate. This requirement is also necessary in broth and thus does not necessarily represent an active host defense process to deplete cysteine. However, in the host, cysteine is present within glutathione (GSH). The ability to utilize GSH is thus a required component of *Francisella* intracellular growth. Indeed, *F. tularensis* mutants lacking a transpeptidase (*ggt*) necessary for cleavage of GSH are severely attenuated during infection of macrophages and mice (3).

The requirement for other biosynthetic pathways during host infection, such as purine and pyrimidine biosynthesis, is well established for *Francisella* and other bacterial pathogens (10, 149). Furthermore, the importance of central metabolism (e.g., glycolysis) has also been shown to play a role during infection (149). Additionally, there is evidence that nutritional status may play a role in allowing *Francisella* to sense the host phagosome compared to being in the host cytosol (40) and to induce expression of virulence genes, including those required for phagosomal escape (40, 67, 191). Mutants that are unable to recognize particular metabolites, such as polyamines present in the host cytosol, are significantly attenuated and unable to alter temporal expression of virulence factors (191). Taken together, these data highlight the importance in the outcome of infection of host and pathogen proteins involved in this nutritional tug-of-war.

Modulation of Adaptive Immune Responses

We have focused a great deal of attention on the ways in which *Francisella* modulates the immune responsiveness of the cells that it directly infects. We now discuss the effect that these interactions have on the ability of other immune cells to fight infection and the development of an effective adaptive immune response. As noted previously, pulmonary infection caused by *F. tularensis* in humans is characterized by an initial delay in inflammatory responses during the first 72 h (58). Although it is not entirely clear how *F. tularensis* evades early immune responses, modulating the activity of innate immune cells that contribute to early cell-mediated immunity likely plays a significant role. Antigen-presenting cells (APCs), such as macrophages and dendritic cells, play an important role in early innate defense against *Francisella* infection. The ability of these cells to present microbial antigens and activate T cells enables them to serve as a bridge between the innate and adaptive immune systems. During the earliest stages of infection, *Francisella* resides primarily in macrophages (97). Therefore, it is not surprising that this pathogen uses multiple subversion mechanisms (e.g., facilitating cell entry via nonactivating macrophage receptors, escaping phagosomal killing, and modulating cytosolic defense pathways) to systematically disarm macrophage defenses. However, when activated by the proinflammatory cytokine IFN-γ, these phagocytes are capable of overcoming the modula-

tory effects exerted by *Francisella*, preventing its replication in the cytosol (68, 126). Primarily produced by NK cells and dendritic cells during infection, IFN-γ regulates over 200 genes, many of which are involved in host defense pathways important for enhancing nitric oxide production, inducing autophagy, and increasing major histocompatibility complex (MHC) class I and II antigen presentation (32, 226). Activation of these pathways could collectively enhance *Francisella* clearance and promote host survival. Moreover, a lack of IFN-γ *in vivo*, through either genetic disruption (76) or anticytokine treatment (126), increased the susceptibility of mice to *Francisella* infection, indicating that this cytokine is an important mediator of host defense *in vivo*.

The exact mechanism of IFN-γ-mediated clearance of *Francisella* from activated macrophages is unclear. IFN-γ can hinder *F. novicida* and LVS escape from the phagosomes of human monocyte-derived macrophages and murine peritoneal exudate cells, respectively (131, 195). This prolonged retention of *Francisella* in the phagosome would expose bacteria to phagosomal defenses such as the NADPH oxidase, nitric oxide, and lysosomal enzymes if phagolysosomal fusion occurred (201), all of which are upregulated by IFN-γ, leading to bacterial clearance. In contrast, escape of highly virulent *F. tularensis* from the phagosome is not affected by IFN-γ activation of macrophages, although its cytosolic replication is nonetheless restricted (74). Therefore, IFN-γ-mediated activation of macrophages leads to both phagosomal and cytosolic defenses that control the virulence of multiple *Francisella* species.

Since IFN-γ has such a pleiotropic effect on macrophage activation, any mechanism of suppressing the action of this cytokine would likely have broad effects on promoting *Francisella* pathogenesis. *Francisella* directly impairs the ability of macrophages to respond to IFN-γ stimulation during infection by downregulating the expression of the alpha subunit of the IFN-γ receptor (IFNGR), which is critical for signaling (189). Nallaparaju et al. found that in the event that signaling through the IFNGR does occur, *Francisella* uses FopC to indirectly block the phosphorylation and subsequent activation of Stat1 (a transcriptional regulator that is required for IFNGR signaling) (159a, 166). The IFN-γ signaling pathway is further decommissioned during infection as the bacteria induce an increase in the expression of SOCS3, a protein that negatively regulates this pathway (38). Activation of the TLR signaling pathway enhances IFN-γ-dependent cytokine production in macrophages (242). Therefore, suppression of TLR signaling by mechanisms discussed earlier in this review (prevention of PAMP release, modification of LPS/lipid A structure to prevent TLR4 activation, and downregulation of TLR expression) could also dampen activation of the IFN-γ pathway.

In addition to suppressing IFN-γ signaling, *F. tularensis* induces macrophages to produce the immunomodulatory lipid prostaglandin E_2 (PGE_2) (236). PGE_2 inhibits T cells from producing IFN-γ, favoring bacterial replication (Fig. 7) (175). PGE_2 also induces the expression of a >10-kDa protease-resistant host factor that promotes ubiquitin-dependent lysosomal degradation of MHC class II molecules, resulting in a nearly complete absence of MHC class II on the surface of macrophages (235). Therefore, by inducing PGE_2, *Francisella* inhibits bacterial killing mediated by IFN-γ and also dampens the induction of adaptive immune responses by limiting antigen presentation through MHC class II.

Dendritic cells play a critical role in directing cell-mediated immunity by producing cytokines that control the way in which T cells are activated and the immune responses that they subsequently promote. In accordance with this pathogen's ability to dampen cell-mediated immune responses, *F. tularensis* suppresses proinflammatory cytokine production from these cells (35). Among these cytokines is IL-12, which is important for the development of IFN-γ-producing T cells (75). Surprisingly, inhibition of IL-12 by *F. tularensis* is mediated by IFN-β production (Fig. 7) (24). As described previously in this review, type I IFNs contribute to inflammasome activation by *Francisella*. However, there was no correlation between IFN-β production and inflammasome activation during *F. tularensis* infection. Considering that *F. tularensis* dampens the expression of genes in the type I IFN pathway, it is possible that this pathogen suppresses the expression of type I IFNs to a level that is below the threshold for inflammasome activation but adequate for IL-12 suppression.

F. tularensis also redirects macrophages to become alternatively activated (207). Alternatively activated macrophages exhibit a skewed inflammatory profile that is less antimicrobial, with decreased levels of nitric oxide production upon IFN-γ stimulation and an impaired ability to kill bacteria (78, 93). Additionally, *F. tularensis* directs dendritic cells to produce the anti-inflammatory cytokines transforming growth factor β (TGF-β) and IL-10 (35, 236). This greatly contributes to the absence of an inflammatory response early in infection because IL-10 inhibits macrophage proliferation and proinflammatory cytokine production (164). In addition, it can lead to reduced MHC class II expression, which would suppress adaptive immune responses (139).

IL-10 or TGF-β can direct dendritic cells to become tolerogenic, inhibiting their ability to activate T cells that induce an inflammatory response (Fig. 7) (139). These cytokines also promote the development of regulatory T cells that can suppress the inflammatory activity of other T cells (85). In fact, pulmonary regulatory T cells develop in the lungs during *F. tularensis* infection, and this development correlates with an increase in bacterial burden (173). Though it is currently unclear how *F. tularensis* redirects APCs toward an anti-inflammatory response, inducing immune tolerance through the induction of IL-10 or TGF-β is a survival strategy used by pathogens such as *Yersinia pestis*, *Coxiella burnetii*, and *Chlamydia pneumoniae* (63). In the case of *Yersinia pestis*, IL-10 production is induced by the type III secretion system effector protein LcrV (124, 208). Further characterization of *Francisella* secretion systems and effector proteins may shed light on similar mechanisms of immune modulation.

Cell-mediated immunity is generally accepted as being essential for controlling intracellular bacterial infection. In accordance with this dogma, antibodies have been shown to provide little protection against *Francisella* infection, but antibody-independent B cell responses are important for early protection (62). However, *Francisella*, like some other intracellular bacterial pathogens (83), is also capable of infecting and replicating inside B cells (119), although it is not known whether it can modulate B cell activity in order to evade immune detection. *Salmonella enterica* serovar Typhimurium has been shown to induce MyD88-dependent IL-10 production in splenic B cells during systemic infection, promoting its survival *in vivo* (163). As discussed above, IL-10 induces a tolerogenic state in immune cells, and it is possible that *Francisella*-induced IL-10 production in APCs could also alter the function of B cells during infection.

Francisella uses multiple strategies to modulate APCs in order to subvert subsequent activation of the adaptive immune system. This modulation not only contributes to the failure in immune

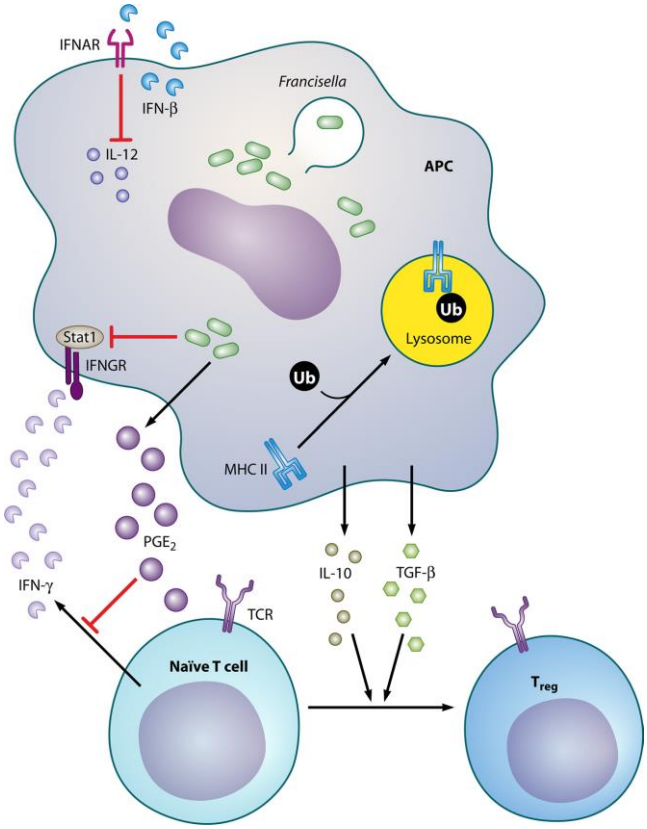

FIG 7 Subversion of adaptive immune responses by *Francisella*. *Francisella* infects antigen-presenting cells (APCs) and dampens their ability to produce proinflammatory cytokines. IL-12 is blocked via the induction of beta interferon (IFN-β). IFN-γ is produced by dendritic cells and T cells during *Francisella* infection, and it induces macrophages to kill the bacteria. *Francisella* blocks signal transduction through the IFN-γ receptor (IFNGR) by inhibiting Stat1 phosphorylation and through the induction of prostaglandin E2 (PGE_2), which inhibits IFN-γ production by T cells. *Francisella* also hampers T cell activation by inducing the degradation of major histocompatibility complex class II (MHC II) (indicated by its absence from the cell surface, tagging with ubiquitin [Ub], and trafficking toward the lysosome) and directing APCs to produce the anti-inflammatory cytokines TGF-β and IL-10, which promote the development of regulatory T cells (T_{reg}) that are able to suppress inflammation and cell-mediated immune responses.

activation during the initial stages of infection but also helps provide a suitable environment for replication in subsequent phases of infection by dampening adaptive responses such as the activation of CD8 T cells, which could kill infected host cells harboring *Francisella*.

CONCLUDING REMARKS

Francisella uses a vast arsenal of virulence mechanisms to subvert host defenses and promote intracellular replication. The main overarching strategy is to prevent the initiation of host inflammatory responses. Since the inflammatory response operates in a positive-feedback loop, it is powerful once started and very difficult, if not impossible, to reign in. If initiated, host defenses encountered by the bacteria (extracellular, phagosomal, and cytosolic defenses) are heightened at each step of infection, taking a toll on replication levels. This is highlighted by comparing the intracellular fates of *Francisella* in unstimulated or IFN-γ-stimulated macrophages. While *Francisella* is able to grow rapidly in unstimulated macrophages, IFN-γ-stimulated macrophages are not permissive for replication and are instead able to kill the bacteria. Therefore, if inflammatory processes leading to IFN-γ production are initiated, this drastically alters the course of infection in favor of the host.

Since PAMPs activate inflammatory pathways during infection, a critical aspect of subverting the inflammatory response is preventing PAMP recognition by the host. *Francisella* achieves this in large part by devoting considerable resources to resisting

damage (capsule, LPS O antigen, lipid A modifications, efflux pumps, detoxifying ROS, etc.) induced by antimicrobials that would lead to the release of PAMPs. When PAMPs are inevitably liberated and recognized by the host at some level, *Francisella* suppresses the signaling of host PRRs, although the mechanisms by which this occurs are not defined and will be a critical area of future research. The importance of subverting early inflammatory responses can be seen when studying numerous mutant strains that lack virulence traits required in the first hours of infection (resistance to complement and phagosomal defenses, defects in phagosome escape, etc), which are often hyperinflammatory and severely attenuated for virulence.

Remaining immunologically "silent" allows the bacteria to reach the host cytosol, where they can replicate. However, an often overlooked virulence trait is the ability to acquire sufficient nutrients to facilitate rapid intracellular replication. *Francisella* has several strategies to acquire iron and synthesize tryptophan *de novo* to subvert specific host defense pathways. As mentioned, numerous metabolic genes have been identified in virulence screens and may lead to the elucidation of novel mechanisms by which the bacteria subvert "nutritional defenses." This is a subject of great interest not just for *Francisella* pathogenesis but also in the field of bacterial pathogenesis as a whole. As it is one of the most virulent bacterial pathogens known, continued research into how *Francisella* subverts innate and adaptive host responses will lead to novel discoveries that will enhance our understanding of host-pathogen interactions.

ACKNOWLEDGMENTS

We thank Thomas Kawula for critical reading of the manuscript.

We attempted to mention all of the relevant studies and have undoubtedly omitted some. We apologize in advance to those authors whose work we did not cite.

This work was supported by NIH grants U54-AI057157 from the Southeastern Regional Center of Excellence for Emerging Infections and Biodefense and R56-AI087673 (D.S.W.), the National Science Foundation Graduate Research Fellowship (C.L.J. and T.R.S.), and the ARCS Foundation (T.R.S.).

The contents of this article are solely the responsibility of the authors and do not necessarily represent the official views of the NIH.

REFERENCES

1. **Abplanalp AL, Morris IR, Parida BK, Teale JM, Berton MT.** 2009. TLR-dependent control of Francisella tularensis infection and host inflammatory responses. PLoS One **4**:e7920.
2. **Akimana C, Kwaik Y.** 2011. Francisella-arthropod vector interaction and its role in patho-adaptation to infect mammals. Front. Microbiol. **2**:34.
3. **Alkhuder K, Meibom KL, Dubail I, Dupuis M, Charbit A.** 2009. Glutathione provides a source of cysteine essential for intracellular multiplication of Francisella tularensis. PLoS Pathog. **5**:e1000284.
4. **Allen LA, Beecher BR, Lynch JT, Rohner OV, Wittine LM.** 2005. Helicobacter pylori disrupts NADPH oxidase targeting in human neutrophils to induce extracellular superoxide release. J. Immunol. **174**: 3658–3667.
5. **Amer LS, Bishop BM, van Hoek ML.** 2010. Antimicrobial and antibiofilm activity of cathelicidins and short, synthetic peptides against Francisella. Biochem. Biophys. Res. Commun. **396**:246–251.
6. **Ancuta P, Pedron T, Girard R, Sandstrom G, Chaby R.** 1996. Inability of the Francisella tularensis lipopolysaccharide to mimic or to antagonize the induction of cell activation by endotoxins. Infect. Immun. **64**:2041–2046.
7. **Andersson H, et al.** 2006. Transcriptional profiling of host responses in mouse lungs following aerosol infection with type A Francisella tularensis. J. Med. Microbiol. 55:263–271.
8. **Anthony LS, Skamene E, Kongshavn PA.** 1988. Influence of genetic background on host resistance to experimental murine tularemia. Infect. Immun. **56**:2089–2093.
9. **Apicella MA, et al.** 2010. Identification, characterization and immunogenicity of an O-antigen capsular polysaccharide of Francisella tularensis. PLoS One **5**:e11060.
10. **Appelberg R.** 2006. Macrophage nutriprive antimicrobial mechanisms. J. Leukoc. Biol. **79**:1117–1128.
11. **Asare R, Abu Kwaik Y.** 2010. Molecular complexity orchestrates modulation of phagosome biogenesis and escape to the cytosol of macrophages by Francisella tularensis. Environ. Microbiol. **12**:2559–2586.
12. **Asong J, Wolfert MA, Maiti KK, Miller D, Boons GJ.** 2009. Binding and cellular activation studies reveal that Toll-like receptor 2 can differentially recognize peptidoglycan from Gram-positive and Gram-negative bacteria. J. Biol. Chem. **284**:8643–8653.
13. **Atianand MK, et al.** 2011. Francisella tularensis reveals a disparity between human and mouse NLRP3 inflammasome activation. J. Biol. Chem. **286**:39033–39042.
14. **Babior BM.** 2002. The leukocyte NADPH oxidase. Isr. Med. Assoc. J. **4**:1023–1024.
15. **Bakshi CS, et al.** 2008. An improved vaccine for prevention of respiratory tularemia caused by Francisella tularensis SchuS4 strain. Vaccine **26**:5276–5288.
16. **Bakshi CS, et al.** 2006. Superoxide dismutase B gene (sodB)-deficient mutants of Francisella tularensis demonstrate hypersensitivity to oxidative stress and attenuated virulence. J. Bacteriol. **188**:6443–6448.
17. **Balagopal A, et al.** 2006. Characterization of the receptor-ligand pathways important for entry and survival of Francisella tularensis in human macrophages. Infect. Immun. **74**:5114–5125.
18. **Bandara AB, et al.** 2011. Isolation and mutagenesis of a capsule-like complex (CLC) from Francisella tularensis, and contribution of the CLC to F. tularensis virulence in mice. PLoS One **6**:e19003.
19. **Barel M, et al.** 2008. A novel receptor-ligand pathway for entry of Francisella tularensis in monocyte-like THP-1 cells: interaction between surface nucleolin and bacterial elongation factor Tu. BMC Microbiol. **8**:145.
20. **Barker JH, et al.** 2009. The role of complement opsonization in interactions between F. tularensis subsp. novicida and human neutrophils. Microbes Infect. **11**:762–769.
21. **Barker JR, et al.** 2009. The Francisella tularensis pathogenicity island encodes a secretion system that is required for phagosome escape and virulence. Mol. Microbiol. **74**:1459–1470.
22. **Baron GS, Reilly TJ, Nano FE.** 1999. The respiratory burst-inhibiting acid phosphatase AcpA is not essential for the intramacrophage growth or virulence of Francisella novicida. FEMS Microbiol. Lett. **176**:85–90.
23. **Baucheron S, et al.** 2004. AcrAB-TolC directs efflux-mediated multidrug resistance in Salmonella enterica serovar Typhimurium DT104. Antimicrob. Agents Chemother. **48**:3729–3735.
24. **Bauler TJ, Chase JC, Bosio CM.** 2011. IFN-beta mediates suppression of IL-12p40 in human dendritic cells following infection with virulent Francisella tularensis. J. Immunol. **187**:1845–1855.
25. **Beasley AS, et al.** 2012. A variety of novel lipid a structures obtained from Francisella tularensis live obtained from Francisella tularensis live. Innate Immun. **18**:268–278.
26. **Beatty WL, Belanger TA, Desai AA, Morrison RP, Byrne GI.** 1994. Tryptophan depletion as a mechanism of gamma interferon-mediated chlamydial persistence. Infect. Immun. **62**:3705–3711.
27. **Beauregard KE, Lee KD, Collier RJ, Swanson JA.** 1997. pH-dependent perforation of macrophage phagosomes by listeriolysin O from Listeria monocytogenes. J. Exp. Med. **186**:1159–1163.
28. **Ben Nasr A, et al.** 2006. Critical role for serum opsonins and complement receptors CR3 (CD11b/CD18) and CR4 (CD11c/CD18) in phagocytosis of Francisella tularensis by human dendritic cells (DC): uptake of Francisella leads to activation of immature DC and intracellular survival of the bacteria. J. Leukoc. Biol. **80**:774–786.
29. **Ben Nasr A, Klimpel GR.** 2008. Subversion of complement activation at the bacterial surface promotes serum resistance and opsonophagocytosis of Francisella tularensis. J. Leukoc. Biol. **84**:77–85.
30. **Bina XR, Lavine CL, Miller MA, Bina JE.** 2008. The AcrAB RND efflux system from the live vaccine strain of Francisella tularensis is a multiple drug efflux system that is required for virulence in mice. FEMS Microbiol. Lett. **279**:226–233.
31. **Birdsell D, et al.** 2009. Francisella tularensis subsp. novicida isolated from a human in Arizona. BMC Res. Notes **2**:223.

32. **Boehm U, Klamp T, Groot M, Howard JC.** 1997. Cellular responses to interferon-gamma. Annu. Rev. Immunol. **15**:749–795.
33. **Boneca IG, et al.** 2007. A critical role for peptidoglycan N-deacetylation in Listeria evasion from the host innate immune system. Proc. Natl. Acad. Sci. U. S. A. **104**:997–1002.
34. **Bosio CM, Bielefeldt-Ohmann H, Belisle JT.** 2007. Active suppression of the pulmonary immune response by Francisella tularensis Schu4. J. Immunol. **178**:4538–4547.
35. **Bosio CM, Dow SW.** 2005. Francisella tularensis induces aberrant activation of pulmonary dendritic cells. J. Immunol. **175**:6792–6801.
36. **Braun V.** 2001. Iron uptake mechanisms and their regulation in pathogenic bacteria. Int. J. Med. Microbiol. **291**:67–79.
37. **Bridges K, Seligman P.** 1995. Disorders of iron metabolism. JB Lippincott Company, London, United Kingdom.
38. **Butchar JP, et al.** 2008. Microarray analysis of human monocytes infected with Francisella tularensis identifies new targets of host response subversion. PLoS One **3**:e2924.
39. **Campos M, et al.** 2004. Capsule polysaccharide mediates bacterial resistance. Infect. Immun. **72**:7107–7114.
40. **Carlson PE, Jr, et al.** 2009. Global transcriptional response to spermine, a component of the intramacrophage environment, reveals regulation of Francisella gene expression through insertion sequence elements. J. Bacteriol. **191**:6855–6864.
41. **Cartron ML, Maddocks S, Gillingham P, Craven CJ, Andrews SC.** 2006. Feo-transport of ferrous iron into bacteria. Biometals **19**:143–157.
42. **Cederlund A, Gudmundsson G, Agerberth B.** 2011. Antimicrobial peptides important in innate immunity. FEBS J. **278**:3942–3951.
43. **Champion MD, et al.** 2009. Comparative genomic characterization of Francisella tularensis strains belonging to low and high virulence subspecies. PLoS Pathog. **5**:e1000459.
44. **Chase JC, Celli J, Bosio CM.** 2009. Direct and indirect impairment of human dendritic cell function by virulent Francisella tularensis Schu S4. Infect. Immun. **77**:180–195.
45. **Checroun C, Wehrly TD, Fischer ER, Hayes SF, Celli J.** 2006. Autophagy-mediated reentry of Francisella tularensis into the endocytic compartment after cytoplasmic replication. Proc. Natl. Acad. Sci. U. S. A. **103**:14578–14583.
46. **Chen W, KuoLee R, Shen H, Busa M, Conlan JW.** 2004. Toll-like receptor 4 (TLR4) does not confer a resistance advantage on mice against low-dose aerosol infection with virulent type A Francisella tularensis. Microb. Pathog. **37**:185–191.
47. **Chen W, Kuolee R, Shen H, Busa M, Conlan JW.** 2005. Toll-like receptor 4 (TLR4) plays a relatively minor role in murine defense against primary intradermal infection with Francisella tularensis LVS. Immunol. Lett. **97**:151–154.
48. **Child R, Wehrly TD, Rockx-Brouwer D, Dorward DW, Celli J.** 2010. Acid phosphatases do not contribute to the pathogenesis of type A Francisella tularensis. Infect. Immun. **78**:59–67.
49. **Chong A, et al.** 2008. The early phagosomal stage of Francisella tularensis determines optimal phagosomal escape and Francisella pathogenicity island protein expression. Infect. Immun. **76**:5488–5499.
50. **Chu P, Rodriguez AR, Arulanandam BP, Klose KE.** 2011. Tryptophan prototrophy contributes to Francisella tularensis evasion of gamma interferon-mediated host defense. Infect. Immun. **79**:2356–2361.
51. **Clay CD, Soni S, Gunn JS, Schlesinger LS.** 2008. Evasion of complement-mediated lysis and complement C3 deposition are regulated by Francisella tularensis lipopolysaccharide O antigen. J. Immunol. **181**:5568–5578.
52. **Clemens DL, Lee BY, Horwitz MA.** 2005. Francisella tularensis enters macrophages via a novel process involving pseudopod loops. Infect. Immun. **73**:5892–5902.
53. **Clemens DL, Lee BY, Horwitz MA.** 2009. Francisella tularensis phagosomal escape does not require acidification of the phagosome. Infect. Immun. **77**:1757–1773.
54. **Clinton SR, Bina JE, Hatch TP, Whitt MA, Miller MA.** 2010. Binding and activation of host plasminogen on the surface of Francisella tularensis. BMC Microbiol. **10**:76.
55. **Cole LE, et al.** 2007. Toll-like receptor 2-mediated signaling requirements for Francisella tularensis live vaccine strain infection of murine macrophages. Infect. Immun. **75**:4127–4137.
56. **Collazo CM, Sher A, Meierovics AI, Elkins KL.** 2006. Myeloid differentiation factor-88 (MyD88) is essential for control of primary in vivo Francisella tularensis LVS infection, but not for control of intramacrophage bacterial replication. Microbes Infect. **8**:779–790.
57. **Colquhoun D, Duobu S.** 2011. Francisella infections in farmed and wild aquatic organisms. Vet. Res. **42**:47.
58. **Conlan JW, Chen W, Shen H, Webb A, KuoLee R.** 2003. Experimental tularemia in mice challenged by aerosol or intradermally with virulent strains of Francisella tularensis: bacteriologic and histopathologic studies. Microb. Pathog. **34**:239–248.
59. **Crane DD, Warner SL, Bosio CM.** 2009. A novel role for plasmin-mediated degradation of opsonizing antibody in the evasion of host immunity by virulent, but not attenuated, Francisella tularensis. J. Immunol. **183**:4593–4600.
60. **Cremer TJ, Amer A, Tridandapani S, Butchar JP.** 2009. Francisella tularensis regulates autophagy-related host cell signaling pathways. Autophagy **5**:125–128.
61. **Cremer TJ, et al.** 2011. Akt-mediated proinflammatory response of mononuclear phagocytes infected with Burkholderia cenocepacia occurs by a novel GSK3β-dependent, IκB kinase-independent mechanism. J. Immunol. **187**:635–643.
62. **Culkin SJ, Rhinehart-Jones T, Elkins KL.** 1997. A novel role for B cells in early protective immunity to an intracellular pathogen, Francisella tularensis strain LVS. J. Immunol. **158**:3277–3284.
63. **Cyktor JC, Turner J.** 2011. Interleukin-10 and immunity against prokaryotic and eukaryotic intracellular pathogens. Infect. Immun. **79**:2964–2973.
64. **de Bruin OM, et al.** 2011. The biochemical properties of the Francisella pathogenicity island (FPI)-encoded proteins IglA, IglB, IglC, PdpB and DotU suggest roles in type VI secretion. Microbiology **157**:3483–3491.
65. **de Bruin OM, Ludu JS, Nano FE.** 2007. The Francisella pathogenicity island protein IglA localizes to the bacterial cytoplasm and is needed for intracellular growth. BMC Microbiol. **7**:1.
66. **Decker T, Muller M, Stockinger S.** 2005. The yin and yang of type I interferon activity in bacterial infection. Nat. Rev. Immunol. **5**:675–687.
67. **Deng K, Blick R, Liu W, Hansen E.** 2006. Identification of Francisella tularensis genes affected by iron limitation. Infect. Immun. **74**:4224–4236.
68. **De Pascalis R, Taylor BC, Elkins KL.** 2008. Diverse myeloid and lymphoid cell subpopulations produce gamma interferon during early innate immune responses to Francisella tularensis live vaccine strain. Infect. Immun. **76**:4311–4321.
69. **Deretic V, Levine B.** 2009. Autophagy, immunity, and microbial adaptations. Cell Host Microbe **5**:527–549.
70. **Desvaux M, Hébraud M.** 2006. The protein secretion systems in Listeria: inside out bacterial virulence. FEMS Microbiol. Rev. **30**:774–805.
71. **Drysdale M, et al.** 2005. Capsule synthesis by Bacillus anthracis is required for dissemination in murine inhalation anthrax. EMBO J. **24**:221–227.
72. **Duenas AI, et al.** 2006. Francisella tularensis LPS induces the production of cytokines in human monocytes and signals via Toll-like receptor 4 with much lower potency than E. coli LPS. Int. Immunol. **18**:785–795.
73. **Dziarski R, Gupta D.** 2005. Staphylococcus aureus peptidoglycan is a Toll-like receptor 2 activator: a reevaluation. Infect. Immun. **73**:5212–5216.
74. **Edwards JA, Rockx-Brouwer D, Nair V, Celli J.** 2010. Restricted cytosolic growth of Francisella tularensis subsp. tularensis by IFN-gamma activation of macrophages. Microbiology **156**:327–339.
75. **Elkins KL, Cooper A, Colombini SM, Cowley SC, Kieffer TL.** 2002. In vivo clearance of an intracellular bacterium, Francisella tularensis LVS, is dependent on the p40 subunit of interleukin-12 (IL-12) but not on IL-12 p70. Infect. Immun. **70**:1936–1948.
76. **Elkins KL, Rhinehart-Jones TR, Culkin SJ, Yee D, Winegar RK.** 1996. Minimal requirements for murine resistance to infection with Francisella tularensis LVS. Infect. Immun. **64**:3288–3293.
77. **Elkins KL, Rhinehart-Jones TR, Stibitz S, Conover JS, Klinman DM.** 1999. Bacterial DNA containing CpG motifs stimulates lymphocyte-dependent protection of mice against lethal infection with intracellular bacteria. J. Immunol. **162**:2291–2298.
78. **Elser B, et al.** 2002. IFN-gamma represses IL-4 expression via IRF-1 and IRF-2. Immunity **17**:703–712.
79. **Eneslatt K, et al.** 2011. Persistence of cell-mediated immunity three decades after vaccination with the live vaccine strain of Francisella tularensis. Eur. J. Immunol. **41**:974–980.
80. **Fadok VA, et al.** 1998. Macrophages that have ingested apoptotic cells in vitro inhibit proinflammatory cytokine production through autocrine/

paracrine mechanisms involving TGF-beta, PGE2, and PAF. J. Clin. Invest. **101**:890–898.
81. **Fernandes-Alnemri T, Yu JW, Datta P, Wu J, Alnemri ES.** 2009. AIM2 activates the inflammasome and cell death in response to cytoplasmic DNA. Nature **458**:509–513.
82. **Fernandes-Alnemri T, et al.** 2010. The AIM2 inflammasome is critical for innate immunity to Francisella tularensis. Nat. Immunol. **11**:385–393.
83. **Fillatreau S.** 2011. Novel regulatory functions for Toll-like receptor-activated B cells during intracellular bacterial infection. Immunol. Rev. **240**:52–71.
84. **Fink SL, Cookson BT.** 2005. Apoptosis, pyroptosis, and necrosis: mechanistic description of dead and dying eukaryotic cells. Infect. Immun. **73**:1907–1916.
85. **Fontenot JD, Rudensky AY.** 2005. A well adapted regulatory contrivance: regulatory T cell development and the forkhead family transcription factor Foxp3. Nat. Immunol. **6**:331–337.
86. **Forestal CA, et al.** 2008. A conserved and immunodominant lipoprotein of Francisella tularensis is proinflammatory but not essential for virulence. Microb. Pathog. **44**:512–523.
87. **Forestal CA, et al.** 2007. Francisella tularensis has a significant extracellular phase in infected mice. J. Infect. Dis. **196**:134–137.
88. **Fujita T, Matsushita M, Endo Y.** 2004. The lectin-complement pathway—its role in innate immunity and evolution. Immunol. Rev. **198**:185–202.
89. **Gallois A, Klein JR, Allen LA, Jones BD, Nauseef WM.** 2001. Salmonella pathogenicity island 2-encoded type III secretion system mediates exclusion of NADPH oxidase assembly from the phagosomal membrane. J. Immunol. **166**:5741–5748.
90. **Geier H, Celli J.** 2011. Phagocytic receptors dictate phagosomal escape and intracellular proliferation of Francisella tularensis. Infect. Immun. **79**:2204–2214.
91. **Gil H, et al.** 2006. Deletion of TolC orthologs in Francisella tularensis identifies roles in multidrug resistance and virulence. Proc. Natl. Acad. Sci. U. S. A. **103**:12897–12902.
92. **Golovliov I, Baranov V, Krocova Z, Kovarova H, Sjöstedt A.** 2003. An attenuated strain of the facultative intracellular bacterium Francisella tularensis can escape the phagosome of monocytic cells. Infect. Immun. **71**:5940–5950.
93. **Gordon S, Martinez FO.** 2010. Alternative activation of macrophages: mechanism and functions. Immunity **32**:593–604.
94. **Gunn JS, Ernst RK.** 2007. The structure and function of Francisella lipopolysaccharide. Ann. N. Y. Acad. Sci. **1105**:202–218.
95. **Hagman KE, et al.** 1995. Resistance of Neisseria gonorrhoeae to antimicrobial hydrophobic agents is modulated by the mtrRCDE efflux system. Microbiology **141**:611–622.
96. **Hajjar AM, et al.** 2006. Lack of in vitro and in vivo recognition of Francisella tularensis subspecies lipopolysaccharide by Toll-like receptors. Infect. Immun. **74**:6730–6738.
97. **Hall JD, et al.** 2008. Infected-host-cell repertoire and cellular response in the lung following inhalation of Francisella tularensis Schu S4, LVS, or U112. Infect. Immun. **76**:5843–5852.
98. **Han S, Bishop BM, van Hoek ML.** 2008. Antimicrobial activity of human beta-defensins and induction by Francisella. Biochem. Biophys. Res. Commun. **371**:670–674.
99. **Henry T, Brotcke A, Weiss DS, Thompson LJ, Monack DM.** 2007. Type I interferon signaling is required for activation of the inflammasome during Francisella infection. J. Exp. Med. **204**:987–994.
100. **Hirakata Y, et al.** 2002. Multidrug efflux systems play an important role in the invasiveness of Pseudomonas aeruginosa. J. Exp. Med. **196**:109–118.
101. **Hornung V, et al.** 2009. AIM2 recognizes cytosolic dsDNA and forms a caspase-1-activating inflammasome with ASC. Nature **458**:514–518.
102. **Horwitz MA.** 1982. Phagocytosis of microorganisms. Rev. Infect. Dis. **4**:104–123.
103. **Horwitz MA.** 1984. Phagocytosis of the Legionnaires' disease bacterium (Legionella pneumophila) occurs by a novel mechanism: engulfment within a pseudopod coil. Cell **36**:27–33.
104. **Hoyal CR, et al.** 2003. Modulation of p47PHOX activity by site-specific phosphorylation: Akt-dependent activation of the NADPH oxidase. Proc. Natl. Acad. Sci. U. S. A. **100**:5130–5135.
105. **Hrstka R, et al.** 2007. Francisella tularensis strain LVS resides in MHC II-positive autophagic vacuoles in macrophages. Folia Microbiol. (Praha) **52**:631–636.
106. **Huang MT, et al.** 2010. Deletion of ripA alleviates suppression of the inflammasome and MAPK by Francisella tularensis. J. Immunol. **185**:5476–5485.
107. **Ishikawa H, Ma Z, Barber GN.** 2009. STING regulates intracellular DNA-mediated, type I interferon-dependent innate immunity. Nature **461**:788–792.
108. **Ishimoto H, et al.** 2006. Identification of hBD-3 in respiratory tract and serum: the increase in pneumonia. Eur. Respir. J. **27**:253–260.
109. **Janeway CA, Jr, Medzhitov R.** 2002. Innate immune recognition. Annu. Rev. Immunol. **20**:197–216.
110. **Jia Q, et al.** 2010. A Francisella tularensis live vaccine strain (LVS) mutant with a deletion in capB, encoding a putative capsular biosynthesis protein, is significantly more attenuated than LVS yet induces potent protective immunity in mice against F. tularensis challenge. Infect. Immun. **78**:4341–4355.
111. **Jones CL, Weiss DS.** 2011. TLR2 signaling contributes to rapid inflammasome activation during F. novicida infection. PLoS One **6**:e20609.
112. **Jones JW, et al.** 2010. Absent in melanoma 2 is required for innate immune recognition of Francisella tularensis. Proc. Natl. Acad. Sci. U. S. A. **107**:9771–9776.
113. **Kang PB, et al.** 2005. The human macrophage mannose receptor directs Mycobacterium tuberculosis lipoarabinomannan-mediated phagosome biogenesis. J. Exp. Med. **202**:987–999.
114. **Kanistanon D, et al.** 2008. A Francisella mutant in lipid A carbohydrate modification elicits protective immunity. PLoS Pathog. **4**:e24.
115. **Kawai T, Akira S.** 2010. The role of pattern-recognition receptors in innate immunity: update on Toll-like receptors. Nat. Immunol. **11**:373–384.
116. **Kieffer TL, Cowley S, Nano FE, Elkins KL.** 2003. Francisella novicida LPS has greater immunobiological activity in mice than F. tularensis LPS, and contributes to F. novicida murine pathogenesis. Microbes Infect. **5**:397–403.
117. **Kiss K, Liu W, Huntley JF, Norgard MV, Hansen EJ.** 2008. Characterization of fig operon mutants of Francisella novicida U112. FEMS Microbiol. Lett. **285**:270–277.
118. **Kofoed EM, Vance RE.** 2011. Innate immune recognition of bacterial ligands by NAIPs determines inflammasome specificity. Nature **477**:592–595.
119. **Krocova Z, et al.** 2008. Interaction of B cells with intracellular pathogen Francisella tularensis. Microb. Pathog. **45**:79–85.
120. **Lai XH, Golovliov I, Sjostedt A.** 2001. Francisella tularensis induces cytopathogenicity and apoptosis in murine macrophages via a mechanism that requires intracellular bacterial multiplication. Infect. Immun. **69**:4691–4694.
121. **Laird MH, et al.** 2009. TLR4/MyD88/PI3K interactions regulate TLR4 signaling. J. Leukoc. Biol. **85**:966–977.
122. **Larsson P, et al.** 2005. The complete genome sequence of Francisella tularensis, the causative agent of tularemia. Nat. Genet. **37**:153–159.
123. **Law HT, et al.** 2011. Francisella tularensis uses cholesterol and clathrin-based endocytic mechanisms to invade hepatocytes. Sci. Rep. **1**:192.
124. **Lee VT, Tam C, Schneewind O.** 2000. LcrV, a substrate for Yersinia enterocolitica type III secretion, is required for toxin targeting into the cytosol of HeLa cells. J. Biol. Chem. **275**:36869–36875.
125. **Leelaporn A, Yongyod S, Limsrivanichakorn S, Yungyuen T, Kiratisin P.** 2008. Francisella novicida bacteremia, Thailand. Emerg. Infect. Dis. **14**:1935–1937.
126. **Leiby DA, Fortier AH, Crawford RM, Schreiber RD, Nacy CA.** 1992. In vivo modulation of the murine immune response to Francisella tularensis LVS by administration of anticytokine antibodies. Infect. Immun. **60**:84–89.
127. **Levine B, Mizushima N, Virgin HW.** 2011. Autophagy in immunity and inflammation. Nature **469**:323–335.
128. **Li H, Nookala S, Bina XR, Bina JE, Re F.** 2006. Innate immune response to Francisella tularensis is mediated by TLR2 and caspase-1 activation. J. Leukoc. Biol. **80**:766–773.
129. **Li J, et al.** 2007. Attenuation and protective efficacy of an O-antigen-deficient mutant of Francisella tularensis LVS. Microbiology **153**:3141–3153.
130. **Lindemann SR, et al.** 2011. Francisella tularensis Schu S4 O-antigen and capsule biosynthesis gene mutants induce early cell death in human macrophages. Infect. Immun. **79**:581–594.
131. **Lindgren H, et al.** 2004. Factors affecting the escape of Francisella tularensis from the phagolysosome. J. Med. Microbiol. **53**:953–958.
132. **Lindgren H, et al.** 2009. The 58-kilodalton major virulence factor of

Francisella tularensis is required for efficient utilization of iron. Infect. Immun. **77**:4429–4436.
133. **Lindgren H, et al.** 2011. Iron content differs between Francisella tularensis subspecies tularensis and subspecies holarctica strains and correlates to their susceptibility to H_2O_2-induced killing. Infect. Immun. **79**:1218–1224.
134. **Lindgren H, et al.** 2007. Resistance of Francisella tularensis strains against reactive nitrogen and oxygen species with special reference to the role of KatG. Infect. Immun. **75**:1303–1309.
135. **Llewellyn AC, Jones CL, Napier BA, Bina JE, Weiss DS.** 2011. Macrophage replication screen identifies a novel Francisella hydroperoxide resistance protein involved in virulence. PLoS One **6**:e24201.
136. **Long GW, et al.** 1993. Detection of Francisella tularensis in blood by polymerase chain reaction. J. Clin. Microbiol. **31**:152–154.
137. **Lucas MA, Fretto LJ, McKee PA.** 1983. The binding of human plasminogen to fibrin and fibrinogen. J. Biol. Chem. **258**:4249–4256.
138. **Macela A, et al.** 1996. The immune response against Francisella tularensis live vaccine strain in Lps(n) and Lps(d) mice. FEMS Immunol. Med. Microbiol. **13**:235–238.
139. **Mahnke K, Schmitt E, Bonifaz L, Enk AH, Jonuleit H.** 2002. Immature, but not inactive: the tolerogenic function of immature dendritic cells. Immunol. Cell Biol. **80**:477–483.
140. **Maier TM, et al.** 2007. Identification of Francisella tularensis Himar1-based transposon mutants defective for replication in macrophages. Infect. Immun. **75**:5376–5389.
141. **Mariathasan S, Weiss DS, Dixit VM, Monack DM.** 2005. Innate immunity against Francisella tularensis is dependent on the ASC/caspase-1 axis. J. Exp. Med. **202**:1043–1049.
142. **Mariathasan S, et al.** 2006. Cryopyrin activates the inflammasome in response to toxins and ATP. Nature **440**:228–232.
143. **Marshall JG, et al.** 2001. Restricted accumulation of phosphatidylinositol 3-kinase products in a plasmalemmal subdomain during Fc gamma receptor-mediated phagocytosis. J. Cell Biol. **153**:1369–1380.
144. **Martinon F, Mayor A, Tschopp J.** 2009. The inflammasomes: guardians of the body. Annu. Rev. Immunol. **27**:229–265.
145. **McCaffrey RL, Allen LA.** 2006. Francisella tularensis LVS evades killing by human neutrophils via inhibition of the respiratory burst and phagosome escape. J. Leukoc. Biol. **80**:1224–1230.
146. **McCaffrey RL, et al.** 2010. Multiple mechanisms of NADPH oxidase inhibition by type A and type B Francisella tularensis. J. Leukoc. Biol. **88**:791–805.
147. **McCoy GW.** 1911. Some features of the squirrel plague problem. Cal. State J. Med. **9**:105–109.
148. **Medina EA, Morris IR, Berton MT.** 2010. Phosphatidylinositol 3-kinase activation attenuates the TLR2-mediated macrophage proinflammatory cytokine response to Francisella tularensis live vaccine strain. J. Immunol. **185**:7562–7572.
149. **Meibom KL, Charbit A.** 2010. Francisella tularensis metabolism and its relation to virulence. Front. Microbiol. **1**:140.
150. **Melillo AA, Bakshi CS, Melendez JA.** 2010. Francisella tularensis antioxidants harness reactive oxygen species to restrict macrophage signaling and cytokine production. J. Biol. Chem. **285**:27553–27560.
151. **Melillo AA, et al.** 2009. Identification of Francisella tularensis live vaccine strain CuZn superoxide dismutase as critical for resistance to extracellularly generated reactive oxygen species. J. Bacteriol. **191**:6447–6456.
152. **Miao EA, et al.** 2010. Innate immune detection of the type III secretion apparatus through the NLRC4 inflammasome. Proc. Natl. Acad. Sci. U. S. A. **107**:3076–3080.
153. **Michell S, et al.** 2010. Deletion of the Bacillus anthracis capB homologue in Francisella tularensis subspecies tularensis generates an attenuated strain that protects mice against virulent tularaemia. J. Med. Microbiol. **59**:1275–1284.
154. **Miethke M, Marahiel MA.** 2007. Siderophore-based iron acquisition and pathogen control. Microbiol. Mol. Biol. Rev. **71**:413–451.
155. **Mohapatra NP, et al.** 2010. Francisella acid phosphatases inactivate the NADPH oxidase in human phagocytes. J. Immunol. **184**:5141–5150.
156. **Mohapatra NP, et al.** 2008. Combined deletion of four Francisella novicida acid phosphatases attenuates virulence and macrophage vacuolar escape. Infect. Immun. **76**:3690–3699.
157. **Monroe KM, McWhirter SM, Vance RE.** 2010. Induction of type I interferons by bacteria. Cell. Microbiol. **12**:881–890.
158. **Mulero V, Brock JH.** 1999. Regulation of iron metabolism in murine J774 macrophages: role of nitric oxide-dependent and -independent pathways following activation with gamma interferon and lipopolysaccharide. Blood **94**:2383–2389.
159. **Murray P, Rosentthal K, Pfaller M.** 2005. Medical microbiology, 5th ed. Elsevier Mosby, Philadelphia, PA.
159a. **Nallaparaju KC, et al.** 31 March 2011. Evasion of IFN-γ signaling by Francisella novicida is dependent upon Francisella outer membrane protein C. PLoS One **6**:e18201.
160. **Nano FE, Schmerk C.** 2007. The Francisella pathogenicity island. Ann. N. Y. Acad. Sci. **1105**:122–137.
161. **Nauseef WM.** 2004. Assembly of the phagocyte NADPH oxidase. Histochem. Cell Biol. **122**:277–291.
162. **Nemeth E, et al.** 2004. Hepcidin regulates cellular iron efflux by binding to ferroportin and inducing its internalization. Science **306**:2090–2093.
163. **Neves P, et al.** 2010. Signaling via the MyD88 adaptor protein in B cells suppresses protective immunity during Salmonella typhimurium infection. Immunity **33**:777–790.
164. **O'Farrell AM, Liu Y, Moore KW, Mui AL.** 1998. IL-10 inhibits macrophage activation and proliferation by distinct signaling mechanisms: evidence for Stat3-dependent and -independent pathways. EMBO J. **17**:1006–1018.
165. **Pan X, Tamilselvam B, Hansen EJ, Daefler S.** 2010. Modulation of iron homeostasis in macrophages by bacterial intracellular pathogens. BMC Microbiol. **10**:64.
166. **Parsa KV, et al.** 2008. Francisella gains a survival advantage within mononuclear phagocytes by suppressing the host IFNgamma response. Mol. Immunol. **45**:3428–3437.
167. **Parsa KV, et al.** 2006. Macrophage pro-inflammatory response to Francisella novicida infection is regulated by SHIP. PLoS Pathog. **2**:e71.
168. **Parsot C.** 1994. Shigella flexneri: genetics of entry and intercellular dissemination in epithelial cells. Curr. Top. Microbiol. Immunol. **192**:217–241.
169. **Pechous R, et al.** 2006. Construction and characterization of an attenuated purine auxotroph in a Francisella tularensis live vaccine strain. Infect. Immun. **74**:4452–4461.
170. **Pekarek RS, Bostian KA, Bartelloni PJ, Calia FM, Beisel WR.** 1969. The effects of Francisella tularensis infection on iron metabolism in man. Am. J. Med. Sci. **258**:14–25.
171. **Peng K, Broz P, Jones J, Joubert LM, Monack D.** 2011. Elevated AIM2-mediated pyroptosis triggered by hypercytotoxic Francisella mutant strains is attributed to increased intracellular bacteriolysis. Cell Microbiol. **13**:1586–1600.
172. **Peng K, Monack DM.** 2010. Indoleamine 2,3-dioxygenase 1 is a lung-specific innate immune defense mechanism that inhibits growth of Francisella tularensis tryptophan auxotrophs. Infect. Immun. **78**:2723–2733.
173. **Periasamy S, et al.** 2011. Development of tolerogenic dendritic cells and regulatory T cells favors exponential bacterial growth and survival during early respiratory tularemia. J. Leukoc. Biol. **90**:493–507.
174. **Philpott DJ, Girardin SE.** 2010. Nod-like receptors: sentinels at host membranes. Curr. Opin. Immunol. **22**:428–434.
175. **Phipps RP, Stein SH, Roper RL.** 1991. A new view of prostaglandin E regulation of the immune response. Immunol. Today **12**:349–352.
176. **Pierini LM.** 2006. Uptake of serum-opsonized Francisella tularensis by macrophages can be mediated by class A scavenger receptors. Cell. Microbiol. **8**:1361–1370.
177. **Pilatz S, et al.** 2006. Identification of Burkholderia pseudomallei genes required for the intracellular life cycle and in vivo virulence. Infect. Immun. **74**:3576–3586.
178. **Platz GJ, et al.** 2010. A tolC mutant of Francisella tularensis is hypercytotoxic compared to the wild type and elicits increased proinflammatory responses from host cells. Infect. Immun. **78**:1022–1031.
179. **Poole K, Krebes K, McNally C, Neshat S.** 1993. Multiple antibiotic resistance in Pseudomonas aeruginosa: evidence for involvement of an efflux operon. J. Bacteriol. **175**:7363–7372.
180. **Raetz CR, et al.** 2009. Discovery of new biosynthetic pathways: the lipid A story. J. Lipid Res. **50**(Suppl.):S103–S108.
181. **Rajaram MV, et al.** 2009. Akt and SHIP modulate Francisella escape from the phagosome and induction of the Fas-mediated death pathway. PLoS One **4**:e7919.
182. **Ramakrishnan G, Meeker A, Dragulev B.** 2008. fslE is necessary for siderophore-mediated iron acquisition in Francisella tularensis Schu S4. J. Bacteriol. **190**:5353–5361.
183. **Rathinam VA, et al.** 2010. The AIM2 inflammasome is essential for host

defense against cytosolic bacteria and DNA viruses. Nat. Immunol. **11**: 395–402.
184. **Ray K, Marteyn B, Sansonetti PJ, Tang CM.** 2009. Life on the inside: the intracellular lifestyle of cytosolic bacteria. Nat. Rev. Microbiol. **7**:333–340.
185. **Recalcati S, Taramelli D, Conte D, Cairo G.** 1998. Nitric oxide-mediated induction of ferritin synthesis in J774 macrophages by inflammatory cytokines: role of selective iron regulatory protein-2 downregulation. Blood **91**:1059–1066.
186. **Reilly TJ, Baron GS, Nano FE, Kuhlenschmidt MS.** 1996. Characterization and sequencing of a respiratory burst-inhibiting acid phosphatase from Francisella tularensis. J. Biol. Chem. **271**:10973–10983.
187. **Roberts TL, et al.** 2009. HIN-200 proteins regulate caspase activation in response to foreign cytoplasmic DNA. Science **323**:1057–1060.
188. **Rohmer L, et al.** 2007. Comparison of Francisella tularensis genomes reveals evolutionary events associated with the emergence of human pathogenic strains. Genome Biol. **8**:R102.
189. **Roth KM, Gunn JS, Lafuse W, Satoskar AR.** 2009. Francisella inhibits STAT1-mediated signaling in macrophages and prevents activation of antigen-specific T cells. Int. Immunol. **21**:19–28.
190. **Rus H, Cudrici C, Niculescu F.** 2005. The role of the complement system in innate immunity. Immunol. Res. **33**:103–112.
191. **Russo BC, et al.** 2011. A Francisella tularensis locus required for spermine responsiveness is necessary for virulence. Infect. Immun. **79**:3665–3676.
192. **Sandstrom G, Lofgren S, Tarnvik A.** 1988. A capsule-deficient mutant of Francisella tularensis LVS exhibits enhanced sensitivity to killing by serum but diminished sensitivity to killing by polymorphonuclear leukocytes. Infect. Immun. **56**:1194–1202.
193. **Sansonetti PJ, Ryter A, Clerc P, Maurelli AT, Mounier J.** 1986. Multiplication of Shigella flexneri within HeLa cells: lysis of the phagocytic vacuole and plasmid-mediated contact hemolysis. Infect. Immun. **51**:461–469.
194. **Santic M, Asare R, Skrobonja I, Jones S, Abu Kwaik Y.** 2008. Acquisition of the vacuolar ATPase proton pump and phagosome acidification are essential for escape of Francisella tularensis into the macrophage cytosol. Infect. Immun. **76**:2671–2677.
195. **Santic M, Molmeret M, Abu Kwaik Y.** 2005. Modulation of biogenesis of the Francisella tularensis subsp. novicida-containing phagosome in quiescent human macrophages and its maturation into a phagolysosome upon activation by IFN-gamma. Cell. Microbiol. **7**:957–967.
196. **Santic M, Molmeret M, Klose KE, Jones S, Kwaik YA.** 2005. The Francisella tularensis pathogenicity island protein IglC and its regulator MglA are essential for modulating phagosome biogenesis and subsequent bacterial escape into the cytoplasm. Cell. Microbiol. **7**:969–979.
197. **Sasakawa C, et al.** 1989. Functional organization and nucleotide sequence of virulence region-2 on the large virulence plasmid in Shigella flexneri 2a. Mol. Microbiol. **3**:1191–1201.
198. **Schaller-Bals S, Schulze A, Bals R.** 2002. Increased levels of antimicrobial peptides in tracheal aspirates of newborn infants during infection. Am. J. Respir. Crit. Care Med. **165**:992–995.
199. **Schlesinger LS, Bellinger-Kawahara CG, Payne NR, Horwitz MA.** 1990. Phagocytosis of Mycobacterium tuberculosis is mediated by human monocyte complement receptors and complement component C3. J. Immunol. **144**:2771–2780.
200. **Schlesinger LS, Horwitz MA.** 1990. Phagocytosis of leprosy bacilli is mediated by complement receptors CR1 and CR3 on human monocytes and complement component C3 in serum. J. Clin. Invest. **85**: 1304–1314.
201. **Schroder K, Hertzog PJ, Ravasi T, Hume DA.** 2004. Interferon-gamma: an overview of signals, mechanisms and functions. J. Leukoc. Biol. **75**: 163–189.
202. **Schulert GS, Allen LA.** 2006. Differential infection of mononuclear phagocytes by Francisella tularensis: role of the macrophage mannose receptor. J. Leukoc. Biol. **80**:563–571.
203. **Schulert GS, et al.** 2009. Francisella tularensis genes required for inhibition of the neutrophil respiratory burst and intramacrophage growth identified by random transposon mutagenesis of strain LVS. Infect. Immun. **77**:1324–1336.
204. **Sebastian S, et al.** 2007. A defined O-antigen polysaccharide mutant of Francisella tularensis live vaccine strain has attenuated virulence while retaining its protective capacity. Infect. Immun. **75**:2591–2602.
205. **Sen B, Meeker A, Ramakrishnan G.** 2010. The fslE homolog, FTL_0439 (fupA/B), mediates siderophore-dependent iron uptake in Francisella tularensis LVS. Infect. Immun. **78**:4276–4285.
206. **Shi CS, et al.** 2012. Activation of autophagy by inflammatory signals limits IL-1beta production by targeting ubiquitinated inflammasomes for destruction. Nat. Immunol. **13**:255–263.
207. **Shirey KA, Cole LE, Keegan AD, Vogel SN.** 2008. Francisella tularensis live vaccine strain induces macrophage alternative activation as a survival mechanism. J. Immunol. **181**:4159–4167.
208. **Sing A, et al.** 2002. Yersinia V-antigen exploits Toll-like receptor 2 and CD14 for interleukin 10-mediated immunosuppression. J. Exp. Med. **196**:1017–1024.
209. **Sjöstedt A.** 2007. Tularemia: history, epidemiology, pathogen physiology, and clinical manifestations. Ann. N. Y. Acad. Sci. **1105**:1–29.
210. **Sjostedt A, Conlan JW, North RJ.** 1994. Neutrophils are critical for host defense against primary infection with the facultative intracellular bacterium Francisella tularensis in mice and participate in defense against reinfection. Infect. Immun. **62**:2779–2783.
211. **Sorokin VM, Pavlovich NV, Prozorova LA.** 1996. Francisella tularensis resistance to bactericidal action of normal human serum. FEMS Immunol. Med. Microbiol. **13**:249–252.
212. **Stinavage P, Martin L, Spitznagel J.** 1989. O antigen and lipid A phosphoryl groups in resistance of Salmonella typhimurium LT-2 to nonoxidative killing in human polymorphonuclear neutrophils. Infect. Immun. **57**:3894–3900.
213. **Su J, et al.** 2011. The capBCA locus is required for intracellular growth of Francisella tularensis LVS. Front. Microbiol. **2**:83.
214. **Su J, et al.** 2007. Genome-wide identification of Francisella tularensis virulence determinants. Infect. Immun. **75**:3089–3101.
215. **Sullivan JT, Jeffery EF, Shannon JD, Ramakrishnan G.** 2006. Characterization of the siderophore of Francisella tularensis and role of fslA in siderophore production. J. Bacteriol. **188**:3785–3795.
216. **Takeda K, Akira S.** 2004. TLR signaling pathways. Semin. Immunol. **16**:3–9.
217. **Tamilselvam B, Daefler S.** 2008. Francisella targets cholesterol-rich host cell membrane domains for entry into macrophages. J. Immunol. **180**: 8262–8271.
218. **Taylor MW, Feng GS.** 1991. Relationship between interferon-gamma, indoleamine 2,3-dioxygenase, and tryptophan catabolism. FASEB J. **5**:2516–2522.
219. **Telepnev M, Golovliov I, Grundstrom T, Tarnvik A, Sjostedt A.** 2003. Francisella tularensis inhibits Toll-like receptor-mediated activation of intracellular signalling and secretion of TNF-alpha and IL-1 from murine macrophages. Cell. Microbiol. **5**:41–51.
220. **Thakran S, et al.** 2008. Identification of Francisella tularensis lipoproteins that stimulate the Toll-like receptor (TLR) 2/TLR1 heterodimer. J. Biol. Chem. **283**:3751–3760.
221. **Thomas RM, et al.** 2007. The immunologically distinct O antigens from Francisella tularensis subspecies tularensis and Francisella novicida are both virulence determinants and protective antigens. Infect. Immun. **75**:371–378.
222. **Travassos LH, et al.** 2004. Toll-like receptor 2-dependent bacterial sensing does not occur via peptidoglycan recognition. EMBO Rep. **5**:1000–1006.
223. **Twine S, et al.** 2005. A mutant of Francisella tularensis strain SCHU S4 lacking the ability to express a 58-kilodalton protein is attenuated for virulence and is an effective live vaccine. Infect. Immun. **73**:8345–8352.
224. **Ulland TK, et al.** 2010. Mutation of Francisella tularensis mviN leads to increased macrophage absent in melanoma 2 inflammasome activation and a loss of virulence. J. Immunol. **185**:2670–2674.
225. **Underhill DM, Ozinsky A.** 2002. Phagocytosis of microbes: complexity in action. Annu. Rev. Immunol. **20**:825–852.
226. **Virgin HW, Levine B.** 2009. Autophagy genes in immunity. Nat. Immunol. **10**:461–470.
227. **Wandersman C, Delepelaire P.** 1990. TolC, an Escherichia coli outer membrane protein required for hemolysin secretion. Proc. Natl. Acad. Sci. U. S. A. **87**:4776–4780.
228. **Wandersman C, Stojiljkovic I.** 2000. Bacterial heme sources: the role of heme, hemoprotein receptors and hemophores. Curr. Opin. Microbiol. **3**:215–220.
229. **Wang X, Ribeiro AA, Guan Z, Abraham SN, Raetz CR.** 2007. Attenuated virulence of a Francisella mutant lacking the lipid A 4′-phosphatase. Proc. Natl. Acad. Sci. U. S. A. **104**:4136–4141.
230. **Wang X, et al.** 2006. Structure and biosynthesis of free lipid A molecules

that replace lipopolysaccharide in Francisella tularensis subsp. novicida. Biochemistry **45**:14427–14440.
231. **Weinberg ED.** 1974. Iron and susceptibility to infectious disease. Science **184**:952–956.
232. **Weiss DS, et al.** 2007. In vivo negative selection screen identifies genes required for Francisella virulence. Proc. Natl. Acad. Sci. U. S. A. **104**: 6037–6042.
233. **Whitnack E, Beachey EH.** 1985. Inhibition of complement-mediated opsonization and phagocytosis of Streptococcus pyogenes by D fragments of fibrinogen and fibrin bound to cell surface M protein. J. Exp. Med. **162**:1983–1997.
234. **Wickstrum JR, et al.** 2009. Francisella tularensis induces extensive caspase-3 activation and apoptotic cell death in the tissues of infected mice. Infect. Immun. **77**:4827–4836.
235. **Wilson JE, Katkere B, Drake JR.** 2009. Francisella tularensis induces ubiquitin-dependent major histocompatibility complex class II degradation in activated macrophages. Infect. Immun. **77**:4953–4965.
236. **Woolard MD, et al.** 2007. Francisella tularensis-infected macrophages release prostaglandin E2 that blocks T cell proliferation and promotes a Th2-like response. J. Immunol. **178**:2065–2074.
237. **Yoshida R, Hayaishi O.** 1978. Induction of pulmonary indoleamine 2,3-dioxygenase by intraperitoneal injection of bacterial lipopolysaccharide. Proc. Natl. Acad. Sci. U. S. A. **75**:3998–4000.
238. **Yoshida R, Oku T, Imanishi J, Kishida T, Hayaishi O.** 1986. Interferon: a mediator of indoleamine 2,3-dioxygenase induction by lipopolysaccharide, poly(I) X poly(C), and pokeweed mitogen in mouse lung. Arch. Biochem. Biophys. **249**:596–604.
239. **Yu JJ, et al.** 2008. The presence of infectious extracellular Francisella tularensis subsp. novicida in murine plasma after pulmonary challenge. Eur. J. Clin. Microbiol. Infect. Dis. **27**:323–325.
240. **Zarrella TM, et al.** 2011. Host-adaptation of Francisella tularensis alters the bacterium's surface-carbohydrates to hinder effectors of innate and adaptive immunity. PLoS One **6**:e22335.
241. **Zegarra-Moran O, et al.** 2004. Double mechanism for apical tryptophan depletion in polarized human bronchial epithelium. J. Immunol. **173**: 542–549.
242. **Zhao J, et al.** 2006. IRF-8/interferon (IFN) consensus sequence-binding protein is involved in Toll-like receptor (TLR) signaling and contributes to the cross-talk between TLR and IFN-gamma signaling pathways. J. Biol. Chem. **281**:10073–10080.
243. **Zhao J, Raetz CR.** 2010. A two-component Kdo hydrolase in the inner membrane of Francisella novicida. Mol. Microbiol. **78**:820–836.

Crystal L. Jones obtained her B.S. in biology with honors from Georgia State University in 2005. There she studied the molecular mechanisms of iron uptake in *Bartonella quintana*. She is currently a Ph.D. candidate in the Microbiology and Molecular Genetics Program at Emory University, conducting research in the laboratory of Dr. David Weiss. Her research focuses on understanding the role of TLR2 in host defense against *Francisella* infection. She was awarded the National Science Foundation Graduate Research Fellowship.

Anna Llewellyn completed her B.S. at Georgia State University in 2006. Her undergraduate research project focused on quorum sensing and interspecies signaling. After a three-month appointment in a Peruvian multidrug-resistant tuberculosis clinical laboratory, she began working on her Ph.D. in microbiology and molecular genetics at Emory University in 2007. As a member of Dr. David Weiss' laboratory, her dissertation work has concentrated on elucidation of *Francisella* virulence mechanisms and intracellular host-pathogen interactions.

Brooke Napier obtained her undergraduate degree in neuroscience from Agnes Scott College in 2007. She then worked with Dr. Monica Farley's group in the Division of Infectious Diseases, Emory University School of Medicine, examining capsule-related sequences in the nonencapsulated human pathogen *Haemophilus influenzae.* She is currently working on a Ph.D. in microbiology and molecular genetics at Emory University in the lab of Dr. David Weiss. Her dissertation work focuses on elucidating novel mechanisms that pathogenic bacteria employ to evade the host immune response.

Max R. Schroeder is a graduate student at Emory University. He obtained his B.A. in microbiology from Ohio Wesleyan University, Delaware, OH. There, he studied the evolution of avian plumage coloration and bacterial feather degradation. His research interests are in molecular pathogenesis, and he is currently working on the genetic determinants of *Streptococcus pneumoniae* pathogenesis.

Tim Sampson received his B.S. in microbiology from the University of Pittsburgh, where he studied mycobacteriophage genetics with Dr. Graham Hatfull. There, he helped identify the first transposons within the mycobacteriophage population. He is currently a Ph.D. student in microbiology at Emory University, studying under Dr. David Weiss. He is a recipient of the NSF Graduate Research Fellowship and was named an ARCS Scholar. His current work focuses on the genetic mechanisms utilized by *Francisella* to evade recognition by the innate immune system, and he hopes to apply this knowledge to the development of novel vaccination strategies.

David S. Weiss is an Assistant Professor of Infectious Diseases at the Emory University School of Medicine and Emory Vaccine Center. He completed his Ph.D. on Toll-like receptors at the New York University School of Medicine under the guidance of Dr. Arturo Zychlinsky. His postdoctoral work in Dr. Denise Monack's lab at Stanford University focused on *Francisella tularensis* pathogenesis and inflammasome activation. His lab currently studies mechanisms of bacterial pathogenesis and host defense using *Francisella*, as well as mechanisms of antibiotic resistance using the nosocomial pathogen *Acinetobacter baumannii*.

Appendix B: Rapid killing of *Acinetobacter baumannii* by polymyxins is mediated by a hydroxyl radical death pathway

Timothy R. Sampson,[a,b,c] Xiang Liu,b,[c,d] Max R. Schroeder,[a] Colleen S. Kraft,[e,f] Eileen M. Burd,[e,f] and David S. Weiss[b,c,f]

Department of Microbiology and Immunology, Microbiology and Molecular Genetics Program,[a] Emory Vaccine Center,[b] Department of Pathology and Laboratory Medicine,[e] and Division of Infectious Diseases, Department of Medicine,[f] Emory University School of Medicine, and Yerkes National Primate Research Center[c] and Emory College,[d] Emory University, Atlanta, Georgia

Published in

Antimicrobial Agents and Chemotherapy

November 2012 Volume 56 Number 11 pages 5642–5649

M.R.S. performed killing experiments and assisted with writing and editing the paper.

AAC Journals.ASM.org

Rapid Killing of *Acinetobacter baumannii* by Polymyxins Is Mediated by a Hydroxyl Radical Death Pathway

Timothy R. Sampson,[a,b,c] Xiang Liu,[b,c,d] Max R. Schroeder,[a] Colleen S. Kraft,[e,f] Eileen M. Burd,[e,f] and David S. Weiss[b,c,f]

Department of Microbiology and Immunology, Microbiology and Molecular Genetics Program,[a] Emory Vaccine Center,[b] Department of Pathology and Laboratory Medicine,[e] and Division of Infectious Diseases, Department of Medicine,[f] Emory University School of Medicine, and Yerkes National Primate Research Center[c] and Emory College,[d] Emory University, Atlanta, Georgia

***Acinetobacter baumannii* is an opportunistic pathogen that is a cause of clinically significant nosocomial infections. Increasingly, clinical isolates of *A. baumannii* are extensively resistant to numerous antibiotics, and the use of polymyxin antibiotics against these infections is often the final treatment option. Historically, the polymyxins have been thought to kill bacteria through membrane lysis. Here, we present an alternative mechanism based on data demonstrating that polymyxins induce rapid cell death through hydroxyl radical production. Supporting this notion, we found that inhibition of radical production delays the ability of polymyxins to kill *A. baumannii*. Notably, we demonstrate that this mechanism of killing occurs in multidrug-resistant clinical isolates of *A. baumannii* and that this response is not induced in a polymyxin-resistant isolate. This study is the first to demonstrate that polymyxins induce rapid killing of *A. baumannii* and other Gram-negatives through hydroxyl radical production. This significantly augments our understanding of the mechanism of polymyxin action, which is critical knowledge toward the development of adjunctive therapies, particularly given the increasing necessity for treatment with these antibiotics in the clinical setting.**

Acinetobacter baumannii is an increasingly prevalent opportunistic pathogen that causes nosocomial infections (5, 6, 11, 34, 43, 47). This Gram-negative, aerobic, coccobacillus is responsible for a significant number of hospital-acquired infections, including those of the skin and bloodstream, as well as pneumonia and meningitis (5, 6, 18, 34, 47). Importantly, *A. baumannii* is able to persist on hospital surfaces for weeks to months, providing an environmental reservoir for its transmission (44–46). Compounding this problem, multidrug-resistant (MDR) strains of *A. baumannii* have been isolated with increasing frequency, and strains with pan-drug resistance (PDR) have been described as well, particularly among vulnerable patients within intensive care units or military hospitals (3, 11, 15, 33, 36, 39, 41). The polymyxin class of antibiotics is generally considered a final option of antibiotic therapy against MDR strains of *A. baumannii*, in large part due to the high potential for nephrotoxicity. Nonetheless, clinical use of the polymyxins, including polymyxin B and polymyxin E (colistin), to treat *A. baumannii* infection is increasing out of necessity due to antibiotic resistance (25, 26, 50).

Polymyxins are non-ribosomally synthesized, cationic antimicrobial peptides that bind to lipid A in the outer leaflet of the Gram-negative outer membrane (10, 32). Positively charged amino acid residues in the polymyxins form a ring that associates with negatively charged residues within lipid A through electrostatic interactions, causing membrane perturbations (10). In addition, polymyxins contain a string of hydrophobic amino acids which insert into the outer membrane, increasing bacterial membrane permeability (10). It has often been assumed that these membrane disruptions cause bacterial cell death directly through membrane lysis. However, reports from as far back as the late 1970s indicate that under certain conditions, polymyxins are capable of killing bacteria without lysis, suggesting that another mechanism of bacterial cell death may also be induced by treatment with these antibiotics (8, 21).

Recently, it has been demonstrated that a number of classes of antibiotics induce the production of lethal hydroxyl radicals within bacteria through the Fenton reaction (12, 22). Briefly, this reaction occurs when superoxides are converted to peroxides by superoxide dismutases present in the cell. Peroxides are capable of interacting with ferric iron associated with a number of biological molecules within the bacterial cell, oxidizing the iron and forming hydroxyl radicals in the process (16, 17, 22, 49). Ultimately, the concentration of hydroxyl radicals reaches levels that cannot be controlled, and the subsequent oxidative damage to DNA, lipids, and proteins eventually causes cell death (12, 22). Although hydroxyl radical-mediated cell death has been demonstrated with antibiotics that target intracellular proteins (12, 22), it is not known whether the classes of antibiotics that directly target the outer membrane (such as the polymyxins) cause cell death through a similar mechanism.

Here, we demonstrate that polymyxin B and colistin initiate rapid killing of both sensitive and MDR isolates of *A. baumannii*, as well as other Gram-negative species, through hydroxyl radical production. Treatment of *A. baumannii* with these antibiotics caused an increase in hydroxyl radicals and, furthermore, killing of *A. baumannii* by the polymyxins was delayed in the presence of inhibitors that both directly and indirectly block the production of oxygen radicals through the Fenton reaction. To our knowledge, this is the first demonstration of how the polymyxin family in-

Received 13 April 2012 **Returned for modification** 27 May 2012
Accepted 12 August 2012
Published ahead of print 20 August 2012
Address correspondence to David S. Weiss, david.weiss@emory.edu.
X.L. and M.R.S. contributed equally to this article.
Supplemental material for this article may be found at http://aac.asm.org/.

doi:10.1128/AAC.00756-12

TABLE 1 MICs for strains utilized in this study

Antibiotic	MICs (μg/ml)[a]			
	ATCC 17978	CI-2	CI-3	CI-4
Amikacin	≤16 (S)	≤16 (S)	>32 (R)	>32 (R)
Ampicillin-sulbactam	≤8/4 (S)	16/8 (I)	>16/8 (R)	16/8 (I)
Cefepime	≤8 (S)	>16 (R)	>16 (R)	>16 (R)
Ceftazidime	4 (S)	>16 (R)	>16 (R)	>16 (R)
Gentamicin	≤4 (S)	>8 (R)	>8 (R)	>8 (R)
Levofloxacin	≤2 (S)	≤2 (S)	>4 (R)	>4 (R)
Meropenem	≤4 (S)	≤4 (S)	>8 (R)	8 (I)
Ticarcillin-clavulanate	≤16 (S)	≤16 (S)	>64 (R)	>64 (R)
Tobramycin	≤4 (S)	8 (I)	>8 (R)	>8 (R)
Trimethoprim-sulfamethoxazole	>2/38 (R)	>2/38 (R)	>2/38 (R)	>2/38 (R)
Colistin	0.19 (S)	0.5 (S)	0.19 (S)	>256 (R)

[a] R, resistant; I, intermediate resistance; S, sensitive. For drug combinations, the two respective MICs are separated by a slash ("/").

duces rapid killing of *A. baumannii* and provides a rationale for previous observations of polymyxin-induced death without lysis observed in other species. With an increasing number of *A. baumannii* isolates demonstrating multidrug resistance, this study may provide clues as to how to exploit hydroxyl radical-mediated cell death to combat drug resistance in this and other drug-resistant bacterial pathogens.

MATERIALS AND METHODS

Bacterial strains and growth conditions. All *A. baumannii* strains (ATCC 17978, CI-2, CI-3, and CI-4), as well as *Escherichia coli* DH5α (Invitrogen, Grand Island, NY), were routinely grown from frozen stock in Mueller-Hinton (MH) broth (BD Biosciences, Sparks, MD) at 37°C with aeration. For *Francisella novicida* U112 (a gift from Denise Monack, Stanford University), 0.2% L-cysteine was added to the growth medium. CI-2, CI-3, and CI-4 were kindly provided by Brandi Limbago, Division of Health Care Quality Promotion, Centers for Disease Control and Prevention, Atlanta, GA. CI-2 was isolated in the District of Columbia in 2005, CI-3 was isolated in Ohio in 2006 by endotrachial aspirate, and CI-4 was isolated in Mississippi in 2010 from sputum.

Determination of MICs. Identification and antimicrobial susceptibility testing were performed using the MicroScan WalkAway Plus automated system (Siemens Medical Solutions Diagnostics, Deerfield, IL). Organism suspensions were prepared using the Prompt system (Siemens Medical Solutions Diagnostics) to inoculate Neg Combo 41 conventional identification susceptibility panels (Siemens Medical Solutions Diagnostics). Manual susceptibility testing using Etest strips (bioMérieux, Durham, NC) on MH agar was performed for colistin since it is not included on the MicroScan panel. Multidrug resistance (MDR) was defined as resistance to at least one member of three or more classes of antibiotic: aminoglycosides, beta-lactams, cephalosporins, or fluoroquinolones (29). Pan-drug resistance (PDR) was defined as resistance to all antibiotic therapies tested, including colistin (29).

Detection of hydroxyl radicals. Overnight cultures were subcultured 1:50 into MH broth for 2 h to an optical density at 600 nm of ~2. Cultures were centrifuged at 5,000 × *g* for 10 min, washed twice in phosphate-buffered saline (PBS; Lonza, Walkersville, MD), and diluted to 10^7 CFU/ml in PBS. The cells were subsequently treated with polymyxin B (USB, Cleveland, OH) or polymyxin E (colistin; Sigma-Aldrich, St. Louis, MO) at a final concentration of 2 μg/ml or with hydrogen peroxide at a final concentration of 0.15%, followed by incubation at 37°C with gentle shaking for 30 min. After treatment, the hydroxyl radical-specific fluorescent dye 3′-(*p*-hydroxyphenyl) fluorescein (HPF; Life Technologies, Grand Island, NY) was added to treated or untreated cultures at a final concentration of 5 μM. Fluorescence was immediately measured in a BioTek Synergy MX plate reader (BioTek, Winooski, VT) with an excitation setting of 490 nm and an emission setting of 515 nm, both with a 9-nm bandwidth.

Time-kill assays. To determine the levels of killing by antimicrobial compounds, time-kill experiments were performed as previously described (28). Overnight cultures were subcultured as described above and then diluted to a final concentration of 10^7 CFU/ml in MH broth. Samples were treated with 2 μg of either polymyxin B or colistin/ml (or 400 μg of colistin/ml for the *F. novicida* experiments) and incubated with aeration at 37°C. At the indicated time points, aliquots of treated cells were harvested, suitable dilutions were performed, and then the cells were plated onto MH agar plates. After overnight incubation of the plates at 37°C, CFU were enumerated. Thiourea (Sigma-Aldrich) was added to cultures concurrently at the indicated doses. When 2,2′-dipyridyl (MP Biomedical, Solon, OH) was utilized, the cells were pretreated for 20 min at 37°C with the indicated doses, before treatment with polymyxins. The addition of thiourea or 2,2′-dipyridyl did not alter growth kinetics in broth (see Fig. S1A and B in the supplemental material).

Statistics. All experiments were analyzed using a two-tailed, unpaired Student *t* test.

RESULTS

Polymyxins induce hydroxyl radical production. Polymyxins are thought to kill Gram-negative bacteria by binding to lipid A in the outer membrane and subsequently disrupting the stability of both the outer and inner membranes, ultimately leading to cell lysis (10, 32). Due to the observations that bactericidal antibiotic treatment induces the production of hydroxyl radicals within bacteria and that these radicals play a significant role in causing bacterial cell death through oxidative damage to DNA, lipids, and proteins (22), we sought to determine whether the last line polymyxin antibiotics induced hydroxyl radical-mediated cell death in *A. baumannii*.

In order to first establish a baseline of *A. baumannii* sensitivities to polymyxins, MICs were determined for the type strain, ATCC 17978 (Table 1). We next determined the kinetics of polymyxin-mediated killing of this strain. Time-kill assays revealed that polymyxin B-mediated killing of *A. baumannii* occurred quickly, with a >3-log reduction of viable cells within 30 min (Fig. 1). Furthermore, similar rapid killing kinetics occurred upon treatment with colistin (polymyxin E) at an identical dose (Fig. 1).

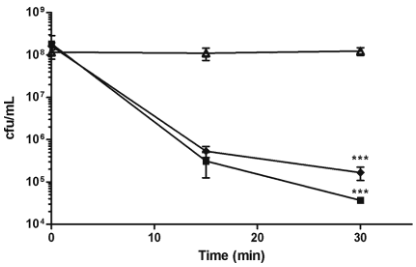

FIG 1 Polymyxins induce rapid killing of *A. baumannii*. *A. baumannii* cultures were treated with 2 μg of polymyxin B/ml (■) or colistin/ml (◆) or left untreated (△). At 0, 15, and 30 min, cultures were plated, and the CFU were enumerated. The data are representative of three independent experiments. Points represent the means and bars represent the standard deviation of triplicate samples. ***, $P < 0.0001$.

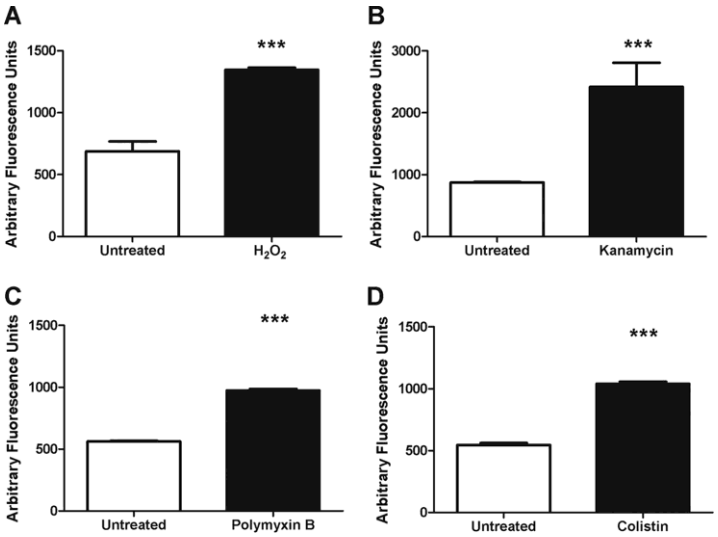

FIG 2 Polymyxins induce hydroxyl radical production. *A. baumannii* cultures were left untreated or were treated with 0.15% hydrogen peroxide (H_2O_2) (A), 5 μg of kanamycin/ml (B), 2 μg of polymyxin B/ml (C), or 2 μg of colistin/ml (D) for 30 min. After treatment, the hydroxyl radical specific fluorescent dye 3′-(*p*-hydroxyphenyl) fluorescein was added, and the fluorescence was measured (490 nm/515 nm). The data are representative of three independent experiments. Bars represent the means and standard deviations of triplicate samples. ***, $P < 0.0001$.

In order to determine whether hydroxyl radicals were induced during the observed rapid polymyxin killing, we utilized the cell permeable, hydroxyl radical-specific fluorescent dye, 3′-(*p*-hydroxyphenyl) fluorescein (HPF) (12). As positive controls, we treated cultures with hydrogen peroxide or kanamycin (previously demonstrated to induce hydroxyl radicals [22]) for 30 min and measured HPF fluorescence compared to untreated cultures (Fig. 2A and B). We observed an ~2-fold increase in fluorescence, indicating an increase in hydroxyl radical production. We next assayed the *A. baumannii* cultures treated with either polymyxin B or colistin and observed that both treatments induced an ~2-fold increase in fluorescence compared to the untreated control (Fig. 2C and D). To demonstrate that the increased fluorescence was not simply due to bacterial lysis, we sonicated *A. baumannii* and observed that the resulting lysates did not produce increased HPF fluorescence above the untreated control (see Fig. S2 in the supplemental material). These data indicate that lysis is not sufficient to cause an induction of HPF fluorescence and, furthermore, that hydroxyl radicals are induced by treatment with the polymyxins.

To determine whether polymyxin-mediated radical production was limited to its action on *A. baumannii*, we utilized the Gram-negative species *Escherichia coli* and *Francisella novicida*, a model intracellular pathogen (19). We first determined the kinetics of colistin-mediated killing in these species (see Fig. S3A and B in the supplemental material) and observed that both species were killed with similar kinetics as *A. baumannii* at the doses utilized. We subsequently measured hydroxyl radical production and observed a significant increase in HPF fluorescence following both kanamycin and colistin treatment of these strains (see Fig. S4A to D in the supplemental material). Together, these data indicate that treatment with polymyxins induces the production of hydroxyl radicals, and that radical production is concurrent with rapid killing of these Gram-negative species by polymyxins.

Rapid polymyxin killing of *A. baumannii* is mediated by hydroxyl radicals. Due to our observations that polymyxin B and colistin treatment induced hydroxyl radical production in *A. baumannii*, we sought to determine whether hydroxyl radicals were required for the rapid killing of *A. baumannii*. We therefore utilized a hydroxyl radical scavenging compound, thiourea (35), and assessed its ability to prevent polymyxin killing of *A. baumannii*. If hydroxyl radicals do indeed mediate the rapid killing of *A. baumannii*, then concurrent treatment with thiourea would be hypothesized to prevent cell death. In fact, when we performed time-kill assays in the presence of thiourea, we found a striking decrease in the ability of both polymyxin B and colistin to kill *A. baumannii* compared to treatment with either antibiotic alone (Fig. 3A and B). Notably, treatment with thiourea rescued survival to nearly the level observed in bacteria not treated with either antibiotic and markedly inhibited the rapid decrease in viability. We further examined the ability of thiourea to rescue colistin-mediated killing in *E. coli* and *F. novicida* and observed similar magnitudes of rescue in these organisms as well (see Fig. S3A and B in the supplemental material). As an additional control, we directly assayed the ability of thiourea to prevent colistin-mediated radical formation. We observed that thiourea significantly dampened the

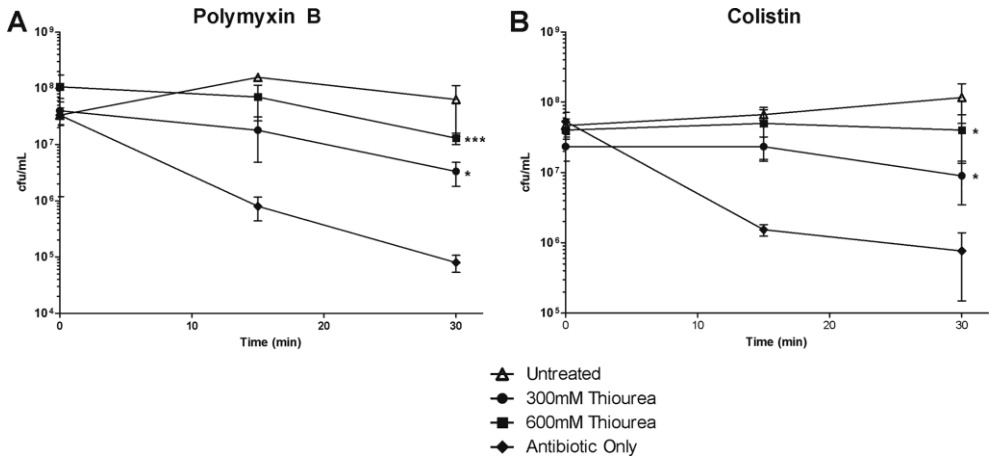

FIG 3 Polymyxin killing is delayed by hydroxyl radical quenching. *A. baumannii* cultures were treated with either 2 μg of polymyxin B/ml (A) or 2 μg of colistin/ml (B) alone (◆) or in combination with either 300 mM thiourea (●) or 600 mM thiourea (■), or they were left untreated in culture medium (△). At 0, 15, and 30 min, the cultures were plated, and the CFU were enumerated. The data are representative of three independent experiments. Points represent the means and bars represent the standard deviations of triplicate samples. ***, $P < 0.0001$; *, $P < 0.05$.

amount of colistin-mediated radical formation in *A. baumannii*, as well as in *E. coli* and *F. novicida* (see Fig. S5A to C in the supplemental material). Since quenching hydroxyl radicals delays killing, these data indicate that the radicals induced by the polymyxins play a significant role in mediating rapid cell death in *A. baumannii* and other Gram-negative species.

Polymyxin killing of *A. baumannii* is delayed by inhibition of the Fenton reaction. Previous studies have indicated that reactive oxygen species initiate an exponential increase in hydroxyl radical production through an intracellular Fenton reaction (12, 16, 22). The iron chelator, 2,2′-dipyridyl (dipyridyl), has previously been shown to be a potent inhibitor of the Fenton reaction by sequestering available iron, thereby preventing its interaction with peroxides (16). In order to determine whether Fenton chemistry was indeed playing a role in the killing of *A. baumannii* during polymyxin action, we assayed the ability of dipyridyl to prevent polymyxin-mediated killing. Treatment of *A. baumannii* with dipyridyl significantly inhibited killing by both polymyxin B and colistin (Fig. 4A and B). Furthermore, we determined that dipyridyl was also capable of rescuing colistin-mediated killing of *E. coli* and *F. novicida* (see Fig. S3A and B in the supplemental material). We further examined whether dipyridyl prevented colistin-mediated radical production, in *A. baumannii*, *E. coli*, and *F. novicida*. Similar to our results with thiourea, we observed a significant decrease in colistin-mediated hydroxyl radical production following treatment with dipyridyl (see Fig. S5A to C in the supplemental material). Since dipyridyl is capable of inhibiting the rapid loss of viability observed during polymyxin-mediated death, as well as the induction of hydroxyl radicals, these data implicate the involvement of the Fenton reaction in the rapid killing of *A. baumannii*, as well as other Gram-negative organisms, by the polymyxins. Together with the ability of the hydroxyl radical scavenger thiourea to inhibit polymyxin-mediated death, these iron depletion data strongly suggest that polymyxins induce rapid killing of Gram-negative bacteria through Fenton chemistry-mediated hydroxyl radical production.

Drug-resistant clinical isolates of *A. baumannii* are killed through hydroxyl radicals after polymyxin treatment. MDR and PDR clinical isolates of *A. baumannii* have been identified with increasing frequency and present a significant problem in health care settings (3, 33, 36, 39, 41). We therefore sought to determine whether the hydroxyl radical-mediated cell death pathway was induced in recent clinical isolates recalcitrant to the majority of current therapies. These isolates would therefore represent potential candidates for treatment with the polymyxins, including colistin. We first examined the ability of colistin to induce hydroxyl radical production in two MDR clinical isolates of *A. baumannii*, CI-2 and CI-3, both of which are colistin sensitive (Table 1). Consistent with our previous results, following 30 min of treatment with colistin, we observed a significant increase in hydroxyl radical production (Fig. 5A and B). Furthermore, we examined whether treatment of a PDR isolate, CI-4, which has significant resistance to colistin (Table 1), would induce the production of hydroxyl radicals. Interestingly, colistin treatment did not cause an induction of hydroxyl radicals in this strain (Fig. 5C), indicating that sublethal levels of colistin are not able to induce hydroxyl radicals, which is consistent with data on other antibiotic treatments (22). Together, these data suggest that the induction of hydroxyl radicals following colistin treatment is conserved in recent clinical isolates, and that colistin resistance prevents their induction.

To determine whether these hydroxyl radicals were participating in rapid killing by colistin, we utilized time-kill assays and assessed the ability of thiourea and dipyridyl to prevent colistin-mediated death in these clinical isolates of *A. baumannii*. We observed that by quenching radical oxygen species or depleting iron to suppress the Fenton reaction, the rapid killing of CI-2 and CI-3

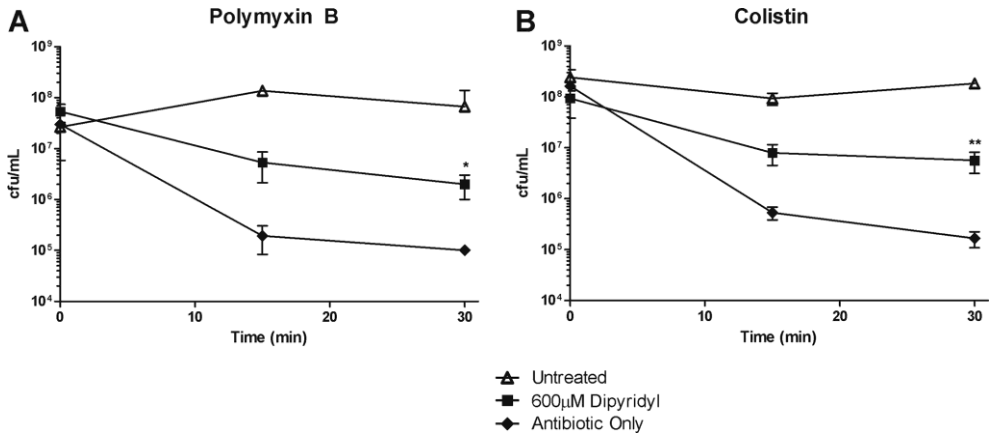

FIG 4 Polymyxin killing is mediated by iron. *A. baumannii* cultures were treated with either 2 μg of polymyxin B/ml (A) or 2 μg of colistin (B) alone (◆) or in combination with 600 μM dipyridyl (■), or they were left untreated in culture medium (△). At 0, 15, and 30 min, the cultures were plated, and the CFU were enumerated. The data are representative of three independent experiments. Points represent the means and bars the standard deviations of triplicate samples. **, $P < 0.005$; *, $P < 0.05$.

by colistin was significantly inhibited (Fig. 6A and B). Furthermore, the PDR/colistin-resistant isolate CI-4 did not demonstrate a significant change in viability following treatment with colistin, alone or in combination with thiourea or dipyridyl (Fig. 6C). In total, these data demonstrate that the induction of hydroxyl radicals by colistin is responsible for the rapid killing of sensitive *A. baumannii* isolates, including clinically important MDR strains, and that resistance to the polymyxins prevents hydroxyl radical production.

DISCUSSION

Classically, the polymyxins have been thought to kill bacteria through membrane disruptions and, ultimately, cell lysis (10). However, there exist historical reports of polymyxins killing bacteria without actively lysing those cells (8, 21). Here, we demonstrated that treatment with polymyxins induces hydroxyl radical production through the Fenton reaction and that this radical production mediates the rapid killing of *A. baumannii*, as well as *E. coli* and *F. novicida*.

Other bactericidal antibiotics, including the quinolones, β-lactams, and aminoglycosides, have previously been shown to induce the production of hydroxyl radicals, which ultimately mediate killing of *Escherichia coli* and *Staphylococcus aureus* (12, 22). Notably, each of these antibiotic classes interact directly with enzymes involved in different aspects of bacterial physiology: DNA replication, cell wall synthesis, and translation, respectively. Conversely, the polymyxins are not known to interact with bacterial enzymes and instead target lipid A in the outer membrane of Gram-negative bacteria (10, 32). Thus, their ability to both induce hydroxyl radicals and kill *A. baumannii* through hydroxyl radical production is somewhat surprising. To our knowledge, this is the first demonstration that the polymyxins induce an oxidative cell death pathway.

The mechanism by which polymyxin treatment induces the

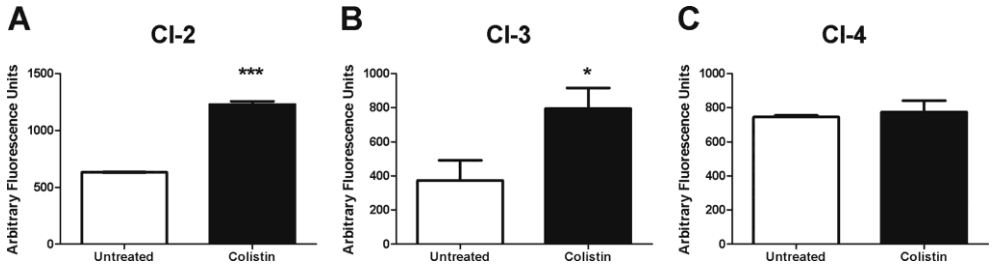

FIG 5 Colistin induces hydroxyl radical production in MDR clinical isolates. Cultures of colistin-sensitive MDR strain CI-2 (A) or CI-3 (B) or a colistin-resistant PDR *A. baumannii* strain CI-4 (C) were treated with 2 μg of colistin/ml or left untreated for 30 min. After treatment, the hydroxyl radical specific fluorescent dye 3′-(*p*-hydroxyphenyl) fluorescein was added, and fluorescence was measured (490 nm/515 nm). The data are representative of two independent experiments. Bars represent the means and standard deviations of triplicate samples. ***, $P < 0.0001$; *, $P < 0.05$.

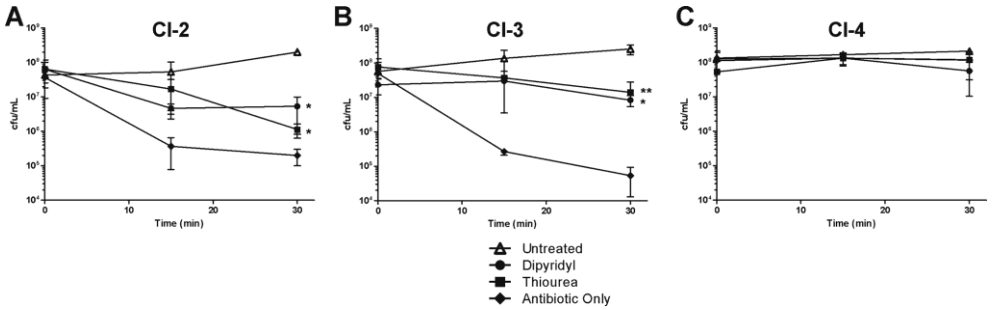

FIG 6 Clinical isolates are killed through hydroxyl radical production during polymyxin treatment. The colistin-sensitive MDR clinical isolates CI-2 (A) and CI-3 (B) or the colistin-resistant PDR *A. baumannii* strain CI-4 (C) were treated with 2 μg of colistin/ml (◆) alone or in combination with either 600 μM dipyridyl (●) or 600 mM thiourea (■), or they were left untreated in culture medium (△). At 0, 15, and 30 min, the cultures were plated, and the CFU were enumerated. The data are representative of two independent experiments. Points represent the means and bars represent the standard deviation of triplicate samples. **, $P < 0.005$; *, $P < 0.05$.

production of hydroxyl radicals in *A. baumannii* is not completely clear. Other bactericidal antibiotics were shown to induce a stress response in *E. coli*, disrupting the production of NADH by inhibiting the tricarboxylic acid cycle and thus ultimately causing aberrant respiration in the electron transport chain (12, 22). Disruptions in the electron transport chain promote the production of superoxide that can participate in the Fenton reaction and induce production of hydroxyl radicals (12, 16, 22). In addition, it has been demonstrated that the mistranslation of membrane proteins following treatment with aminoglycosides or the mammalian peptidoglycan recognition proteins activates the CpxAR two-component system in *E. coli*, which is involved in the bacterial envelope stress response, and subsequently triggers the depletion of NADH and production of hydroxyl radicals through the process described above (20, 23). It is therefore tempting to posit that the polymyxins may induce hydroxyl radicals in a similar fashion, by activating an envelope stress response in the bacterial cell, which shifts the metabolic state and causes aberrant electron transport. In fact, *Vibrio cholerae* treated with polymyxin B exhibits an increase in the transcriptional levels of *rpoE*, the sigma factor involved in envelope and oxidative stress responses (37). Interestingly, previous studies have indicated that polymyxin B treatment can induce aberrant oxidative respiration (31, 40, 42). In organisms with no experimentally identified CpxAR envelope stress-sensing two-component system, such as *A. baumannii* and *F. novicida*, this envelope stress response may be triggered by other, as-yet-unidentified, sensory systems. In total, these past observations are consistent with the data presented here and together suggest that killing of Gram-negative bacteria, including *A. baumannii*, by the polymyxins may follow the proposed conserved pathway of hydroxyl radical-mediated cell death. It is also interesting to consider the possibility that other membrane-targeting antibiotics, such as daptomycin, which depolarizes the bacterial membrane and also kills bacteria without causing lysis, induce this cell death pathway as well (7, 13).

Since polymyxin treatment is increasingly the last line therapeutic option for patients infected with MDR strains of *A. baumannii*, we further elucidated the conserved nature of hydroxyl radical-mediated killing in MDR clinical isolates. Not only did colistin treatment induce hydroxyl radical production in colistin-sensitive strains, but both thiourea and dipyridyl were able to inhibit the ability of colistin to kill these strains, indicating that hydroxyl radical-mediated cell death can occur in MDR nosocomial isolates of *A. baumannii* (Fig. 5 and 6). We also note that colistin resistance prevented the induction of hydroxyl radicals in *A. baumannii*.

Colistin resistance in *A. baumannii* has primarily been linked to changes in its lipid A, dampening or preventing the initial interaction between colistin and the bacterial envelope. These changes include complete loss of lipid A or additions of phosphoethanolamine to mask negatively charged phosphate moieties (2, 4, 14, 30, 38). *A. baumannii* can become resistant through mutations in genes necessary to produce lipid A or through mutations in the PmrAB two-component system, which signals for lipid A alterations (1, 2, 4). The PmrAB system is activated by ferric iron, and growth in iron replete conditions has been shown to provide a slight increase in the *A. baumannii* MIC for colistin, likely due to PmrAB activation of lipid A alterations (1, 2, 4). This is not contrary to our data, which suggests that when colistin interacts with the bacterial envelope, intracellular iron potentiates killing through the Fenton reaction and the induction of hydroxyl radicals (16). Thus, as we demonstrate, iron depletion prevents Fenton chemistry from potentiating the production of hydroxyl radicals following polymyxin treatment. Notably, it has been demonstrated that some pathogenic bacterial species limit intracellular iron, and those with lower levels have increased resistance to oxidative killing (27). It is interesting to consider the possibility that this intracellular iron limitation may provide resistance to a broad range of host defenses, as well as the polymyxins.

With the increasing frequency of *A. baumannii* as a nosocomial pathogen, a rising percentage of these infections requiring treatment with polymyxins, as well as the growing cost of treatment of infections with this pathogen, understanding the precise mechanism of action of these last line therapeutics is imperative (3, 5, 6, 24, 34, 36, 43, 47). Our findings not only

augment our knowledge of the mechanism of polymyxin action but also provide support to current concepts of utilizing hydroxyl radical-inducing agents as therapies against extensively drug-resistant pathogens (9, 48).

ACKNOWLEDGMENTS

We thank William Shafer, Emory University, for critical review of the manuscript; Philip Rather, Emory University, for critical review, reagents, and helpful discussion; Brandi Limbago, Division of Health Care Quality Promotion, Centers for Disease Control and Prevention, Atlanta, Georgia, for acquisition of the clinical isolates used in this study; and Crystal Jones, Emory University, for superb technical assistance.

This study was supported by National Institutes of Health (NIH) grants U54-AI057157 from the Southeastern Regional Center of Excellence for Emerging Infections and Biodefense and R21-AI098800. T.R.S. was supported by a National Science Foundation Graduate Research Fellowship, as well as the ARCS Foundation. C.S.K. was supported by KL2 RR025009.

The contents of this paper are solely the responsibility of the authors and do not necessarily represent the official views of the NIH.

REFERENCES

1. **Adams MD, et al.** 2009. Resistance to colistin in *Acinetobacter baumannii* associated with mutations in the PmrAB two-component system. Antimicrob. Agents Chemother. **53**:3628–3634.
2. **Arroyo LA, et al.** 2011. The *pmrCAB* operon mediates polymyxin resistance in *Acinetobacter baumannii* ATCC 17978 and clinical isolates through phosphoethanolamine modification of lipid A. Antimicrob. Agents Chemother. **55**:3743–3751.
3. **Baang JH, et al.** 2012. Longitudinal epidemiology of multidrug-resistant (MDR) *Acinetobacter* species in a tertiary care hospital. Am. J. Infect. Control **40**:134–137.
4. **Beceiro A, et al.** 2011. Phosphoethanolamine modification of lipid A in colistin-resistant variants of *Acinetobacter baumannii* mediated by the *pmrAB* two-component regulatory system. Antimicrob. Agents Chemother. **55**:3370–3379.
5. **Bergogne-Berezin E.** 2001. The increasing role of *Acinetobacter* species as nosocomial pathogens. Curr. Infect. Dis. Rep. **3**:440–444.
6. **Bergogne-Berezin E, Towner KJ.** 1996. *Acinetobacter* spp. as nosocomial pathogens: microbiological, clinical, and epidemiological features. Clin. Microbiol. Rev. **9**:148–165.
7. **Cotroneo N, Harris R, Perlmutter N, Beveridge T, Silverman JA.** 2008. Daptomycin exerts bactericidal activity without lysis of *Staphylococcus aureus*. Antimicrob. Agents Chemother. **52**:2223–2225.
8. **David HL, Rastogi N.** 1985. Antibacterial action of colistin (polymyxin E) against *Mycobacterium aurum*. Antimicrob. Agents Chemother. **27**:701–707.
9. **Davies BW, et al.** 2009. Hydroxyurea induces hydroxyl radical-mediated cell death in *Escherichia coli*. Mol. Cell **36**:845–860.
10. **Dixon RA, Chopra I.** 1986. Polymyxin B and polymyxin B nonapeptide alter cytoplasmic membrane permeability in *Escherichia coli*. J. Antimicrob. Chemother. **18**:557–563.
11. **Durante-Mangoni E, Zarrilli R.** 2011. Global spread of drug-resistant *Acinetobacter baumannii*: molecular epidemiology and management of antimicrobial resistance. Future Microbiol. **6**:407–422.
12. **Dwyer DJ, Kohanski MA, Hayete B, Collins JJ.** 2007. Gyrase inhibitors induce an oxidative damage cellular death pathway in *Escherichia coli*. Mol. Syst. Biol. **3**:91.
13. **Eisenstein BI.** 2008. Treatment of staphylococcal infections with cyclic lipopeptides. Clin. Microbiol. Infect. **14**(Suppl 2):10–16.
14. **Henry R, et al.** 2012. Colistin-resistant, lipopolysaccharide-deficient *Acinetobacter baumannii* responds to lipopolysaccharide loss through increased expression of genes involved in the synthesis and transport of lipoproteins, phospholipids, and poly-β-1,6-*N*-acetylglucosamine. Antimicrob. Agents Chemother. **56**:59–69.
15. **Hong KB, et al.** 2012. Investigation and control of an outbreak of imipenem-resistant *Acinetobacter baumannii* infection in a pediatric intensive care unit. Pediatr. Infect. Dis. J. **31**:685–690.
16. **Imlay JA, Chin SM, Linn S.** 1988. Toxic DNA damage by hydrogen peroxide through the Fenton reaction in vivo and in vitro. Science **240**:640–642.
17. **Imlay JA, Linn S.** 1988. DNA damage and oxygen radical toxicity. Science **240**:1302–1309.
18. **Jimenez-Mejias ME, et al.** 1997. Treatment of multidrug-resistant *Acinetobacter baumannii* meningitis with ampicillin/sulbactam. Clin. Infect. Dis. **24**:932–935.
19. **Jones CL, et al.** 2012. Subversion of host recognition and defense systems by *Francisella* spp. Microbiol. Mol. Biol. Rev. **76**:383–404.
20. **Kashyap DR, et al.** 2011. Peptidoglycan recognition proteins kill bacteria by activating protein-sensing two-component systems. Nat. Med. **17**:676–683.
21. **Klemperer RM, Gilbert P, Meier AM, Cozens RM, Brown MR.** 1979. Influence of suspending media upon the susceptibility of *Pseudomonas aeruginosa* NCTC 6750 and its spheroplasts to polymyxin B. Antimicrob. Agents Chemother. **15**:147–151.
22. **Kohanski MA, Dwyer DJ, Hayete B, Lawrence CA, Collins JJ.** 2007. A common mechanism of cellular death induced by bactericidal antibiotics. Cell **130**:797–810.
23. **Kohanski MA, Dwyer DJ, Wierzbowski J, Cottarel G, Collins JJ.** 2008. Mistranslation of membrane proteins and two-component system activation trigger antibiotic-mediated cell death. Cell **135**:679–690.
24. **Lee BY, McGlone SM, Doi Y, Bailey RR, Harrison LH.** 2010. Economic impact of *Acinetobacter baumannii* infection in the intensive care unit. Infect. Control Hosp. Epidemiol. **31**:1087–1089.
25. **Li J, et al.** 2006. Colistin: the re-emerging antibiotic for multidrug-resistant Gram-negative bacterial infections. Lancet Infect. Dis. **6**:589–601.
26. **Lim LM, et al.** 2010. Resurgence of colistin: a review of resistance, toxicity, pharmacodynamics, and dosing. Pharmacotherapy **30**:1279–1291.
27. **Lindgren H, et al.** 2011. Iron content differs between *Francisella tularensis* subspecies *tularensis* and subspecies *holarctica* strains and correlates to their susceptibility to H_2O_2-induced killing. Infect. Immun. **79**:1218–1224.
28. **Mai J, et al.** 2011. A novel target-specific, salt-resistant antimicrobial peptide against the cariogenic pathogen *Streptococcus mutans*. Antimicrob. Agents Chemother. **55**:5205–5213.
29. **Manchanda V, Sanchaita S, Singh N.** 2010. Multidrug resistant acinetobacter. J. Global Infect. Dis. **2**:291–304.
30. **Moffatt JH, et al.** 2010. Colistin resistance in *Acinetobacter baumannii* is mediated by complete loss of lipopolysaccharide production. Antimicrob. Agents Chemother. **54**:4971–4977.
31. **Mogi T, et al.** 2009. Polymyxin B identified as an inhibitor of alternative NADH dehydrogenase and malate: quinone oxidoreductase from the Gram-positive bacterium *Mycobacterium smegmatis*. J. Biochem. **146**:491–499.
32. **Morrison DC, Jacobs DM.** 1976. Binding of polymyxin B to the lipid A portion of bacterial lipopolysaccharides. Immunochemistry. **13**:813–818.
33. **Park YK, et al.** 2009. Extreme drug resistance in *Acinetobacter baumannii* infections in intensive care units, South Korea. Emerg. Infect. Dis. **15**:1325–1327.
34. **Peleg AY, Seifert H, Paterson DL.** 2008. *Acinetobacter baumannii*: emergence of a successful pathogen. Clin. Microbiol. Rev. **21**:538–582.
35. **Repine JE, Fox RB, Berger EM.** 1981. Hydrogen peroxide kills *Staphylococcus aureus* by reacting with staphylococcal iron to form hydroxyl radical. J. Biol. Chem. **256**:7094–7096.
36. **Sengstock DM, et al.** 2010. Multidrug-resistant *Acinetobacter baumannii*: an emerging pathogen among older adults in community hospitals and nursing homes. Clin. Infect. Dis. **50**:1611–1616.
37. **Sikora AE, Beyhan S, Bagdasarian M, Yildiz FH, Sandkvist M.** 2009. Cell envelope perturbation induces oxidative stress and changes in iron homeostasis in *Vibrio cholerae*. J. Bacteriol. **191**:5398–5408.
38. **Soon RL, et al.** 2011. Different surface charge of colistin-susceptible and -resistant *Acinetobacter baumannii* cells measured with zeta potential as a function of growth phase and colistin treatment. J. Antimicrob. Chemother. **66**:126–133.
39. **Sutter DE, et al.** 2011. High incidence of multidrug-resistant gram-negative bacteria recovered from Afghan patients at a deployed US military hospital. Infect. Control Hosp. Epidemiol. **32**:854–860.
40. **Terce F, Gillois M, Laneelle G.** 1979. Respiratory chain inhibition by

polymyxin b in a gram-positive bacterium (*Micrococcus luteus*). FEMS Microbiol. Lett. **6**:357–360.
41. **Tien HC, et al.** 2007. Multidrug resistant *Acinetobacter* infections in critically injured Canadian forces soldiers. BMC Infect. Dis. 7:95. doi: 10.1186/1471-2334-7-95.
42. **Tochikubo K, Yasuda Y, Kozuka S.** 1986. Decreased particulate NADH oxidase activity in *Bacillus subtilis* spores after polymyxin B treatment. J. Gen. Microbiol. **132**:277–287.
43. **Villers D, et al.** 1998. Nosocomial Acinetobacter baumannii infections: microbiological and clinical epidemiology. Ann. Intern. Med. **129**:182–189.
44. **Weber DJ, Rutala WA, Miller MB, Huslage K, Sickbert-Bennett E.** 2010. Role of hospital surfaces in the transmission of emerging health care-associated pathogens: norovirus, *Clostridium difficile*, and *Acinetobacter* species. Am. J. Infect. Control. **38**:S25–S33.
45. **Webster C, Towner KJ, Humphreys H.** 2000. Survival of Acinetobacter on three clinically related inanimate surfaces. Infect. Control Hosp. Epidemiol. **21**:246.
46. **Wendt C, Dietze B, Dietz E, Ruden H.** 1997. Survival of *Acinetobacter baumannii* on dry surfaces. J. Clin. Microbiol. **35**:1394–1397.
47. **Wolff M, et al.** 1997. The changing epidemiology of severe infections in the ICU. Clin. Microbiol. Infect. **3**:s36–s47.
48. **Wright GD.** 2007. On the road to bacterial cell death. Cell **130**:781–783.
49. **Yeom J, Imlay JA, Park W.** 2010. Iron homeostasis affects antibiotic-mediated cell death in *Pseudomonas* species. J. Biol. Chem. **285**:22689–22695.
50. **Zavascki AP, Goldani LZ, Li J, Nation RL.** 2007. Polymyxin B for the treatment of multidrug-resistant pathogens: a critical review. J. Antimicrob. Chemother. **60**:1206–1215.

Appendix C: A CRISPR-Cas system enhances envelope integrity mediating antibiotic resistance and inflammasome evasion

Timothy R. Sampson[a,b,c], Brooke A. Napier[a,b,c,*], Max R. Schroeder[a,*], Rogier Louwen[d], Jinshi Zhao[e], Chui-Yoke Chin[b,c], Hannah K. Ratner[a,b,c], Anna C. Llewellyn[a,b,c], Crystal L. Jones[a,b,c], Hamed Laroui[f], Didier Merlin[f], Pei Zhou[e], Hubert P. Endtz[d], and David S. Weiss[b,c,g]

[a]Department of Microbiology and Immunology, Microbiology and Molecular Genetics Program, [b]Emory Vaccine Center, and [c]Yerkes National Primate Research Center, Emory University, Atlanta, GA 30329; [d]Department of Medical Microbiology and Infectious Diseases, Erasmus Medical Center, University Medical Centre Rotterdam, Rotterdam, The Netherlands; [e]Department of Biochemistry, Duke University Medical Center, Durham, NC 27710; [f]Department of Biology, Center for Diagnostics and Therapeutics, Georgia State University, Atlanta, GA 30302; and [g]Division of Infectious Diseases, Department of Medicine, Emory University School of Medicine, Atlanta, GA 30322

*B.A.N. and M.R.S. contributed equally to this work.

Published in

Proceedings of the National Academy of Sciences

July 29, 2014 Volume 111 Number 30 pages 11163–11168

M.R.S. developed and executed the polymyxin B screen and assisted in editing the paper.

A CRISPR-Cas system enhances envelope integrity mediating antibiotic resistance and inflammasome evasion

Timothy R. Sampson[a,b,c], Brooke A. Napier[a,b,c,1,2], Max R. Schroeder[a,1], Rogier Louwen[d], Jinshi Zhao[e], Chui-Yoke Chin[b,c], Hannah K. Ratner[a,b,c], Anna C. Llewellyn[a,b,c,3], Crystal L. Jones[a,b,c,4], Hamed Laroui[f], Didier Merlin[f], Pei Zhou[e], Hubert P. Endtz[d], and David S. Weiss[b,c,g,5]

[a]Department of Microbiology and Immunology, Microbiology and Molecular Genetics Program, [b]Emory Vaccine Center, and [c]Yerkes National Primate Research Center, Emory University, Atlanta, GA 30329; [d]Department of Medical Microbiology and Infectious Diseases, Erasmus Medical Center, University Medical Centre Rotterdam, Rotterdam, The Netherlands; [e]Department of Biochemistry, Duke University Medical Center, Durham, NC 27710; [f]Department of Biology, Center for Diagnostics and Therapeutics, Georgia State University, Atlanta, GA 30302; and [g]Division of Infectious Diseases, Department of Medicine, Emory University School of Medicine, Atlanta, GA 30322

Edited by Ralph R. Isberg, Howard Hughes Medical Institute/Tufts University School of Medicine, Boston, MA, and approved June 13, 2014 (received for review December 12, 2013)

Clustered, regularly interspaced, short palindromic repeats–CRISPR associated (CRISPR-Cas) systems defend bacteria against foreign nucleic acids, such as during bacteriophage infection and transformation, processes which cause envelope stress. It is unclear if these machineries enhance membrane integrity to combat this stress. Here, we show that the Cas9-dependent CRISPR-Cas system of the intracellular bacterial pathogen *Francisella novicida* is involved in enhancing envelope integrity through the regulation of a bacterial lipoprotein. This action ultimately provides increased resistance to numerous membrane stressors, including antibiotics. We further find that this previously unappreciated function of Cas9 is critical during infection, as it promotes evasion of the host innate immune absent in melanoma 2/apoptosis associated speck-like protein containing a CARD (AIM2/ASC) inflammasome. Interestingly, the attenuation of the *cas9* mutant is complemented only in mice lacking both the AIM2/ASC inflammasome and the bacterial lipoprotein sensor Toll-like receptor 2, but not in single knockout mice, demonstrating that Cas9 is essential for evasion of both pathways. These data represent a paradigm shift in our understanding of the function of CRISPR-Cas systems as regulators of bacterial physiology and provide a framework with which to investigate the roles of these systems in myriad bacteria, including pathogens and commensals.

gene regulation | innate immune evasion

Clustered, regularly interspaced, short palindromic repeats–CRISPR associated (CRISPR-Cas) systems are adaptive bacterial defenses against foreign nucleic acids derived from bacteriophages, plasmids, and other sources (1–4). Foreign nucleic acids are targeted by direct hybridization of small CRISPR RNAs (crRNAs), which act in conjunction with conserved Cas proteins to mediate cleavage of the target. Interestingly, there is evidence that CRISPR-Cas components are up-regulated in the presence of bacteriophages or due to perturbations in the cell envelope (5–7), suggesting that CRISPR-Cas systems are induced in response to envelope stresses. Despite this up-regulation, it is unknown whether CRISPR-Cas systems function to counteract the stresses occurring at the envelope.

We demonstrated a role for components of a type II-B CRISPR-Cas system, which are encoded predominantly in pathogens and commensals (8–10), in the regulation of a membrane lipoprotein produced by the intracellular pathogen *Francisella novicida* (11). Through the action of the RNA-directed endonuclease Cas9 and two small RNAs, tracrRNA and scaRNA, the transcript for a bacterial lipoprotein (BLP; *FTN_1103*) is targeted and its stability altered, resulting in a decrease in protein production (*SI Appendix*, Fig. S1) (11). As this is the only known direct and natural example of CRISPR-Cas–mediated endogenous gene regulation, the *F. novicida* type II-B CRISPR-Cas system represents an important model to understand how these common prokaryotic genetic elements can act as regulators to control microbial physiology.

F. novicida is capable of causing disease in a number of mammalian species, including humans (12–14). During infection, *F. novicida* must resist the action of numerous antimicrobials that are present on mucosal surfaces and within phagosomes of innate immune cells such as macrophages (15). Compared with

Significance

Increasing the integrity of the bacterial envelope is necessary to allow the successful survival of bacterial pathogens within the host and allow them to counteract damage caused by membrane-targeting antibiotics. We demonstrate that components of a clustered, regularly interspaced, short palindromic repeats–CRISPR associated (CRISPR-Cas) system, a prokaryotic defense against viruses and foreign nucleic acid, act to regulate the permeability of the bacterial envelope, ultimately providing these cells with the capability to resist membrane damage caused by antibiotics. This regulation further allows bacteria to resist detection by multiple host receptors to promote virulence. Overall, this study demonstrates the breadth of function of CRISPR-Cas systems in regulation, antibiotic resistance, innate immune evasion, and virulence.

Author contributions: T.R.S. and D.S.W. designed research; T.R.S., B.A.N., M.R.S., R.L., J.Z., C.-Y.C., H.K.R., A.C.L., C.L.J., P.Z., and H.P.E. performed research; H.L. and D.M. contributed new reagents/analytic tools; T.R.S., B.A.N., M.R.S., R.L., J.Z., C.-Y.C., H.K.R., C.L.J., P.Z., H.P.E., and D.S.W. analyzed data; B.A.N. performed the immunofluorescence staining and imaging; M.R.S. developed and executed the polymyxin B screen; R.L. and H.P.E. performed experiments with *C. jejuni*; J.Z. and P.Z. isolated and analyzed the lipid A; C.-Y.C. performed surface charge analysis; H.K.R. performed susceptibility assays; A.C.L. generated the *FTN_1254* and *FTN_0109* mutants; C.L.J. made fundamental contributions to experimental direction; T.R.S. performed all other experiments; and T.R.S. and D.S.W. wrote the paper.

The authors declare no conflict of interest.

This article is a PNAS Direct Submission.

[1]B.A.N. and M.R.S. contributed equally to this work.

[2]Present address: Department of Microbiology and Immunology, Stanford University, Stanford, CA 94305.

[3]Present address: Coxiella Pathogenesis Section, Laboratory of Intracellular Parasites, Rocky Mountain Laboratories, National Institute of Allergy and Infectious Diseases, National Institutes of Health, Hamilton, MT 59840.

[4]Present address: Department of Wound Infections, Walter Reed Army Institute of Research, Silver Spring, MD 20910.

[5]To whom correspondence should be addressed. Email: david.weiss@emory.edu.

This article contains supporting information online at www.pnas.org/lookup/suppl/doi:10.1073/pnas.1323025111/-/DCSupplemental.

other Gram-negative species, *F. novicida* is highly resistant to the effects of several antimicrobials, including cationic antimicrobial peptides that disrupt bacterial membranes causing lysis and death (16–18). These cationic antimicrobial peptides act similarly to polymyxin antibiotics which are often used as surrogates for their study, and *F. novicida* is also extremely resistant to polymyxins. Following phagocytosis by macrophages, *F. novicida* escapes the phagosome and replicates to high titers in the cytosol (19). Throughout this cycle, the macrophage employs numerous pattern recognition receptors to respond to *F. novicida* infection. This includes the BLP receptor Toll-like receptor 2 (TLR2), present at both the plasma membrane and in the phagosome, which initiates a proinflammatory response (20). Additionally, *F. novicida* can be recognized in the host cytosol by the absent in melanoma 2/apoptosis associated speck-like protein containing a CARD (AIM2/ASC) inflammasome (21–23). This protein complex triggers activation of the cysteine protease caspase-1, which mediates an inflammatory host cell death. Cell death results in the loss of the intracellular replicative niche for *F. novicida*, and as such, plays an important role in controlling infection. Because both TLR2 and the AIM2/ASC inflammasome are important for host defense against *F. novicida* infection, dampening the activation of these innate signaling pathways is critical for *F. novicida* pathogenesis (24–26).

We initially sought to identify genes that allow *F. novicida* to resist antimicrobials, using polymyxin for these studies. Surprisingly, we identified the CRISPR-Cas gene *cas9* as being required for *F. novicida* resistance to this membrane-targeting antibiotic. We subsequently found that tracrRNA and scaRNA, two small RNAs that function with Cas9, were also necessary for polymyxin resistance, and that this process was dependent on their ability to repress production of the FTN_1103 BLP. We further observed that this regulation was critical for the enhancement of envelope integrity, which facilitated resistance to other antimicrobials as well. This process also occurred during infection of host cells and subsequently dampened AIM2/ASC inflammasome activation. The importance of Cas9-mediated evasion of the inflammasome, as well as evasion of TLR2, in *F. novicida* pathogenesis was highlighted by the demonstration that the *cas9* deletion mutant was rescued for virulence in mice lacking both ASC and TLR2, but not either component alone. Thus, the work presented here demonstrates that CRISPR-Cas systems are capable of enhancing the integrity of the bacterial envelope, a previously unappreciated role in bacterial physiology. This promotes resistance to antimicrobials and, during infection, facilitates the evasion of multiple innate defense pathways. This represents a previously unappreciated CRISPR-Cas function that is likely relevant to numerous bacteria, including pathogenic and commensal species.

Results

Cas9 Regulatory Axis Promotes Enhancement of Envelope Integrity. We sought to determine if CRISPR-Cas systems could enhance bacterial membrane integrity, because they are known to be upregulated in response to nucleic acid transfer events associated with envelope stress. A genetic screen for determinants of *F. novicida* resistance to the membrane targeting antibiotic polymyxin B (details of which can be found in the *SI Appendix*, Figs. S2 and S3 and Tables S1–S3) identified the gene encoding the CRISPR-Cas endonuclease Cas9 (*FTN_0757*). The *cas9* mutant was significantly hindered in its ability to grow in the presence of polymyxin, even at doses that had little effect on the growth of WT bacteria (Fig. 1*A* and *SI Appendix*, Fig. S4), and was also unable to resist a lethal dose of this antimicrobial (Fig. 1*B*). This defect could be successfully complemented by restoration of the *cas9* gene to the deletion mutant (*SI Appendix*, Fig. S5). In contrast, mutants lacking *cas1*, *cas2*, *cas4*, or the CRISPR locus were not defective in their ability to survive in the presence of polymyxin B (*SI Appendix*, Fig. S6). Resistance to polymyxin is often mediated by alterations to the structure of lipid A in the outer membrane and an increase in surface charge. However, the *cas9* deletion mutant produced a lipid A identical to WT cells (*SI Appendix*, Fig. S7) and had similar total surface charge (*SI Appendix*, Fig. S8). Together, these data clearly demonstrate the importance of Cas9 in the enhancement of resistance against a membrane-damaging antibiotic through a mechanism independent of lipid A modifications.

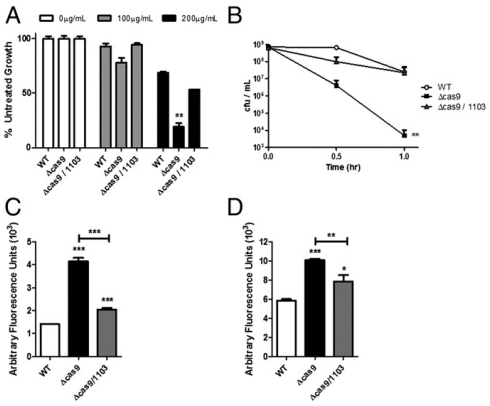

Fig. 1. The Cas9 regulatory axis is necessary for polymyxin resistance. (*A*) WT, *cas9*, or *cas9/1103* deletion mutants were grown overnight in broth culture containing the indicated concentration of polymyxin B. Percent growth compared with untreated cultures is plotted ($n = 3$). (*B*) 10^9 cfu of WT, *cas9*, or *cas9/1103* deletion mutants were treated with 800 μg/mL of polymyxin B, and cfu were enumerated at the indicated times to quantify antimicrobial killing. (*C* and *D*) WT, *cas9*, or *cas9/1103* deletion mutants were grown to midlog phase, washed, and stained with (*C*) propidium iodide or (*D*) ethidium bromide, and fluorescence was measured ($n = 3$). $*P \leq 0.05$; $**P \leq 0.005$; $***P \leq 0.001$.

Because *F. novicida* Cas9 functions with two small RNAs (tracrRNA and scaRNA; the three components are together referred to as the Cas9 regulatory system) to regulate an endogenous transcript encoding a membrane-localized BLP (FTN_1103) (11), we tested whether mutants lacking these small RNAs had a diminished ability to grow in the presence of polymyxin. tracrRNA and scaRNA deletion mutants exhibited an increase in susceptibility, similar to the *cas9* deletion strain (*SI Appendix*, Fig. S9 *A* and *B*). Furthermore, deletion of *FTN_1103* from the *cas9*, tracrRNA, or scaRNA mutants restored their resistance to polymyxin to near WT levels (Fig. 1*A* and *SI Appendix*, Fig. S9 *A* and *B*). In addition, we observed that the Cas9 regulatory axis mutants displayed a modest increase in susceptibility to the nonionic surfactant, Triton-X, but not hydrogen peroxide (*SI Appendix*, Figs. S10 and S11). We further found that these strains were more susceptible to streptomycin and kanamycin, first-line choices for treatment of *Francisella* infection (27) (*SI Appendix*, Figs. S12 and S13), in a manner dependent on overproduction of FTN_1103. These surprising observations suggest that the regulatory action of these CRISPR-Cas components promotes resistance to multiple antimicrobials through regulation of FTN_1103.

Because we observed a marked defect in antimicrobial resistance, we sought to address whether Cas9, tracrRNA, and scaRNA promoted resistance by enhancing the integrity of the bacterial envelope. We therefore directly analyzed the permeability of the *cas9* deletion mutant by measuring its uptake of propidium iodide (PI), which fluoresces when bound to nucleic acid. The *cas9* deletion mutant demonstrated a limited, yet significant, increase in fluorescence compared with WT bacteria,

indicating that it is more permeable to PI (Fig. 1*C*). Importantly, similar levels of colony-forming units were recovered from the mutant and WT bacteria during this experiment (*SI Appendix*, Fig. S14), and we observed no significant difference in the ability of the strains to grow in rich or minimal media (*SI Appendix*, Fig. S15), together indicating that although envelope permeability was altered, bacterial viability was unaffected. As a further proof of principle, we performed similar experiments with the nucleic acid-staining dye ethidium bromide (EtBr) and observed a near-identical increase in fluorescence in the *cas9* mutant (Fig. 1*D*). Comparable effects were observed in both the tracrRNA and scaRNA deletion mutants (*SI Appendix*, Fig. S16), which also did not display an observable defect during growth in broth (*SI Appendix*, Fig. S15). Furthermore, the increased permeability of all three mutant strains could be restored to near WT levels through deletion of *FTN_1103* (Fig. 1 *C* and *D* and *SI Appendix*, Fig. S16), demonstrating that overproduction of this envelope lipoprotein results in decreased envelope integrity. Thus, the Cas9 regulatory axis acts to directly enhance envelope integrity in part through regulation of a BLP and thereby mediates resistance to multiple antimicrobials.

Cas9 Regulatory Axis Promotes Enhanced Bacterial Integrity During Intracellular Infection. Because these data demonstrated a role for CRISPR-Cas components in enhancing envelope integrity during growth in broth culture, we examined whether they were necessary for a similar function during infection of macrophages, an important replicative niche for *F. novicida*. Importantly, Cas9 regulatory axis mutants and double mutants lacking *FTN_1103* survived and replicated to WT levels in macrophages (Fig. 2*A* and *SI Appendix*, Fig. S17*A*). However, during intracellular infection we observed that *cas9*, tracrRNA, and scaRNA deletion mutants displayed an almost 10-fold increase in PI staining, a measure of membrane permeability (Fig. 2 *B* and *C* and *SI Appendix*, Fig. S17 *B* and *C*). Additionally, intracellular permeability to PI was dependent on *FTN_1103*, further demonstrating the importance of repression of this membrane lipoprotein for the enhancement of envelope stability during infection of host cells (Fig. 2 *B* and *C* and *SI Appendix*, Fig. S17 *B* and *C*).

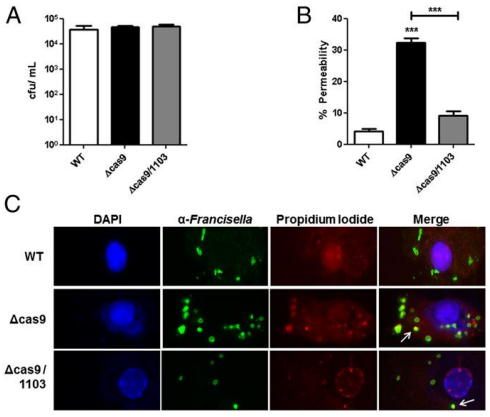

Fig. 2. Cas9 is necessary for enhanced envelope integrity during intracellular infection. (*A*) Bone marrow-derived macrophages were infected with WT, *cas9*, or *cas9/1103* deletion mutants at a multiplicity of infection (MOI) of 20:1 (bacteria per macrophage). At 4 h postinfection, macrophages were lysed and plated to enumerate colony-forming units. (*B* and *C*) Macrophages were infected as above, and at 4 h postinfection, were permeabilized with saponin and stained with anti-*Francisella* antibody (green), propidium iodide (nucleic acids, red), and DAPI (DNA, blue). Colocalization was determined as no less than 50% PI overlap with anti-*Francisella*. One thousand bacteria were counted per strain and quantified in *B*. Representative fluorescence micrographs are shown in *C*. Arrows indicate representative PI and anti-*Francisella* colocalization. Data are representative of at least three independent experiments in *A*, whereas *B* and *C* are compiled from four independent experiments. $***P \leq 0.001$.

Cas9, tracrRNA, and scaRNA Are Required for Evasion of Inflammasome Activation. Because we observed an increase in the permeability of Cas9 regulatory axis mutants during intracellular infection, we sought to determine if the lack of enhanced membrane integrity might correlate with increased recognition of bacterial components by host cytosolic receptors that activate innate immune signaling pathways. *Francisella* is recognized in the cytosol by the AIM2 inflammasome, which contains the adaptor protein ASC, and is partially activated in a TLR2-dependent manner (21–23, 28). Inflammasome activation leads to an inflammatory host cell death and loss of *Francisella*'s intracellular replicative niche. To determine if the loss of envelope integrity in the Cas9 regulatory axis mutants could result in an inability to dampen inflammasome activation, we measured cell death following infection of bone marrow-derived macrophages. Mutants lacking *cas9*, tracrRNA, or scaRNA (but not other components of the CRISPR-Cas system) displayed significantly higher levels of cytotoxicity than WT bacteria (Fig. 3*A* and *SI Appendix*, Figs. S18 and S19), through a signaling pathway that was partially dependent on TLR2 and completely dependent on ASC (Fig. 3*A*). We further found that in the absence of *FTN_1103*, cytotoxicity decreased to near WT levels (Fig. 3*A* and *SI Appendix*, Fig. S18), demonstrating that dysregulation of the FTN_1103 BLP is indeed the primary factor responsible for the increased activation of ASC-dependent cell death in the Cas9 regulatory axis mutants.

To directly address whether loss of envelope integrity could lead to increased inflammasome activation, we treated WT bacteria with a sublethal dose of polymyxin B. Although this dose did not result in a loss of cellular viability (*SI Appendix*, Fig. S20*A*), it resulted in an increase in envelope permeability as measured by EtBr staining (*SI Appendix*, Fig. S20*B*), similar in magnitude to that observed in the *cas9* deletion mutant (Fig. 1*C*). Upon infection of macrophages, WT bacteria pretreated with polymyxin B showed significantly more cytotoxicity than untreated bacteria in a manner that was partially TLR2-dependent and completely ASC-dependent (Fig. 3*B*), similar to the cell death elicited by the *cas9* deletion mutant (Fig. 3*A*). Thus, these data directly show that loss of envelope integrity can lead to increased inflammasome activation. Along with both the increased permeability and cytotoxicity of Cas9 regulatory axis mutants, these data demonstrate that Cas9-dependent enhancement of envelope integrity acts to promote evasion of the inflammasome.

The *cas9* Mutant Is Rescued for Virulence in ASC/TLR2-Deficient Mice. *cas9* deletion mutants are severely attenuated and unable to cause lethal infection in mice (11). However, the cause of this attenuation in vivo is not clear. Because Cas9 is important for evasion of both the inflammasome and TLR2, we tested whether the *cas9* mutant was rescued for virulence in the absence of these innate inflammatory pathways. Mice lacking ASC alone were able to control infection by the *cas9* deletion mutant, since the bacteria were undetectable in the spleen following infection (*SI Appendix*, Fig. S21*A*) and were unable to cause morbidity in these mice (*SI Appendix*, Fig. S21*B*). Similarly, mice lacking TLR2 alone were also capable of controlling infection by the *cas9* deletion mutant (*SI Appendix*, Fig. S21 *A* and *C*). We therefore generated mice lacking both of these innate immune

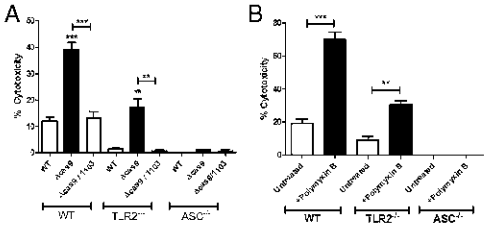

Fig. 3. Cas9 and enhanced envelope integrity promote evasion of inflammasome activation. (A) WT, TLR2$^{-/-}$, and ASC$^{-/-}$ bone marrow-derived macrophages were infected with WT, cas9, or cas9/1103 deletion mutants at a multiplicity of infection (MOI) of 20:1 (bacteria per macrophage). At 5.5 h postinfection, cells were assayed for cytotoxicity using the lactate dehydrogenase release assay (n = 3). (B) WT bacteria were untreated or pretreated for 30 min with 40 μg/mL polymyxin B and subsequently used to infect macrophages, and cytotoxicity was measured as in A (n = 3). Data are representative of at least three independent experiments. **P ≤ 0.005; ***P ≤ 0.001.

proteins, and infection of macrophages derived from these mice validated that the induction of both cell death and the inflammatory cytokine response by the cas9 deletion mutant were completely abrogated (SI Appendix, Fig. S22 A and B). Strikingly, during infection of these mice, the cas9 deletion mutant was significantly rescued for survival and replication (Fig. 4 A and B and SI Appendix, Fig. S21A). The level of the cas9 mutant increased at least 3 logs in the spleen and 2–3 logs in the liver (above the limit of detection) of infected ASC/TLR2-deficient mice, reaching the levels of WT bacteria observed in WT mice (Fig. 4 A and B). This robust increase in bacterial burden correlated with mortality, because >90% of infected ASC/TLR2-deficient mice succumbed to infection with the cas9 deletion mutant (Fig. 4 C and D). This increase in virulence of the cas9 mutant in ASC/TLR2-deficient mice highlights the essential role that Cas9 plays in facilitating the evasion of two distinct and critical host innate immune receptors, providing further evidence of the important roles that CRISPR-Cas systems can play in bacterial pathogenesis.

Discussion

Here, we demonstrate that the CRISPR-Cas endonuclease Cas9, working in conjunction with tracrRNA and scaRNA, is critical for enhancing the stability of the bacterial envelope and promoting resistance to polymyxin B, as well as other antibiotics. Expression of CRISPR-Cas components can be induced by bacterial envelope stress, disruptions in envelope protein localization (5), the presence of bacteriophage (6, 7), and during infection of host cells (11, 29, 30). Taken together, this suggests that CRISPR-Cas systems are induced in response to membrane stressors, and their regulatory activity can subsequently result in the enhancement of envelope integrity to promote resistance to such stressors. It is therefore tempting to speculate that the CRISPR-Cas response to envelope stress serves two distinct purposes: (i) the activation of its canonical function as the adaptive, foreign nucleic acid restriction system and (ii) the regulation of envelope structure and content to enhance the integrity of the bacterial envelope and combat membrane stress, which represents a previously unappreciated role in bacterial physiology and a shift in the understanding of these systems.

Our data demonstrate a role for CRISPR-Cas systems in promoting antibiotic resistance, whereas previous studies have focused instead on their ability to limit this process by restricting the acquisition of mobile elements, including those which carry resistance cassettes. Studies in several bacterial species revealed a correlation between increased antibiotic resistance and nonfunctional CRISPR-Cas systems (31–33). In fact, it has been demonstrated that acquisition of resistance traits can be restricted by CRISPR-Cas systems in vivo (34). In contrast, the

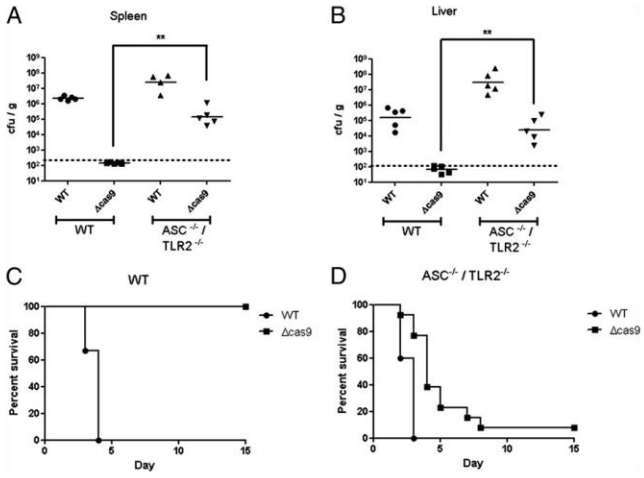

Fig. 4. A cas9 deletion mutant is rescued for virulence in mice lacking both ASC and TLR2. (A and B) WT or ASC/TLR2-deficient mice were inoculated s.c. with 10^5 cfu of WT or the cas9 deletion strain. Forty-eight hours postinfection, the (A) spleen and (B) liver were harvested and plated to quantify bacterial levels (n = 5). (C and D) Groups of 15 (C) WT or (D) ASC/TLR2-deficient mice were inoculated s.c. with 10^8 cfu of WT or cas9 deletion strains. Mice were monitored for survival over 15 d. Data are representative of at least two independent experiments in A and B; data are compiled from three independent experiments for C and D. **P ≤ 0.005.

data presented here suggest that CRISPR-Cas systems with regulatory functions may provide bacteria with the capacity to resist certain antibiotics. Thus, loss of these systems in antibiotic-resistant species may have unappreciated regulatory effects leading to altered bacterial physiology (i.e., envelope structure) and enhanced susceptibility to certain antibiotics. Delineating the regulatory functions of CRISPR-Cas systems in diverse bacteria will be required to more broadly assess their potential roles as antibiotic resistance determinants.

During infection, the ability of CRISPR-Cas systems to enhance envelope integrity has important ramifications for the virulence of *F. novicida*. We demonstrate here that Cas9 regulatory axis-mediated envelope enhancement is necessary to inhibit activation of the inflammasome and host cell death. This is broadly in agreement with the idea that mutant strains with membrane defects induce increased levels of inflammasome activation (24). Furthermore, we directly demonstrate that an increase in envelope permeability induced by polymyxin B treatment leads to enhanced inflammasome activation. Because the AIM2/ASC inflammasome responds to DNA released from *Francisella*, it is likely that increased envelope stability serves to prevent the release of nucleic acid, thereby subverting inflammasome activation (21, 23, 24). It has been posited that the AIM2/ASC inflammasome has a low threshold for activation, perhaps requiring only a single bacterium to release DNA (24). Therefore, small changes in envelope integrity may have drastic effects on inflammasome activation, while not having any observable effects on a bacterial population's viability as a whole. The regulation of BLP expression by the Cas9 regulatory axis thus limits the levels of this TLR2 ligand and subsequent activation of TLR2 (11), as well as promoting enhanced envelope integrity and subversion of the inflammasome. In the absence of both ASC and TLR2, the virulence of the *cas9* mutant is significantly restored (Fig. 4 *A*, *B*, and *D*), demonstrating the importance of Cas9-mediated innate immune evasion in the ability of *F. novicida* to cause disease.

Although *F. novicida* is the only known bacterial species in which Cas9 plays a clearly demonstrated regulatory role, it is likely that Cas9-dependent regulation contributes to the virulence of other pathogens encoding this protein including *Streptococcus* spp., *Legionella pneumophila*, *Listeria monocytogenes*, *Staphylococcus aureus*, and *Haemophilus parainfluenzae* (8, 9, 11, 29). In fact, a role for Cas9 in controlling virulence traits has been demonstrated in *Neisseria meningitidis* and *Campylobacter jejuni*. Each has been observed to require Cas9 for both invasion and replication in eukaryotic cells (11, 35). In addition, both of these species require Cas9 to attach to host cells, further supporting the hypothesis that CRISPR-Cas systems can have effects on the bacterial envelope (11, 35). Interestingly, we have additionally observed defects in the *C. jejuni* envelope in the absence of Cas9. A *cas9* deletion mutant in *C. jejuni* displays an increase in envelope permeability, similar to that observed in *F. novicida* (*SI Appendix*, Fig. S23*A*), and is significantly more sensitive to erythromycin, a first-line treatment for invasive campylobacteriosis (*SI Appendix*, Fig. S23*B*) (36). Therefore, although it is yet unknown how Cas9 may function as a regulator in *C. jejuni*, it is clear that these findings represent a broader role for Cas9 systems in modulating this important aspect of bacterial physiology.

CRISPR-Cas systems have more broadly been linked to other processes that involve the bacterial envelope and extracellular structures. For instance, the type I CRISPR-Cas system in *Pseudomonas aeruginosa* is capable of modulating biofilm formation (37, 38), and the type I system in *Myxococcus xanthus* is an essential component in regulating the development of fruiting bodies (39–41). These examples provide further support for a broader CRISPR-Cas function in the modification and regulation of the envelope and extracellular structures, extending beyond those organisms that encode Cas9. This unappreciated role for CRISPR-Cas systems would allow the myriad bacterial species encoding them to respond to envelope stresses that occur as a result of not only bacteriophage attack but also infection of host cells and exposure to other environmental conditions.

Experimental Procedures

Bacterial Manipulations. *F. novicida* strain U112 and all derivatives used in this study were routinely grown at 37 °C with aeration in tryptic soy broth (TSB) supplemented with 0.2% L-cysteine (BD Biosciences), or on tryptic soy agar plates supplemented with 0.1% L-cysteine. Cas9 regulatory axis deletion mutants and complementation strains were described previously (11, 42). *FTN_1254* and *FTN_0109* mutants were constructed by allelic exchange as described previously (43, 44) using primers in *SI Appendix*, Table S3.

Polymyxin Treatments. The indicated strains were grown overnight and subsequently diluted to an OD_{600} of 0.03 in Mueller-Hinton/cation-adjusted broth with 0.2% L-cysteine containing the specified doses of polymyxin B (USB Corporation). Following overnight growth at 37 °C with aeration, OD_{600} was measured and used to calculate the percent growth compared with the growth of the strain in media alone. For the killing assay, cultures were treated with 800 μg/mL of polymyxin B, incubated at 37 °C with aeration, and plated for colony-forming units at the indicated time points. For sublethal treatments with polymyxin, bacterial cultures were washed once and resuspended in media containing 40 μg/mL polymyxin B for 30 min. Treated cells were subsequently washed twice before preparing for infections as described below.

In Vitro Permeability. The indicated strains were grown overnight and subsequently subcultured 1:50 in TSB and grown to an OD_{600} of ∼0.8–0.9. Cells were washed twice in 50 mM phosphate buffer and resuspended in 50 mM phosphate buffer containing 30 μg/mL EtBr (Fisher Scientific) or 200 μM PI (Life Technologies). Fluorescence was measured immediately in a Biotek Synergy Mx plate reader using an excitation of 250 nm and emission of 605 nm for EtBr or excitation of 534 nm and emission of 617 nm for PI, correcting with samples lacking bacteria.

Macrophage Culture and Infection. Murine bone marrow-derived macrophages were prepared from WT C57BL/6 mice or the indicated knockout strains and cultured as described previously (42). Macrophages were seeded overnight and infected with overnight cultures of the indicated bacterial strains at a MOI of 20:1 bacteria per macrophage. Plates were centrifuged for 15 min at 335 × *g* at room temperature to promote bacterial uptake. Infected macrophages were incubated for 30 min at 37 °C and washed twice before adding DMEM containing 10 μg/mL gentamicin.

Intracellular Permeability. WT murine bone marrow-derived macrophages were seeded onto glass coverslips and infected as above. At 4 h postinfection, macrophages were gently permeabilized for 15 min at room temperature with 0.1% saponin/3% (wt/vol) BSA in PBS. Cells were first stained with 2.6 μM PI and chicken–anti-*F. novicida* antibody (a kind gift from Denise Monack, Stanford University) for 12 min at 37 °C. Following washing, cells were fixed with 4% (vol/vol) paraformaldehyde and incubated with FITC-labeled anti-chicken antibody. Coverslips were mounted onto glass slides with SlowFade Gold reagent with DAPI (Life Technologies). Slides were imaged on a Zeiss Axioscope Z.1 microscope and a Zeiss Imager 2.1 camera. Images were analyzed with Volocity 5.5 software (Perkin–Elmer). Colocalization was determined by no less than 50% overlap between PI and *Francisella*-positive cells, and 1,000 cells were counted for each strain.

Cytotoxicity Assays. Murine bone marrow-derived macrophages prepared from the indicated mice were infected with bacterial strains as described above. At 5.5 h postinfection, supernatants were collected and assayed for levels of lactate dehydrogenase using the nonradioactive cytotoxicity assay kit (Promega).

Murine Infections. $ASC^{-/-}$ and $TLR2^{-/-}$ C57BL/6 mice were a generous gift from Bali Pulendran, Emory Vaccine Center, Atlanta (with much appreciated assistance from Paul Hakimpour) and were bred together to generate mice deficient in both ASC and TLR2. Mice were bred and kept under specific-pathogen free conditions in filter-top cages at Yerkes National Primate Center, Emory University, and provided food and water ad libitum. For bacterial burden assays, female WT or ASC/TLR2-deficient mice (of 8–10 wk of age) were infected s.c. with 2×10^5 cfu of the indicated bacterial strains in sterile PBS. At 48 h postinfection, liver and spleen were harvested,

weighed, and homogenized in PBS, and serial dilutions were plated to enumerate colony-forming units. For survival experiments, mice were infected with 10^8 cfu s.c. and monitored for signs of illness. Mice were killed when they appeared moribund. All experimental procedures were approved by the Emory University Institutional Animal Care and Use Committee (Protocol #069-2008Y).

Statistics. Two-tailed, Student *t* tests were performed to analyze pairs of data as indicated, excluding the experiments in Fig. 4 *A* and *B*, which were analyzed with the Mann–Whitney test.

ACKNOWLEDGMENTS. We thank Emily Crispell, Thayer King, William Shafer, and Eric Skaar for helpful discussions and critical reading of this manuscript. This work was supported by National Institutes of Health (NIH) Grants U54-AI057157 from the Southeastern Regional Center of Excellence for Emerging Infections and Biodefense, R56-AI87673, and R01-AI110701 (to D.S.W., a Burroughs Wellcome Fund Investigator in the Pathogenesis of Infectious Disease). T.R.S. was supported by the National Science Foundation Graduate Research Fellowship Program and the Achievement Rewards for College Scientists Foundation. J.Z. and P.Z. were supported by NIH R01-AI055588 and GM5-1310.

1. Richter C, Chang JT, Fineran PC (2012) Function and regulation of clustered regularly interspaced short palindromic repeats (CRISPR) / CRISPR associated (Cas) systems. *Viruses* 4(10):2291–2311.
2. Fineran PC, Charpentier E (2012) Memory of viral infections by CRISPR-Cas adaptive immune systems: Acquisition of new information. *Virology* 434(2):202–209.
3. Sorek R, Lawrence CM, Wiedenheft B (2013) CRISPR-mediated adaptive immune systems in bacteria and archaea. *Annu Rev Biochem* 82:237–266.
4. Barrangou R, Marraffini LA (2014) CRISPR-Cas systems: Prokaryotes upgrade to adaptive immunity. *Mol Cell* 54(2):234–244.
5. Perez-Rodriguez R, et al. (2011) Envelope stress is a trigger of CRISPR RNA-mediated DNA silencing in *Escherichia coli*. *Mol Microbiol* 79(3):584–599.
6. Quax TE, et al. (2013) Massive activation of archaeal defense genes during viral infection. *J Virol* 87(15):8419–8428.
7. Young JC, et al. (2012) Phage-induced expression of CRISPR-associated proteins is revealed by shotgun proteomics in *Streptococcus thermophilus*. *PLoS ONE* 7(5): e38077.
8. Chylinski K, Le Rhun A, Charpentier E (2013) The tracrRNA and Cas9 families of type II CRISPR-Cas immunity systems. *RNA Biol* 10(5):726–737.
9. Chylinski K, Makarova KS, Charpentier E, Koonin EV (2014) Classification and evolution of type II CRISPR-Cas systems. *Nucleic Acids Res*, 10.1093/nar/gku241.
10. Schunder E, Rydzewski K, Grunow R, Heuner K (2013) First indication for a functional CRISPR/Cas system in *Francisella tularensis*. *Int J Med Microbiol* 303(2):51–60.
11. Sampson TR, Saroj SD, Llewellyn AC, Tzeng YL, Weiss DS (2013) A CRISPR/Cas system mediates bacterial innate immune evasion and virulence. *Nature* 497(7448):254–257.
12. Hand J, Scott-Waldron C, Balsamo G (2012) Outbreak of *Francisella novicida* infections among occupants at a long-term residential facility - Louisiana, April-July, 2011. *Louisiana Morbidity Rep* 23(1):1–6.
13. Birdsell DN, et al. (2009) *Francisella tularensis* subsp. *novicida* isolated from a human in Arizona. *BMC Res Notes* 2:1–6.
14. Leelaporn A, Yongyod S, Limsrivanichakorn S, Yungyuen T, Kiratisin P (2008) *Francisella novicida* Bacteremia, Thailand. *Emerg Infect Dis* 14(12):1935–1937.
15. Jones CL, et al. (2012) Subversion of host recognition and defense systems by *Francisella* spp. *Microbiol Mol Biol Rev* 76(2):383–404.
16. Han S, Bishop BM, van Hoek ML (2008) Antimicrobial activity of human beta-defensins and induction by *Francisella*. *Biochem Biophys Res Commun* 371(4):670–674.
17. Mohapatra NP, et al. (2007) Identification of an orphan response regulator required for the virulence of *Francisella* spp. and transcription of pathogenicity island genes. *Infect Immun* 75(7):3305–3314.
18. Urban C, Tiruvury H, Mariano N, Colon-Urban R, Rahal JJ (2011) Polymyxin-resistant clinical isolates of *Escherichia coli*. *Antimicrob Agents Chemother* 55(1):388–389.
19. Golovliov I, Baranov V, Krocova Z, Kovarova H, Sjöstedt A (2003) An attenuated strain of the facultative intracellular bacterium *Francisella tularensis* can escape the phagosome of monocytic cells. *Infect Immun* 71(10):5940–5950.
20. Cole LE, et al. (2010) Phagosomal retention of *Francisella tularensis* results in TIRAP/Mal-independent TLR2 signaling. *J Leukoc Biol* 87(2):275–281.
21. Fernandes-Alnemri T, et al. (2010) The AIM2 inflammasome is critical for innate immunity to *Francisella tularensis*. *Nat Immunol* 11(5):385–393.
22. Jones JW, et al. (2010) Absent in melanoma 2 is required for innate immune recognition of *Francisella tularensis*. *Proc Natl Acad Sci USA* 107(21):9771–9776.
23. Rathinam VA, et al. (2010) The AIM2 inflammasome is essential for host defense against cytosolic bacteria and DNA viruses. *Nat Immunol* 11(5):395–402.
24. Peng K, Broz P, Jones J, Joubert LM, Monack D (2011) Elevated AIM2-mediated pyroptosis triggered by hypercytotoxic *Francisella* mutant strains is attributed to increased intracellular bacteriolysis. *Cell Microbiol* 13(10):1586–1600.
25. Jones CL, Sampson TR, Nakaya HI, Pulendran B, Weiss DS (2012) Repression of bacterial lipoprotein production by *Francisella novicida* facilitates evasion of innate immune recognition. *Cell Microbiol* 14(10):1531–1543.
26. Mariathasan S, Weiss DS, Dixit VM, Monack DM (2005) Innate immunity against *Francisella tularensis* is dependent on the ASC/caspase-1 axis. *J Exp Med* 202(8): 1043–1049.
27. Word Health Organization (2007) WHO Guidelines on Tularaemia. *WHO Library Cataloguing-in Publication Data* (World Health Organization, Geneva), 978 92 4 154737 6.
28. Jones CL, Weiss DS (2011) TLR2 signaling contributes to rapid inflammasome activation during *F. novicida* infection. *PLoS ONE* 6(6):e20609.
29. Louwen R, Staals RH, Endtz HP, van Baarlen P, van der Oost J (2014) The role of CRISPR-Cas systems in virulence of pathogenic bacteria. *Microbiol Mol Biol Rev* 78(1): 74–88.
30. Gunderson FF, Cianciotto NP (2013) The CRISPR-associated gene cas2 of *Legionella pneumophila* is required for intracellular infection of amoebae. *MBio* 4(2): e00074–e13.
31. Palmer KL, Gilmore MS (2010) Multidrug-resistant enterococci lack CRISPR-cas. *MBio* 1(4):e00227–e10.
32. Dang TN, et al. (2013) Uropathogenic *Escherichia coli* are less likely than paired fecal *E. coli* to have CRISPR loci. *Infect Genet Evol* 19:212–218.
33. Burley KM, Sedgley CM (2012) CRISPR-Cas, a prokaryotic adaptive immune system, in endodontic, oral, and multidrug-resistant hospital-acquired *Enterococcus faecalis*. *J Endod* 38(11):1511–1515.
34. Bikard D, Hatoum-Aslan A, Mucida D, Marraffini LA (2012) CRISPR interference can prevent natural transformation and virulence acquisition during in vivo bacterial infection. *Cell Host Microbe* 12(2):177–186.
35. Louwen R, et al. (2013) A novel link between *Campylobacter jejuni* bacteriophage defence, virulence and Guillain-Barré syndrome. *Eur J Clin Microbiol Infect Dis* 32(2): 207–226.
36. Allos BM (2001) *Campylobacter jejuni* infections: Update on emerging issues and trends. *Clin Infect Dis* 32(8):1201–1206.
37. Cady KC, O'Toole GA (2011) Non-identity-mediated CRISPR-bacteriophage interaction mediated via the Csy and Cas3 proteins. *J Bacteriol* 193(14):3433–3445.
38. Zegans ME, et al. (2009) Interaction between bacteriophage DMS3 and host CRISPR region inhibits group behaviors of *Pseudomonas aeruginosa*. *J Bacteriol* 191(1): 210–219.
39. Viswanathan P, Murphy K, Julien B, Garza AG, Kroos L (2007) Regulation of dev, an operon that includes genes essential for *Myxococcus xanthus* development and CRISPR-associated genes and repeats. *J Bacteriol* 189(10):3738–3750.
40. Boysen A, Ellehauge E, Julien B, Søgaard-Andersen L (2002) The DevT protein stimulates synthesis of FruA, a signal transduction protein required for fruiting body morphogenesis in *Myxococcus xanthus*. *J Bacteriol* 184(6):1540–1546.
41. Thöny-Meyer L, Kaiser D (1993) devRS, an autoregulated and essential genetic locus for fruiting body development in *Myxococcus xanthus*. *J Bacteriol* 175(22):7450–7462.
42. Weiss DS, et al. (2007) In vivo negative selection screen identifies genes required for *Francisella* virulence. *Proc Natl Acad Sci USA* 104(14):6037–6042.
43. Brotcke A, et al. (2006) Identification of MglA-regulated genes reveals novel virulence factors in *Francisella tularensis*. *Infect Immun* 74(12):6642–6655.
44. Anthony LS, Gu MZ, Cowley SC, Leung WW, Nano FE (1991) Transformation and allelic replacement in *Francisella* spp. *J Gen Microbiol* 137(12):2697–2703.

Appendix D: Pleomorphic structures in human blood are red blood cell-derived microvesicles, not bacteria

Adam Mitchell MD[1]; Warren D. Gray PhD[1]; Max Schroeder BA[2]; Hong Yi MS[3]; Jeannette V. Taylor[3], Elizabeth R. Wright, PhD[3, 4]; David Stephens MD[2]; John D. Roback MD, PhD[5]; Charles D. Searles MD[1*]

[1]Division of Cardiology, Department of Medicine, Emory University; [2]Division of Infectious Disease, Department of Medicine, Emory University; [3]Robert P. Apkarian Integrated Electron Microscopy Core, Emory University; [4]Division of Infectious Disease, Department of Pediatrics, Emory University; [5]Center for Transfusion and Cellular Therapy, Department of Pathology and Laboratory Medicine, Emory University

Manuscript Under Review

M.R.S. participated in design and execution of experiments and edited the paper.

Abstract

Background: Red blood cell (RBC) transfusions are a common, life-saving therapy for many patients, but they have also been associated with poor clinical outcomes. We identified unusual, pleomorphic structures in human RBC transfusion units by negative-stain electron microscopy that appeared identical to those previously reported to be bacteria in healthy human blood samples. The presence of viable, replicating bacteria in stored blood could explain poor outcomes in transfusion recipients and have major implications for transfusion medicine. Here, we investigated the possibility that these structures were bacteria.

Results: Flow cytometry, miRNA analysis, protein analysis, and additional electron microscopy studies strongly indicated that the pleomorphic structures in the supernatant of stored RBCs were RBC-derived microvesicles (RMVs). Bacterial 16S rDNA PCR amplicons were sequenced and found to be highly similar to species that commonly contaminate lab reagents.

Conclusions: These studies suggest that pleomorphic structures identified in human blood are RMVs and not bacteria, and they provide an example in which laboratory contaminants may confound interpretation of EM data.

Key words: nanobacteria, healthy human blood, red blood cell, erythrocyte, microvesicle, microparticle

Background:

Red blood cell (RBC) transfusions are a necessary and often life-saving therapy, but have been associated with significant morbidity and mortality, though the mechanisms responsible for this association remain unclear (1). During the course of studying RBC-derived microvesicles (RMVs), that are known to accumulate over time in stored human RBC units, we detected submicron, pleomorphic structures by negative-stain electron microscopy (EM). A review of the literature revealed previous reports of identical, submicron, pleomorphic structures in human blood, that were characterized as bacteria (2, 3). McLaughlin et al. concluded that the pleomorphic structures were bacteria based on bacterial 16S rDNA sequencing, flow cytometry-based fluorescent *in situ* hybridization studies, the apparent ability of the structures to replicate, and their sensitivity to antibiotics (2). However, bacteria could not be cultured by standard techniques. Intrigued by the possibility of viable nanobacteria in RBC transfusion units as a possible etiology of poor clinical outcomes after transfusion, we examined the pleomorphic structures isolated from RBC storage units further, and conclude that these structures are not bacteria, but rather RMVs.

Results and discussion:

Electron microscopy of RMVs

Several groups have published electron micrographs of RMVs, thus we expected to find a mostly spherical morphology (4, 5). However, negative stain EM images (Figure 1A and B) of the unfixed pellet obtained from the supernatant of stored RBC units appeared identical to images published by McLaughlin et al. and Szymanski et al. In both of these

latter cases, the pleomorphic structures were reported to be bacteria. We consistently identified similar pleomorphic structures in RBC units obtained from >6 healthy donors; these structures were present immediately after donation (day 0) as well as after several weeks of storage at 4°C, under standard blood bank conditions. We reasoned that these pleomorphic structures were either RMVs with unusual morphology (possibly due to artifact), or they were in fact microbial in nature. We systematically ruled out possible sources of artifact – RBC centrifugation, washing of the carbon grid with water, a lack of albumin in the isolated pellet - and also performed TEM and SEM of fixed pellets (Figure 1, C-F). Regardless of how the unfixed samples were prepared, negative-stain EM reliably produced images represented in Figure 1 A and B. However, detailed analysis of fixed material by TEM and SEM revealed that, whereas some of the vesicles were pleomorphic and rod-like in shape, many retained the expected ellipsoidal shape (Figure 1, C-F) (4, 5). Further, comparison of fixed and unfixed samples by negative stain EM showed mostly ellipsoidal versus mostly pleomorphic, rod-like shaped vesicles respectively (Figure 1G and H).

Microbial DNA analysis of vesicles identifies common contaminants

To further assess whether bacterial DNA is present in the supernatant of stored RBC units, a large microvesicle pellet was isolated by sequential centrifugation of RBCs (100mL) that had been stored for 42 days under standard blood bank conditions. The pellet contained ~3 billion submicron, calcein-positive vesicles, as determined by flow cytometric analysis. DNA was extracted from the pelleted material and analyzed by standard gel electrophoresis. *S. pneumoniae* was used as a positive control, and molecular

grade water or molecular grade water passed through the Qiagen DNA extraction protocol were negative controls. Despite the isolation of very large numbers of these vesicles, no genomic DNA was observed on gel electrophoresis (Figure 2, A). Similar results were obtained using a phenol-chloroform based DNA extraction protocol. Subsequently, PCR was performed on the pelleted material using the same universal 16S rDNA primers as described by McLaughlin et al. PCR product was observed in pelleted vesicles and both positive and negative controls (Figure 2, B). The PCR product from each sample was purified and sequenced by single pass sequencing (Beckman Coulter Genomics) using the same 16S rDNA primers. BLAST analysis revealed that 16S sequences in the pelleted material were highly similar to *Pelomonas spp.* Sequences from molecular grade water and water passed through the Qiagen extraction protocol were related to *Bradyrhizobium spp.* and *Propionibacterium spp.*, respectively. All three species are known to be common contaminants in laboratory reagents (6). Of note, both species identified by McLaughlin et al. are also now known to be typical contaminants (*Stenotrophomonas spp.*, *Pseudomonas spp.*). As expected, 16S rDNA amplified from *S. pneumonia* DNA was identified as *S. pneumonia* (raw sequences available in supplemental material).

16S rDNA levels are unchanged in human serum incubated for up to 10 days

To further rule out the possibility of viable bacteria in the blood of healthy humans, serum from 3 donors was subjected to 16S rDNA qPCR analysis after incubation for 0, 5, and 10 days. The abundance of 16S rDNA would be expected to increase over time if

viable, replicating bacteria were present. Here, we did not find any change in the amount of 16S rDNA over time (ANOVA, $p = 0.53$) (Figure 2, C).

Flow cytometry, miRNA, and protein analysis indicate isolated structures are RMVs

Flow cytometric analysis demonstrated that all vesicles in the pelleted material from RBC storage units were positive for glycophorin-A (GPA), a RBC specific surface antigen, and calcein-AM (Figure 3, A), suggesting that they were membrane-bound and intact (7). Calcein-AM is a non-fluorescent, membrane permeable dye that becomes fluorescent and membrane impermeant after it is cleaved by esterases. RNA isolated from the vesicles was characterized using an Agilent Bioanalyzer and revealed that it contained only small RNA (Figure 3, B). miR-451, a miRNA known to be highly enriched in RBCs was highly abundant in both RBC and in RMV fractions, as compared to RNA isolated from cultured human aortic endothelial cells (HAECs), which have low levels of miR-451 and were used as a negative control (Figure 3, C). High levels of hemoglobin-alpha were detected in protein lysate of the vesicles and RBCs (Figure 3, D). Since the RMV pellet was washed extensively with PBS prior to RNA or protein isolation, it is not expected that the miR-451 or hemoglobin-alpha was derived from lysed RBCs in the stored unit.

In summary, unfixed negative-stain EM of material in the extracellular fluid of RBC units identified pleomorphic structures that appeared identical to those previously reported to be circulating bacteria. Our results suggest that these pleomorphic structures are RMVs, not viable bacteria. First, genomic DNA was undetectable in the extracellular material, even when very large numbers of vesicles were used for DNA isolation. Second,

incubation of serum samples from healthy humans at 30°C for up to 10 days failed to show any increase in bacterial 16S rDNA content. Third, 16S rDNA sequences amplified by PCR here and previously are known to be common contaminants in laboratory reagents (6). Lastly, isolated vesicles had intact membranes, RBC specific antigen on their surface, and relatively abundant amounts of hemoglobin alpha and miR-451, a miRNA highly expressed in RBCs (8).

The unusual, pleomorphic nature of the vesicles present in unfixed negative stain EM appeared to largely be due to the vesicles remaining flexible and deformable just prior to grid preparation. Whereas, most vesicles were observed to be ellipsoidal when fixed for negative stain EM, thin-section TEM, or SEM. However, a small fraction of particles seemed to have a rod-shaped morphology. Why RBC-derived vesicles would assume this seemingly energetically unfavorable morphology is not clear, though it may be related to the unique structural proteins or lipid content responsible for the biconcave shape of RBCs.

While it is accepted that bacteria transiently transmigrate into healthy human circulation, the concept that naturally occurring, viable nanobacteria routinely circulate in blood is not well supported. In general, the existence of nanobacteria is controversial (9), and, whereas multiple groups have provided evidence that nanobacteria-like structures can form spontaneously in human serum, the consensus opinion is that these structures are likely mineraloprotein complexes rather than microbes (10, 11).

Conclusions

The existence of pleomorphic nanobacteria in healthy human blood has been described elsewhere; however, our study suggests that pleomorphic structures observed in negative stain electron micrographs of human RBC storage units, plasma and serum are MVs and that 16S rDNA PCR products associated with these MVs are contaminants, commonly known to be present in laboratory reagents. In the case of RBC storage units, the pleomorphic structures in the extracellular fluid are RMVs, derived from RBC plasma membranes.

Methods

The Emory University IRB approved all studies and study participants gave written consent prior study participation.

Isolation of RBC-derived vesicles

Leukocyte-depleted RBC transfusion units were obtained from the blood bank at Emory University Hospital and stored from 0-42 days under standard conditions at 4°C. Blood product samples were obtained through a syringe port using a sterile 18-gauge needle under aseptic conditions. Samples were then prepared using a protocol developed to isolate microvesicles (MVs). RBCs were centrifuged at 1900 x g for 1 minute to pellet cells, the supernatant was transferred to a sterile tube, and centrifuged a second time at 800 x g for 10 minutes to pellet any residual RBCs. The supernatant was then centrifuged at 16,100 x g for 20 minutes to pellet MVs. The MV pellet was re-suspended in molecular grade PBS and either studied immediately or frozen in aliquots at minus 80°C.

Electron microscopy

Negative staining

The Robert P. Apkarian Integrated Electron Microscopy Core, Emory University performed transmission electron microscopy of the RBC vesicles using a standard negative staining protocol. Briefly, 400-mesh carbon coated copper grids were made hydrophilic by glow discharging. A 5-µl droplet of the pellet suspension, either unfixed or fixed with 2.5% glutaraldehyde, was placed on the grid, after 5 minutes, the grid with the suspension was rinsed by briefly touching the sample side to three drops of distilled water. The excess water on the grid was then removed by blotting the side of the grid on a piece of filter paper. For negative staining, 5 µl of 1% phosphotungstic acid (PTA) was applied onto the grid immediately after water removal, and then removed as described above after 30 seconds. The grid was allowed to completely dry before viewing in the microscope.

TEM

For thin-section TEM examination of embedded RBC vesicles, the samples were fixed with 2.5% glutaraldehyde in 0.1 M sodium cacodylate (pH 7.4). Samples were then washed with the same buffer twice and post-fixed with 1% osmium tetroxide and 1.5% potassium ferrocyanide in the same buffer, dehydrated through a graded ethanol series to 100%, and embedded in Eponate 12 resin (Ted Pella Inc., Redding, CA). Ultrathin sections were cut on a Leica UltraCut S ultramicrotome (Leica Microsystems Inc., Buffalo Grove, IL) at 70 nm, and counter-stained with 4% aqueous uranyl acetate and 2%

lead citrate. Sections were examined using a 120 kV JEOL JEM-1400 LaB_6 transmission electron microscope (JEOL, Ltd., Japan) equipped with a Gatan 2k x 2k US1000 CCD camera (Gatan, Inc., Pleasanton, CA).

SEM

For SEM examination of RBC vesicles, the samples were fixed with 2.5% glutaraldehyde in 0.1 M sodium cacodylate buffer (pH 7.4). The samples were then placed onto poly-L-lysine coated silicon chips and washed with the same buffer twice before post-fixation with 1% osmium tetroxide in the same buffer and dehydration through a graded ethanol series to 100%. Silicon chips with vesicles were then loaded into a Polaron E3000 critical point drying apparatus to exchange 100% ethanol for liquid CO_2. Once liquid CO_2 was brought to its critical point, it was vented slowly. The samples on the silicon chips were coated with 8 nm chromium in a Denton DV-602 Turbo Magnetron Sputter Coater (Denton Vacuum, LLC, Moorestown, NJ) before imaging on the upper-stage of a Topcon DS-150 field emission-scanning electron microscope (FE-SEM).

Microbial DNA analysis

DNA was isolated from microvesicle pellets, molecular grade water, and a colony of *Streptococcus pneumoniae* using a QIAamp DNA Mini Kit according to the manufacturer's specified protocol for bacteria (Qiagen). As an alternative, DNA was extracted using a conventional phenol-chlorophorm extraction protocol (12). Standard agarose gel electrophoresis was carried out on a 1% agarose accompanied by a 1kb DNA

ladder (NEB). The same universal 16S PCR primers used by McLaughlin et al. were utilized to amplify 16S rDNA: BSF8/20 (5′-AGAGTTTGATCCTGGCTCAG-3′) and the reverse primer BSR1541/20 (5′-AAGGAGGTGATCCAGCCGCA-3′) (2). PCRs were performed in 20µl reaction volumes with 1X Q5 High Fidelity Master Mix (New England Biolabs), 1µM forward and reverse primer, and 6ul of DNA template. Reactions were carried out on a Biorad C1000 Touch Thermocycler with the following conditions: 98°C x 10 minutes, (98°C x 10 seconds, 70°C x 30 seconds, 72°C x 30 seconds) x 38 cycles, 72°C x 2 minutes. PCR products were purified using a Qiaquick PCR Purification Kit per the manufacturer's protocol and sent for commercial first pass sequencing (Beckman Coulter) using the BSF8/20 and BSR1541/20 primers.

16S rDNA qPCR of human serum

Under aseptic conditions, blood was collected into serum vacutainers (BD) from 3 healthy donors (no medications). Cells were removed by centrifugation (3,000 x g for 7 minutes) and serum was incubated for 0, 5, or 10 days at 30°C. DNA was extracted from 100ul of serum as described above and used as a template for qPCR. Universal 16S primers developed previously for 16S rDNA qPCR were utilized: EUBAC-F (5′-TCCTACGGGAGGCAGCAGT-3′) and EUBAC-R (5′-GGACTACCAGGGTATCTAATCCTGTT-3′)(13). These primers were selected for qPCR because the amplicon size was more appropriate for qPCR studies than the primers used by McLaughlin et al. Reactions were performed in 20µl volumes with 1X Quantitect SYBR Green Master Mix, 300nM forward and reverse primers, and 8.8µl DNA. Thermocycler conditions were: 95C x 10 minutes, (95°C x 15 seconds, 60°C x 1 minute)

x 40 cycles. All reactions were performed in triplicate. Relative expression was calculated as 2^{dCt} and converted to fold-change by normalizing to the mean expression at day 0. Data was analyzed using a one-way ANOVA with the assistance of Prism (Graphpad).

Flow cytometry

Isolated particles were stained with 10μM calcein-AM (Life Technologies) and anti-CD235a (GPA) fluorescently labeled antibody (PE/Cy7; BioLegend), incubated at room temperature for 20 minutes, and analyzed on a BD LSR flow cytometer (BD Biosciences). The concentration of RMVs in a sample was calculated by ratiometric comparison after adding a known concentration of Flow-Check Fluoroshperes (Beckman).

miRNA analysis

Total RNA was isolated using a miRNeasy Mini Kit according to the manufacturer's protocol (Qiagen) and analyzed on an Agilent Bioanalyzer with the RNA 6000 Pico Kit by standard protocol. qRT-PCR analysis of miR-451 was performed using Qiagen products (miScript II RT Kit, miScript Primer assay) and analyzer on a StepOne Real-Time PCR System (ThermoFisher).

Western blot

Particles were lysed in RIPA buffer, exposed to brief sonication, and protein was quantified using the BCA assay. 30μg of protein was separated by gel electrophoresis,

transferred to a nitrocellulose membrane, and probed using an anti-hemoglobin-alpha antibody (Santa Cruz Biotechnology; sc-21005).

Funding Information

This work was supported by the National Institutes of Health (R01HL109559, R01HL124879, R01HL095476, S10RR025679), and a VA Merit Award (I01 BX000704). Research reported in this publication was also supported by the National Heart, Lung, and Blood Institute of the National Institutes of Health under Award Number T32HL007745. The JEOL JEM-1400 transmission electron microscope was acquired with an NIH S10 grant (1 S10RR025679 01). The content is solely the responsibility of the authors and does not necessarily represent the official views of the National Institutes of Health.

Figure Legends

Figure 1. Representative electron micrographs of pelleted material from supernatant of RBC storage units. A, B, Negative stain EM images of the unfixed material, showing pleomorphic structures. C,D, Thin-section TEM images, showing membrane encapsulate vesicles. E,F, SEM images. G,H, Negative stain EM of fixed (G) versus unfixed (H) structures. Vesicles were isolated and imaged as described in Methods section.

Figure 2. Analysis of bacterial DNA in pelleted material from RBC storage units and serum. RMVs were isolated from ~100mL of RBCs stored under standard conditions for 42 days. A, Genomic DNA was isolated and analyzed by gel electrophoresis. Molecular grade water and DNA from *S. Pneumoniae* served as negative and positive controls, respectively. Band reflective of genomic DNA was only observed in positive control lane. B, Isolated DNA was also subjected to 16S rDNA PCR analysis, using universal primers. PCR product was observed for all samples assessed. C, Serum from 3 healthy donors was incubated at 30°C for 5 and 10 days, and then analyzed using a 16S rDNA qPCR assay. No significant difference in 16S rDNA was observed between the different time points.

Figure 3. Vesicles isolated from supernatant of RBC storage units are membrane-bound, intact, and contain RBC surface antigen and RBC-specific miRNA. A, Unstained vesicles (red, bottom left) or vesicles co-stained with calcein-AM and fluorescent anti-GPA (blue, top right) were analyzed by flow cytometry. >99% of the vesicles were positive for calcein-AM and anti-GPA. B, RNA from vesicles was analyzed by Agilent Bioanalyzer.

Peak on electropherogram at 25 nt is internal standard and small peak to the right reflects small RNA. This electropherogram is representative of Bioanlyzer data from six different RBC storage units. C, Levels (Ct values) of miR-451 were assessed by qRT-PCR in stored RBCs, the RMV pellet, and in human aortic endothelial cells (HAECs, negative control). D, Hemoglobin-alpha content of RMV pellet and stored RBCs, as assessed by Western blot. Blot is representative of six different RBC storage units.

Figure 1.

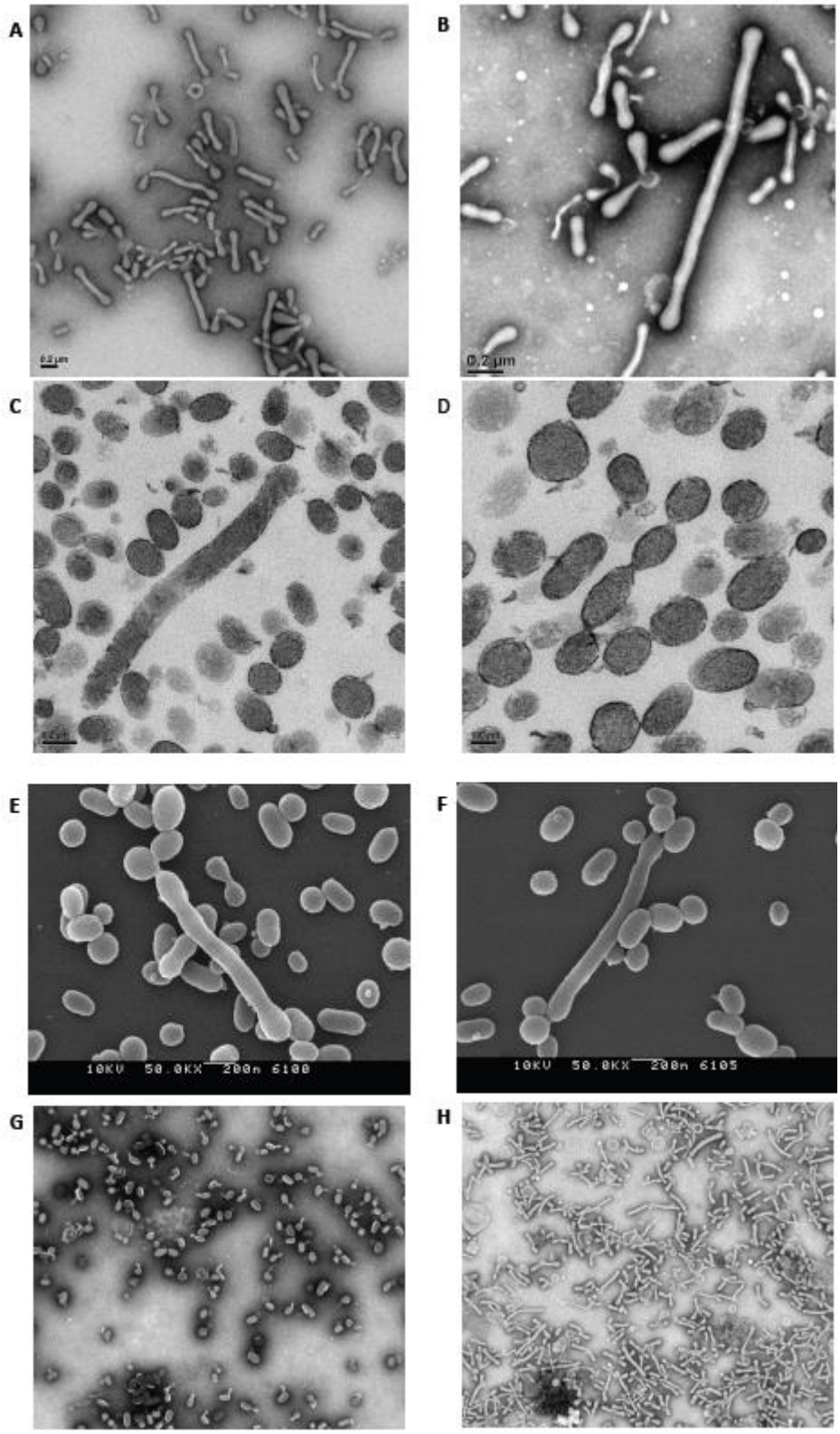

Figure 2.

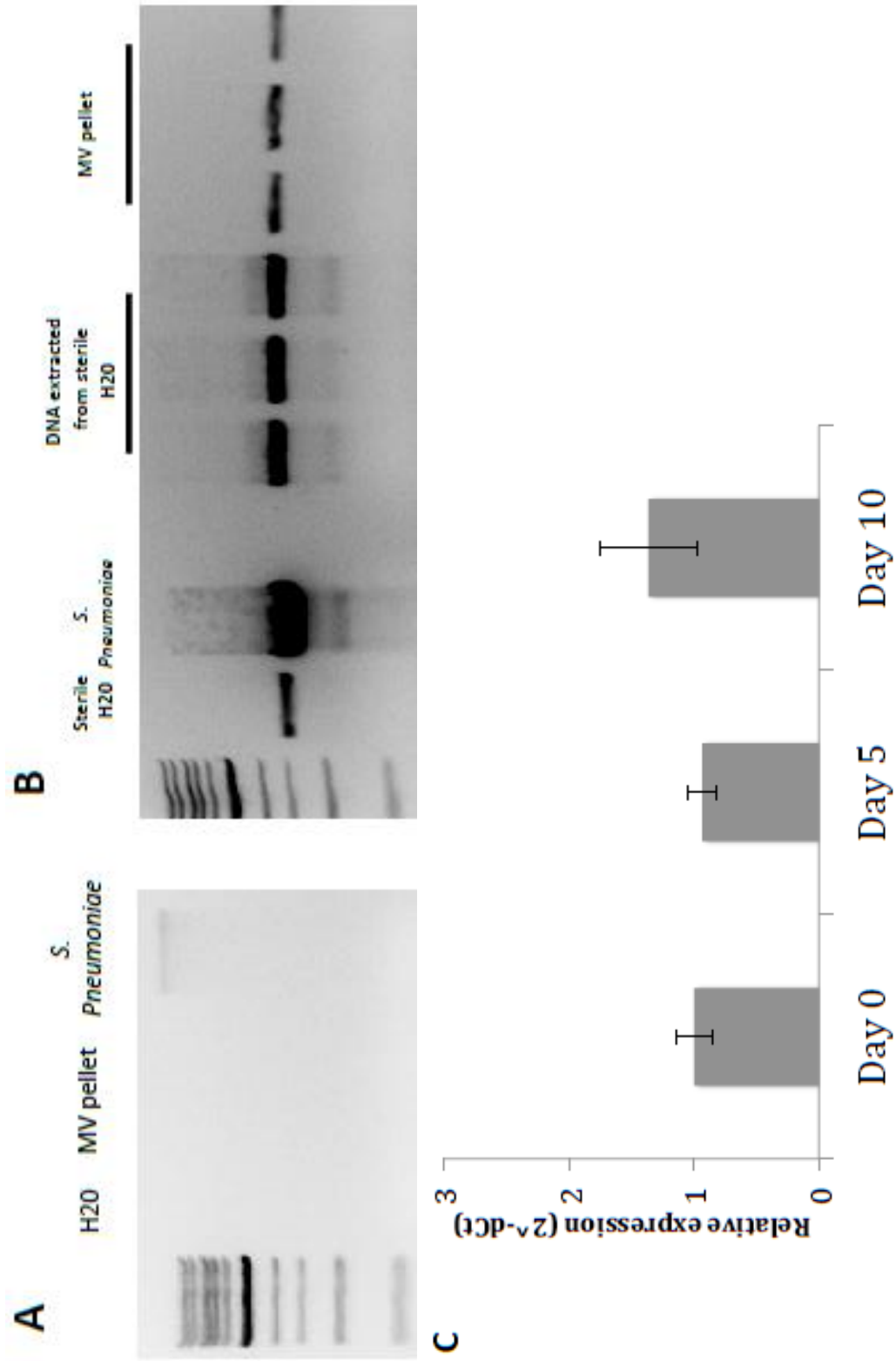
A
H20
MV pellet
S. Pneumoniae
B
Sterile H20
S. Pneumoniae
DNA extracted from sterile H20
MV pellet
C
Relative expression (2^-dCt)
0
1
2
3
Day 0
Day 5
Day 10

Figure 3.

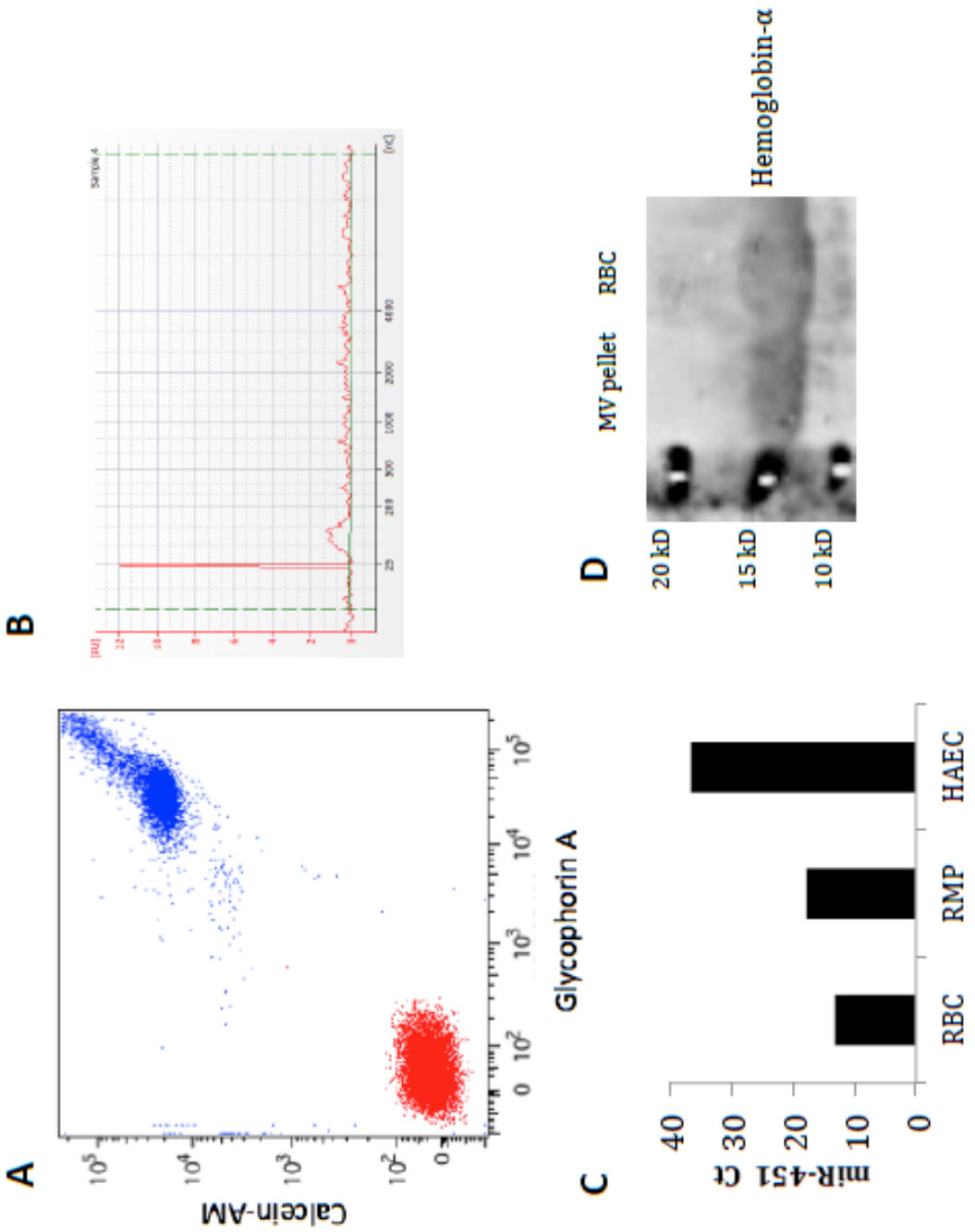
A
Calcein-AM
Glycophorin A
B
C
miR-451 Ct
RBC
RMP
HAEC
D
MV pellet
RBC
Hemoglobin-α
20 kD
15 kD
10 kD

References

1. **Hopewell S, Omar O, Hyde C, Yu LM, Doree C, Murphy MF.** 2013. A systematic review of the effect of red blood cell transfusion on mortality: evidence from large-scale observational studies published between 2006 and 2010. BMJ Open **3**.
2. **McLaughlin RW, Vali H, Lau PC, Palfree RG, De Ciccio A, Sirois M, Ahmad D, Villemur R, Desrosiers M, Chan EC.** 2002. Are there naturally occurring pleomorphic bacteria in the blood of healthy humans? J Clin Microbiol **40:**4771-4775.
3. **Szymanski M, Petric M, Saunders FE, Tellier R.** 2002. Mycoplasma pneumoniae pericarditis demonstrated by polymerase chain reaction and electron microscopy. Clin Infect Dis **34:**E16-17.
4. **Rubin O, Canellini G, Delobel J, Lion N, Tissot JD.** 2012. Red blood cell microparticles: clinical relevance. Transfus Med Hemother **39:**342-347.
5. **Dinkla S, Brock R, Joosten I, Bosman GJ.** 2013. Gateway to understanding microparticles: standardized isolation and identification of plasma membrane-derived vesicles. Nanomedicine (Lond) **8:**1657-1668.
6. **Salter SJ, Cox MJ, Turek EM, Calus ST, Cookson WO, Moffatt MF, Turner P, Parkhill J, Loman NJ, Walker AW.** 2014. Reagent and laboratory contamination can critically impact sequence-based microbiome analyses. BMC Biol **12:**87.
7. **Gray WG, Mitchell AJ, Searles CS.** 2015. An accurate, precise method for general labeling of extracellular vesicles. MethodsX **2:**360-367.

8. **Azzouzi I, Moest H, Wollscheid B, Schmugge M, Eekels JJ, Speer O.** 2015. Deep sequencing and proteomic analysis of the microRNA-induced silencing complex in human red blood cells. Exp Hematol **43:**382-392.

9. **Young JD, Martel J.** 2010. The rise and fall of nanobacteria. Sci Am **302:**52-59.

10. **Martel J, Young JD.** 2008. Purported nanobacteria in human blood as calcium carbonate nanoparticles. Proc Natl Acad Sci U S A **105:**5549-5554.

11. **Raoult D, Drancourt M, Azza S, Nappez C, Guieu R, Rolain JM, Fourquet P, Campagna B, La Scola B, Mege JL, Mansuelle P, Lechevalier E, Berland Y, Gorvel JP, Renesto P.** 2008. Nanobacteria are mineralo fetuin complexes. PLoS Pathog **4:**e41.

12. **Bergallo M, Costa C, Gribaudo G, Tarallo S, Baro S, Negro Ponzi A, Cavallo R.** 2006. Evaluation of six methods for extraction and purification of viral DNA from urine and serum samples. New Microbiol **29:**111-119.

13. **Dinakaran V, Rathinavel A, Pushpanathan M, Sivakumar R, Gunasekaran P, Rajendhran J.** 2014. Elevated levels of circulating DNA in cardiovascular disease patients: metagenomic profiling of microbiome in the circulation. PLoS One **9:**e105221.